HOW TO SURVIVE AN INFECTION:
LESSONS FROM THE FLY

A Dissertation

Presented to the Faculty of the Graduate School

of Cornell University

in Partial Fulfillment of the Requirements for the Degree of

Doctor of Philosophy

by

Katia Ana Maria Sotelo Troha

December 2018

HOW TO SURVIVE AN INFECTION:
LESSONS FROM THE FLY

Katia Ana Maria Sotelo Troha, Ph. D.

Cornell University 2018

How an organism is able to combat infection and survive has been a central and longstanding question in the field of infection biology. To fight infection, a host activates a combination of immune and physiological responses. While detection of microbial presence is sufficient to stimulate the immune response, some physiological responses to infection occur as a consequence of microbial growth and virulence, and can therefore be very specific to the particular microbe the host interacts with. Despite recent advances, our knowledge of the different processes that are activated or repressed in response to infection, and of how such responses contribute to organismal survival, remains limited.

To identify new biological processes required to survive infection, we used RNA-seq to profile the *D. melanogaster* response to infection with 10 different bacterial pathogens. We found that each bacterium triggers a unique transcriptional response. However, we also identified a core set of 252 genes that are differentially expressed in response to the majority of bacteria tested. Among these, we determined that the transcription factor *CrebA* is a novel regulator of infection tolerance that acts to promote host survival during infection. Knock-down of *CrebA* significantly increased mortality from microbial infection without any concomitant change in bacterial number. Upon infection, *CrebA* is upregulated by both the Toll and Imd pathways in the fat body, where it is required to induce the expression of secretory pathway genes. Loss of *CrebA* during infection triggered endoplasmic reticulum (ER) stress and activated the unfolded protein response (UPR),

which contributed to infection-induced mortality. Altogether, our study reveals essential features of the response to bacterial infection and elucidates the function of a novel regulator of infection tolerance that promotes survival to infection.

The second research project of this dissertation assesses the role of a different biological process, hemolymph (extracellular fluid analogous to blood) filtration, in the host response to infection. Nephrocytes are podocyte-like cells that regulate hemolymph composition by filtration. Flies deficient for *Klf15*, a transcription factor required for nephrocyte development and function, are viable but lack nephrocytes. Surprisingly, we found that *Klf15* mutants display constitutively elevated Toll pathway activity, and as a consequence, are more resistant to microbial infection. Our analysis revealed that nephrocytes uptake Lys-type peptidoglycan from systemic circulation and degrade it inside lysosomes. Without nephrocyte function, microbiota-derived peptidoglycan accumulates in circulation, triggering Toll pathway activation even in the absence of infection. These results unveil a role for hemolymph filtration in the maintenance of immune tolerance to microbiota. Although our study was not able to address whether nephrocytes filter Lys-type peptidoglycan from circulation in the context of a systemic bacterial infection, we found a novel and important physiological connection between hemolymph filtration and the immune system, and learned that disruption of this process actually increases survival to infection.

BIOGRAPHICAL SKETCH

Katia Troha received B.A. in Molecular and Cell Biology with a concentration in Genetics, Genomics, and Development from the University of California, Berkeley. After graduation, she joined the laboratory of Dr. Russell Vance at UC Berkeley as a research assistant, where she became interested in infection biology. In 2012, Katia formally began her Ph.D. work at Cornell University under the guidance of Dr. Nicolas Buchon and Dr. Brian Lazzaro. Katia's research interests include immunity, host-microbe interactions, and disease tolerance

ACKNOWLEDGMENTS

I would like to thank both of my advisors, Dr. Nicolas Buchon and Dr. Brian Lazzaro, for their guidance and support during my Ph.D. I would also like to thank my committee members Dr. David Russell, Dr. Sylvia Lee, and Dr. Chun Han for all their help and encouragement during my time as a graduate student. Finally, I would like to thank all members, past and present, of both the Buchon and Lazzaro labs for their friendship and helpful contributions to my research.

TABLE OF CONTENTS

CHAPTER I

INTRODUCTION

1. Central question

Survival is arguably the ultimate goal of a pathogen-infected organism. How an organism is able to combat infection and survive has therefore been a central and longstanding question in the field of infection biology. To overcome infection, a host will deploy a combination of immune and physiological responses [1] [2] [3] [4]. Following microbial challenge, immune responses are triggered by the detection of microbe-associate molecular patterns (MAMPs) and damage-associated molecular patterns (DAMPs) by the host [5]. The function of these immune responses, which are also known as resistance mechanisms, is to clear and or limit pathogen burden [3]. Because host physiology can be negatively affected by pathogens and/or the immune responses that they elicit, the mechanisms that customarily maintain homeostasis of various host physiological systems are expected to counter, limit, or prevent the pathological alterations caused by infection [6]. Some of these physiological responses contribute to disease tolerance (also referred to as resilience or infection tolerance), which is defined as the ability to withstand the infection and/or its deleterious consequences [2] [7]. Despite an ever-growing body of literature on infection biology, our knowledge of the different host processes that are activated or repressed in response to infection, and of how such responses contribute to host survival, remains incomplete. The present work, therefore, seeks to identify novel biological processes involved in the host response to infection, determine how these host responses contribute to organismal survival, and finally ascertain how generic or specific host responses to various pathogens are.

2. The *Drosophila melanogaster* model

Drosophila melanogaster is a powerful system to study the host response to microbial infection [4]. Thanks, in part, to the high degree of evolutionary conservation between mammalian

and fly signaling pathways and organ systems, studies using the *Drosophila* model have shed light not only on the basic molecular mechanisms of pathogen recognition and nuclear factor-κB (NF-κB) signaling, but also on the nature of physiological responses activated in the host by infection and how dysregulation of these responses contributes to disease [4] [8] [9]. In the wild, *Drosophila* is naturally infected by viruses, bacteria, fungi, and parasites, and in the laboratory, flies can be experimentally infected with diverse human pathogens, making it an attractive model to study infectious diseases [10] [11] [12]. The availability of a vast arsenal of genetic tools is arguably the most attractive asset that *Drosophila* has over other model organisms for the study of immunity. This advantage has allowed for the fine manipulation of cells and tissues both spatially and temporally, as well as the generation of countless reporter lines that have facilitated the study of immune and immune-related processes in both a qualitative and quantitative manner [13]. In combination with genomic technologies, these tools have contributed to the advancement of our knowledge of the host response to infection in both flies and mammals.

To resist infection, *Drosophila* deploys cellular and humoral innate immune responses. The cellular response consists of encapsulation and phagocytosis, while the humoral response involves the melanization cascade and the synthesis of antimicrobial peptides (AMPs) by the fat body (an organ analogous to the liver and adipose tissue of mammals) [8] [4]. Production of AMPs is controlled by two principal signaling cascades, the Toll and Imd pathways [14]. Both pathways are activated in response to peptidoglycan (PGN): Lys-type PGN from Gram-positive bacteria triggers the Toll pathway, while DAP-type PGN from Gram-negative bacteria induces the Imd pathway [8] [4]. The Toll and Imd pathways are the major regulators of the immune response in *Drosophila*, and as such, control a majority of genes induced or repressed in response to microbial infection [14].

3. The effects of infection on *Drosophila* physiology

In the early 2000s, microarray studies characterizing the transcriptional response to bacterial infection were conducted in *Drosophila*. These experiments were based on infection with a mixture of two non-pathogenic bacteria, *Micrococcus luteus* (a Gram-positive) and *Escherichia coli* (a Gram-negative) [15] [14] [16]. This approach successfully identified a set of genes that are differentially expressed upon infection, which became known as the *Drosophila* Immune-Regulated Genes (DIRGs) [15] [14]. A majority of the DIRGs were functionally assigned to specific aspects of the immune response—phagocytosis, antimicrobial peptide synthesis, and production of reactive oxygen species among others. However, a fraction of the DIRGs fell under biological processes that would not be considered classical immune reactions, such as metabolism, wound healing, and stress response [15] [14]. Subsequent studies confirmed some of these findings. For example, with regards to metabolism, it was demonstrated that infection with *L. monocytogenes* alters energy metabolism, with flies gradually losing their energy stores (triglycerides and glycogen) [17]. It was also shown that flies infected with *M. marinum* become hyperglycemic and undergo a process like wasting [18]. Additionally, it was found that anorexia is induced by infection with certain microbes [19]. Furthermore, recent studies have established that tissue repair is an integral part of the response to some infections, as flies that cannot repair infection-induced gut damage are rendered more susceptible to infection [20] [21]. In sum, evidence from several infection studies indicate that the infection alters host physiology in the fly in various ways.

The aforementioned studies established that the response to infection includes a physiological response by the host, yet the extent of this response remains an open question.

Because physiological responses to infection occur as a consequence of microbial growth and virulence, they can be very specific to the particular pathogen the host interacts with [22] [23]. Given that *Drosophila* infection responses have been historically studied in the context of challenge with a few, mostly avirulent microbes [15] [14] [16], we currently have limited knowledge of the kinds of physiological responses induced by infection, of how generic or specific the physiological response to various microbes is, and to what extent these responses contribute to organismal survival. Furthermore, a lot of the studies that first identified physiological changes in response to infection were based on gene expression experiments that used whole flies as samples [15] [14]. One of the drawbacks of this approach is that it is possible to miss small but relevant transcriptional changes in tissues made up of only a few cells, as these alterations may be drowned out by stronger mRNA signal coming from larger tissues. Thus, it is likely that these early studies may have missed important physiological reactions in smaller tissues, opening the door for future work to look into this possibility.

4. Outline of dissertation research

The central focus of my PhD work has been to identify novel processes that allow an organism to survive microbial challenge, with a special focus on host physiological responses to infection. I began my PhD work by learning about my model organism, *Drosophila melanogaster*, and various assays and techniques to study *Drosophila* immunity. I have compiled my knowledge of the methods and protocols I have used throughout my PhD into a review manuscript titled "Methods for the Study of Innate Immunity in *D. melanogaster*". This manuscript is presented as Chapter II of this dissertation.

Chapter III covers the results of a collaborative project that addresses the key questions of my PhD. To identify all the different biological processes regulated by infection, as well as their

regulators, we transcriptionally profiled the response to infection at the level of the whole organism by doing RNA-seq on whole flies following systemic infection. In order to determine whether the host response to microbial challenge is generic or specific to individual pathogens, we employed 10 different bacteria that varied in their level of virulence and Gram-type. We found that each bacterium triggers a unique transcriptional response, with distinct genes making up to one third of the response elicited by highly virulent bacteria. We also identified a core set of 252 genes that are differentially expressed in response to the majority of bacteria tested. Among these, we determined that the transcription factor *CrebA* is a novel regulator of infection tolerance/disease tolerance. Knock-down of *CrebA* significantly increased mortality from microbial infection without any concomitant change in bacterial number. Upon infection, *CrebA* is upregulated by both the Toll and Imd pathways in the fat body, where it is required to induce the expression of secretory pathway genes. Loss of *CrebA* during infection leads to endoplasmic reticulum (ER) stress, a disruption of protein folding in the ER resulting in the accumulation of unfolded or misfolded proteins [24], which increased infection-induced mortality. In this work, we proposed a model in which *CrebA* is upregulated early during infection by the host to adapt the fat body cells for infection, thus preventing ER stress that would otherwise be triggered by the response to infection. In this context, *CrebA* is a novel regulator of the physiological response to infection that promotes host survival by preventing deleterious, infection-induced ER stress. The results of this project were assembled into a manuscript titled "Comparative transcriptomics reveals *CrebA* as a novel regulator of infection tolerance in *D. melanogaster*" and are presented here as Chapter III [25].

The second research project of my dissertation focused on characterizing the role of hemolymph (extracellular fluid analogous to blood) filtration in the host response to infection. This project was based on the hypothesis that hemolymph filtration could be an important

component of the physiological response to infection because hosts may want to remove harmful molecules, such as bacterial toxins, from circulation during the course of infection. In the fly, hemolymph filtration is performed by nephrocytes, a cell type that acts as a filtration device. Each adult fly has, on average, a total of ~40 pericardial nephrocytes [26]. Given the particular limitation of using whole fly samples for gene expression studies (missing small but significant transcriptional changes in tissues made up of only a few cells—as discussed above), this hemolymph filtration project is complementary to the RNA-seq project of Chapter III. In this work, we found that nephrocytes filter Lys-type peptidoglycan from Gram-positive microbiota from systemic circulation and degrade it inside lysosomes. Without nephrocyte function, microbiota-derived peptidoglycan accumulates in circulation, triggering Toll pathway activation even in the absence of infection. Lack of nephrocytes also results in increased resistance to infection and a shorter lifespan. These results unveil a role for hemolymph (insect blood) filtration in the maintenance of immune tolerance (defined as lack of an immune response to a substance that has the potential to induce an immune reaction [27]) to microbiota. Although our study was not able to address whether nephrocytes filter immunostimulatory peptidoglycan from circulation in the context of a pathogenic infection (as opposed to peptidoglycan from resident microbiota), we did find a novel and important physiological connection between the filtration system of the fly and the immune system that serves to maintain immune homeostasis and learned that disruption of this process actually increases survival to infection. The results of this project have been summarized in a manuscript titled "Nephrocytes mediate immune tolerance to microbiota by removing peptidoglycan from systemic circulation" and are presented as Chapter IV of this dissertation.

Finally, Chapter V contains a discussion of my findings as they relate to the central questions of my dissertation, as well as a perspective on future directions for each project.

REFERENCES

1. Shirasu-Hiza MM, Schneider DS. Confronting physiology: how do infected flies die? Cellular Microbiology. Wiley/Blackwell (10.1111); 2007;9: 2775–2783. doi:10.1111/j.1462-5822.2007.01042.x

2. Ayres JS, Schneider DS. Tolerance of infections. Annu Rev Immunol. Annual Reviews; 2012;30: 271–294. doi:10.1146/annurev-immunol-020711-075030

3. Schneider DS, Ayres JS. Two ways to survive infection: what resistance and tolerance can teach us about treating infectious diseases. Nat Rev Immunol. 2008;8: 889–895. doi:10.1038/nri2432

4. Buchon N, Silverman N, Cherry S. Immunity in Drosophila melanogaster--from microbial recognition to whole-organism physiology. Nat Rev Immunol. 2014;14: 796–810. doi:10.1038/nri3763

5. Newton K, Dixit VM. Signaling in Innate Immunity and Inflammation. Cold Spring Harbor Perspectives in Biology. 2012;4: a006049–a006049. doi:10.1101/cshperspect.a006049

6. Medzhitov R, Schneider DS, Soares MP. Disease tolerance as a defense strategy. Science. 2012;335: 936–941. doi:10.1126/science.1214935

7. Ferrandon D. The complementary facets of epithelial host defenses in the genetic model organism Drosophila melanogaster: from resistance to resilience. Curr Opin Immunol. 2013;25: 59–70. doi:10.1016/j.coi.2012.11.008

8. Lemaitre B, Hoffmann J. The host defense of Drosophila melanogaster. Annu Rev Immunol. Annual Reviews; 2007;25: 697–743. doi:10.1146/annurev.immunol.25.022106.141615

9. Padmanabha D, Baker KD. Drosophila gains traction as a repurposed tool to investigate metabolism. Trends Endocrinol Metab. 2014;25: 518–527. doi:10.1016/j.tem.2014.03.011

10. Carpenter JA, Obbard DJ, Maside X, Jiggins FM. The recent spread of a vertically transmitted virus through populations of Drosophila melanogaster. Mol Ecol. Blackwell Publishing Ltd; 2007;16: 3947–3954. doi:10.1111/j.1365-294X.2007.03460.x

11. Galac MR, Lazzaro BP. Comparative pathology of bacteria in the genus Providencia to a natural host, Drosophila melanogaster. Microbes and Infection. 2011;13: 673–683. doi:10.1016/j.micinf.2011.02.005

12. Panayidou S, Ioannidou E, Apidianakis Y. Human pathogenic bacteria, fungi, and viruses in Drosophila: disease modeling, lessons, and shortcomings. Virulence. Taylor & Francis; 2014;5: 253–269. doi:10.4161/viru.27524

13. Venken KJT, Bellen HJ. Chemical mutagens, transposons, and transgenes to interrogate gene function in Drosophila melanogaster. Methods. 2014;68: 15–28.

doi:10.1016/j.ymeth.2014.02.025

14. De Gregorio E, Spellman PT, Tzou P, Rubin GM, Lemaitre B. The Toll and Imd pathways are the major regulators of the immune response in Drosophila. EMBO J. EMBO Press; 2002;21: 2568–2579. doi:10.1093/emboj/21.11.2568

15. De Gregorio E, Spellman PT, Rubin GM, Lemaitre B. Genome-wide analysis of the Drosophila immune response by using oligonucleotide microarrays. Proc Natl Acad Sci USA. 2001;98: 12590–12595. doi:10.1073/pnas.221458698

16. Irving P, Troxler L, Heuer TS, Belvin M, Kopczynski C, Reichhart JM, et al. A genome-wide analysis of immune responses in Drosophila. Proc Natl Acad Sci USA. 2001;98: 15119–15124. doi:10.1073/pnas.261573998

17. Chambers MC, Song KH, Schneider DS. Listeria monocytogenes Infection Causes Metabolic Shifts in Drosophila melanogaster. Freitag NE, editor. PLoS ONE. Public Library of Science; 2012;7: e50679. doi:10.1371/journal.pone.0050679

18. Dionne MS, Pham LN, Shirasu-Hiza M, Schneider DS. Akt and FOXO dysregulation contribute to infection-induced wasting in Drosophila. Curr Biol. 2006;16: 1977–1985. doi:10.1016/j.cub.2006.08.052

19. Ayres JS, Schneider DS. The role of anorexia in resistance and tolerance to infections in Drosophila. Promislow D, editor. PLoS Biol. Public Library of Science; 2009;7: e1000150. doi:10.1371/journal.pbio.1000150

20. Buchon N, Broderick NA, Poidevin M, Pradervand S, Lemaitre B. Drosophila intestinal response to bacterial infection: activation of host defense and stem cell proliferation. Cell Host Microbe. Elsevier; 2009;5: 200–211. doi:10.1016/j.chom.2009.01.003

21. Buchon N, Broderick NA, Kuraishi T, Lemaitre B. Drosophila EGFR pathway coordinates stem cell proliferation and gut remodeling following infection. BMC Biol. BioMed Central; 2010;8: 152. doi:10.1186/1741-7007-8-152

22. Chakrabarti S, Liehl P, Buchon N, Lemaitre B. Infection-induced host translational blockage inhibits immune responses and epithelial renewal in the Drosophila gut. Cell Host Microbe. 2012;12: 60–70. doi:10.1016/j.chom.2012.06.001

23. Hooper P, Selleck P. **Pathology of Low and High Virulent Influenza Virus Infections**. Avian Diseases. 1997;: 134–141.

24. Yoshida H. ER stress and diseases. FEBS Journal. Wiley/Blackwell (10.1111); 2007;274: 630–658. doi:10.1111/j.1742-4658.2007.05639.x

25. Troha K, Im JH, Revah J, Lazzaro BP, Buchon N. Comparative transcriptomics reveals CrebA as a novel regulator of infection tolerance in D. melanogaster. Schneider DS, editor. PLoS Pathog. 2018;14: e1006847. doi:10.1371/journal.ppat.1006847

26. Denholm B, Skaer H. Bringing together components of the fly renal system. Curr Opin Genet Dev. 2009;19: 526–532. doi:10.1016/j.gde.2009.08.006

27. Belkaid Y, Harrison OJ. Homeostatic Immunity and the Microbiota. Immunity. 2017;46: 562–576. doi:10.1016/j.immuni.2017.04.008

CHAPTER II

METHODS FOR THE STUDY OF INNATE IMMUNITY IN *D. MELANOGASTER**

* Adapted from Katia Troha and Nicolas Buchon. Methods for the Study of Innate Immunity in *D. melanogaster*. Submitted to WIREs Developmental Biology.

Abstract

From flies to humans, many components of the innate immune system have been conserved during metazoan evolution. This foundational observation has allowed us to develop *Drosophila melanogaster*, the fruit fly, into a powerful model to study innate immunity in animals. Thanks to an ever-growing arsenal of genetic tools, an easily manipulated genome, and its winning disposition, *Drosophila* is now employed to study not only basic molecular mechanisms of pathogen recognition and immune signaling, but also the nature of physiological responses activated in the host by microbial challenge and how dysregulation of these processes contributes to disease. Here, we present a collection of methods and protocols to challenge the fly with an assortment of microbes, both systemically and orally, and assess its humoral, cellular, and epithelial response to infection. Our review covers techniques for measuring the reaction to microbial infection both qualitatively and quantitatively. Specifically, we describe survival, bacterial load, *BLUD* (a measure of disease tolerance), phagocytosis, melanization, clotting, and ROS production assays, as well as efficient protocols to collect hemolymph and measure immune gene expression. We also offer an updated catalog of online resources and a collection of popular reporter lines and mutants to facilitate research efforts.

I. Introduction

Over the last 25 years, the fruit fly, *Drosophila melanogaster*, has emerged as a leading model to study host-microbe interactions. Thanks, in part, to the high degree of evolutionary conservation between mammalian and fly signaling pathways and organ systems, studies using the *Drosophila* model have shed light not only on the basic molecular mechanisms of pathogen recognition and nuclear factor-κB (NF-κB) signaling, but also on the nature of physiological responses activated in the host by infection and how dysregulation of these responses contributes to disease (Buchon et al., 2014; Lemaitre and Hoffmann, 2007; Padmanabha and Baker, 2014). In the wild, *Drosophila* is naturally infected by viruses, bacteria, fungi, and parasites, and in the laboratory, flies can be experimentally infected with diverse human pathogens, making it an attractive model to study infectious diseases (Carpenter et al., 2007; Galac and Lazzaro, 2011; Panayidou et al., 2014). *Drosophila* has played a role in identifying virulence factors of opportunistic human pathogens (Kim et al., 2008). To a large extent, many microbes employ similar mechanisms to infect mammals and flies, and several virulence factors necessary for invasion and colonization of mammals are also effective against flies (Alarco et al., 2004; Chamilos et al., 2009; Fauvarque, 2014). The availability of a vast array of genetic tools is arguably the most attractive asset that *Drosophila* has over other model organisms for the study of immunity. This advantage has allowed for the fine manipulation of cells and tissues both spatially and temporally, as well as the generation of innumerable reporter lines that have facilitated the study of immune and immune-related processes in both a qualitative and quantitative manner (Venken and Bellen, 2014). In combination with genomic technologies, these tools have contributed to the advancement of our knowledge of the host response to infection in both flies and mammals.

To combat infection, *Drosophila* relies on both cellular and humoral innate immune

responses. The cellular response consists of phagocytosis and encapsulation (Guillou et al., 2016; Kocks et al., 2005). The humoral response includes the pro-phenoloxidase cascade, which leads to the generation of reactive oxygen species and clotting, and the production of antimicrobial peptides (AMPs) primarily by the fat body, an organ functionally analogous to the liver and adipose tissues of mammals (Boman et al., 1972; Tauszig et al., 2000; Buchon et al., 2014). The Toll and Imd pathways are the principal signaling cascades responsible for AMP production (Lemaitre and Hoffmann, 2007). Although *Drosophila* can mount effective immune responses at all stages of development, some responses appear to be stage-specific. For example, proliferation of lamellocytes, large cells that primarily function in encapsulation, upon infection is only observed in the larval stage (Lanot et al., 2001). Immune reactions in *Drosophila* include both systemic and local responses. The hallmark of the systemic response is the inducible synthesis and secretion of AMPs into the hemolymph by the fat body and hemocytes (Lemaitre and Hoffmann, 2007). In contrast, local immune responses take place in barrier epithelia, such as the gut, which is capable of producing tissue-specific AMPs and reactive oxygen species (ROS) in response to microbes (Buchon et al., 2009b; Ha et al., 2005). Although both the local and systemic responses include the generation of AMPs, the molecular mechanisms regulating AMP gene expression have been shown to differ between the two (Tzou et al., 2000). These systemic and local immune responses are complemented by other potent defense mechanisms, such as RNA interference (RNAi), which *Drosophila* employs to combat viral infection (Wang et al., 2006) (Figure 1).

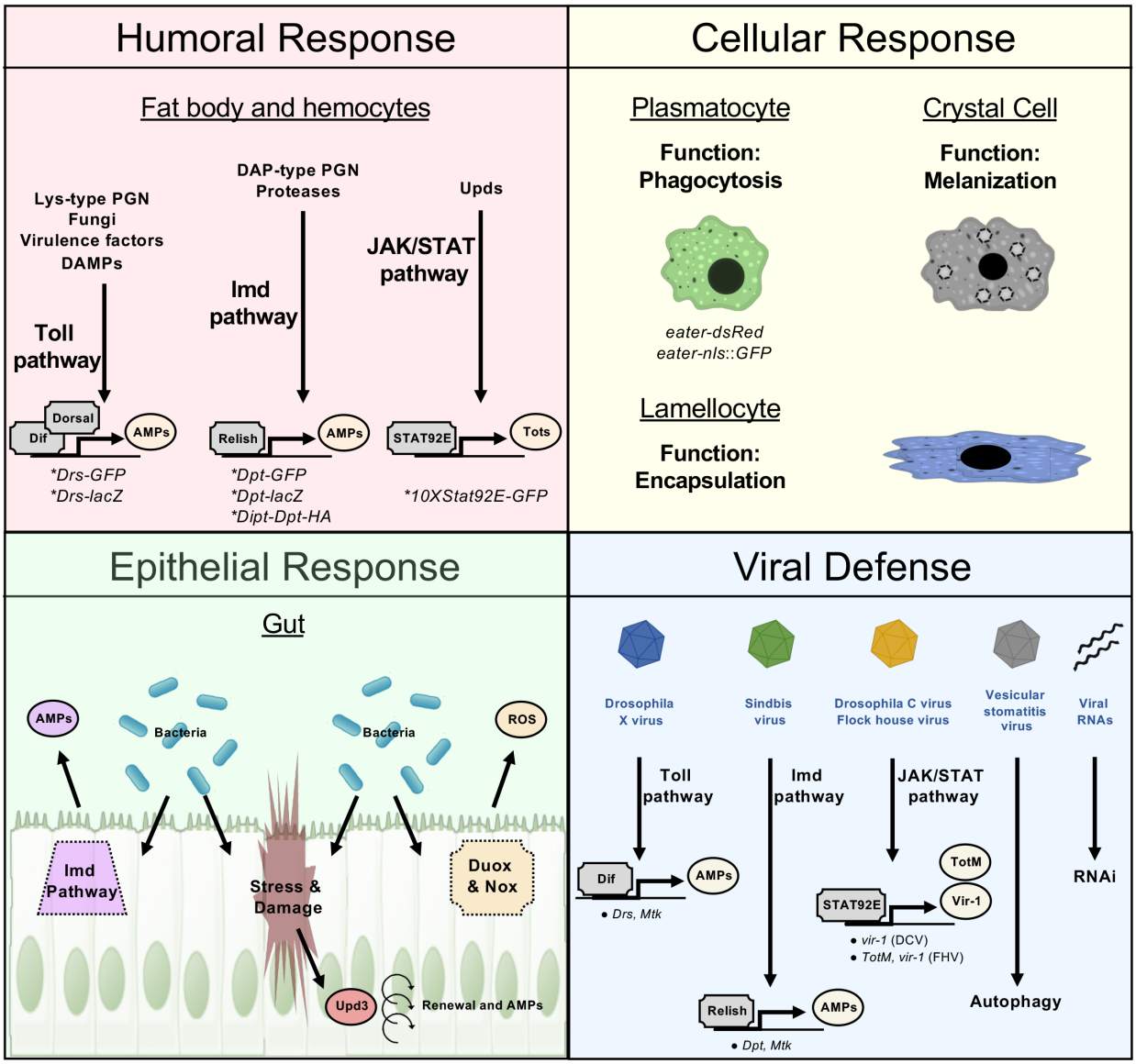

Figure II.1. The response to infection in *Drosophila melanogaster*.
Schematic overview of *Drosophila* host defense. Detection of an array of elicitors triggers a coordinated and synergistic activation of defense modules in the fly. *Denotes reporter lines associated with select pathways. ●Indicates reporter genes linked to individual pathways. Detailed information on these reporter lines and reporter genes can be found in Tables 2 and 3, respectively.

The nature of the immune response in *Drosophila* can be affected by environmental, physiological, and genetic factors; therefore, special attention should be paid to control these experimental variables, whenever possible. For instance, starvation increases susceptibility to

infection in both insects and humans, and changes in the ratios of specific dietary components, such as carbohydrates, proteins, and fat, have been implicated in shaping the immune response to infection (Cotter et al., 2010; Moret and Schmid-Hempel, 2000; Schaible and Kaufmann, 2007). Studies have also found that circadian rhythm mutants have immune phenotypes and that the temperature at which flies are maintained can affect host survival following infection (Linder et al., 2008; Stone et al., 2012). Variations in the composition of environmental microbes can have significant effects on host physiology and immune responsiveness; thus, standardization of microbiota is recommended at the beginning of every project (Fast et al., 2018; Gould et al., 2017; Rosshart et al., 2017). Basic protocols to homogenize environmental microbes have been described previously (Koyle et al., 2016). Special consideration should also be paid to the presence of viruses and endosymbionts in laboratory stocks, as some of these agents are reported to have significant effects on infection outcome (Palmer et al., 2018; Teixeira et al., 2008; Xu and Cherry, 2014). Protocols for the eradication of both are described in subsequent sections of this article. *Drosophila* exhibits marked sexual dimorphism in response to infection; female flies customarily have lower survival rates compared to males after infection (Duneau et al., 2017a; Shahrestani et al., 2018). Additionally, mating status has a substantial impact on the outcome of infection, with mated females typically presenting with increased susceptibility and higher pathogen loads compared to virgin females (Schwenke and Lazzaro, 2017; Short and Lazzaro, 2010). As aging flies are generally more susceptible to infection compared to their younger counterparts, age at infection also appears to play a role in the host response (Ramsden et al., 2008). Finally, immune performance varies across genetic backgrounds. A recent study comparing 5 commonly used reference strains (*Canton*^{s}, *Oregon*^{R}, *w*^{1118}, *cinnabar brown*, and *yellow white*) detected sizeable differences upon infection in host survival, bacterial load, expression of antimicrobial peptide

genes, number of circulating hemocytes, and levels of phenol-oxidase activity between all 5 strains (Eleftherianos et al., 2014). Because of potential interactions between mutations and specific genetic backgrounds, it is recommended that mutations of interest be tested in the context of different genetic backgrounds, particularly when the mutant phenotype is small and or subtle.

The host response to infection is also shaped by the type of pathogen used. For example, in flies, the transcriptional response to bacterial challenge differs from that to fungal infection (De Gregorio et al., 2001; 2002). Recent work has also shown that different bacterial pathogens elicit largely unique gene expression profiles in the host, with differences in the transcriptional magnitude of the host response and the type of peptidoglycan found on bacteria (Lys-type versus DAP-type peptidoglycan) predominantly accounting for the transcriptional differences observed (Troha et al., 2018). Selection of suitable microbes is a key consideration in all immune studies. Pathogen virulence, LT50 values (median time required to kill 50% of subjects after exposure to a known concentration of a pathogen), whether the microbe is cleared or enters a chronic infection, and the ability of the pathogen to suppress or avoid the immune response are all important factors to be considered. Lastly, infection route can determine the outcome of infection in flies. For instance, a number of microbes capable of causing mortality via systemic infection display no lethality during oral challenge (Martins et al., 2013).

After highlighting these key considerations for the study of immunity, we present below common methodologies to study the immune response in *Drosophila*.

II. Frequently used microbes and immune elicitors

Drosophila is amenable to infection with a large variety of microbes. Both human pathogens and entomopathogenic microbes have been used in the study of immunity (Chakrabarti et al., 2012; Neyen et al., 2014; Troha et al., 2018). The availability of genetically tractable microorganisms is an important factor in the selection of microbes for immune investigation, as they allow for the parallel study of pathogen virulence factors and host immune genes. Here, we describe a select group of microbes and immune elicitors commonly used across research groups for the study of *Drosophila* immunity. A more comprehensive list of the pathogens used in the field—including classification, culture conditions, typical dose, and usual route of infection—is provided in Table 1.

Bacteria	Gram and Peptidoglycan Type	Growth Conditions	Route of Infection	Dose
Escherichia coli	Gram-negative, DAP-type	LB media, 29-37 °C	Systemic	OD_{600}= 100 for needle pricking OD_{600}= 0.1 for microinjection
Serratia marcescens	Gram-negative, DAP-type	LB media, 29-37 °C	Systemic	OD_{600}= 1 for needle pricking OD_{600}= 0.1 for microinjection
Pectinobacterium carotovora 15 (Ecc15)	Gram-negative, DAP-type	LB media, 29 °C	Systemic & Oral	OD_{600}= 1 for needle pricking OD_{600}= 0.1 for microinjection OD_{600}= 200 for oral infection
Salmonella typhimurium	Gram-negative, DAP-type	LB media, 37 °C	Systemic	OD_{600}= 1 for needle pricking OD_{600}= 0.1 for microinjection
Providencia rettgeri	Gram-negative, DAP-type	LB media, 29-37 °C	Systemic	OD_{600}= 1 for needle pricking OD_{600}= 0.1 for microinjection
Pseudomonas entomophila	Gram-negative, DAP-type	LB media, 29 °C	Systemic & Oral	OD_{600}= 1 for needle pricking OD_{600}= 0.1 for microinjection OD_{600}= 200 for oral infection
Micrococcus luteus	Gram-positive, Lys-type	LB media, 29-37 °C	Systemic	OD_{600}= 100 for needle pricking OD_{600}= 0.1 for microinjection
Bacillus subtilis	Gram-positive, DAP-type	LB media, 37 °C	Systemic	OD_{600}= 1 for needle pricking OD_{600}= 0.1 for microinjection
Listeria monocytogenes	Gram-positive, DAP-type	BHI media, 37 °C	Systemic	OD_{600}= 1 for needle pricking OD_{600}= 0.1 for microinjection
Enterococcus faecalis	Gram-positive, Lys-type	LB media, 29-37 °C	Systemic	OD_{600}= 1 for needle pricking OD_{600}= 0.1 for microinjection
Staphylococcus aureus	Gram-positive, Lys-type	LB media, 29-37 °C	Systemic	OD_{600}= 1 for needle pricking OD_{600}= 0.1 for microinjection
Staphylococcus saprophyticus	Gram-positive, Lys-type	LB media, 37 °C	Systemic	OD_{600}= 1 for needle pricking OD_{600}= 0.1 for microinjection
Fungi	**Growth Conditions**	**Route of Infection**	**Dose**	
Candida albicans	YPG media, 29 °C	Systemic	OD_{600}= 200 for needle pricking	
Beauveria bassiana	Malt agar, 25-29 °C	Cuticle breach (natural infection)	Roll flies in a sporulating plate for ~15 seconds	
Metarhizium anisopliae	Malt agar, 25-29 °C	Cuticle breach (natural infection)	Roll flies in a sporulating plate for ~15 seconds	

Table II.1. Frequently used microbes.
Abbreviations: Luria Bertani (LB), Brain Heart Infusion (BHI), and Yeast Peptone Glucose (YPG).

A. Bacteria

The type of bacterial peptidoglycan (PGN) is one of the most important factors shaping the host response to infection, as Lys-type (Gram-positive) and DAP-type (Gram-negative) PGN bacteria activate both the Toll and Imd pathways to quantitatively different levels (Lemaitre and Hoffmann, 2007; Troha et al., 2018).

1. DAP-type peptidoglycan bacteria

Providencia rettgeri is an opportunistic pathogen of hospitalized patients and a causative agent of traveler's diarrhea (Sagar et al., 2017; Sharma et al., 2017; Yoh et al., 2005). This extracellular, Gram-negative bacterium also infects *Drosophila* in the wild (Corby-Harris et al., 2007; Juneja and Lazzaro, 2009; Galac et al., 2011). *P. rettgeri* activates a robust immune response in flies, as indicated by strong induction of the antimicrobial peptide genes *Diptericin* and *Drosomycin*. Systemic infection with *P. rettgeri* causes ~50% mortality in wildtype flies; half of the subjects die with a high pathogen burden, while the other 50% survive indefinitely with an asymptomatic, low-burden, chronic infection (Galac and Lazzaro, 2011; Duneau et al., 2017b; Troha et al., 2018). This feature of *P. rettgeri* infection provides two advantages. First, the intermediate mortality allows researchers to observe not only host and bacterial mutations that increase susceptibility to infection, but also those that increase host survival. Second, as it establishes a persistent infection in surviving hosts, *P. rettgeri* can also be used to study the biology of chronic infection. The transcriptional profile of adult wildtype flies infected with *P. rettgeri* has been published (Short and Lazzaro, 2013; Troha et al., 2018). Additionally, the *P. rettgeri* genome is fully sequenced, and the data is publicly available (Galac and Lazzaro, 2012; Marquez-Ortiz et al., 2017). *P. rettgeri* is grown as a shaking culture in Luria Bertani (LB) medium at 29 °C. For

faster growth, the bacteria can also be cultured at 37 °C. To infect flies, an overnight culture (~16 h) of 10 mL is pelleted by centrifugation (4 min at 1700 *g*, 4 °C) and resuspended in sterile PBS buffer to reach an OD_{600} = 1 for the needle-prick method or an OD_{600} = 0.1 for the injector protocol (infection techniques are described in detail in subsequent sections of this article). Both approaches result in inoculation with ~3,000 CFU. Fresh cultures should be used for infection whenever possible, as they tend to give more consistent results; however, unpelleted cultures can be kept at 4 °C and used for up to a week if necessary. *P. rettgeri* LB plates can be stored at 4 °C for a month to inoculate liquid cultures. This bacterium is naturally resistant to the antibiotic tetracycline (10 μg/mL of LB media), which can aid to restrict the growth of other bacteria when plating fly homogenates.

Pectinobacterium (previously known as *Erwinia*) *carotovora carotovora* is a Gram-negative, extracellular bacterium employed in the study of both systemic and gut immunity in *Drosophila*. Naturally transmitted by insects, this phytopathogenic organism causes soft rot in fruits (Barras et al., 1994). Strain 15 (*Ecc15*) is genetically tractable and resistant to rifampicin (100 μg/mL of LB media). A spectinomycin-resistant GFP-transformed strain (25 μg/mL of LB media) is available to track the location of bacteria inside the host (Basset et al., 2000). *Ecc15* is also a strong inducer of the immune response (Buchon et al., 2009b; 2013; Troha et al., 2018). Unlike *P. rettgeri*, systemic infection with *Ecc15* causes little mortality (~15%) in healthy wildtype flies, which mostly clear the infection after ~5.5 days. This feature makes *Ecc15* a good choice for a screen of immune-deficient mutant flies (Troha et al., 2018). *Ecc15* is grown in LB broth as a shaking culture at 29 °C; it will not grow at 37 °C. For systemic infection, set up a 10 mL culture following the protocol outlined above for *P. rettgeri*. To orally infect flies, pellet an overnight culture (~16 h) of 500 mL by centrifugation (10 min at 2400 g, 4°C) and resuspend the pellet in

sterile PBS to reach an OD_{600} = 200. Oral infection with *Ecc15* should cause little to no mortality in wildtype flies (Buchon et al., 2009a). The transcriptional profiles of flies infected systemically and orally with *Ecc15* are available online (Buchon et al., 2013; Troha et al., 2018).

For readers especially interested in gut infection models, two other Gram-negative bacteria commonly used in the field are *Pseudomonas entomophila* and *Serratia marcescens*. Ingestion of *P. entomophila* induces irreversible damage in the *Drosophila* gut, killing a majority of hosts. This infection is known to trigger a global translational blockage that impairs both immune and repair mechanisms in the fly gut (Vodovar et al., 2005; Liehl et al., 2006; Chakrabarti et al., 2012; Dutta et al., 2015). *Serratia marcescens* Db11 strain is an entomopathogenic bacterium that opportunistically infects a wide range of hosts, including humans. Following oral infection, this bacterium crosses the gut barrier, resulting in a systemic infection. In this model, flies succumb to infection after only ~6 days (Nehme et al., 2007; Lee et al., 2016).

In terms of intracellular models, *Salmonella typhimurium* and *Francisella tularensis* infections have been characterized in *Drosophila*. Both bacteria are pathogenic to flies (Ayres and Schneider, 2009; Vonkavaara et al., 2008).

2. Lys-type peptidoglycan bacteria

Enterococcus faecalis is a nosocomial, opportunistic human pathogen that also infects flies in the wild (Huycke et al., 1991; Lazzaro et al., 2006). This extracellular, Gram-positive bacterium is a strong inducer of the Toll but not the Imd pathway during systemic challenge. Like *P. rettgeri*, this microbe causes an intermediate mortality (~60%) and leads to a persistent infection in surviving hosts (Troha et al., 2018). An advantage of *E. faecalis* is that transposon insertion mutant libraries are available for screening (Gao et al., 2013; Rigottier-Gois et al., 2011). The

transcriptional profile of flies infected with *E. faecalis* is publicly available, and the bacterium's genome is fully sequenced (Brede et al., 2011; Troha et al., 2018).

One of the most classically used bacteria for the study of innate immunity in the fly is *Micrococcus luteus* (De Gregorio et al., 2001; 2002). Typically found in water, soil, and as part of the normal flora of human skin, this Gram-positive, extracellular bacterium is easily recognizable because of the small size and bright yellow color of the colonies it forms (Kloos and Musselwhite, 1975; Tuleva et al., 2009). *M. luteus* is a strong inducer of the Toll pathway, and it causes almost no lethality (<5%) in flies. Some strains of this bacterium can be cleared by the fly in as little as ~6 h (Troha et al., 2018).

Infections with a few intracellular, Gram-positive bacteria have been characterized in the fly. Both *Listeria monocytogenes* and *Staphylococcus aureus* are pathogenic to flies (Mansfield et al., 2003). *S. aureus* is a particularly good choice to probe the role of melanization and phagocytosis during infection (this bacterium is almost exclusively cleared by phagocytosis and also tends to induce larger melanization spots) (Kocks et al., 2005; Shiratsuchi et al., 2012; Atilano et al., 2011; Ayres and Schneider, 2008; Binggeli et al., 2014; Chung and Kocks, 2011; Nehme et al., 2011).

B. Viruses

Several viruses have been used to study antiviral immunity in *Drosophila*. Some are natural pathogens that infect *Drosophila* in the wild, such as *Drosophila* C virus ((+) ssRNA) and Sigma virus ((-) ssRNA), while others, like Invertebrate iridescent virus-6 (dsDNA), are viruses originally identified in other insects. Several viruses trigger classical immune pathways

in the fly. For example, *Drosophila* X virus induces the Toll pathway, Sindbis virus stimulates the Imd pathway, and *Drosophila* C virus (DCV) activates the JAK/STAT pathway (Avadhanula et al., 2009; Dostert et al., 2005; Zambon et al., 2005). DCV is reported to propagate in various tissues, including the fat body and gut, and it has been implied that Sigma virus infects the glial cells, which may account for the CO_2 sensitivity observed in these flies (Bussereau, 1970a; 1970b; Chow et al., 2017). Sigma virus, Invertebrate iridescent virus-6, and DCV are capable of replication in Schneider 2 (S2) cells. Specific protocols to propagate and isolate these viruses have been described before (Merkling and van Rij, 2015). Of note, virus stocks must always be prepared using cell lines that are free from persistent infection with other viruses. Viral contamination of cell lines can be assessed by RT-qPCR. A comprehensive list of published *Drosophila* viruses can be found in the Obbard lab's website (http://obbard.bio.ed.ac.uk/data.html) (Obbard., 2018).

C. Fungi and yeasts

Beauveria bassiana and *Metarhizium anisopliae* are two naturally occurring entomopathogenic fungi used to probe the response to fungal infection in *Drosophila* (De Gregorio et al., 2001; Lu et al., 2015). When fungal spores come into contact with the body of a fly, they germinate, penetrate the cuticle, and grow inside, killing the host in a matter of days. *B. bassiana* grows on malt agar plates at 25 to 29 °C, preferentially in the dark. Culture plates should be kept dry at all times. If condensation droplets form on the lids of culture plates, either replace the lid with a new, dry lid or wipe the lid dry with a clean paper towel. To induce sporulation, switch culture plates to 29 °C; this process may take up to a month. To check if a plate is sporulating,

gently tap the plate while holding it upside down. A sporulating plate will release dust-like spores, which should now be visible on the lid of the plate. Culture plates can be stored for up to a month at 18 °C. To propagate cultures, flip sporulating plates onto new malt agar plates (Neyen et al., 2014).

Candida albicans, a human pathogen, has also been used to infect *Drosophila* (Davis et al., 2011). A strong inducer of the Toll pathway, this yeast causes mild mortality in adult flies when administered systemically. For readers interested in studying a behavior-manipulating pathogen, the Eisen lab recently discovered a strain of *Entomophthora muscae* capable of such a feat. *E. muscae* is known to invade the nervous system, and flies infected with this fungus display unique behaviors. Hours before their death, the flies climb upward and extend their proboscides, affixing in place. This is followed by a raising of their wings, which clears a path for infectious fungal spores to launch from their abdomens (Elya et al., 2018).

D. Parasites

Parasitoid wasps infect up to 70% of *Drosophila* larvae in the wild (Fleury et al., 2004). These wasps inject eggs into the bodies of fly larvae, which, upon hatching, slowly kill their hosts by feeding on their internal tissues. Some parasitoid wasps, such as *Leptopilina boulardi*, are specific to *Drosophila*, while others, like *Leptopilina heterotoma*, are generalists (Schlenke et al., 2007). Wasps can be propagated in the laboratory using larvae of the permissive *Drosophila yellow white* genotype (grown at 24 °C). On average, new wasps eclose after 25-30 days. Adult wasps can be maintained on a honey diet. For detailed methods on wasp rearing, we refer the reader to the protocols developed by the Govind lab (Small et al., 2012).

E. Immune Elicitors

Infection with live microbes elicits a complex host response, part reaction to the presence of microbe-associated molecular patterns (MAMPs), such as peptidoglycan (PGN), and part response to microbial growth and virulence (Newton and Dixit, 2012). To separate the response to MAMPs from that to live pathogens, purified elicitors or heat-killed microbes can be used. Commonly used elicitors include: DAP-type PGN, TCT (the minimum PGN motif capable of inducing the Imd pathway), Lys-type PGN, β-glucan, and proteases. Purified elicitors are available for purchase from Sigma or InvivoGen. It is important to note that LPS itself does not induce the Imd pathway (which detects the presence of Gram-negative bacteria) in *Drosophila* (Leulier et al., 2003). However, because commercial preparations of LPS are oftentimes contaminated with trace amounts of PGN, LPS has been recorded to induce immune activation on occasion (Kaneko et al., 2004). To heat-kill bacteria for injection, prepare a fresh bacterial solution, adjust it to the desired OD_{600}, and heat the bacteria to 70 °C for 1 h. To confirm that the bacteria are dead, plate 10 µl of this solution on the proper nutrient agar plate and incubate the plate overnight. If successful, no colonies should grow. To kill fungal spores, collect dust-like spores and incubate them in a 1.5 M NaOH solution for 30 min twice at 70 °C. Immediately follow by washing the spores 4 times with PBS 0.01% Tween 20 (Gottar et al., 2006). A fraction of the spores should also be plated on nutrient agar plates to confirm the efficiency of the alkali treatment.

III. Routes of infection

A. Systemic infection

1. Needle pricking

In this method, a 0.1mm stainless steel needle (Fine Science Tools, catalog #26002-10) is dipped into a concentrated bacterial, viral, or fungal spore solution and used to prick previously anesthetized adult flies in the thorax or abdomen (Figure 2A-B). Inoculation into either site results in systemic infection in the fly. Historically, thorax inoculation has been the preferred method to introduce microbes into the insect body cavity. However, compared to abdomen inoculation, inoculation via the thorax leads to higher mortality and bacterial load within the first few days of infection (Chambers et al., 2014). Fly pricking should be gentle; it should breach the cuticle with minimal damage to internal tissues/organs, and the needle must never pierce through the entire fly. Typically, flies recover from this procedure within a few minutes. Infected flies should be laid down on the side of a new media tube while they recover from anesthesia to prevent them from sticking to the food. A dark spot, corresponding to the activation of the melanization cascade, will appear at the site of injury in a matter of hours. The presence of this spot can be used to ensure that the flies have been infected. To avoid scoring lethally injured flies (i.e., flies dying from lethal wounding as opposed to infection), dead subjects should be counted ~2 h after inoculation and excluded from further analysis (Khalil et al., 2015). Needle pricking is a fast and efficient method that allows for large numbers of flies to be tested in a short period of time (>250 adult flies can be infected per hour). The disadvantage is that dosing cannot be precisely controlled. Following the procedure, subjects should be transferred to the appropriate temperature for experimentation.

For larval infections, wash larvae in sterile PBS buffer and place them in a small drop of PBS on a pre-chilled rubber pad (the cold temperature helps to immobilize them). Prick larvae on their posterior lateral side using a very fine tungsten needle as described here (Kenmoku et al., 2017). After, transfer larvae to petri dishes containing apple juice agar or normal fly medium (Neyen et al., 2014).

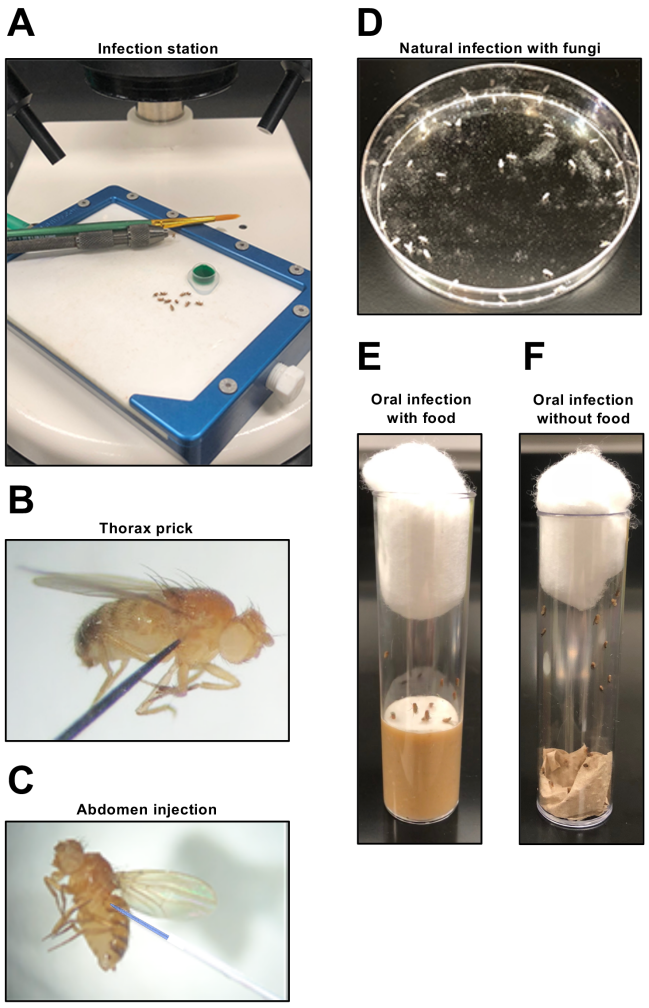

Figure II.2. *Drosophila* infection techniques.
(A) Infection station setup. (B) Anesthetized fly pricked in the thorax with a stainless-steel needle. (C) Fly injected in the abdomen with a defined volume using a microinjector. Two methods are available for oral infection. (D) In the first, previously starved flies are orally infected using a pre-cut Whatman Filter Paper disk soaked in a bacterial solution. The paper disk sits atop food in a fly vial. This placement ensures that the flies receive the inoculum as well as nutrients, which are

absorbed through the filter. (E) The second protocol places flies in a vial devoid of food, where they feed on a small piece of a Tork napkin that has been soaked in a bacterial solution. The availability of a nutrient source beyond the bacterial solution distinguishes the two methods. (F) Flies coated in fungal spores during natural infection.

2. Microinjection

When inoculation with exact doses of microbes or immune elicitors is required, injection of a defined volume using a microinjector (Drummond, catalog #3-000-204) is the preferred method (Figure 2C). An injection volume of ~23 nL is recommended for both thorax and abdomen injections (Khalil et al., 2015). Disadvantages of this method include: slower speed compared to needle pricking and heavy injector equipment.

3. Natural infection with fungi

While injection of fungal spores is a reliable method to challenge flies, natural infection is the preferred method to achieve systemic infection with fungi. In this method, CO_2-anaestethized flies are placed directly on the sporulating lawn of a fungal culture plate, and the plate is shaken for ~15 seconds to coat the flies in spores (Figure 2D). Flies are then transferred to a new, clean food vial to recover. Larvae can also be rolled on sporulating plates for infection. Flies and larvae will become infected as the spores germinate and breach the cuticle. A sporulating plate can be reused for multiple infections (Tzou et al., 2002).

4. Sexual transmission

Although not commonly used, sexual transmission is a viable method to establish systemic infection in the fly. Briefly, male flies are anesthetized and laid ventral side up on the fly pad. Next, a pipette is used to place a large drop of a bacterial solution directly on the male genitalia,

covering it fully. After treatment, each male is placed in a sterile food vial with a single virgin female to recover and mate. This arrangement leaves little, if no time for males to groom themselves before mating (Gendrin et al., 2009; Miest and Bloch-Qazi, 2008).

B. Oral infection

Three model pathogens are commonly used to study the response to oral infection in the fly gut: *Ecc15*, *P. entomophila*, and *S. marcescens* Db11 (a description of these pathogens is provided in the section of the article dealing with bacteria). To orally infect flies, five- to eight-day-old adult flies are starved in empty vials for 2 h at 29 °C. This starvation treatment ensures that all flies are receptive to consuming a large amount of the oral inoculum. Next, the flies are transferred to infection vials and returned to 29 °C, the optimal infection temperature for traditional *Drosophila* gut pathogens. Flies are left to feed on the infection vials for 4 to 12 h, after which they are transferred to fresh food vials (Figure 2E-F). Infection vials should be prepared fresh while the flies undergo starvation. To prepare an infection vial, take a standard food vial and cover the media fully using a pre-cut Whatman Filter Paper disk. No traces of food should be visible above the paper disk. This guarantees that the flies will only feed on the bacterial solution provided. Next, pipette 150 µl of either the control solution (5% sucrose) or the control solution mixed in a 1:1 ratio with the concentrated bacterial suspension (combine 75 µl of 5% sucrose with 75 µl of concentrated bacteria at OD_{600} = 200) onto the paper disk, making sure that the disk is completely and evenly covered by this mixture. Let the vials settle for ~15 min to allow for the entire solution to be absorbed into the filter disk before starting the infections. It is important that the surface of the media tubes used for infection be somewhat dry. If the vials are damp, the paper disks will become saturated before the addition of the infection solution. As a result, the inoculum will not

be absorbed, and the flies will drown in these wet vials. This protocol can also be used to introduce viruses and fungi into the fly gut (Figure 2E). An alternative infection method places the flies in vials containing only a pile of folded papers (Tork) or cotton balls soaked in 2.5 mL of a concentrated bacterial solution (Figure 2F) (Houtz and Buchon, 2014; Nehme et al., 2007). Unlike the former, this latter method does not provide access to nutrients (from the regular food source), thereby altering host physiology and susceptibility to infection.

To orally infect larvae, place larvae in an Eppendorf tube containing 400 µl of crushed banana mixed with 200 µl of control solution (1X PBS, sterile) or with 200 µl of a concentrated bacterial suspension (the OD_{600} used should be 3X the final desired OD_{600}, e.g., use 200 µl of an OD_{600} = 300 solution to achieve a terminal OD_{600}= 100 for infection). After adding the larvae, cap the tube with a foam plug and gently flick it to mix the contents. Let larvae feed on the bacteria for ~30 min at 29 °C, then transfer them to fresh food vials by inverting the contents of the Eppendorf into the new vial. Optional: Ingestion of bacteria can be stopped immediately by washing infected larvae with 1X PBS, but the extra handling might kill additional larvae (Neyen et al., 2014).

C. Wasp infection

For wasp infection, place 6 female wasps in a 35-mm petri dish filled with 2 mL of fly food and ~50 fly larvae for 2 h. Parasitized larvae are kept at 25 °C. Capsules can be dissected 4 to 6 days after infection (Small et al., 2012).

D. Generation of germ-free flies

Although flies feed on microbes and live in microbe-rich settings, the *Drosophila* gut lumen is an environment with relatively low bacterial diversity and bacterial numbers. Typically,

only ~100 CFU/fly are found, with *Acetobacter* and *Lactobacillus* spp. comprising the majority of the associated species (Blum et al., 2013; Wong et al., 2011). The production of germ-free flies has allowed for the study of the effects of gut microbes on fly physiology.

Generation of germ-free flies begins with the collection of large numbers of fly eggs. A sizable number is required because many eggs will not survive the chemical treatment applied. Collected eggs (exclude larvae) are placed in a mesh sieve (Genesee Scientific, catalog #46-102 for the mesh basket and FlyStuff.com, catalog #57-102 for the 120 μm nitex nylon mesh). To surface sterilize the eggs, dip the mesh basket in a beaker of 70% ethanol for 2 min. Next, immerse the mesh basket in a separate beaker containing a 10% bleach solution for 10 min (longer treatments up to 30 min are possible, but they will result in increased mortality). The bleach treatment serves to dechorionate the eggs. This is followed by rinsing the eggs in sterile water 3 times to remove any residual bleach (dip the mesh basket in 3 separate beakers with H_2O). Using a sterile pipette tip, transfer the eggs in a small amount of 70% ethanol to pre-autoclaved media vials and allow them to develop (Koyle et al., 2016; Broderick et al., 2014). This procedure should be performed using sterile technique in a laminar flow hood. Bacterial sterilization can be confirmed by performing 16S PCR on the resulting flies or by plating a homogenate of the same flies on De Man, Rogosa and Sharpe (MRS) media.

To clear *Drosophila* lines of the endosymbiont Wolbachia, flies are treated with the antibiotic tetracycline (0.05 mg/mL) for two generations, as previously described (Teixeira et al., 2008). Additionally, several viral infections can be eliminated using the protocols referenced here (Brun and Plus, 1980; Teixeira et al., 2008).

IV. Tools and assays to evaluate the response to infection

Over the past decade, it has become increasingly evident that a successful response to infection requires a combinatorial approach, involving both resistance mechanisms, which target the pathogen for elimination, and tolerance responses, which induce tissue-protective programs (Ayres and Schneider, 2012). Disease tolerance mechanisms involve many different biological processes, from metabolic adaptation and stress responses to tissue repair (Soares et al., 2014; Troha et al., 2018; Weis et al., 2017). In light of this, this section outlines methods to score both resistance and tolerance responses to infection.

A. Tools

1. Frequently used *Drosophila* lines

Commonly used fly stocks can be requested directly from laboratories or purchased from the principal *Drosophila* stock centers:

Bloomington *Drosophila* Stock Center	https://bdsc.indiana.edu
Vienna *Drosophila* Resource Center	https://stockcenter.vdrc.at
Kyoto Stock Center	https://kyotofly.kit.jp
The Exelixis Collection at the Harvard Medical School	https://drosophila.med.harvard.edu

Toll and Imd are the canonical immune signaling pathways in *Drosophila*, responsible for the production of antimicrobial peptides (AMPs) (De Gregorio et al., 2002; Lemaitre and Hoffmann, 2007). Several mutants, RNAi lines, and overexpression stocks of key component

genes of both pathways are publicly available (see Table 2). Among many non-immune functions, Toll signaling plays a critical role during embryonic development; therefore, many Toll-deficient mutants exhibit some degree of lethality during the embryonic stage (Anderson et al., 1985). Nevertheless, viable mutants, such as *spz*^{rm7}, are amenable to experimentation (Michel et al., 2001). To activate the pathway in the absence of infection, recent studies have favored the use of gain-of-function mutations, such as *UAS-Toll*^{10B} or *UAS-spz** (Buchon et al., 2009c; DiAngelo et al., 2009). The current model of Toll pathway activation has three distinct upstream signaling cascades controlling the activation of Spz. Two of these cascades are initiated upon detection of Lys-type peptidoglycan by PGRP-SA and β-glucan by GNBP3, leading to the activation of ModSP, a modular serine protease that integrates signals from these sensors to activate Spz (Buchon et al., 2009). A third cascade is mediated by the protease Psh, which senses virulence factors as well as damage-associated molecular patterns (DAMPs) (Valanne et al., 2011). Mutants of all these genes are available, allowing for genetic dissection of the three branches controlling Toll activation. For the Imd pathway, the mutant *Rel*^{E20} exhibits complete abrogation of antimicrobial peptide induction, making it one of the best options available (Hedengren et al., 1999). Other mutants, such as the hypomorph *imd*^{1}, are suitable alternatives (Lemaitre et al., 1995). The best way to induce the Imd pathway artificially is to overexpress *imd* (Georgel et al., 2001).

Plasmatocytes are the primary phagocytic cells in *Drosophila*, and it is possible to generate viable flies that lack all phagocytes, named phagoless (Defaye et al., 2009). To generate these flies, *Hml-Gal4*, a hemocyte-specific driver, is crossed to *UAS-Bax*, which encodes a pro-apoptotic factor. Additionally, many mutants that affect phagocytosis, such as the CD36 homologue *crq*, have been described before (Guillou et al., 2016). To study melanization, a *PPO1*,

PPO2 double mutant, which lacks complete PO activity in the hemolymph, is available (Binggeli et al., 2014). In addition to the mutants described here, RNAi lines present a suitable alternative to target these genes. All mutants, overexpression, and RNAi lines mentioned in this section are listed in Table 2.

Mutant	Line Description	Recently Used By
PGRP-SA^{seml}	Mutant (Toll pathway)	Michel et al., 2001
GNBP3^{Hades}	Mutant (Toll pathway)	Matskevich et al., 2011
modSP^{1}	Mutant (Toll pathway)	Buchon et al., 2009
psh^{1}	Mutant (Toll pathway)	Gottar et al., 2006
spz^{rm7}	Mutant (Toll pathway)	Buchon et al., 2009
UAS-Toll^{10B}	Expresses a constitutively active form of Toll	DiAngelo et al., 2009
Drs-GFP	Expresses *GFP* under the control of the *Drs* promoter. Toll pathway reporter.	Wu et al., 2015
Drs-lacZ	Expresses *lacZ* under the control of the *Drs* promoter. Toll pathway reporter.	Foley et al., 2003
Rel^{E20}	Mutant (Imd pathway)	Guillou et al., 2016
imd^{1}	Mutant (Imd pathway)	Zerofsky et al., 2005
UAS-imd	Overexpresses *imd*	Georgel et al., 2001
Dpt-GFP	Expresses *GFP* under the control of the *Dpt* promoter. Imd pathway reporter.	Flatt et al., 2009
Dpt-lacZ	Expresses *lacZ* under the control of the *Dpt* promoter. Imd pathway reporter.	Chakrabarti et al., 2012
Dipt-Dpt-HA	Carries the *Dpt* CDS + HA tag under the control of the *Dpt* promoter. Imd pathway reporter.	Chakrabarti et al., 2012
10XStat92-GFP	Expresses *GFP* under the control of the *Stat92E* promoter. JAK/STAT pathway reporter.	Bach et al., 2007
PPO1$^{\Delta}$, *PPO2*$^{\Delta}$	Double mutant (melanization)	Binggeli et al., 2014
crq^{ko}	Mutant (phagocytosis)	Guillou et al., 2016
eater-dsRed	Plasmatocyte marker used to visualize hemocytes	Guillou et al., 2016
eater-nls::*GFP*	Plasmatocyte marker used to visualize hemocytes	Guillou et al., 2016
Hml-Gal4	Hemocyte driver	Guillou et al., 2016
UAS-BAX	Induces apoptosis. Used in combination with *Hml-Gal4* to generate phagoless flies.	Regan et al., 2013

Table II.2 List of frequently used *Drosophila* lines

2. Reporter lines

One of the biggest advantages of working with Drosophila is the availability of large numbers of reporter lines that allow for quick examination of various phenotypes. These reporters place immune-inducible promoter regions upstream of fluorescent proteins, such as GFP, or reporter enzymes, such as lacZ, and they provide a fast alternative to measurements of gene expression. In general, GFP reporters are best suited for qualitative analysis, while lacZ reporters are recommended for quantitative evaluations; lacZ encodes β-galactosidase, an enzyme whose activity can be measured (as described later in this section).

Fluorescent reporters, such as *Drs-GFP* (Toll pathway reporter) or *Dpt-GFP* (measures Imd pathway activity), can be used to assess antimicrobial peptide gene expression in the fly (Ferrandon et al., 1998; Vodovar et al., 2005). Similarly, in the gut, the reporters *10XStat92-GFP* and $esg^{F/O}$ (*esg-Gal4, Gal80*^{ts}*, UAS-FLP, act > CD2 > Gal4, UAS-GFP*) can be used to track midgut renewal following enteric infection (Figure 3A) (Buchon et al., 2009a; 2010; Houtz and Buchon, 2014). *10XStat92-GFP* is a reliable indicator of JAK/STAT activity, which is required for gut renewal, and $esg^{F/O}$ is a tracing tool to monitor new epithelial cells generated during tissue repair. Flies or larvae carrying these reporters can be scored visually under a fluorescence dissecting microscope, where not only the presence but also the specific location of fluorescent signal can be deduced. Typically, GFP can be detected in as little as 6 h post treatment; however, the amount of signal at this very early time point will be relatively weak. More time is normally required for a stronger GFP signal.

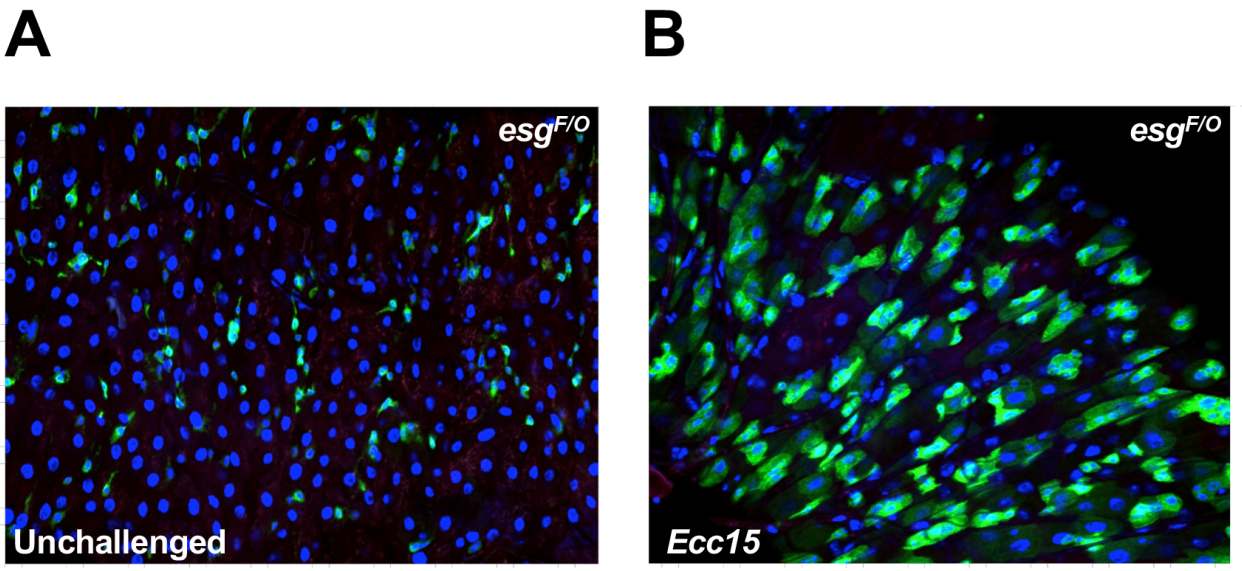

Figure II.3. Tracking midgut renewal following enteric infection
Fluorescent reporter line *esg$^{F/O}$-Gal4>UAS-GFP,* which strongly labels intestinal stem cells, enteroblasts, and newly synthesized enterocytes, can be used to detect midgut renewal following oral infection with a pathogen. (A) Unchallenged adult midgut. (B) Adult midgut after enteric infection with *Ecc15*.

Enzymatic titration of a reporter enzyme, such as β-galactosidase, under the control of a promoter region belonging to a gene of interest is another classical method of assessing gene expression in the fly. *P[lac-Z]* insertion lines are available for a large number of genes at the Bloomington Drosophila Stock Center. To quantify gene expression using the β-galactosidase titration assay, dissected tissues (~20 guts or carcasses) or whole animals (~5 larvae or flies) are homogenized in Eppendorf tubes containing 100 µl of Buffer Z (60mM Na2HPO4, 60mM NaH2PO4, 10mM KCl, 1mM MgSO4, 50mM β-mercaptoethanol, adjusted pH to 8 with NaOH). Samples are then centrifuged for 1 min at 4 °C to pellet any debris. 40 µl of clear supernatant per sample is then loaded onto a 96-well plate. Next, 250 µl of Buffer Z – o-nitrophenol-β-D-galactoside (0.35 mg/mL ONPG in Buffer Z)—preheated to 37 °C before addition—is added to each well. Plates are then incubated in a microplate reader at 37 °C, with measurements taken

every minute at OD_{420} for 1 hr (Broderick et al., 2014; Houtz et al., 2017). Because melanization can interfere with this assay, it is recommended that samples be processed quickly. β-galactosidase activity is typically normalized to the amount of protein present in each sample using the Bradford or BCA assays.

X-gal staining can also be used to evaluate gene expression in P[lac-Z]-expressing flies. In this protocol, tissues are dissected in PBS buffer and fixed in 0.5–1% glutaraldehyde in PBS at 4 °C. The size and thickness of the tissue will dictate the length of fixation. For example, hemocytes can be fixed in as little as ~20 s, while gut tissue requires ~4 min. Tissues are then washed 3X in PBS buffer. Next, fixed tissues are incubated in staining buffer containing X-gal at room temperature or 37 °C. The staining buffer is composed of 150 mM NaCl, 3.5 mM K_3FeCN_6,10 mM NaH_2PO_4/Na_2HPO_4, 1 mM $MgCl_2$, and 3.5 mM K_4FeCN_6. NaOH is used to adjust the pH to 7.2. X-gal stock is prepared as a 5% solution in dimethylformamide, and it is stored at −20 °C. Prior to staining, 20 µl of 5% X-gal stock is added to each milliliter of staining buffer to be used. Incubation length is dependent on the amount of enzyme expressed (Neyen et al., 2014).

3. Online resources

Microarray and RNA-seq studies have resulted in the creation of online databases that allow users to look up the expression value of any gene in response to both oral and systemic infection. FlySick-seq (http://flysick.buchonlab.com) is an interactive databank that provides gene expression data for every gene following systemic infection with 10 distinct bacterial pathogens (Troha et al., 2018). Flygut (http://flygut.epfl.ch) hosts an atlas of the *Drosophila* midgut, including an exhaustive description of the different regions of the gut and microarray data of flies orally infected with the pathogens *Ecc15* and *P. entomophila* (Buchon et al., 2013). Flygut-seq

(http://flygutseq.buchonlab.com) provides cell- and region-specific transcriptomic data of the fly midgut, including cell-specific expression values under infection conditions (Dutta et al., 2015). The Lemaitre lab's website (http://lemaitrelab.epfl.ch/resources) also offers an assortment of microarray data profiling the host response to tracheal, systemic, and intestinal infection. Of particular interest, this resource includes expression data from *spz* and *rel* mutant flies, which can help to ascertain whether an immune gene is regulated in a Toll- or Imd-specific manner (De Gregorio et al., 2002). Finally, the *Drosophila* Interactions Database (DroID) is a comprehensive gene and protein interactions database that includes protein-protein, transcription factor-gene, miRNA-gene, and genetic interactions (http://www.droidb.org).

4. Methods to identify novel genes involved in the response to infection

Although ethyl methanesulfonate (EMS) treatment was the standard approach for mutagenesis during the era of forward genetic screens in *Drosophila*, the advent of large collections of efficient RNAi lines has propelled a shift toward RNAi-based screens. Both *in vivo* and *in vitro*, RNAi screens have successfully identified novel components of immune responsive pathways, as well as other key regulators of the host response to infection (Echeverri and Perrimon, 2006; Kambris et al., 2006). Targeted expression of RNAi constructs using the Gal4/UAS system can be used for tissue- or –cell specific interrogation of gene function. Coupled with a thermosensitive version of the Gal80 inhibitor ($Gal80^{ts}$), this technique can be used to block gene expression in a time-controlled manner, preventing developmental effects (McGuire et al., 2004). However, the use of RNAi lines is not without its caveats. First, a number of RNAi lines have been shown to exhibit residual gene expression of 25% or more (Heigwer et al., 2018; Perkins et al., 2015). Hence, RNAi is more likely to give rise to hypomorphic phenotypes, which can

conceal the phenotypes of genes that only require a low level of gene expression to execute their function. Second, there is typically no information available on the half-life of the gene product of interest. Therefore, it is possible that targeted protein levels remain stable despite efficient knockdown, thus obscuring a potential phenotype. Lastly, off-target effects could lead to the erroneous attribution of phenotypes to specific genes (Kulkarni et al., 2006; Perrimon and Mathey-Prevot, 2007). Given the aforementioned drawbacks, we recommend verifying the results of RNAi studies through the following methods: using multiple RNAi lines to target the same gene, quantifying the level of knockdown via RT-qPCR or similar method, and testing whether a mutant of the gene of interest (if available) replicates the RNAi phenotype observed.

Another approach to identify original genes involves the use of the *Drosophila* Genetic Reference Panel (DGRP) (Mackay et al., 2012). The DGRP consists of >200 fully sequenced lines that have been inbred to homozygosity. These stocks have facilitated an expansion of genome-wide association studies (GWAS). DGRP-based screens can identify genetic polymorphisms associated with differences in the host response to infection (Howick and Lazzaro, 2017; Wang et al., 2017). Moreover, this approach has the advantage that it can detect variants not only in protein-coding genes, but also in the regulatory regions that coordinate expression of immune-related genes.

5. Generation of immune-deficient mutants

CRISPR/Cas9 is quickly becoming the most efficient method to engineer the genome of many organisms, including *Drosophila*. Several CRISPR/Cas9-derived knock-out mutants already exist, and the protocols used to generate them have been described extensively (Bassett and Liu, 2014; Bassett et al., 2014; Gratz et al., 2015). Transposon mutagenesis represents another approach

to edit the genome. Newer generations of engineered transposable elements, such as the *Minos*–mediated integration cassette (MiMIC), have vastly expanded the capabilities of this tool. MiMIC, which integrates into the genome almost at random, carries a gene-trap cassette flanked by two inverted ΦC31 integrase *attP* sites. The *attP* sites allow for the replacement of the intervening sequence of the transposon with any other sequence through recombinase-mediated cassette exchange (Venken et al., 2011). In combination, these two features allow for virtually limitless gene modifications. A large collection of MiMIC lines is available at the Bloomington *Drosophila* Stock Center.

When loss of gene expression results in tissue or cell death, clonal analysis can be used to study the cell-autonomous function of a gene. For more information on both MARCM and twin-spot clonal analysis protocols, the reader is referred to the following studies (Wu and Luo, 2006; Griffin et al., 2009).

B. Assays

1. Survival

Survival or death is the terminal outcome of infection. Therefore, survival analysis provides a comprehensive test to measure differences in the host response to infection. In a survival assay, 20 flies are placed together in a media vial following infection, and the number of dead flies is scored daily (Tzou et al., 2002). Only "healthy-looking" flies (no missing legs and no clipped wings) should be included in the experiment. Any subjects that die within the first 2 h following infection should be counted and excluded from further analysis, as these flies are dying from excessive injury rather than infection. A minimum of three biological replicates is required. It is

important to transfer the flies to new vials every ~3 days. In the case of females, this is done because the food becomes gooey as their eggs develop, which can trap and kill flies. Since a shiny, pinkish film, which signals microbial contamination, tends to develop on the surface of food vials with no larvae to churn the food (after a few days), it is recommended that male flies be flipped periodically into new tubes. The length of a survival assay depends mostly on how fast the pathogen can kill its host. For example, the fraction of subjects that succumb to *P. rettgeri* infection do so within the first 3 days following challenge. Therefore, survival is typically recorded over a period of no more than 7 days for this infection. Similarly, a pathogen that takes longer to kill flies will require a lengthier scoring window. If working with mutants, it is imperative to use a reference strain that matches the mutant background, as divergent wildtype lines (e.g., $Canton^{s}$ vs. w^{1118}) can display vastly different susceptibilities to the same pathogen (Eleftherianos et al., 2014).

2. Quantification of microbial load

There are many techniques, both quantitative and qualitative, to measure microbial load following infection (Figure 4A). Below, we describe 3 distinct approaches.

Counting the number of Colony Forming Units (CFU) per fly at defined time points post-infection is perhaps the most commonly used method, and it has the advantage of being both quantitative and representative of live bacteria. Briefly, individual flies (or larvae) are deposited into autoclaved Eppendorf tubes containing 500 µL of sterile PBS buffer. Flies are then manually homogenized using a Squisher (Zymo Research, catalog #H1001). If working with a sizeable number of samples, an automated homogenizer that can simultaneously process large batches (MP Biomedicals, catalog #116004500) is recommended. In this case, a single sterile metal bead (Omni International, catalog #19-640) is added to the Eppendorf tube prior to loading the samples into

the machine. Flies should be homogenized to the point where no large body parts are identifiable (Figure 4B). Next, samples are serially diluted in sterile PBS to reach countable dilutions and plated on agar plates of the appropriate media. To plate manually, pipette 50 µL of sample per plate and spread the solution using either sterile glass beads or a glass spreader. Plating can also be done via a semi-automated plater (Microbiology International, catalog #WASP 2). It is recommended that at least 2 separate dilutions be plated the first time an experiment is performed (Figure 4C). On average, bacteria remain viable in PBS for up to 2 days at 4 °C; therefore, if the initial dilutions prove to be uncountable once plated, it is possible to go back and re-plate a different dilution. Dilution factors will vary depending on the initial dose administered, the capacity of the microbe to grow within the host, the ability of the host to eliminate the microorganism, and the sampling time point. CFUs can be counted either manually or using an automated plate counter (Microbiology International, catalog #ProtoCOL 3). This protocol can also be used to measure CFUs in specific tissues (with some adjustments to the volume of PBS used per sample). Lastly, bacterial quantification of orally infected flies presents an extra consideration. Because microbial contamination on the fly's appendages could, in principle, obfuscate the results, an additional step must be taken to eliminate surface microbes. Prior to homogenization, flies are quickly dunked in 70% EtOH, rinsed in sterile PBS, and dried by placing them on tissue paper (Neyen et al., 2014).

A second method to measure microbial abundance relies on the use of fluorescently labeled bacteria. For example, the presence or absence of *Ecc15*-GFP can be qualitatively scored visually using a fluorescence dissecting microscope (Figure 4D-E) (Acosta Muniz et al., 2007). Additionally, several research groups have published protocols to quantify microbial genes of in fly extracts using PCR (Dionne et al., 2006; Dostálová et al., 2017).

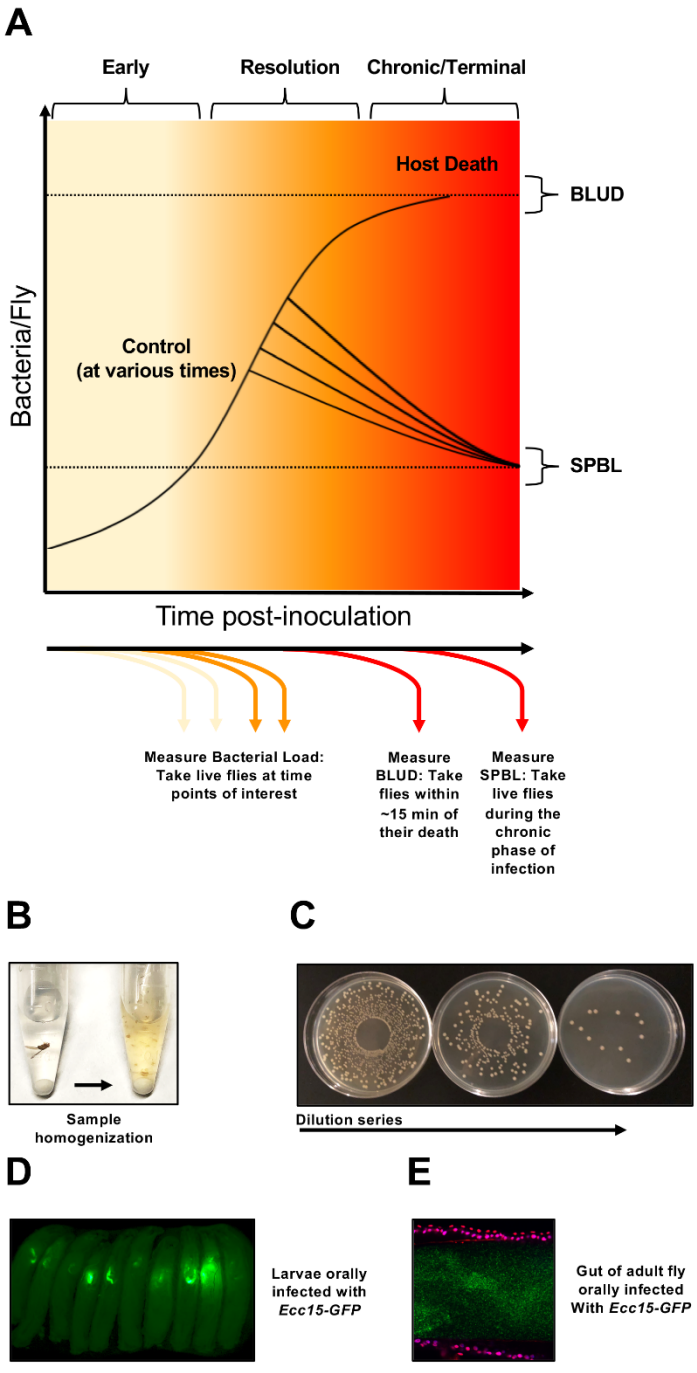

Figure II.4. Qualitative and quantitative methods of pathogen detection

(A) Schematic representation of a model for bacterial growth within the host during the course of a chronic infection. During the early phase of infection, which precedes effective control by the immune system, bacteria grow exponentially inside the host. This is followed by the second stage of infection, called resolution, in which some of the hosts start to control bacterial proliferation, lowering their total CFU (colony forming units). Hosts that fail to control their pathogen load early on enter the terminal phase of infection, where bacteria continue to divide until reaching a load that cannot be sustained by the host. Upon reaching this load, termed the Bacterial Load Upon Death or *BLUD,* the host dies. Hosts that survive the infection by controlling their bacterial burden enter the chronic phase of infection, where they sustain a persistent pathogen load called the Set-Point Bacterial Load (*SPBL*). To measure bacterial load, live flies can be sampled at points of interest during both the early and resolution phases of infection. To measure the *BLUD*, dead flies are collected within 15 minutes of their death. To quantify the *SPBL*, live flies should be sampled during the chronic phase of infection (approximately 5 days after infection is a good starting point for bacteria such as *P. rettgeri* and *E. faecalis*). (B) To quantify bacteria, individual flies are placed in single Eppendorf tubes containing 500 µl of sterile PBS buffer and a metal bead. The sample is then homogenized. (C) Following homogenization, samples are plated using the appropriate agar media. We advise that at least 2 dilutions of each sample are plated the first time an experiment is conducted so as to ensure that individual colonies are visible and therefore countable. (D) *Drosophila* larvae orally infected with *Ecc15-GFP*, which is visible in the gut of the larvae. (E) Gut of an adult fly orally infected with *Ecc15-GFP*.

3. *BLUD*

The Bacterial Load Upon Death (*BLUD*) represents the maximal quantity of bacteria that a fly can sustain while alive. Every bacterium has an associated *BLUD* for a given fly genotype, and *BLUD* values differ across bacteria. *BLUD* can be used as a measure of disease tolerance (the ability of the host to withstand infection) (Duneau et al., 2017b; Troha et al., 2018). In a *BLUD* assay, flies are collected within 15 min of their death, and CFU counting is used to determine the number of bacteria in each individual fly. For the purpose of this assay, flies that fall on their side and are unable to stand up again are considered dead (Figure 4A).

4. *SPBL*

Stereotypically, flies that survive bacterial infection rarely clear their infectious microbes. Instead, they often develop a chronic infection characterized by a persistent, low-level pathogen burden termed the Set-Point Bacterial Load (*SPBL*). The *SPBL* varies with both host and pathogen genotype (Duneau et al., 2017b). To quantify the *SPBL*, collect live flies during the chronic phase of infection (approximately 7 days after infection is a good starting point for bacteria such as *P. rettgeri* and *E. faecalis*) and process them as described earlier to count CFUs (Figure 4A).

5. mRNA quantification

Assessment of endogenous RNA transcript levels is fundamental for understanding transcriptional regulation and monitor the level of activation of immune pathways. It is also important for independent confirmation of data generated using techniques such as RNAi

knockdown or RNA-seq. RT-qPCR is an accurate, sensitive, and quantitative method to measure gene expression in the fly. Trizol extraction from a single fly can yield sufficient, albeit very low, levels of RNA for RT-qPCR. For convenience, most laboratories prefer to pool large numbers of larvae or adults per sample. Typically, 10 to 20 larvae or adult flies are combined for RNA extraction. If performing RT-qPCR on individual tissues, the number of necessary subjects will vary depending on the size of the tissue. For instance, while ~15 to 20 guts or fat bodies will produce an adequate amount of RNA, harvesting RNA from Malpighian tubules requires dissection of over 50 subjects. Of note, while column extraction often gives cleaner RNA compared to the Trizol method, it also yields considerably less RNA than Trizol extraction. For this reason, it is recommended that single fly and pooled tissue extraction be done via the Trizol protocol (Khalil et al., 2015).

FlyPrimerBank (http://www.flyrnai.org/flyprimerbank) is a searchable database that provides a list of pre-designed qPCR primer pairs for each *Drosophila* gene (Hu et al., 2013). When validating RNAi knockdown, it is important to avoid amplifying the reagent itself. Instead, qPCR analysis should be performed on a different section of the transcript. One of the advantages of using FlyPrimerBank is that it includes the predicted overlap of each amplified sequence with RNAi constructs from various public resources (DRSC, VDRC, TRiP, and NIG-Japan collections). In *Drosophila*, *RpL32* is the choice reference gene for normalization of RT-qPCR data (Neyen et al., 2014). A list of popular immune reporter genes (including qPCR primer pairs for their amplification) is available in Table 3.

Gene Name	Forward Primer	Reverse Primer	Pathway
RpL32	GACGCTTCAAGGGACAGTATCTG	AAACGCGGTTCTGCATGAG	Reference gene
Drs	CGTGAGAACCTTTTCCAATATGATG	TCCCAGGACCACCAGCAT	Toll pathway (Antimicrobial peptide)
IM2	ACCGTCTTTGTGTTCGGTCT	TGCAGTCCCCGTTGATTACC	Toll pathway (Antimicrobial peptide, Bomanin)
CG15067	GAGCCTGACGTTATTGGCG	CCTTTTCCACTTGTTGGCTTGT	Toll pathway (Antimicrobial peptide, Bomanin)
Mtk	AACTTAATCTTGGAGCGA	CGGTCTTGGTTGGTTAG	Toll pathway (Antimicrobial peptide)
Dpt	GCTGCGCAATCGCTTCTACT	TGGTGGAGTGGGCTTCATG	Imd pathway (Antimicrobial peptide)
AttA	CCCGGAGTGAAGGATG	GTTGCTGTGCGTCAAG	Imd pathway (Antimicrobial peptide)
CecA1	GAACTTCTACAACATCTTCGT	TCCCAGTCCCTGGATT	Imd pathway (Antimicrobial peptide)
vir-1	GATCCCAATTTTCCCATCAA	GATTACAGCTGGGTGCACAA	JAK/STAT
upd3	GCGGGGAGGATGTACC	GTCTTCATGGAATGAGCC	JAK/STAT
TotA	CCCAGTTTGACCCCTGAG	GCCCTTCACACCTGGAGA	JAK/STAT
TotM	TCGACAGCCTGGTCACTTTC	ACCAAGACCACACGAGCATT	JAK/STAT
Socs36E	GCACAGAAGGCAGACC	ACGTAGGAGACCCGTAT	JAK/STAT
puc	TGGCTCTGTTCAAGCG	CCTTATCTCAGTCCCTCG	JNK

Table II.3. List of commonly used primers

An important consideration when measuring gene expression is circadian control of the immune system. It has been previously reported that immune genes display circadian rhythmicity, and differences in the time of day at infection significantly change survival outcomes in the fly (Lee and Edery, 2008; McDonald and Rosbash, 2001). For these reasons, it is recommended that experimental flies be kept under a strict 12 h light: 12 h dark cycle, and that infections be performed at the same time of day, whenever possible.

Although measuring mRNA provides an accurate representation of the transcriptional response in the fly, it does not offer much information on the availability of the encoded proteins. Recent studies have shown that translational inhibition is a property of some infections (Chakrabarti et al., 2012; Fontana et al., 2011). Therefore, it is strongly recommended that, whenever possible, protein levels also be measured in parallel. This can be done indirectly through *enzymatic titration of a reporter enzyme* (*Drs-lacZ* for the Toll pathway and *Dpt-lacZ* for the Imd pathway) or directly via Western blotting using antibodies against the same antimicrobial peptides or against HA tags present in reporter lines such as *Dipt-Dpt-HA* (Foley and O'Farrell, 2003; Chakrabarti et al., 2012).

6. Phagocytosis Assays

Plasmatocytes, the most abundant hemocytes in flies, are very proficient phagocytic cells (Lemaitre and Hoffmann, 2007). Many protocols have been developed to both visualize and quantify phagocytosis in adult flies and larvae. These techniques benefit from the use of both fluorescent bacteria and transgenic plasmatocyte reporter lines, such as *Hml-Gal4>UAS-GFP*, *eater-dsRed*, *and eater-nls*::*GFP* (Guillou et al., 2016).

To visualize phagocytosis *in vivo*, flies (or larvae) are injected in the thorax with 69 nL of pHrodo red bacteria (Life Technologies, #P35361) using a microinjector (Drummond, catalog #3-000-204). pHrodo red bacteria are non-fluorescent outside the cell, but fluoresce brightly red in acidic compartments such as maturing phagolysosomes. The fluorescence signal within the abdomen of flies or the body of larvae is then imaged using a fluorescence microscope and quantified using Image J (NIH) (Figure 5A) (Guillou et al., 2016).

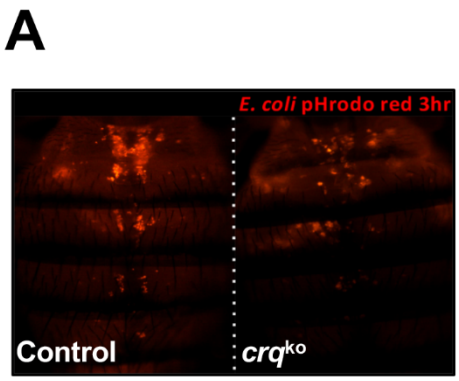

Figure II.5. Tracking phagocytosis *in vivo*

Fluorescent images of the abdomen following injection with pHrodo red-*E. coli*, which allows for visualization of phagocytosis *in vivo*. pHrodo red bacteria are non-fluorescent outside the cell, but fluoresce brightly red once inside phagosomes. (A) Abdomen of wildtype fly and abdomen of phagocytosis-deficient *crq* mutant fly.

For *ex vivo* imaging of adults, reporter flies (e.g., *eater-dsRed*) are injected with 46 nL of PBS following infection with fluorescent bacteria (e.g., GFP-labelled bacteria to contrast with the dsRed reporter) to loosen the hemocytes. Next, the abdomens of ~10 flies are torn open with tweezers and mechanically scraped so as to release all hemocytes onto a drop of sterile PBS on a lysine-coated slide (the poly-L-lysine coat promotes adhesion). Hemocytes are then quickly dried and mounted using Citifluor AF1 Mountant Solution (Electron Microscopy Sciences, catalog #17970-100). Slides are scanned using a confocal microscope, and the number of plasmatocytes as well as the average fluorescence signal per plasmatocyte is quantified (Guillou et al., 2016). This protocol is compatible with larval samples.

A different method for larval *ex vivo* studies involves collecting hemocytes, incubating them with fluorescent heat-killed bacteria, and then running the sample on a flow cytometer, which will both quantify the fraction of cells that phagocytosed bacteria and measure the intensity of the phagocytic uptake (Kurucz et al., 2007). Prior to bleeding, L3 larvae should be washed in PBS buffer to remove any remaining food. Larvae are then placed in a small drop of PBS on a pre-

chilled rubber pad, which helps to immobilize them during the procedure. To bleed larvae, 2 pairs of tweezers are used to tear open chilled larvae on a glass slide containing 120 µL of cold Schneider's *Drosophila* media. The glass slide should be sitting atop a chilled block so the cells remain cold. Next, 100 µL of the media containing the plasmatocytes is transferred to a low binding 96-well plate (Corning, catalog #3474) and incubated for 10 min at room temperature. *E. coli* or *S. aureus* Alexa Fluor 488 conjugate bacteria is then added, using doses ranging from 10^6 to 10^8 bacteria (Molecular Probes, catalog #E13231). Plasmatocytes and bacteria are gently mixed by pipetting, and the cells are incubated together for 20 min at room temperature to allow for phagocytosis. After, 50 µL of 0.4% Trypan blue (Sigma, catalog #T8154-20ML) is introduced to the wells to quench the fluorescence of extracellular bacteria. The sample is then immediately run on a flow cytometer, and the mean fluorescence intensity of the cell population is measured relative to a control sample that lacks fluorescent bacteria. The percentage of cells that have taken up bacteria is calculated by dividing the number of cells in the fluorescence positive gate by the number of cells in the fluorescence negative gate and then multiplying by 100. The phagocytic index (PI) is computed by dividing the mean fluorescence intensity of bacteria-treated hemocyte samples over the mean fluorescence intensity of bacteria-free control samples. Of note, the number of circulating plasmatocytes in L3 larvae varies substantially by genotype. For instance, bleeding 20 *Oregon*^{R} larvae will result in collection ~5,000 individual plasmatocytes, while 20 w^{1118} larvae will yield ~8,000 cells. Therefore, the number of larvae bled for experimentation should be adjusted to compensate for any genotypic differences (Neyen et al., 2014).

Commonly used phagocytosis mutants are listed in Table 2. Phagocytosis can also be inhibited by injecting polystyrene beads into the hemocoel (Elrod-Erickson et al., 2000).

7. Melanization Assays

Melanization is an immediate immune response in *Drosophila*, which results in the synthesis and deposition of melanin as well as oxidative byproducts, which are microbicidal. This reaction requires enzymatic cleavage of prophenoloxidase (PPO) into its active form phenoloxidase (PO). Once activated, this enzyme catalyzes the oxidation of monophenols and diphenols to orthoquinones, which polymerize into melanin (Lemaitre and Hoffmann, 2007). Here, we describe commonly used assays to monitor PO activity.

a. Hemolymph collection

Collection of hemolymph is the first step to measure PO activity. To collect hemolymph from adult flies, ~100 anesthetized flies are loaded into a modified spin column (Qiagen, catalog #74104), in which the filter was removed and thoroughly washed with water before use, and 2 metal beads are placed on top of the flies. The purpose of the column is to filter out cell debris. Flies are then centrifuged twice at 5,000 g for 5 minutes at 4 °C. The resultant hemolymph is immediately diluted in a 1:10 ratio using a protease inhibitor cocktail (Sigma, catalog #11697498001, one tablet dissolved in 4 mL of PBS buffer), which prevents proteolytic activation of PO, and kept on ice. Finally, samples are normalized using protein concentration obtained via a Bradford assay or similar method (Park et al., 2014). Pricking adults with a sterile needle before centrifugation can increase hemolymph yield, but it is not necessary. The same procedure can be used for larval hemolymph extraction using ~30 larvae, but pricking the larvae prior to centrifugation may be required. Samples must be kept on ice at all times.

b. DOPA Assay

The DOPA assay is a robust method for quantification of PO activity in the insect hemolymph. In this assay, PO present in the hemolymph catalyzes the conversion of L-DOPA substrate into an orange to red pigment called dopachrome, whose absorbance can be measured at OD_{492}.

Briefly, combine 50 µL of your previously diluted hemolymph sample (5 µL of hemolymph in 45 µL of protease inhibitor cocktail) with 150 μl of a 5 mM $CaCl_2$ solution in a clean Eppendorf tube. Next, add 800 µL of L-DOPA (Sigma, catalog #D9628-5G) reagent to each sample. L-DOPA reagent is prepared by dissolving 0.3944g of L-DOPA in 130 mL of dH_2O using constant (~45 min) mixing. Because L-DOPA is rapidly oxidized by air and darkens upon exposure to air and light, the reagent should be prepared fresh each time. Following thorough mixing, load 200 μl of sample/well in triplicate into a 96-well plate. Using a spectrophotometer set to 29 °C, perform a kinetic assay at OD_{492}. The intensity of the color observed will depend on the initial amount of cleaved PO in the sample. Due to the presence of protease inhibitors in the wells, the data from this assay conveys PO activity at the time of collection. To quantify both PPO and PO activity, protease inhibitors are replaced by chymotrypsin, which enables the cleavage of PPO into PO (Neyen et al., 2014).

Frequently used melanization mutants, which can be used as negative controls for this assay, can be found in Table 2.

c. PPO cleavage test

PPO1 and PPO2 both contribute to PO activity in the hemolymph of *Drosophila*. Performing Western blot analysis on hemolymph extracts using antibodies against PPO1 and PPO2 is another method to evaluate PPO activation (Binggeli et al., 2014). This method allows for

the detection of both naive PPO (75 kDA) and mature PO (70 kDA) in samples following microbial challenge. The assay can be performed on both larval and adult extracts.

d. Imaging of crystal cells

Crystal cells are larval hemocytes involved in the melanization process; they are responsible for the synthesis and release of PPOs (Lemaitre and Hoffmann, 2007). Visualization of crystal cells is relatively easy. The cells can be observed using transgenic reporter lines, such as *lz-Gal4>UAS-GFP* (*lz-Gal4* is a crystal cell-specific driver), or by heating larvae for 10 min at 70 °C in a water bath. The latter treatment induces a blackening of crystal cells, making them easily visible through the cuticle (Neyen et al., 2014).

e. Scoring melanization spots

The simplest qualitative test to evaluate melanization in flies involves pricking flies in the thorax with a needle, similar to how systemic infection is performed. A black spot, corresponding to the activation of the melanization cascade, will appear at the site of wounding as early as 30 min post-injury. However, the final size and coloring of the spot will not be apparent for 4 h. The characteristics (hue and dimensions) of the melanization dot can be recorded using a camera attached to a microscope. Of note, if scoring melanization spots following microbial challenge, careful consideration should be paid to the infecting agent, as infection with distinct bacterial species gives rise to different wound site melanization responses. For example, inoculation with *S. aureus* tends to produce a larger melanization dot (Ayres and Schneider, 2008; Neyen et al., 2014). Melanization spots can also be observed in larvae following needle pricking, with the first signs of a spot appearing in as little as ~5 min post-injury. Typically, the size and color of the dot

is fully developed after 1 h, at which point it can be recorded by a camera (Dudzic et al., 2015). Finally, because the melanization response can vary substantially between subjects, it is crucial to repeat this experiment several times to have an accurate representation of the reaction.

8. Quantification of ROS production

Several methods to measure ROS production have been developed over the past few years. Below, we describe three commonly used methods. Of note, when quantifying ROS production in gut tissue, the addition of live yeast to the diet of experimental stocks should be controlled because their presence can alter basal levels of ROS in the intestine (Neyen et al., 2014).

ROS production in *Drosophila* can be evaluated using 2′,7′-dichlorofluorescein-diacetate (DCFH-DA) to sense H_2O_2, which facilitates detection of ROS levels in gut tissue (Chakrabarti et al., 2012; Wu et al., 2012). Briefly, adult female guts are dissected in a buffer solution containing 20 mM N-ethylmaleimide (Sigma, catalog #E3876). Immediately following dissection, a 100 μM DCF-DA fluorescent dye solution (Invitrogen, catalog #C400) is added to the gut tissue, and the guts are incubated in this dye for 30 min. The tissues are then mounted in 70% glycerol, and the anterior portion of the midguts are imaged. Analysis of DCF-DA fluorescent signal requires excitation at 488 nm and emission at 529 nm using a confocal microscope. To quantify signal intensity, average the signal measured on representative fields in a minimum of 6 guts (using Fiji) (Neyen et al., 2014). With small modifications, similar protocols can be easily adapted for use in any *Drosophila* tissue (Owusu-Ansah et al., 2008).

Another option for ROS quantification in the gut involves the use of R19S, a recently developed HOCl-specific rhodamine-based dye, which is unable to react with various other ROS. A detailed description of this technique was previously published (Lee et al., 2013).

Finally, transgenic flies carrying genetically encoded redox probes to visualize redox differences are also available. Glutathione peroxidases reduce H_2O_2 to water by oxidizing GSH to GSSG. The Dick group has generated transgenic flies carrying redox-sensitive GFPs (roGFPs) targeted to the cytosol or mitochondria that can be used to measure the GSSG/GSH ratio and H_2O_2 levels in various *Drosophila* tissues (Albrecht et al., 2011).

9. Clotting assay

Numerous protocols to evaluate clotting have been developed, including the bead aggregation test and the draw-out assay among others. A thorough methodological guide specific to clotting assays can be found here (Lesch and Ulrich, 2008).

Acknowledgments

We thank J. Rossi, J.J. Hodgson, P. Nagy, A. Bonfini, and B.P. Lazzaro for assistance with manuscript editing, and V. Gupta, P. Nagy, and P. Houtz for contributing images. We also thank all members of the Buchon and Lazzaro labs for helpful suggestions.

REFERENCES

Acosta Muniz, C., Jaillard, D., Lemaitre, B., and Boccard, F. (2007). Erwinia carotovora Evf antagonizes the elimination of bacteria in the gut of Drosophila larvae. Cellular Microbiology *9*, 106–119.

Alarco, A.-M., Marcil, A., Chen, J., Suter, B., Thomas, D., and Whiteway, M. (2004). Immune-deficient Drosophila melanogaster: a model for the innate immune response to human fungal pathogens. J. Immunol. *172*, 5622–5628.

Albrecht, S.C., Barata, A.G., Grosshans, J., Teleman, A.A., and Dick, T.P. (2011). In vivo mapping of hydrogen peroxide and oxidized glutathione reveals chemical and regional specificity of redox homeostasis. Cell Metabolism *14*, 819–829.

Anderson, K.V., Bokla, L., and Nüsslein-Volhard, C. (1985). Establishment of dorsal-ventral polarity in the Drosophila embryo: the induction of polarity by the Toll gene product. Cell *42*, 791–798.

Atilano, M.L., Yates, J., Glittenberg, M., Filipe, S.R., and Ligoxygakis, P. (2011). Wall teichoic acids of Staphylococcus aureus limit recognition by the drosophila peptidoglycan recognition protein-SA to promote pathogenicity. PLoS Pathog. *7*, e1002421.

Avadhanula, V., Weasner, B.P., Hardy, G.G., Kumar, J.P., and Hardy, R.W. (2009). A novel system for the launch of alphavirus RNA synthesis reveals a role for the Imd pathway in arthropod antiviral response. PLoS Pathog. *5*, e1000582.

Ayres, J.S., and Schneider, D.S. (2008). A signaling protease required for melanization in Drosophila affects resistance and tolerance of infections. PLoS Biol. *6*, 2764–2773.

Ayres, J.S., and Schneider, D.S. (2009). The role of anorexia in resistance and tolerance to infections in Drosophila. PLoS Biol. *7*, e1000150.

Ayres, J.S., and Schneider, D.S. (2012). Tolerance of infections. Annu. Rev. Immunol. *30*, 271–294.

Barras, F., van Gijsegem, F., and Chatterjee, A. (1994). EXTRACELLULAR ENZYMES AND PATHOGENESIS OF SO -ROT ERWINIA. Annual Review of Phytopathology *32:201-34*, 1–34.

Basset, A., Khush, R.S., Braun, A., Gardan, L., Boccard, F., Hoffmann, J.A., and Lemaitre, B. (2000). The phytopathogenic bacteria Erwinia carotovora infects Drosophila and activates an immune response. Proc. Natl. Acad. Sci. U.S.a. *97*, 3376–3381.

Bassett, A.R., and Liu, J.-L. (2014). CRISPR/Cas9 and genome editing in Drosophila. J Genet Genomics *41*, 7–19.

Bassett, A.R., Tibbit, C., Ponting, C.P., and Liu, J.-L. (2014). Highly Efficient Targeted Mutagenesis of Drosophila with the CRISPR/Cas9 System. Cell Rep *6*, 1178–1179.

Binggeli, O., Neyen, C., Poidevin, M., and Lemaitre, B. (2014). Prophenoloxidase activation is required for survival to microbial infections in Drosophila. PLoS Pathog. *10*, e1004067.

Blum, J.E., Fischer, C.N., Miles, J., and Handelsman, J. (2013). Frequent replenishment sustains the beneficial microbiome of Drosophila melanogaster. MBio *4*, e00860–13.

Boman, H.G., Nilsson, I., and Rasmuson, B. (1972). Inducible antibacterial defence system in Drosophila. Nature *237*, 232–235.

Brede, D.A., Snipen, L.G., Ussery, D.W., Nederbragt, A.J., and Nes, I.F. (2011). Complete genome sequence of the commensal Enterococcus faecalis 62, isolated from a healthy Norwegian infant. J. Bacteriol. *193*, 2377–2378.

Broderick, N.A., Buchon, N., and Lemaitre, B. (2014). Microbiota-induced changes in drosophila melanogaster host gene expression and gut morphology. MBio *5*, e01117–14.

Brun, G., and Plus, N. (1980). The viruses of *Drosophila* (New York: Academic Press).

Buchon, N., Broderick, N.A., Chakrabarti, S., and Lemaitre, B. (2009a). Invasive and indigenous microbiota impact intestinal stem cell activity through multiple pathways in Drosophila. Genes Dev. *23*, 2333–2344.

Buchon, N., Broderick, N.A., Kuraishi, T., and Lemaitre, B. (2010). Drosophila EGFR pathway coordinates stem cell proliferation and gut remodeling following infection. BMC Biol. *8*, 152.

Buchon, N., Broderick, N.A., Poidevin, M., Pradervand, S., and Lemaitre, B. (2009b). Drosophila intestinal response to bacterial infection: activation of host defense and stem cell proliferation. Cell Host Microbe *5*, 200–211.

Buchon, N., Osman, D., David, F.P.A., Fang, H.Y., Boquete, J.-P., Deplancke, B., and Lemaitre, B. (2013). Morphological and molecular characterization of adult midgut compartmentalization in Drosophila. Cell Rep *3*, 1725–1738.

Buchon, N., Poidevin, M., Kwon, H.-M., Guillou, A., Sottas, V., Lee, B.L., and Lemaitre, B. (2009c). A single modular serine protease integrates signals from pattern-recognition receptors upstream of the Drosophila Toll pathway. Proc. Natl. Acad. Sci. U.S.a. *106*, 12442–12447.

Buchon, N., Silverman, N., and Cherry, S. (2014). Immunity in Drosophila melanogaster--from microbial recognition to whole-organism physiology. Nat. Rev. Immunol. *14*, 796–810.

Bussereau, F. (1970a). [Study of CO2 sensitivity symptom induced by sigma virus in Drosophila. I. Influence of inoculation place on delay of symptom appearance]. Ann Inst Pasteur (Paris) *118*, 367–385.

Bussereau, F. (1970b). [Study of the symptom of CO2 sensitivity induced by sigma virus in Drosophila. II. Comparative course of yield of nervous centers and of some organs after inoculation in the abdomen and thorax]. Ann Inst Pasteur (Paris) *118*, 626–645.

Carpenter, J.A., Obbard, D.J., Maside, X., and Jiggins, F.M. (2007). The recent spread of a vertically transmitted virus through populations of Drosophila melanogaster. Mol. Ecol. *16*, 3947–3954.

Chakrabarti, S., Liehl, P., Buchon, N., and Lemaitre, B. (2012). Infection-induced host translational blockage inhibits immune responses and epithelial renewal in the Drosophila gut. Cell Host Microbe *12*, 60–70.

Chambers, M.C., Jacobson, E., Khalil, S., and Lazzaro, B.P. (2014). Thorax injury lowers resistance to infection in Drosophila melanogaster. Infect. Immun. *82*, 4380–4389.

Chamilos, G., Nobile, C.J., Bruno, V.M., Lewis, R.E., Mitchell, A.P., and Kontoyiannis, D.P. (2009). Candida albicans Cas5, a regulator of cell wall integrity, is required for virulence in murine and toll mutant fly models. J. Infect. Dis. *200*, 152–157.

Chow, J., Márka, Z., Bartos, I., Márka, S., and Kagan, J.C. (2017). Environmental Stress Causes Lethal Neuro-Trauma during Asymptomatic Viral Infections. Cell Host Microbe *22*, 48–60.e5.

Chung, Y.-S.A., and Kocks, C. (2011). Recognition of Pathogenic Microbes by the DrosophilaPhagocytic Pattern Recognition Receptor Eater. J. Biol. Chem. *286*, 26524–26532.

Corby-Harris, V., Pontaroli, A.C., Shimkets, L.J., Bennetzen, J.L., Habel, K.E., and Promislow, D.E.L. (2007). Geographical distribution and diversity of bacteria associated with natural populations of Drosophila melanogaster. Appl. Environ. Microbiol. *73*, 3470–3479.

Cotter, S.C., Simpson, S.J., Raubenheimer, D., and Wilson, K. (2010). Macronutrient balance mediates trade-offs between immune function and life history traits. Functional Ecology *25*, 186–198.

Davis, M.M., Alvarez, F.J., Ryman, K., Holm, Å.A., Ljungdahl, P.O., and Engström, Y. (2011). Wild-type Drosophila melanogaster as a model host to analyze nitrogen source dependent virulence of Candida albicans. PLoS ONE *6*, e27434.

De Gregorio, E., Spellman, P.T., Rubin, G.M., and Lemaitre, B. (2001). Genome-wide analysis of the Drosophila immune response by using oligonucleotide microarrays. Proc. Natl. Acad. Sci. U.S.a. *98*, 12590–12595.

De Gregorio, E., Spellman, P.T., Tzou, P., Rubin, G.M., and Lemaitre, B. (2002). The Toll and Imd pathways are the major regulators of the immune response in Drosophila. Embo J. *21*, 2568–2579.

Defaye, A., Evans, I., Crozatier, M., Wood, W., Lemaitre, B., and Leulier, F. (2009). Genetic ablation of Drosophila phagocytes reveals their contribution to both development and resistance to bacterial infection. J Innate Immun *1*, 322–334.

DiAngelo, J.R., Bland, M.L., Bambina, S., Cherry, S., and Birnbaum, M.J. (2009). The immune response attenuates growth and nutrient storage in Drosophila by reducing insulin signaling. Proc. Natl. Acad. Sci. U.S.a. *106*, 20853–20858.

Dionne, M.S., Pham, L.N., Shirasu-Hiza, M., and Schneider, D.S. (2006). Akt and foxo Dysregulation Contribute to Infection-Induced Wasting in Drosophila. Current Biology *16*, 1977–1985.

Dostálová, A., Rommelaere, S., Poidevin, M., and Lemaitre, B. (2017). Thioester-containing proteins regulate the Toll pathway and play a role in Drosophila defence against microbial pathogens and parasitoid wasps. BMC Biol. *15*, 79.

Dostert, C., Jouanguy, E., Irving, P., Troxler, L., Galiana-Arnoux, D., Hetru, C., Hoffmann, J.A., and Imler, J.-L. (2005). The Jak-STAT signaling pathway is required but not sufficient for the antiviral response of drosophila. Nat. Immunol. *6*, 946–953.

Dudzic, J.P., Kondo, S., Ueda, R., Bergman, C.M., and Lemaitre, B. (2015). Drosophila innate immunity: regional and functional specialization of prophenoloxidases. BMC Biol. *13*, 81.

Duneau, D.F., Kondolf, H.C., Im, J.H., Ortiz, G.A., Chow, C., Fox, M.A., Eugénio, A.T., Revah, J., Buchon, N., and Lazzaro, B.P. (2017a). The Toll pathway underlies host sexual dimorphism in resistance to both Gram-negative and Gram-positive bacteria in mated Drosophila. BMC Biol. *15*, 124.

Duneau, D., Ferdy, J.-B., Revah, J., Kondolf, H., Ortiz, G.A., Lazzaro, B.P., and Buchon, N. (2017b). Stochastic variation in the initial phase of bacterial infection predicts the probability of survival in D. melanogaster. Elife *6*, 245.

Dutta, D., Dobson, A.J., Houtz, P.L., Gläßer, C., Revah, J., Korzelius, J., Patel, P.H., Edgar, B.A., and Buchon, N. (2015). Regional Cell-Specific Transcriptome Mapping Reveals Regulatory Complexity in the Adult Drosophila Midgut. Cell Rep *12*, 346–358.

Echeverri, C.J., and Perrimon, N. (2006). High-throughput RNAi screening in cultured cells: a user's guide. Nat. Rev. Genet. *7*, 373–384.

Eleftherianos, I., More, K., Spivack, S., Paulin, E., Khojandi, A., and Shukla, S. (2014). Nitric oxide levels regulate the immune response of Drosophila melanogaster reference laboratory strains to bacterial infections. Infect. Immun. *82*, 4169–4181.

Elrod-Erickson, M., Mishra, S., and Schneider, D. (2000). Interactions between the cellular and humoral immune responses in Drosophila. Curr. Biol. *10*, 781–784.

Elya, C., Lok, T.C., Spencer, Q.E., McCausland, H., Martinez, C.C., and Eisen, M. (2018). Robust manipulation of the behavior of Drosophila melanogaster by a fungal pathogen in the laboratory. Elife *7*, F463.

Fast, D., Duggal, A., and Foley, E. (2018). Monoassociation with Lactobacillus plantarum Disrupts Intestinal Homeostasis in Adult Drosophila melanogaster. MBio *9*, 603.

Fauvarque, M.-O. (2014). Small flies to tackle big questions: assaying complex bacterial virulence mechanisms using Drosophila melanogaster. Cellular Microbiology *16*, 824–833.

Ferrandon, D., Jung, A.C., Criqui, M., Lemaitre, B., Uttenweiler-Joseph, S., Michaut, L., Reichhart, J., and Hoffmann, J.A. (1998). A drosomycin-GFP reporter transgene reveals a local immune response in Drosophila that is not dependent on the Toll pathway. Embo J. *17*, 1217–1227.

Fleury, F., Ris, N., Allemand, R., Fouillet, P., Carton, Y., and Boulétreau, M. (2004). Ecological and genetic interactions in Drosophila-parasitoids communities: a case study with D. melanogaster, D. simulans and their common Leptopilina parasitoids in south-eastern France. Genetica *120*, 181–194.

Foley, E., and O'Farrell, P.H. (2003). Nitric oxide contributes to induction of innate immune responses to gram-negative bacteria in Drosophila. Genes Dev. *17*, 115–125.

Fontana, M.F., Banga, S., Barry, K.C., Shen, X., Tan, Y., Luo, Z.-Q., and Vance, R.E. (2011). Secreted bacterial effectors that inhibit host protein synthesis are critical for induction of the innate immune response to virulent Legionella pneumophila. PLoS Pathog. *7*, e1001289.

Galac, M.R., and Lazzaro, B.P. (2011). Comparative pathology of bacteria in the genus Providencia to a natural host, Drosophila melanogaster. Microbes and Infection *13*, 673–683.

Galac, M.R., and Lazzaro, B.P. (2012). Comparative genomics of bacteria in the genus Providencia isolated from wild Drosophila melanogaster. BMC Genomics *13*, 612.

Gao, P., Pinkston, K.L., Bourgogne, A., Cruz, M.R., Garsin, D.A., Murray, B.E., and Harvey, B.R. (2013). Library screen identifies Enterococcus faecalis CcpA, the catabolite control protein A, as an effector of Ace, a collagen adhesion protein linked to virulence. J. Bacteriol. *195*, 4761–4768.

Gendrin, M., Welchman, D.P., Poidevin, M., Hervé, M., and Lemaitre, B. (2009). Long-range activation of systemic immunity through peptidoglycan diffusion in Drosophila. PLoS Pathog. *5*, e1000694.

Georgel, P., Naitza, S., Kappler, C., Ferrandon, D., Zachary, D., Swimmer, C., Kopczynski, C., Duyk, G., Reichhart, J.M., and Hoffmann, J.A. (2001). Drosophila immune deficiency (IMD) is a death domain protein that activates antibacterial defense and can promote apoptosis. Dev. Cell *1*, 503–514.

Gottar, M., Gobert, V., Matskevich, A.A., Reichhart, J.-M., Wang, C., Butt, T.M., Belvin, M., Hoffmann, J.A., and Ferrandon, D. (2006). Dual Detection of Fungal Infections in Drosophila via Recognition of Glucans and Sensing of Virulence Factors. Cell *127*, 1425–1437.

Gould, A.L., Zhang, V., Lamberti, L., Jones, E.W., Obadia, B., Gavryushkin, A., Korasidis, N., Carlson, J.M., Beerenwinkel, N., and Ludington, W.B. (2017). High-dimensional microbiome interactions shape host fitness.

Gratz, S.J., Harrison, M.M., Wildonger, J., and O'Connor-Giles, K.M. (2015). Precise Genome Editing of Drosophila with CRISPR RNA-Guided Cas9. Methods Mol. Biol. *1311*, 335–348.

Griffin, R., Sustar, A., Bonvin, M., Binari, R., del Valle Rodriguez, A., Hohl, A.M., Bateman, J.R.,

Villalta, C., Heffern, E., Grunwald, D., et al. (2009). The twin spot generator for differential Drosophila lineage analysis. Nat. Methods *6*, 600–602.

Guillou, A., Troha, K., Wang, H., Franc, N.C., and Buchon, N. (2016). The Drosophila CD36 Homologue croquemort Is Required to Maintain Immune and Gut Homeostasis during Development and Aging. PLoS Pathog. *12*, e1005961.

Ha, E.-M., Oh, C.-T., Bae, Y.S., and Lee, W.-J. (2005). A direct role for dual oxidase in Drosophila gut immunity. Science *310*, 847–850.

Hedengren, M., Asling, B., Dushay, M.S., Ando, I., Ekengren, S., Wihlborg, M., and Hultmark, D. (1999). Relish, a central factor in the control of humoral but not cellular immunity in Drosophila. Mol. Cell *4*, 827–837.

Heigwer, F., Port, F., and Boutros, M. (2018). RNA Interference (RNAi) Screening in Drosophila. Genetics *208*, 853–874.

Houtz, P.L., and Buchon, N. (2014). Methods to assess intestinal stem cell activity in response to microbes in Drosophila melanogaster. Methods Mol. Biol. *1213*, 171–182.

Hout.z, P., Bonfini, A., Liu, X., Revah, J., Guillou, A., Poidevin, M., Hens, K., Huang, H.-Y., Deplancke, B., Tsai, Y.-C., et al. (2017). Hippo, TGF-β, and Src-MAPK pathways regulate transcription of the upd3 cytokine in Drosophila enterocytes upon bacterial infection. PLoS Genet. *13*, e1007091.

Howick, V.M., and Lazzaro, B.P. (2017). The genetic architecture of defence as resistance to and tolerance of bacterial infection in Drosophila melanogaster. Mol. Ecol. *26*, 1533–1546.

Hu, Y., Sopko, R., Foos, M., Kelley, C., Flockhart, I., Ammeux, N., Wang, X., Perkins, L., Perrimon, N., and Mohr, S.E. (2013). FlyPrimerBank: an online database for Drosophila melanogaster gene expression analysis and knockdown evaluation of RNAi reagents. G3 (Bethesda) *3*, 1607–1616.

Huycke, M.M., Spiegel, C.A., and Gilmore, M.S. (1991). Bacteremia caused by hemolytic, high-level gentamicin-resistant Enterococcus faecalis. Antimicrob. Agents Chemother. *35*, 1626–1634.

Juneja, P., and Lazzaro, B.P. (2009). Providencia sneebia sp. nov. and Providencia burhodogranariea sp. nov., isolated from wild Drosophila melanogaster. Int. J. Syst. Evol. Microbiol. *59*, 1108–1111.

Kambris, Z., Brun, S., Jang, I.-H., Nam, H.-J., Romeo, Y., Takahashi, K., Lee, W.-J., Ueda, R., and Lemaitre, B. (2006). Drosophila immunity: a large-scale in vivo RNAi screen identifies five serine proteases required for Toll activation. Curr. Biol. *16*, 808–813.

Kaneko, T., Goldman, W.E., Mellroth, P., Steiner, H., Fukase, K., Kusumoto, S., Harley, W., Fox, A., Golenbock, D., and Silverman, N. (2004). Monomeric and polymeric gram-negative peptidoglycan but not purified LPS stimulate the Drosophila IMD pathway. Immunity *20*, 637–649.

Kenmoku, H., Hori, A., Kuraishi, T., and Kurata, S. (2017). A novel mode of induction of the humoral innate immune response in Drosophila larvae. Dis Model Mech *10*, 271–281.

Khalil, S., Jacobson, E., Chambers, M.C., and Lazzaro, B.P. (2015). Systemic bacterial infection and immune defense phenotypes in Drosophila melanogaster. J Vis Exp e52613–e52613.

Kim, S.-H., Park, S.-Y., Heo, Y.-J., and Cho, Y.-H. (2008). Drosophila melanogaster-based screening for multihost virulence factors of Pseudomonas aeruginosa PA14 and identification of a virulence-attenuating factor, HudA. Infect. Immun. *76*, 4152–4162.

Kloos, W.E., and Musselwhite, M.S. (1975). Distribution and persistence of Staphylococcus and Micrococcus species and other aerobic bacteria on human skin. Appl Microbiol *30*, 381–385.

Kocks, C., Cho, J.H., Nehme, N., Ulvila, J., Pearson, A.M., Meister, M., Strom, C., Conto, S.L., Hetru, C., Stuart, L.M., et al. (2005). Eater, a transmembrane protein mediating phagocytosis of bacterial pathogens in Drosophila. Cell *123*, 335–346.

Koyle, M.L., Veloz, M., Judd, A.M., Wong, A.C.-N., Newell, P.D., Douglas, A.E., and Chaston, J.M. (2016). Rearing the Fruit Fly Drosophila melanogaster Under Axenic and Gnotobiotic Conditions. J Vis Exp.

Kulkarni, M.M., Booker, M., Silver, S.J., Friedman, A., Hong, P., Perrimon, N., and Mathey-Prevot, B. (2006). Evidence of off-target effects associated with long dsRNAs in Drosophila melanogaster cell-based assays. Nat. Methods *3*, 833–838.

Kurucz, É., Márkus, R., Zsámboki, J., Folkl-Medzihradszky, K., Darula, Z., Vilmos, P., Udvardy, A., Krausz, I., Lukacsovich, T., Gateff, E., et al. (2007). Nimrod, a Putative Phagocytosis Receptor with EGF Repeats in Drosophila Plasmatocytes. Current Biology *17*, 649–654.

Lanot, R., Zachary, D., Holder, F., and Meister, M. (2001). Postembryonic hematopoiesis in Drosophila. Dev. Biol. *230*, 243–257.

Lazzaro, B.P., Sackton, T.B., and Clark, A.G. (2006). Genetic variation in Drosophila melanogaster resistance to infection: a comparison across bacteria. Genetics *174*, 1539–1554.

Lee, J.-E., and Edery, I. (2008). Circadian regulation in the ability of Drosophila to combat pathogenic infections. Curr. Biol. *18*, 195–199.

Lee, K.-A., Kim, S.-H., Kim, E.-K., Ha, E.-M., You, H., Kim, B., Kim, M.-J., Kwon, Y., Ryu, J.-H., and Lee, W.-J. (2013). Bacterial-derived uracil as a modulator of mucosal immunity and gut-microbe homeostasis in Drosophila. Cell *153*, 797–811.

Lee, K.-Z., Lestradet, M., Socha, C., Schirmeier, S., Schmitz, A., Spenlé, C., Lefebvre, O., Keime, C., Yamba, W.M., Bou Aoun, R., et al. (2016). Enterocyte Purge and Rapid Recovery Is a Resilience Reaction of the Gut Epithelium to Pore-Forming Toxin Attack. Cell Host Microbe *20*, 716–730.

Lemaitre, B., Kromer-Metzger, E., Michaut, L., Nicolas, E., Meister, M., Georgel, P., Reichhart,

J.M., and Hoffmann, J.A. (1995). A recessive mutation, immune deficiency (imd), defines two distinct control pathways in the Drosophila host defense. Proc. Natl. Acad. Sci. U.S.a. *92*, 9465–9469.

Lemaitre, B., and Hoffmann, J. (2007). The host defense of Drosophila melanogaster. Annu. Rev. Immunol. *25*, 697–743.

Lesch, C., and Ulrich, T. Methods to study hemolymph clotting in insects. In Insect Immunology.

Leulier, F., Parquet, C., Pili-Floury, S., Ryu, J.-H., Caroff, M., Lee, W.-J., Mengin-Lecreulx, D., and Lemaitre, B. (2003). The Drosophila immune system detects bacteria through specific peptidoglycan recognition. Nat. Immunol. *4*, 478–484.

Liehl, P., Blight, M., Vodovar, N., Boccard, F., and Lemaitre, B. (2006). Prevalence of local immune response against oral infection in a Drosophila/Pseudomonas infection model. PLoS Pathog. *2*, e56.

Linder, J.E., Owers, K.A., and Promislow, D.E.L. (2008). The effects of temperature on host-pathogen interactions in D. melanogaster: who benefits? J. Insect Physiol. *54*, 297–308.

Lu, H.-L., Wang, J.B., Brown, M.A., Euerle, C., and St Leger, R.J. (2015). Identification of Drosophila Mutants Affecting Defense to an Entomopathogenic Fungus. Sci Rep *5*, 12350.

Mackay, T.F.C., Richards, S., Stone, E.A., Barbadilla, A., Ayroles, J.F., Zhu, D., Casillas, S., Han, Y., Magwire, M.M., Cridland, J.M., et al. (2012). The Drosophila melanogaster Genetic Reference Panel. Nature *482*, 173–178.

Mansfield, B.E., Dionne, M.S., Schneider, D.S., and Freitag, N.E. (2003). Exploration of host-pathogen interactions using Listeria monocytogenes and Drosophila melanogaster. Cellular Microbiology *5*, 901–911.

Marquez-Ortiz, R.A., Haggerty, L., Sim, E.M., Duarte, C., Castro-Cardozo, B.E., Beltran, M., Saavedra, S., Vanegas, N., Escobar-Perez, J., and Petty, N.K. (2017). First Complete Providencia rettgeri Genome Sequence, the NDM-1-Producing Clinical Strain RB151. Genome Announc *5*, e01472–16.

Martins, N.E., Faria, V.G., Teixeira, L., Magalhães, S., and Sucena, É. (2013). Host adaptation is contingent upon the infection route taken by pathogens. PLoS Pathog. *9*, e1003601.

McDonald, M.J., and Rosbash, M. (2001). Microarray analysis and organization of circadian gene expression in Drosophila. Cell *107*, 567–578.

McGuire, S.E., Mao, Z., and Davis, R.L. (2004). Spatiotemporal gene expression targeting with the TARGET and gene-switch systems in Drosophila. Sci. STKE *2004*, pl6–pl6.

Merkling, S.H., and van Rij, R.P. (2015). Analysis of resistance and tolerance to virus infection in Drosophila. Nat Protoc *10*, 1084–1097.

Michel, T., Reichhart, J.M., Hoffmann, J.A., and Royet, J. (2001). Drosophila Toll is activated by Gram-positive bacteria through a circulating peptidoglycan recognition protein. Nature *414*, 756–759.

Miest, T.S., and Bloch-Qazi, M. (2008). Sick of mating: sexual transmission of a pathogenic bacterium in Drosophila melanogaster. Fly (Austin) *2*, 215–219.

Moret, Y., and Schmid-Hempel, P. (2000). Survival for immunity: the price of immune system activation for bumblebee workers. Science *290*, 1166–1168.

Nehme, N.T., Liégeois, S., Kele, B., Giammarinaro, P., Pradel, E., Hoffmann, J.A., Ewbank, J.J., and Ferrandon, D. (2007). A model of bacterial intestinal infections in Drosophila melanogaster. PLoS Pathog. *3*, e173.

Nehme, N.T., Quintin, J., Cho, J.H., Lee, J., Lafarge, M.-C., Kocks, C., and Ferrandon, D. (2011). Relative roles of the cellular and humoral responses in the Drosophila host defense against three gram-positive bacterial infections. PLoS ONE *6*, e14743.

Newton, K., and Dixit, V.M. (2012). Signaling in Innate Immunity and Inflammation. Cold Spring Harbor Perspectives in Biology *4*, a006049–a006049.

Neyen, C., Bretscher, A.J., Binggeli, O., and Lemaitre, B. (2014). Methods to study Drosophila immunity. Methods *68*, 116–128.

Obbard, D.J. A comprehensive list of published *Drosophila* viruses. Httpobbard.Bio.Ed.Ac.Ukdata.Html.

Owusu-Ansah, E., Yavari, A., and Banerjee, U. (2008). A protocol for _in vivo_ detection of reactive oxygen species.

Padmanabha, D., and Baker, K.D. (2014). Drosophila gains traction as a repurposed tool to investigate metabolism. Trends Endocrinol. Metab. *25*, 518–527.

Palmer, W.H., Medd, N.C., Beard, P.M., and Obbard, D.J. (2018). Isolation of a natural DNA virus of Drosophila melanogaster, and characterisation of host resistance and immune responses. PLoS Pathog. *14*, e1007050.

Panayidou, S., Ioannidou, E., and Apidianakis, Y. (2014). Human pathogenic bacteria, fungi, and viruses in Drosophila: disease modeling, lessons, and shortcomings. Virulence *5*, 253–269.

Park, S., Alfa, R.W., Topper, S.M., Kim, G.E.S., Kockel, L., and Kim, S.K. (2014). A genetic strategy to measure circulating Drosophila insulin reveals genes regulating insulin production and secretion. PLoS Genet. *10*, e1004555.

Perkins, L.A., Holderbaum, L., Tao, R., Hu, Y., Sopko, R., McCall, K., Yang-Zhou, D., Flockhart, I., Binari, R., Shim, H.-S., et al. (2015). The Transgenic RNAi Project at Harvard Medical School: Resources and Validation. Genetics *201*, 843–852.

Perrimon, N., and Mathey-Prevot, B. (2007). Matter arising: off-targets and genome-scale RNAi screens in Drosophila. Fly (Austin) *1*, 1–5.

Ramsden, S., Cheung, Y.Y., and Seroude, L. (2008). Functional analysis of the Drosophila immune response during aging. Aging Cell *7*, 225–236.

Rigottier-Gois, L., Alberti, A., Houel, A., Taly, J.-F., Palcy, P., Manson, J., Pinto, D., Matos, R.C., Carrilero, L., Montero, N., et al. (2011). Large-scale screening of a targeted Enterococcus faecalis mutant library identifies envelope fitness factors. PLoS ONE *6*, e29023.

Rosshart, S.P., Vassallo, B.G., Angeletti, D., Hutchinson, D.S., Morgan, A.P., Takeda, K., Hickman, H.D., McCulloch, J.A., Badger, J.H., Ajami, N.J., et al. (2017). Wild Mouse Gut Microbiota Promotes Host Fitness and Improves Disease Resistance. Cell *171*, 1015–1028.e13.

Sagar, S., Narasimhaswamy, N., and D'Souza, J. (2017). Providencia Rettgeri:

An Emerging Nosocomial Uropathogen in an Indwelling Urinary Catheterised Patient. J Clin Diagn Res *11*, DD01–DD02.

Schaible, U.E., and Kaufmann, S.H.E. (2007). Malnutrition and infection: complex mechanisms and global impacts. PLoS Med. *4*, e115.

Schlenke, T.A., Morales, J., Govind, S., and Clark, A.G. (2007). Contrasting infection strategies in generalist and specialist wasp parasitoids of Drosophila melanogaster. PLoS Pathog. *3*, 1486–1501.

Schwenke, R.A., and Lazzaro, B.P. (2017). Juvenile Hormone Suppresses Resistance to Infection in Mated Female Drosophila melanogaster. Current Biology *27*, 596–601.

Shahrestani, P., Chambers, M., Vandenberg, J., Garcia, K., Malaret, G., Chowdhury, P., Estrella, Y., Zhu, M., and Lazzaro, B.P. (2018). Sexual dimorphism in Drosophila melanogaster survival of Beauveria bassiana infection depends on core immune signaling. Sci Rep *8*, 12501.

Sharma, D., Sharma, P., and Soni, P. (2017). First case report of Providencia Rettgeri neonatal sepsis. BMC Res Notes *10*, 536.

Shiratsuchi, A., Mori, T., Sakurai, K., Nagaosa, K., Sekimizu, K., Lee, B.L., and Nakanishi, Y. (2012). Independent recognition of Staphylococcus aureus by two receptors for phagocytosis in Drosophila. J. Biol. Chem. *287*, 21663–21672.

Short, S.M., and Lazzaro, B.P. (2010). Female and male genetic contributions to post-mating immune defence in female Drosophila melanogaster. Proc. Biol. Sci. *277*, 3649–3657.

Short, S.M., and Lazzaro, B.P. (2013). Reproductive status alters transcriptomic response to infection in female Drosophila melanogaster. G3 (Bethesda) *3*, 827–840.

Small, C., Paddibhatla, I., Rajwani, R., and Govind, S. (2012). An introduction to parasitic wasps of Drosophila and the antiparasite immune response. J Vis Exp e3347.

Soares, M.P., Gozzelino, R., and Weis, S. (2014). Tissue damage control in disease tolerance. Trends Immunol. *35*, 483–494.

Stone, E.F., Fulton, B.O., Ayres, J.S., Pham, L.N., Ziauddin, J., and Shirasu-Hiza, M.M. (2012). The circadian clock protein timeless regulates phagocytosis of bacteria in Drosophila. PLoS Pathog. *8*, e1002445.

Tauszig, S., Jouanguy, E., Hoffmann, J.A., and Imler, J.L. (2000). Toll-related receptors and the control of antimicrobial peptide expression in Drosophila. Proc. Natl. Acad. Sci. U.S.a. *97*, 10520–10525.

Teixeira, L., Ferreira, A., and Ashburner, M. (2008). The bacterial symbiont Wolbachia induces resistance to RNA viral infections in Drosophila melanogaster. PLoS Biol. *6*, e2.

Troha, K., Im, J.H., Revah, J., Lazzaro, B.P., and Buchon, N. (2018). Comparative transcriptomics reveals CrebA as a novel regulator of infection tolerance in D. melanogaster. PLoS Pathog. *14*, e1006847.

Tuleva, B., Christova, N., Cohen, R., Antonova, D., Todorov, T., and Stoineva, I. (2009). Isolation and characterization of trehalose tetraester biosurfactants from a soil strain Micrococcus luteus BN56. Process Biochemistry *44*, 135–141.

Tzou, P., Ohresser, S., Ferrandon, D., Capovilla, M., Reichhart, J.M., Lemaitre, B., Hoffmann, J.A., and Imler, J.L. (2000). Tissue-specific inducible expression of antimicrobial peptide genes in Drosophila surface epithelia. Immunity *13*, 737–748.

Tzou, P., Meister, M., and Lemaitre, B. (2002). 27 Methods for studying infection and immunity in Drosophila. In Molecular Cellular Microbiology, (Elsevier), pp. 507–529.

Valanne, S., Wang, J.-H., and Rämet, M. (2011). The Drosophila Toll signaling pathway. J. Immunol. *186*, 649–656.

Venken, K.J.T., and Bellen, H.J. (2014). Chemical mutagens, transposons, and transgenes to interrogate gene function in Drosophila melanogaster. Methods *68*, 15–28.

Venken, K.J.T., Schulze, K.L., Haelterman, N.A., Pan, H., He, Y., Evans-Holm, M., Carlson, J.W., Levis, R.W., Spradling, A.C., Hoskins, R.A., et al. (2011). MiMIC: a highly versatile transposon insertion resource for engineering Drosophila melanogaster genes. Nat. Methods *8*, 737–743.

Vodovar, N., Vinals, M., Liehl, P., Basset, A., Degrouard, J., Spellman, P., Boccard, F., and Lemaitre, B. (2005). Drosophila host defense after oral infection by an entomopathogenic Pseudomonas species. Proc. Natl. Acad. Sci. U.S.a. *102*, 11414–11419.

Vonkavaara, M., Telepnev, M.V., Rydén, P., Sjöstedt, A., and Stöven, S. (2008). Drosophila melanogaster as a model for elucidating the pathogenicity of Francisella tularensis. Cellular Microbiology *10*, 1327–1338.

Wang, J.B., Lu, H.-L., and St Leger, R.J. (2017). The genetic basis for variation in resistance to

infection in the Drosophila melanogaster genetic reference panel. PLoS Pathog. *13*, e1006260.

Wang, X.-H., Aliyari, R., Li, W.-X., Li, H.-W., Kim, K., Carthew, R., Atkinson, P., and Ding, S.-W. (2006). RNA interference directs innate immunity against viruses in adult Drosophila. Science *312*, 452–454.

Weis, S., Carlos, A.R., Moita, M.R., Singh, S., Blankenhaus, B., Cardoso, S., Larsen, R., Rebelo, S., Schäuble, S., Del Barrio, L., et al. (2017). Metabolic Adaptation Establishes Disease Tolerance to Sepsis. Cell *169*, 1263–1275.e14.

Wong, C.N.A., Ng, P., and Douglas, A.E. (2011). Low-diversity bacterial community in the gut of the fruitfly Drosophila melanogaster. Environ. Microbiol. *13*, 1889–1900.

Wu, J.S., and Luo, L. (2006). A protocol for mosaic analysis with a repressible cell marker (MARCM) in Drosophila. Nat Protoc *1*, 2583–2589.

Wu, S.-C., Liao, C.-W., Pan, R.-L., and Juang, J.-L. (2012). Infection-induced intestinal oxidative stress triggers organ-to-organ immunological communication in Drosophila. Cell Host Microbe *11*, 410–417.

Xu, J., and Cherry, S. (2014). Viruses and antiviral immunity in Drosophila. Dev. Comp. Immunol. *42*, 67–84.

Yoh, M., Matsuyama, J., Ohnishi, M., Takagi, K., Miyagi, H., Mori, K., Park, K.-S., Ono, T., and Honda, T. (2005). Importance of Providencia species as a major cause of travellers' diarrhoea. J. Med. Microbiol. *54*, 1077–1082.

Zambon, R.A., Nandakumar, M., Vakharia, V.N., and Wu, L.P. (2005). The Toll pathway is important for an antiviral response in Drosophila. Proc. Natl. Acad. Sci. U.S.a. *102*, 7257–7262.

CHAPTER III

COMPARATIVE TRANSCRIPTOMICS REVEALS *CREBA* AS A NOVEL REGULATOR OF INFECTION TOLERANCE IN *D. MELANOGASTER**

* Adapted from Katia Troha, Joo Hyun Im, Jonathan Revah, Brian P. Lazzaro and Nicolas Buchon. Copyright 2018. PLOS Pathogens.

Abstract

Host responses to infection encompass many processes in addition to activation of the immune system, including metabolic adaptations, stress responses, tissue repair, and other reactions. The response to bacterial infection in *Drosophila melanogaster* has been classically described in studies that focused on the immune response elicited by a small set of largely avirulent microbes. Thus, we have surprisingly limited knowledge of responses to infection that are outside the canonical immune response, of how the response to pathogenic infection differs from that to avirulent bacteria, or even of how generic the response to various microbes is and what regulates that core response. In this study, we addressed these questions by profiling the *D. melanogaster* transcriptomic response to 10 bacteria that span the spectrum of virulence. We found that each bacterium triggers a unique transcriptional response, with distinct genes making up to one third of the response elicited by highly virulent bacteria. We also identified a core set of 252 genes that are differentially expressed in response to the majority of bacteria tested. Among these, we determined that the transcription factor *CrebA* is a novel regulator of infection tolerance. Knock-down of *CrebA* significantly increased mortality from microbial infection without any concomitant change in bacterial number. Upon infection, *CrebA* is upregulated by both the Toll and Imd pathways in the fat body, where it is required to induce the expression of secretory pathway genes. Loss of *CrebA* during infection triggered endoplasmic reticulum (ER) stress and activated the unfolded protein response (UPR), which contributed to infection-induced mortality. Altogether, our study reveals essential features of the response to bacterial infection and elucidates the function of a novel regulator of infection tolerance.

Introduction

To combat infection, a host activates a combination of immune and physiological responses. While detection of microbial presence is sufficient to stimulate the innate immune response, physiological responses to infection occur as a consequence of microbial growth and virulence, and can therefore be very specific to the particular bacterium the host interacts with. Despite a growing body of literature on immunity, our knowledge of the different host processes that are activated or repressed in response to infection, and of how such responses contribute to host survival, remains limited. To identify new biological processes required to survive infection and to determine how specific or generic the immune and physiological responses to infection are, we surveyed changes in the transcriptome of *Drosophila melanogaster* in response to infection with 10 bacteria that span the spectrum of virulence.

Drosophila is a leading model system for studying how hosts respond to infection at the organismal level. To overcome infection, the fly relies on cellular and humoral innate immune responses. The cellular response consists of phagocytosis and encapsulation [1,2]. The humoral response includes the pro-phenoloxidase cascade, which leads to the generation of reactive oxygen species and clotting, as well as the production of antimicrobial peptides (AMPs) primarily by the fat body, an organ functionally analogous to the liver and adipose tissues of mammals [3-5]. In the early 2000s, microarray studies characterizing the transcriptional response to bacterial infection were conducted in *Drosophila* [6-8]. These experiments were based on infection with two non-pathogenic bacteria, *Micrococcus luteus* and *Escherichia coli*. This approach successfully identified a set of genes that are differentially expressed upon infection, which became known as the *Drosophila* Immune-Regulated Genes (DIRGs). A majority of the DIRGs were functionally assigned to specific aspects of the immune response—phagocytosis, antimicrobial peptide

synthesis, and production of reactive oxygen species among others [6]. These studies also confirmed that the Toll and Imd pathways are the major regulators of the immune response in *Drosophila*, and that both pathways direct expression of the majority of DIRGs [7]. In this model, the host response depends on the sensing of two microbe-associated molecular patterns (MAMPs): Lys-type peptidoglycan from Gram-positive bacteria, which activates the Toll pathway, and DAP-type peptidoglycan from Gram-negative bacteria, which induces the Imd pathway [9-11]. Upon activation, each pathway goes on to regulate a subset of DIRGs.

More recently, new findings have expanded our insight into the *Drosophila* response to infection. First, the Toll and Imd pathways can also be activated by virulence factors and damage-associated molecular patterns (DAMPs) [12-16]. Additionally, biological processes that would not be considered as classic immunological responses, such as tissue repair and regulation of metabolism, are clearly modulated by pathogenic infection [17-20]. These observations beget the idea that microbial virulence—the relative capacity of a microbe to cause damage in a host—could be an important factor in shaping the host response, and suggest that survival from pathogenic infections may require additional biological processes beyond those that are currently known [21].

In this study, we aimed to identify a comprehensive list of genes regulated by pathogenic and avirulent infections, and to determine what responses are general or specific to each infection. To that purpose, we used RNA-seq to profile the *D. melanogaster* transcriptomic response to systemic infection with 10 different species of bacteria that vary in their ability to grow within and kill the host. We found that each bacterium elicits a unique host transcriptional response. However, we also identified a small set of core genes that were differentially regulated by infection with the majority of microbes. These genes are involved in a variety of immune and non-immune functions, and a fraction of them remained highly expressed even after bacteria were cleared from the host.

Among the core genes was *CrebA*, a Creb3-like transcription factor. *CrebA* expression is upregulated through both Toll and Imd signaling in the fat body following infection. Knockdown of *CrebA* significantly increased mortality from bacterial challenge but did not alter bacterial load, indicating that *CrebA* contributes to host tolerance of infection. *CrebA* regulates multiple genes involved in the secretory pathway, and the loss of *CrebA* triggered ER stress upon infection. This suggests that the *CrebA* tolerance phenotype may arise through protection from cellular stress during the rapid and dramatic response to infection.

Results

Identification of bacteria with different virulence levels and peptidoglycan types

We began by assembling a panel of bacteria to probe the host response to infection. We selected bacteria that span the spectrum of virulence (from 0% to 100% mortality), focusing on microbes that are commonly used by the *D. melanogaster* research community and ensuring that we included bacteria with Lys-type or DAP-type peptidoglycan (PGN) in each virulence level. To assess the relative virulence of each bacterium, we measured host survival and bacterial load over time following infection (Fig 1A, Fig S1, and Fig S2). The bacteria with the lowest levels of virulence—*Escherichia coli* (*Ec*), *Micrococcus luteus* (*Ml*), and the Type strain of *Serratia marcescens* (*Sm*)—caused less than 10% mortality and did not grow past initial inoculum levels in the host. Bacteria exhibiting intermediate levels of virulence—*Pectinobacterium* (previously known as *Erwinia*) *carotovora 15* (*Ecc15*), *Providencia rettgeri* (*Pr*), and *Enterococcus faecalis* (*Ef*)—showed the ability to proliferate within the host and killed 15% to 55% of infected hosts. Highly virulent bacteria—*Staphylococcus aureus* (*Sa*), *Providencia sneebia* (*Ps*), *Serratia marcescens* strain Db11 (Db11), and *Pseudomonas entomophila* (*Pe*)—caused 100% mortality in less than 96 h (Fig 1A). *M. luteus*, *E. faecalis*, and *S. aureus* are Gram-positive bacteria (Lys-type PGN); all others are Gram-negative (DAP-type PGN).

A

Bacteria	Gram	PGN	Isolated from *Dmel*	Survival at 7 days (%)	LT_{50} (hours) (95%CI)	Virulence level
E. coli	-	DAP-type	No	98.3	N/A	*
M. luteus	+	Lys-type	No	96.7	N/A	*
S. marcescens Type	-	DAP-type	No	94.9	N/A	*
Ecc15	-	DAP-type	No	85.0	N/A	**
P. rettgeri	-	DAP-type	Yes	48.3	N/A	**
E. faecalis	+	Lys-type	Yes	45.0	N/A	**
S. aureus	+	Lys-type	No	0.0	31.3 (27.2 – 35.4)	***
P. sneebia	-	DAP-type	Yes	0.0	31.2 (27.8 – 34.7)	***
S. marcescens Db11	-	DAP-type	Yes	0.0	13.4 (12.8 – 14.8)	***
P. entomophila	-	DAP-type	Yes	0.0	13.7 (12.7 – 15.8)	***

B

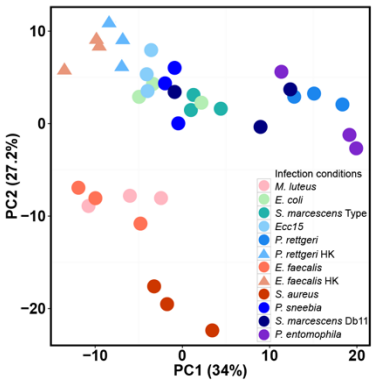

C

PC	Gene name	Function	SW	Pr HK	Ef HK	Ml	Ef	Sa	Ecc	Ec	Ps	Sm	Db11	Pr	Pe
PC1	PGRP-LC	Imd signaling	1.1	1.4	1.3	1.3	1.2	1.3	1.6	1.7	1.9	1.9	2.5	4.4	4.9
PC1	Rel	Imd signaling	1.2	1.3	1.1	1.8	1.8	4.5	1.5	1.5	2.2	2.4	4.5	7.3	8.1
PC1	PGRP-LB	Imd signaling	1.3	1.3	1.1	1.4	1.3	2.5	2.1	2.8	4.3	4.3	8.3	15.9	13.9
PC1	PGRP-SD	Imd signaling	4.2	6.1	4.4	7.2	4.3	6.5	9.1	8.7	9.4	11.8	11.7	20.2	27.5
PC1	AttA	AMP	7.2	10.7	6.5	29.7	16.7	51.2	24.0	35.5	42.7	61.3	65.2	100	100
PC1	Dpt	AMP	35.3	85.1	40.0	52.2	23.3	23.2	100	100	100	100	100	100	100
PC1	Drs	AMP	9.5	11.9	7.5	54.6	42.6	65.6	16.5	27.3	14.9	26.1	20.2	29.9	40.9
PC1	Mtk	AMP	29.0	66.7	34.9	69.5	50.1	72.6	85.5	91.7	69.9	100	92.9	100	100
PC1	Spz	Toll signaling	1.1	1.2	1.3	1.4	1.3	1.7	1.3	1.5	1.4	1.6	1.7	2.9	4.4
PC1	Spirit	Toll signaling	1.0	1.3	1.1	1.7	1.4	2.6	1.1	1.1	-1.0	1.5	1.6	2.9	4.5
PC1	PGRP-SA	Toll signaling	2.1	2.3	1.8	2.9	2.0	3.3	2.7	3.7	2.4	4.3	3.6	4.8	7.6
PC1	Spn88Eb	Toll signaling	1.8	2.2	1.9	4.6	6.0	13.0	1.8	2.9	2.8	3.3	4.5	5.7	6.7
PC1	TotA	stress peptide (JAK)	24.4	72.1	20.6	10.9	4.1	8.9	13.2	43.3	8.3	18.5	18.8	23.7	20.5
PC1	TotC	stress peptide (JAK)	52.2	100	35.3	13.7	4.3	10.6	19.9	69.0	11.6	28.2	33.9	40.6	28.8
PC1	TotM	stress peptide (JAK)	79.8	100	35.2	16.7	6.7	15.3	19.2	99.3	14.0	45.3	35.6	65.8	59.4
PC1	ACC	acetyl-coA-carboxylase	-1.0	-1.0	-1.0	-1.2	-1.2	-1.8	1.2	1.0	-1.2	-1.1	-1.4	-1.9	-2.0
PC1	UGP	glycogen synthesis	-1.2	-1.0	1.0	-1.8	-1.3	-2.5	-1.1	-1.1	-1.3	-1.3	-1.9	-2.1	-2.9
PC1	Galk	galactokinase	-1.3	-1.3	-1.0	-1.3	-1.3	-2.3	-1.3	-1.3	-1.3	-1.2	-2.2	-2.4	-2.8
PC1	Tps1	trehalose 6P synthase	-1.1	-1.1	-1.2	-1.7	-1.9	-2.6	-1.1	-1.5	-1.3	-1.3	-2.0	-3.3	-3.6
PC1	Hex-C	hexokinase	-1.2	-1.4	-1.3	-1.4	-1.6	-2.7	-1.2	-1.3	-1.6	-1.5	-2.2	-2.9	-3.7
PC1	FASN1	Fatty acid synthase	1.0	1.0	1.2	-1.8	-1.4	-2.5	1.1	-1.2	-1.1	-1.4	-2.0	-3.5	-3.3
		Fold regulation vs unchallenged							< -4	< -2	NS	> 2	> 4	> 8	> 32

PC	Gene name	Function	SW	Pr HK	Ef HK	Ml	Ef	Sa	Ecc	Ec	Ps	Sm	Db11	Pr	Pe
PC2	Sp7	Toll signaling	-1.2	-1.1	-1.8	1.2	-1.0	2.0	1.1	-1.2	-1.6	-1.1	1.4	1.6	1.8
PC2	cactus	Toll signaling	1.1	1.2	1.0	1.6	1.8	3.8	1.3	1.2	1.1	1.2	1.3	1.4	1.3
PC2	nec	Toll signaling	1.4	1.5	1.7	2.8	3.4	6.2	1.4	1.5	1.3	1.3	1.6	1.2	1.3
PC2	SPE	Toll signaling	1.3	1.2	1.2	2.5	2.8	3.7	1.5	1.5	1.3	1.5	1.3	1.3	1.2
PC2	fon	coagulation	1.9	1.6	1.8	2.8	2.9	2.5	2.0	2.2	1.8	1.8	1.7	-1.1	1.2
PC2	MP1	melanization	1.6	1.0	-1.1	1.5	2.6	4.9	1.5	1.3	1.4	1.4	-1.2	1.7	1.9
PC1/2	IM2	AMP	3.4	2.1	2.7	12.1	12.1	15.6	2.2	4.1	3.4	3.0	2.8	1.3	2.2
PC1/2	IM3	AMP	3.4	2.3	2.8	14.0	13.9	19.2	2.4	4.5	3.5	3.4	2.9	1.5	2.7
PC1/2	IM1	AMP	4.7	3.5	3.9	33.3	29.9	39.8	4.8	9.6	5.4	6.3	5.2	3.5	6.2
PC1/2	IM23	AMP	4.9	3.5	4.1	46.6	39.0	61.1	5.1	8.7	5.7	6.0	6.1	3.4	6.7
PC2	nimB3	phago	1.7	1.9	1.5	4.8	3.8	5.3	2.3	2.7	2.0	2.3	2.1	1.9	3.2
PC2	Mal-A1	Digestion	-1.3	-1.3	-1.1	-1.5	-1.8	-3.3	-1.3	-1.5	-1.2	-1.1	-2.2	-1.2	-1.2
PC2	Mal-A8	Digestion	-1.4	-1.3	-1.2	-1.4	-1.9	-3.5	-1.3	-1.7	-1.2	-1.5	-2.1	-1.4	-1.2
PC2	Mal-A7	Digestion	-1.6	-1.3	-1.1	-1.6	-1.8	-3.6	-1.3	-1.6	-1.2	-1.4	-2.0	-1.4	-1.4
PC2	Mal-A4	Digestion	-1.3	-1.3	-1.4	-2.1	-2.2	-4.0	-1.4	-1.9	-1.2	-1.6	-1.4	-1.2	-1.1
PC2	Gs1	AA biosynthesis	1.3	1.4	1.4	1.0	-1.0	-1.7	1.6	1.3	1.5	1.5	1.2	-1.1	-1.1
PC2	Spat	AA biosynthesis	-1.2	-1.2	-1.2	-2.0	-2.0	-3.9	-1.1	-1.4	-1.2	-1.5	-2.0	-2.7	-3.3
PC2	Cyp6w1	P450	1.7	1.3	1.5	-2.5	-1.3	-2.3	1.4	-1.2	1.7	-1.4	1.8	1.2	-1.2
PC2	Cyp6g1	P450	-1.3	-1.2	-1.1	-2.0	-1.9	-3.6	-1.3	-1.7	-1.5	-1.9	-2.3	-2.1	-2.4
PC2	Cyp4ac1	P450	1.0	1.0	1.0	-1.6	-1.5	-3.4	1.2	-1.1	-1.2	-1.1	-1.2	-1.1	-1.1
PC2	Cyp309a1	P450	-1.3	-1.1	-1.3	-1.9	-2.9	-6.1	1.1	1.0	1.2	1.0	1.0	1.1	1.3

Figure III.1. Major parameters influencing the global response to infection
(A) List of bacteria used in the RNA-seq experiment, including Gram classification, type of bacterial peptidoglycan (PGN), source of isolate, percent survival at 7 days post-infection, median lethal time (LT_{50}) for each bacterium, and assignment into broad virulence categories. (B) PCA plot showing the first two principal components of the 12 h dataset. Red and orange (warm) colors indicate infections with Lys-type PGN bacteria, while green, blue and purple (cool) colors indicate infections with DAP-type PGN bacteria. Circles indicate infection with live bacteria and triangles denote inoculation with heat-killed bacteria. (C) Genes that contribute the most to PC1 (left column), PC2 (right column), or both PCs (right column) are presented with their associated level of expression change (fold change) at 12 h post-infection. Warm colors indicate the degree of transcriptional induction, while cool colors show the extent of transcriptional downregulation.

Bacterial load time course experiments revealed differences between bacterial species in their ability to grow and persist within the host. For example, only *M. luteus* and *Ecc15* were eliminated from the host (i.e. their levels fall below our detection threshold of ~30 CFU/fly) by 132 h post-infection. In the case of *Ecc15*, most but not all hosts were able to clear the infection (Fig S2A, F). Neither *E. coli* nor *S. marcescens* Type increased in density, but the bacteria persisted

inside the host at ~2^{10} bacteria/fly even after 5 days of infection (Fig S2D-E). *P. rettgeri* and *E. faecalis* grew during the first 24 h of infection, killing a fraction of the hosts. The flies that survived these infections remained chronically infected with ~2^{10} to 2^{13} bacteria per fly (Fig S2B, G) for at least 5.5 days. *P. entomophila*, *S. aureus*, *S. marcescens* Db11, and *P. sneebia* all grew monotonically in the host until death occurred (Fig S2C, H, I, J), causing complete mortality within 96 h (Fig S1E, J, K, L).

Having assembled our panel of bacteria, our next goal was to select relevant time points for transcriptomic analysis. Using our survival and bacterial load data, we identified three time points that are characteristic of different stages of infection: 12, 36, and 132 h. At 12 h post-infection, all flies remain alive, and they face the initial growth of microbes. Thirty-six hours represents an intermediate time point during infection, after the highly virulent bacteria have killed most or all flies and the moderately virulent bacteria have killed 15% to 55% of infected hosts. Finally, at 132 h post-infection (5.5 days), surviving flies are chronically infected with moderate to low levels of bacteria.

A diverse, partly specific *Drosophila* response to infection

To identify novel biological processes required to survive systemic infection, and to assess the level of specificity of the *Drosophila* response to microbes, we used RNA-seq to profile the *D. melanogaster* transcriptome after infection with each of our 10 experimental bacteria. We additionally included the following controls: unchallenged flies (UC), flies challenged with a sterile wound (SW), and flies inoculated with heat-killed *E. faecalis* (*Ef* HK) or heat-killed *P. rettgeri* (*Pr* HK). The purpose of the controls was to distinguish the response to live bacteria from that to aseptic injury and/or inert bacterial compounds (MAMPs) provided by the injection of dead

bacteria. The expression value dataset for the entire experiment can be downloaded or accessed online in our associated database Flysick-seq (http://flysick.buchonlab.com)

We first determined the overall transcriptomic differences between flies infected by each of the 10 bacteria. Principal component analysis (PCA) showed that all three biological replicates clustered together, indicating good replicability of the response for each pathogen (illustrated in Fig 1B-C for the 12 h time point and Fig S3A for the full data set). In total, we identified 2,423 genes (13.7% of the genome) that were differentially expressed upon infection. Of these, 1,286 genes were upregulated and 1,290 genes were downregulated in response to at least one bacterial infection and time point (Fig 2A and Fig S3B). Out of the total number of genes differentially regulated by all 10 live infections, more genes were upregulated than downregulated; 6.1% of the 1,286 upregulated genes were induced in all bacterial infections, while only 0.6% of the 1,290 downregulated genes were repressed by all 10 bacteria (Fig S3B). We also determined that 51.1% of the downregulated genes were repressed in only one bacterial infection, while 38.6% of the upregulated genes were induced by a single bacterial condition (Fig S3B). These data suggest that the host response to infection is highly specific to individual bacteria, but that there is also a core set of genes that are differentially expressed during most bacterial infections. Additionally, our data showed that downregulated genes tend to be unique to each infecting bacterium, perhaps reflecting the singular consequences of each infection to host physiology (Fig S3B).

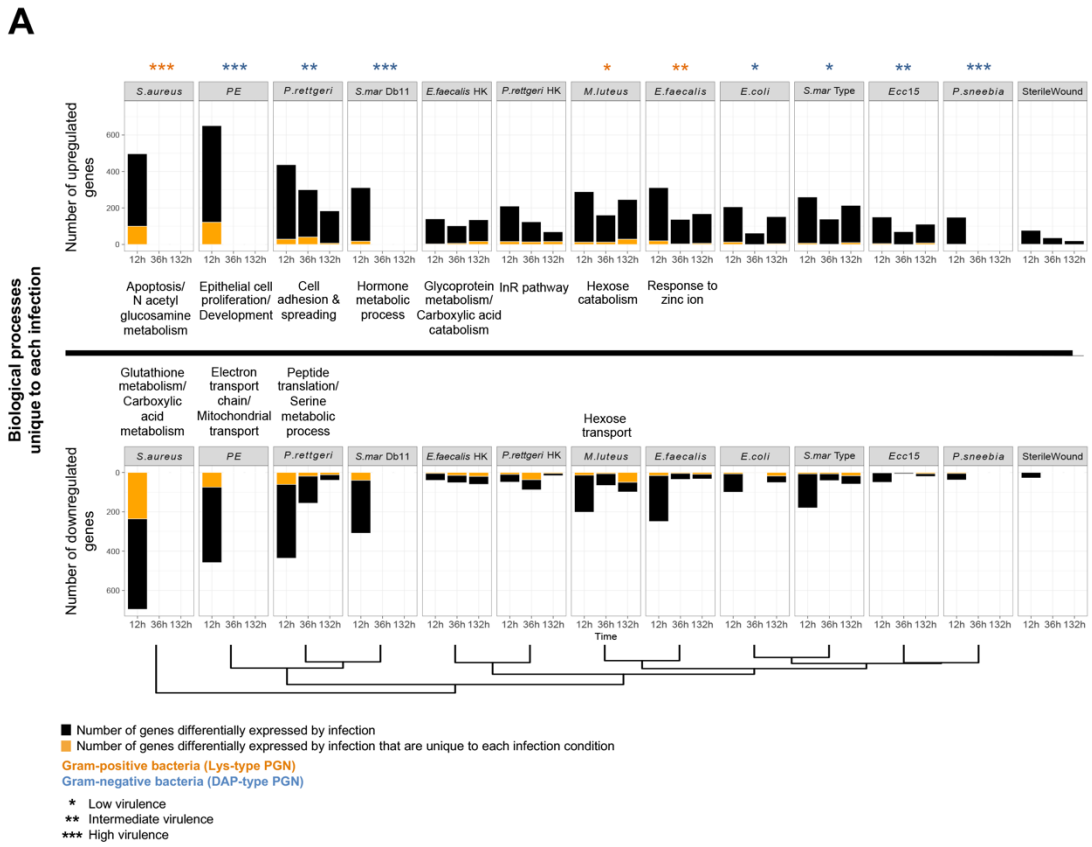

Figure III.2. The host response to bacterial infection is diverse
(A) Number of genes differentially regulated by each infection (black bars) and number of genes differentially expressed by infection that are unique to each individual bacterium (orange bars). This information is listed separately by time point for each infection. Upregulated and downregulated genes are above and below the horizontal demarcation line, respectively. The biological processes regulated exclusively in response to each individual bacterium, if any, are listed adjacent to each bacterium. These biological processes are also separated by the horizontal demarcation line depending on whether they are upregulated (above) or downregulated (below) by each infection. The relative level of virulence of each bacterium is indicated by the number of stars: *Low virulence, **Intermediate virulence, ***High virulence. The type of bacterial peptidoglycan is indicated by the color of the stars: orange (bacteria with Lys-type PGN) and blue (bacteria with DAP-type PGN). The clustering of infection conditions (shown at the bottom of the graph) is based on the similarities of the expression patterns measured at 12 h.

In general, the largest number of differentially expressed genes was observed at 12 h post-infection. However, a substantial number of genes continued to be differentially regulated at 36 h and 132 h post-inoculation (Fig 2A), presumably in part because the hosts continue to carry their bacterial infections at these later time points and/or because infection induces long-term changes

in host physiology. Samples for the 36 h and 132 h time points were not available for infections with the highly virulent bacteria because they rapidly killed all their hosts. For the remaining infections, however, the number of upregulated genes at 12 h after infection was 1.6 times higher than the average number of genes that continued to be induced at 36 h and 132 h post-infection. Likewise, there were 2.8 times as many downregulated genes at 12 h post-infection than there were at later time points. These results demonstrate that the early transcriptional response to infection is larger than the sustained one, probably because the early response includes both an injury-induced transcriptional regulation and an aggressive initial immune response that is not yet tuned to bacterial titer or growth state within the host [22].

Major axes of variation in the transcriptional response to infection

We sought to investigate the source of differences in the host response to various infections. We began by looking at the number of genes regulated by the host in response to each bacterium. The number of differentially regulated genes fluctuated considerably across bacterial infections (Fig 2A). Flies inoculated with heat-killed *E. faecalis* and *P. rettgeri*, as well as flies challenged with avirulent bacteria, such as *E. coli* and *M. luteus*, induced the lowest number of genes. However, the number of genes regulated in the host did not directly correlate with the level of bacterial virulence. For example, despite the fact that both bacteria rapidly killed all flies, infection with *S. aureus* differentially regulated the expression of 1,193 genes, while *P. sneebia* infection altered the transcription of only 187 genes (Fig 2A). In addition, there was a large variability in the number of genes regulated in response to different benign bacteria. Across all time points, *M. luteus* infection changed the expression of 794 genes, while *E. coli* infection affected only 446 genes (Fig 2A). These results indicate that the breadth and the specificity of the host transcriptomic response

is largely independent of virulence.

Next, we aimed to identify specific genes that underlie the transcriptomic differences in response to distinct infections. We focused on the first two principal components of our PCA analysis (Fig 1B), which respectively explain 34.0% and 27.2% of the variance in gene expression. We found that 73 of the top 100 genes contributing to the first principal component (PC1) and 75 of the 100 genes contributing most to the second principal component (PC2) are known targets of the Toll or Imd pathways (Fig 1C and S4 Fig), confirming that these two pathways are key regulators of the specificity of the host response [7]. The genes that contributed most to PC1 included antimicrobial peptide genes (*Dpt, AttA, Drs*, and *Mtk*) as well as signaling components of the Toll (*Spz* and *PGRP-SA*) and Imd (*PGRP-LC*, *PGRP-SD, PGRP-LB,* and *Rel*) pathways themselves (Fig 1C). Additionally, the expression of Turandot genes, stress peptides regulated by the JAK-STAT pathway, was strongly variable between infections, indicating that differential activation of the JAK/STAT pathway also contributes to PC1. Interestingly, metabolic genes involved in lipid synthesis (*ACC*), the Leloir pathway (*Galk*), and trehalose and glycogen synthesis (*Tps1*, *UGP*, and *Hex-C*) were downregulated to different levels depending on the infection, indicating that different bacteria alter host metabolism in unique ways. In general, PC1 appeared to reflect the transcriptional magnitude of the response to infection. Genes that contributed most to PC2 include target genes of the Toll pathway, including melanization and coagulation-related genes (*MP1* and *fondue*) (Fig 1C), as well as immune-induced proteins of the IM cluster. PC2 also included genes downregulated by infection that are involved in sugar digestion (i.e. the *Maltase* cluster), as well as P450 enzymes known for their functions in oxidoreduction reactions (i.e. *Cyp* genes). Flies infected with Gram-positive bacteria (Lys-type PGN) and Gram-negative bacteria (DAP-type PGN) were separated from each other on PC2, confirming that the type of bacterial

peptidoglycan is a major parameter influencing the global response to infection (Fig 1B, Fig S3A) [7]. A heatmap showing the expression level of genes that contribute the most to each PC can be found in Fig S4.

Subsequently, we asked whether any differentially regulated genes were unique to a specific bacterial condition. We defined unique genes as those that significantly changed their expression in one and only one infection condition, regardless of time points, thus reflecting the response to a particular bacterium rather than temporal variations in the response to this bacterium. Without exception, we found that infection with each bacterium regulates an exclusive set of genes. The number of uniquely regulated genes varied dramatically across bacterial infections (Fig 2A). For instance, *P. sneebia* infection resulted in unique regulation of only 6 genes, whereas *S. aureus* infection exclusively regulated 336 genes. In order to determine what portion of the host response is specific to individual bacteria, we calculated the percentage of differentially expressed genes that were unique to each infection (Fig S3C). We found that this number also differs widely between bacteria. For instance, 20.1% of genes upregulated in response to *S. aureus* were exclusive to this infection, while only 7.1% of genes upregulated by *E. faecalis* infection were unique to this condition. Evaluating Gene Ontology (GO) terms associated with the genes uniquely altered by individual infections revealed bacteria-specific responses in some infection conditions (Fig 2A). For example, *S. aureus* infection induced apoptosis-related genes and downregulated genes involved in glutathione and carboxylic acid metabolism. In contrast, infection with *P. entomophila* upregulated genes involved in epithelial cell proliferation and strongly decreased the expression of genes associated with cellular respiration and the electron transport chain. At the same time, infection by *P. rettgeri* specifically downregulated genes involved in the translation machinery (Fig 2A). All the GO gene categories we identified are linked to stress responses that aim to

maintain cell homeostasis (cell death and tissue repair) or metabolic homeostasis, suggesting that the unique physiological and virulence interactions of each bacterium with the host induce a specific set of organismal responses. Altogether, our results demonstrate that the host response to infection is shaped by a combination of immune potency, metabolic impact, and physiological alteration.

Identification of a core host response to infection

Next, we set out to identify the core set of genes that are regulated in response to most or all bacterial infections. We defined the core genes as those that are differentially expressed in response to 7 or more bacteria on at least one time point post-infection. We set the cutoff at 7 bacteria because we were concerned that requiring differential expression in response to all 10 infections would be overly restrictive. Specifically, we had reservations about the artificial omission of genes in cases where the bacteria are rapidly cleared from all or most hosts (e.g. *M. luteus* and *Ecc15*) and in cases where the bacterium might suppress or evade the canonical response (e.g. *P. sneebia*; [23]). Using these criteria, we identified a core response of 252 genes. This included 166 upregulated genes (Fig 3A and S1 Table) and 86 downregulated genes (Fig 3B and S1 Table). The set of core genes is fairly robust to the criteria for inclusion, decreasing only to 135 genes induced and 54 genes repressed when inclusion required differential expression in response to 8 of the bacterial conditions. Similarly, the numbers increased only to 216 genes induced and 136 repressed when inclusion was relaxed to 6 of the bacterial infections.

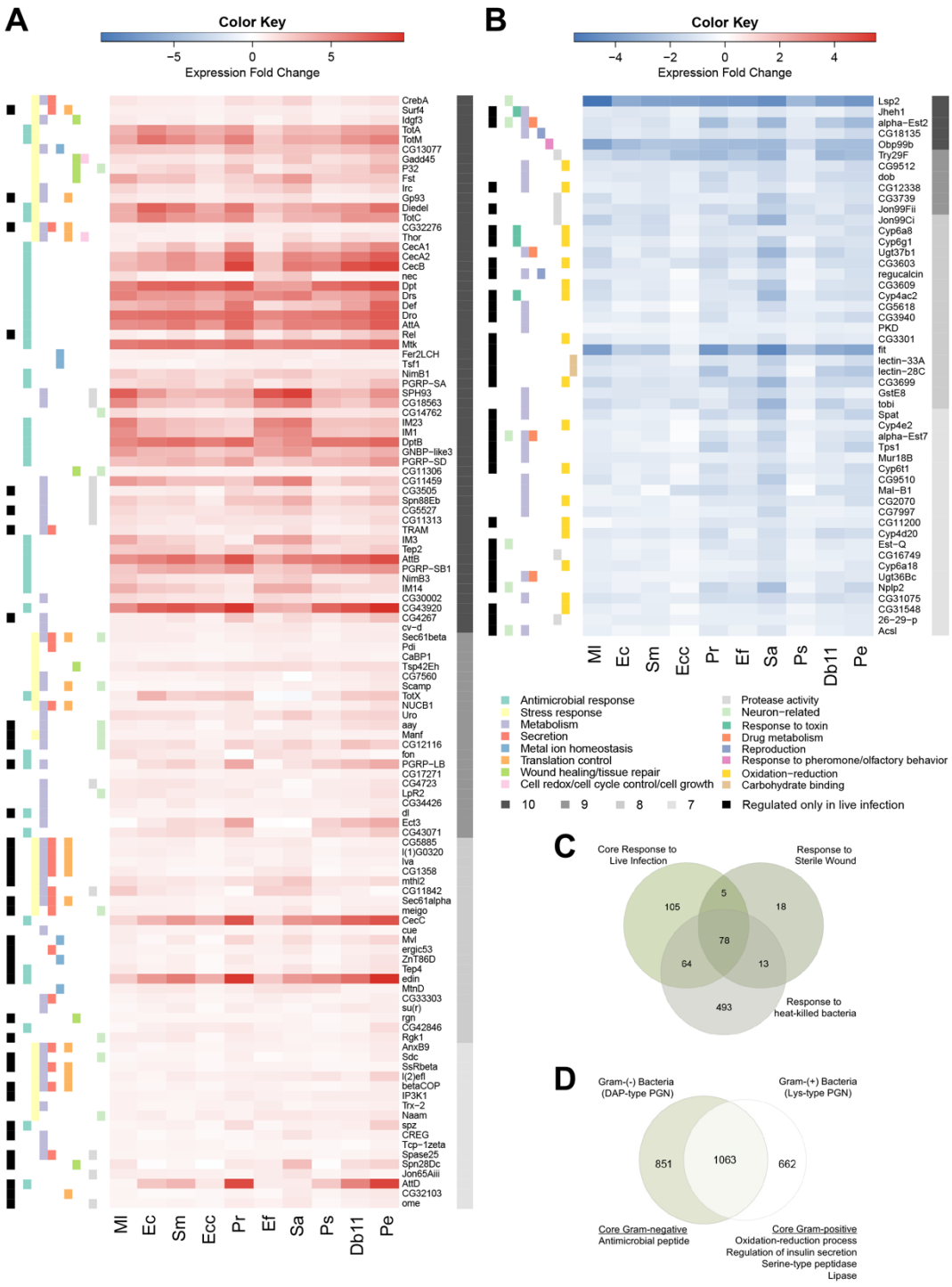

Figure III.3. **Systemic infection triggers a core host response**
Heatmap showing the expression level ($\log_2$ fold change) of selected core upregulated (A) and downregulated (B) genes for all 10 bacteria. Core genes are differentially expressed in response to infection by 7 or more bacteria. A gray scale on the right side of each heatmap indicates the number of bacterial infections that significantly change the expression of a given gene (dark gray = 10, medium gray = 9, light gray = 8, and very light gray = 7). A color scale on the left side of each

heatmap denotes the functional categories that each gene belongs to, and the legend for each color is listed at the bottom of the graph. (C) Venn diagram showing the intersection of core genes, sterile wound genes, and genes differentially regulated by challenge with heat-killed bacteria. (D) Venn diagram indicating the number of genes differentially regulated only in response to infection with Lys-type peptidoglycan (PGN) bacteria (right), DAP-type PGN bacteria (left), and those genes differentially expressed by challenge with both types of bacteria. GO terms associated with genes exclusively regulated by infection with Lys-type PGN bacteria or DAP-type PGN bacteria are listed.

Within the core, 78 genes were also regulated in response to sterile wound alone or to challenge with heat-killed bacteria (Fig 3C). Most of the genes regulated by injury were also regulated by challenge with live or dead bacteria (96/114 genes), which is congruent with the fact that the infection method inherently inflicts injury. However, the core response to live infection was markedly distinct from the response to heat-killed bacteria. Of our core genes, ~40% (105/252 genes) were differentially expressed in response to live infections but not in response to challenge with heat-killed bacteria. Moreover, we found 493 genes that were differentially regulated by treatment with heat-killed bacteria but were not part of the core response to live infection (Fig 3C). Of those 493 genes, 164 were uniquely regulated in response to heat-killed bacteria and not in response to any live infection (Fig S5A). To determine whether genes exclusively regulated in response to heat-killed bacteria are simply artifacts of weak statistical detection, we relaxed the cutoff to a False Discovery Rate (FDR) <0.1 for classifying a gene as differentially expressed during infection. Even with this more lenient threshold, 61.6% of the 164 genes that were uniquely regulated in response to heat-killed bacteria were still not differentially regulated in response to any live infection. Our results, therefore, not only show that the response to live infections is fundamentally different from the biological challenges that simple injury and immune activation pose, but also demonstrate that challenge with dead bacteria induces a response that does not occur as a consequence of infection by live bacteria.

In 2001, a study identified a set of genes that are differentially expressed after infection with a combination of *E. coli* and *M. luteus* [6]. These genes became known as *Drosophila* Immune-Regulated Genes (DIRGs). We compared our set of 252 core response genes to the 381 DIRGs and found that only 84 of them were previously identified as DIRGs (Fig S5B). Intriguingly, the DIRGs identified in the previous study included 279 genes that were neither in our core response nor regulated by challenge with heat-killed bacteria (Fig S5B), and 246 of these DIRGs were not induced in the present study even by infection with *M. luteus* or *E. coli* (Fig S5C). These discrepancies may originate from differences in *Drosophila* genotype or rearing conditions, bacterial genotype, or experimental variation. Alternatively, they could imply that infection with a mixture of two bacteria can lead to the activation of a specific set of genes, different from each mono-microbial infection. When we compared our total number of differentially regulated genes (2,423) to the DIRGs, we found that our study has identified 2,197 novel infection response genes, including 168 new core genes. Thus, our data offer a more comprehensive list of infection-responsive genes that is expanded both because of the sensitivity of RNA-seq technology over the previous microarrays and because of the broader diversity of bacteria used in our experiment.

To investigate the biological functions of our newly identified core response genes, we evaluated GO categories enriched in the core (Fig 3A-B). Upregulated core genes were primarily annotated with immune functions, such as Toll pathway and defense response to Gram-negative bacteria. This group also included genes involved in metabolism, including glycosaminoglycan metabolic process, carbohydrate metabolism, and metal ion transport. Additionally, core upregulated genes have a role in cellular and tissue processes, with genes acting in tissue repair, response to oxidative stress, cellular homeostasis, co-translational protein targeting to membrane, and protein targeting to ER (Fig 3A). The core downregulated genes were annotated with functions

such as oxidation-reduction and starch and sucrose metabolism (Fig 3B). Core genes can be separated into two groups: genes regulated in response to live infections only and genes regulated in response to both live infections and heat-killed bacteria (Fig 3C). The 78 core genes that were also differentially expressed in the wound-only control and in the heat-killed bacteria control included genes coding for AMPs, PGRPs, Turandot (*Tot*) genes, and other classical targets of the Toll and Imd pathways [24]. Genes regulated only in response to live infection included key transcription factors of the immune system, such as *Rel* and *dl*, and were associated with biological processes such as metabolism, oxidation-reduction, regulation of iron ion transmembrane transport, and secretion. Altogether, these data indicate that heat-killed bacteria mostly trigger classically defined immune responses, while live infections regulate a set of additional biological processes that presumably reflect physiological interactions between the host and invading pathogen. These processes, including metabolic rewiring, response to stress and damage, cellular translation, and secretion, could act as physiological adaptations or buffers to the stress and damage imposed by infection.

The hypothesis that *D. melanogaster* has a distinct response to infection by Gram-positive (Lys-type PGN) versus Gram-negative (DAP-type PGN) bacteria dominated the field for most of the 1990s and 2000s [25]. To address this hypothesis, we characterized the transcriptional response to Gram-positive versus Gram-negative bacterial infection in our study. We found that 662 genes are regulated only by infection with Gram-positive bacteria, 851 genes are regulated only by Gram-negative infection, and 1,063 genes are regulated by infections with bacteria of both Gram types (Fig 3D). Of the 662 genes exclusively regulated by Gram-positive bacteria, only 20 (*Cyp309a1*, *daw, CG31326,* etc.) are upregulated and 8 are downregulated by all three Gram-positive bacteria. Similarly, amongst genes regulated specifically by Gram-negative bacteria, only 1 gene is

upregulated (*AttD*) and no genes are downregulated in response to all 7 Gram-negative bacteria. Our data suggest that the stereotypical response to Gram-negative infection also occurs as a consequence of Gram-positive infection, such that there is no large cohort of genes responding exclusively to Gram-negative infection. To confirm this, we performed RT-qPCR on *Dpt* and *Drs* transcripts as a proxy for activity of the Imd and Toll pathways, respectively [7]. We found that infection by most of our 10 bacteria induced both pathways, although to significantly different levels (Fig S6). Our results generally confirm the notion that the Toll pathway is more responsive to infection with Gram-positive (Lys-type PGN) bacteria and the Imd pathway is more reactive to infection with Gram-negative (DAP-type PGN) bacteria, but also make clear that the differences in pathway activation are quantitative and not qualitative or binary.

Infection induces long-term changes in global host transcription

Since the bacteria belonging to the low and intermediate virulence categories do not kill all hosts, we followed the dynamics of gene expression in surviving hosts over several days. In particular, we aimed to contrast the sustained transcriptional response of flies that had cleared their infections to undetectable levels (i.e. after infection with *M. luteus* or *Ecc15*) to that of flies carrying chronic infections (i.e. *E. coli*, *S. marcescens* Type strain, *P. rettgeri* and *E. faecalis*). We hypothesized that persistent bacteria would continue to elicit a response from the host, which would be absent in flies that have cleared all bacteria. To test this idea, we determined whether genes "recover" from bacterial infection. We defined recovery in terms of gene expression: a gene that has recovered is differentially expressed at 12 and/or 36 h post-infection but returns to pre-infection levels by 132 h (5.5 days) after inoculation. We found that, on average, a minimum of 50% of the genes that are differentially regulated by each infection returned to basal levels by our last time

point (Fig 4A), and this was the case even in hosts infected with persistent infections. The percentage of genes that fully recovered was substantially higher in moderately virulent infections (*P. rettgeri*: 79.8% and *E. faecalis*: 71.1%) than in benign infections (*E. coli*: 54.5% and *S. marcescens* Type: 55.5%), perhaps in part as a consequence of the higher number of genes induced upon infection with these bacteria (Fig 4A). Surprisingly, we also observed that only 56.5% and 58.7% of genes recovered in *M. luteus* and *Ecc15* infections, respectively, even though the majority of hosts (≥85%) survive these infections and the bacteria are eliminated (i.e. their levels fall below our detection threshold) within two days. These results demonstrate the complexities of the transcriptional response to infection. While there can be a substantial lingering transcriptional effect in flies that successfully cleared an infection, a subset of differentially regulated genes may return to basal levels even in chronically infected flies that continue to carry bacteria.

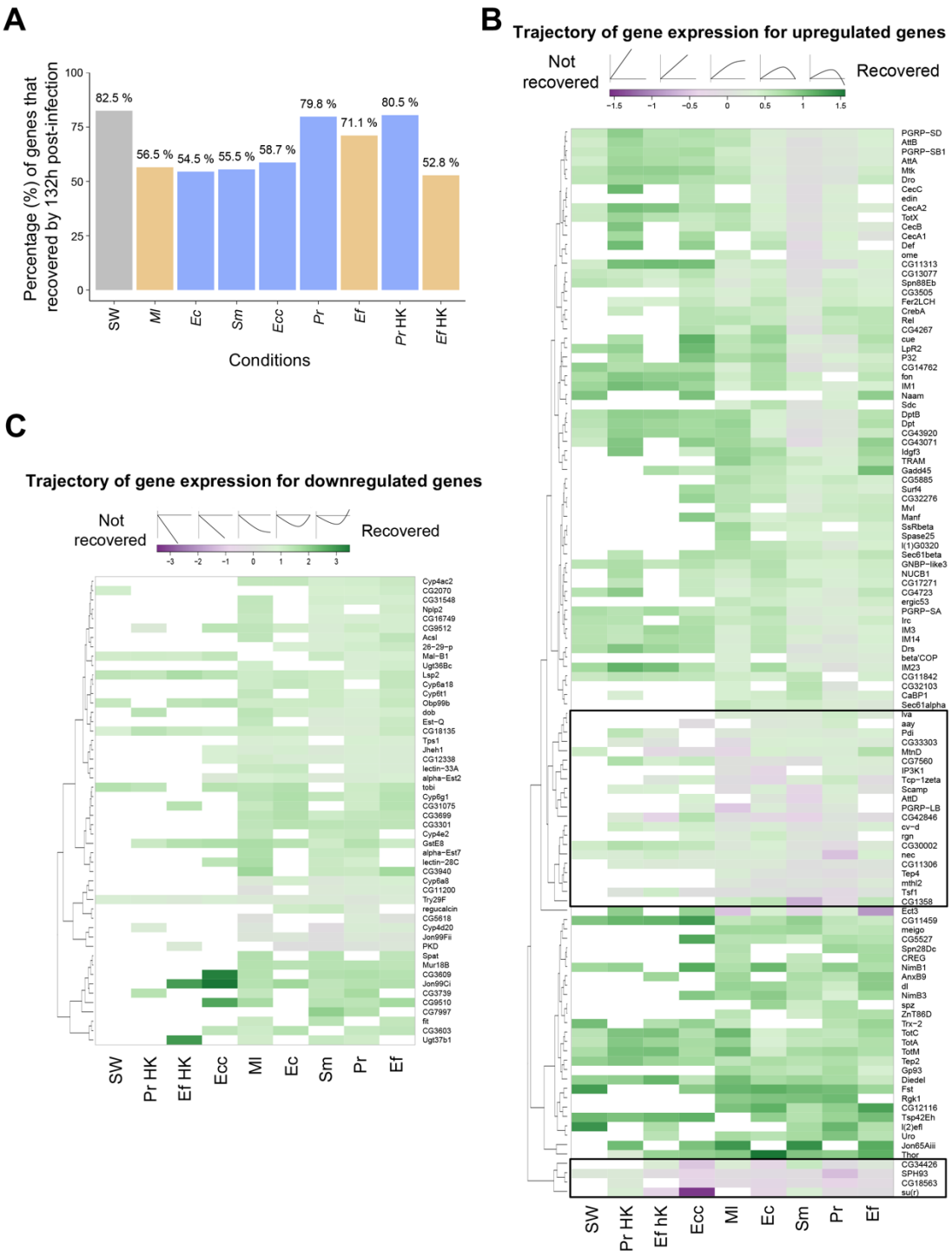

Figure III.4. **Bacterial infection elicits long-term changes in global host transcription**
(A) Percentage of genes found to be differentially expressed at 12 and/or 36 h post-infection in a given condition that returned to basal levels of expression (recovery) by 132 h post-infection. (B) Gene expression trajectory of core upregulated genes. By 132 h post-infection, the expression level of core upregulated genes continued to increase (purple), plateaued (gray), or returned to basal, pre-infection levels (green) as indicated by the graphic above the color key. A black box encloses

genes that did not recover in most infections (as denoted by the purple color). (C) Trajectory of gene expression for core downregulated genes. By the last time point (132 h), the transcript levels of core downregulated genes continued to decrease (purple), plateaued (gray), or returned to basal expression levels (green) as illustrated on the graphic above the color key. Genes that were not differentially regulated by a given condition are marked in white.

Next, we evaluated how the core upregulated and downregulated genes change in expression level over time (Fig 4B-C). We quantified the degree of recovery for each gene by comparing the fold change in expression at 132 h after infection to the fold change at either 12 h or 36 h, whichever was the highest if the gene was upregulated or the lowest if the gene was downregulated. In general, sterile wound and challenge with heat-killed bacteria resulted in the regulation of fewer core genes than live infection, and most of these genes recovered to pre-infection expression levels by 132 h post-challenge (Fig 4B-C). Core genes induced by *Ecc15* and *M. luteus* showed similar kinetics, and most genes had recovered or were on their way to recovery by 132 h, suggesting that the core response is not sustained in the absence of these bacteria. In contrast, core genes induced by *S. marcescens* Type, *P. rettgeri,* and *E. faecalis* did not recover as much, in agreement with the idea that infections with persistent bacteria continuously stimulate the core response. This paradigm was, however, not true for downregulated genes, as most downregulated genes did recover or were in the process of recovery by 132 h regardless of which bacteria was used for infection. Interestingly, we noticed that a group of genes did not recover at all in most conditions but continued to be upregulated over time (boxed in Fig 4B). These included effector genes of the immune response (*AttD* and *Tep4*), regulators of iron homeostasis (*Tsf1* and *MtnD*), and negative regulators of the immune response (*PGRP-LB*, *nec*). Genes like *SPH93* and *su(r)* never returned to their basal expression levels in flies infected with *Ecc15* or *M. luteus*. Additionally, while the transcript levels of most antimicrobial peptide genes decreased over time, they never returned to basal, pre-infection levels, suggesting that the effect of infection lingers for

several days after bacteria are eliminated.

CrebA is regulated in the fat body upon infection by the Toll and Imd pathways

Having identified a core transcriptional response to infection, we set out to find key regulators of that response. We used i-cisTarget to identify transcription factor binding motifs enriched in the regulatory regions of our core genes [26,27]. Using this approach, we found enrichment in putative binding sites for Relish (Rel), Dif/Dorsal, Schnurri (Shn), CrebA, Atf6, Xbp1, and Tbp in the regulatory regions of upregulated core genes (Fig 5A and S2 Table). Dif/Dorsal and Relish are the terminal transcription factors of the Toll and Imd pathways, respectively; therefore, finding enrichment for their predicted binding sites is in agreement with the central role that these pathways play in the immune response. Our data also agree with published reports showing that the TGF-beta pathway upstream of *shn* and the *Atf6* transcription factor are important to survive infection [28,29]. Transcription factor binding site enrichment analysis of the repressed genes revealed putative binding sites for the Lola and GATA transcription factors (S3 Table).

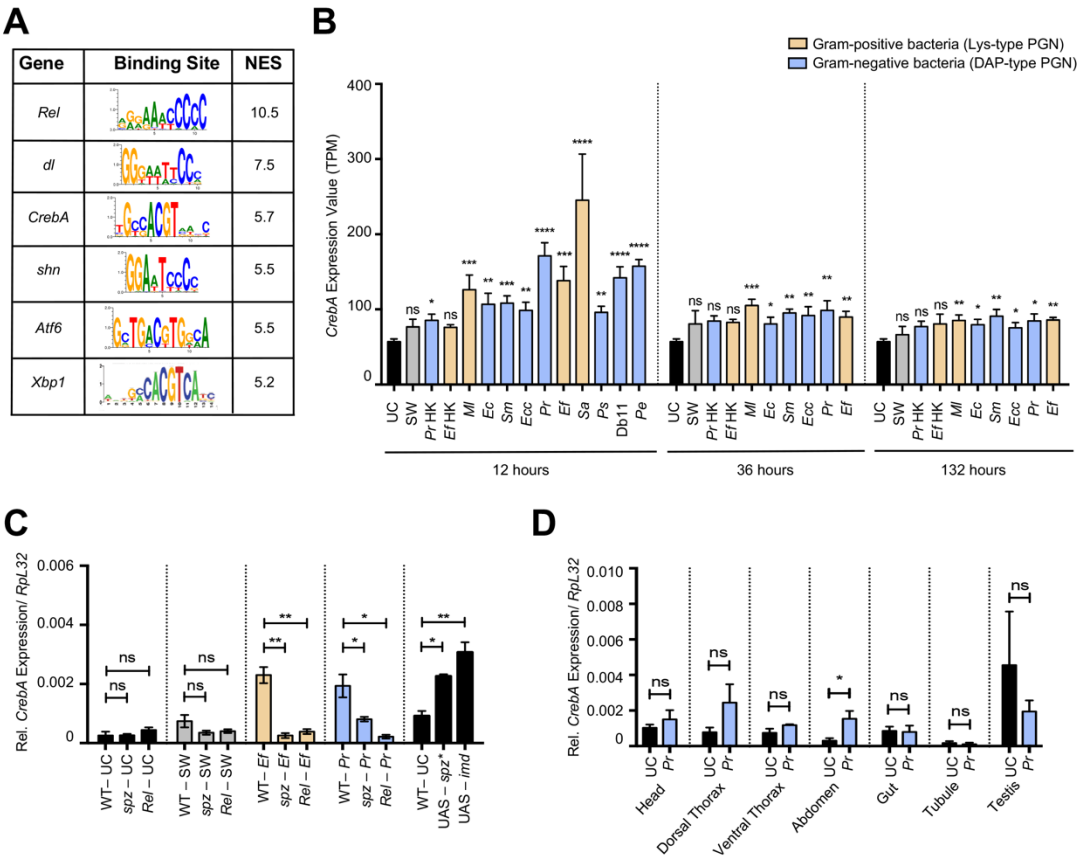

Figure III.5. *CrebA* is a core transcription factor regulated by Toll and Imd in the fat body
(A) Subset of transcription factors whose predicted binding sites are enriched in the promoter regions of core upregulated genes. The table includes the transcription factors' gene symbols, consensus binding sites, and their normalized enrichment scores (NES), which indicate the degree to which a binding site is overrepresented at the top of a ranked list of binding sites. (B) RNA-seq expression values in TPM (transcripts per million) of *CrebA* at 12, 36, and 132 h after infection with all 10 bacteria. (C) RT-qPCR of *CrebA* levels in Rel^{E20} and spz^{rm7} mutants and wildtype flies following: no challenge (UC), sterile wound (SW), infection with *E. faecalis* (*Ef*), and infection with *P. rettgeri* (*Pr*). In the last histogram, WT indicates wildtype flies given no challenge, UAS-spz* denotes *CrebA* expression in the absence of challenge when an activated form of Spz is ubiquitously overexpressed, and UAS-imd shows *CrebA* expression in flies that constitutively overexpress Imd in the absence of challenge. (D) RT-qPCR of *CrebA* levels in dissected organs and body parts (head, dorsal thorax, ventral thorax, abdomen, gut, Malpighian tubule, and testis) following infection with *P. rettgeri*. Mean values of at least three biological replicates are represented ±SE. *p<0.05 **p<0.01 ***p<0.001 ****p<0.0001 in a Student's t-test.

In addition to the i-cisTarget analysis, we searched for genes encoding transcription factors within our list of core upregulated genes. We identified 3 transcription factors in the defined core that are upregulated themselves by infection: *Rel*, *dorsal*, and *CrebA* (Fig 5B). Although *Dif* is

required to activate Toll pathway signaling in response to bacterial infection in *Drosophila* adults and *dorsal* is not [30], we surprisingly found that *Dif* is not significantly upregulated in response to any of the 10 bacteria tested.

CrebA is the single *Drosophila* member of the Creb3-like family of transcription factors [31]. We found the predicted DNA motif bound by CrebA (TGCCACGT, see Fig 5A for position weight matrix [32]) in 71 genes upregulated by infection, including 18 upregulated core genes (Fig S7A). *CrebA* is itself significantly induced upon infection by all 10 bacteria (Fig 3A and 5B). To validate our RNA-seq results on *CrebA* expression, we infected a new group of flies with *P. rettgeri* and *E. faecalis* and measured *CrebA* transcript levels at 12 h post-inoculation. In agreement with our RNA-seq data, we confirmed that *CrebA* expression is upregulated in response to infection with *P. rettgeri* (p=0.0026) and *E. faecalis* (p=0.0147) (Fig S7B). These results demonstrate that *CrebA* is a transcription factor induced by infection and is potentially a key regulator of the core response.

To identify the molecular mechanisms that control *CrebA* transcription in response to infection, we scanned 2 kb upstream and 2 kb downstream of the *CrebA* transcription start site for potential transcription factor binding sites using MatInspector (Genomatix) [33]. Within this region, we found an enrichment of putative binding sites corresponding to the transcription factors Dif/Dorsal and Relish. There were 12 predicted Relish binding sites, 16 predicted Dif binding sites, and 13 predicted Dorsal binding sites flanking the *CrebA* gene, suggesting that immune pathways may induce the expression of *CrebA* (Fig S7C). To confirm regulation of *CrebA* by the Toll and Imd pathways, we quantified *CrebA* expression by RT-qPCR 12 h after infection with *P. rettgeri* and *E. faecalis* in wildtype (WT) flies, flies deficient for the Imd pathway (Rel^{E20}), and flies deficient for the Toll pathway (spz^{rm7}) (Fig 5C). *CrebA* expression was significantly reduced in

both *Rel*^{E20} (p=0.0456 for *P. rettgeri* and p=0.0020 for *E. faecalis*) and *spz*^{rm7} (p=0.0118 for *P. rettgeri* and p=0.0026 for *E. faecalis*) mutants relative to wildtype controls, indicating that both the Imd and Toll pathways contribute to infection-induced *CrebA* upregulation. We then tested whether activation of the Imd or Toll pathway is sufficient to upregulate the level of *CrebA* expression in the absence of infection. Using the temperature-sensitive *UAS/Gal4/Gal80*^{ts} gene expression system to ubiquitously drive Imd or an active form of Spz (Spz*), we stimulated Imd and Toll pathway activity in adult flies [34,35]. Transgenic activation of either the Imd or Toll pathway in the absence of infection was sufficient to significantly increase *CrebA* transcript levels in *D. melanogaster* adults (p=0.0114 for UAS-spz* and p=0.0062 for UAS-imd) (Fig 5C). Altogether, our results demonstrate that the Imd and Toll pathways are both necessary and sufficient to regulate *CrebA* transcription upon infection.

In order to identify the tissue(s) and/or organ(s) within the fly that upregulate *CrebA* expression upon bacterial challenge, we infected wildtype flies with *P. rettgeri* and dissected out the following tissues and body parts at 12 h post-infection: head, dorsal thorax (including wings and heart), ventral thorax (including legs), digestive tract (crop, midgut, and hindgut), Malpighian tubules, testes, and abdomen (abdominal fat body). The abdomen was the only tissue that exhibited significant upregulation of *CrebA* as determined by RT-qPCR (p=0.0315), suggesting that *CrebA* may be regulated in the fat body upon infection (Fig 5D). We therefore knocked down *CrebA* expression by RNAi (via 3 independent RNAi constructs) using 2 separate fat body drivers, *c564-Gal4* and *Lpp-Gal4*, and quantified *CrebA* expression by RT-qPCR in whole flies 12 h after infection with *P. rettgeri*. The combination of 2 *CrebA* RNAi constructs (B and C) with the drivers fully prevented *CrebA* induction upon infection with *P. rettgeri*. In the case of the third RNAi construct (A), *CrebA* was significantly upregulated by infection with *P. rettgeri* (p=0.0002), but

the induction was significantly lower (p=0.0442) than the expression level observed in infected wildtype samples (Fig S7D). These data indicate that the cells of the fat body represent the primary site of *CrebA* induction. In sum, our data suggest that the Toll and Imd pathways regulate the expression of *CrebA* in the fat body in response to infection.

CrebA is required to survive infection and promotes tolerance of infection

We next asked whether *CrebA* is required for the host to survive infection. Since strong loss-of-function *CrebA* mutants are embryonic lethal, we tested the role of *CrebA* in response to infection by knocking it down in the fat body of adult flies using 3 independent RNAi constructs expressed under the control of the *c564-Gal4* driver (*Gal80^{ts}; c564-Gal4 > UAS-CrebA-IR*) and, separately, the *Lpp-Gal4* driver (*Gal80^{ts}; Lpp-Gal4 > UAS-CrebA-IR*) [36]. Because the *c564-Gal4* driver expresses strongly in both the fat body and hemocytes, we additionally tested the requirement for *CrebA* in the response to infection in hemocytes (*Hml-Gal4 > UAS-CrebA-IR)*. All *CrebA* fat body knockdown flies exhibited increased susceptibility to systemic infection with *P. rettgeri* ($p<0.0001$) (Fig 6A and Fig S8A), while hemocyte-specific knockdown did not lead to any significant increase in mortality (Fig S8B). When *CrebA* was knocked down in the fat body, nearly 100% of the flies died, and most of the death occurred during the first 24 h following infection. In contrast, almost 50% of control flies survived the infection for at least 7 days (Fig. 6A and Fig S8A). To confirm that the survival phenotype observed in *CrebA* RNAi flies upon infection was solely due to loss of *CrebA* expression, we co-expressed a *CrebA* RNAi construct and a *CrebA* overexpression construct in flies (*Gal80^{ts}; c564-Gal4 > UAS-CrebA*, *UAS-CrebA-IR*) and infected them with *P. rettgeri*. We observed no significant difference between the survival of infected control flies and that of infected flies co-expressing both the RNAi and overexpression constructs,

indicating that changes in *CrebA* expression are uniquely responsible for the lowered survival phenotype observed (Fig 6A). We also infected *CrebA* RNAi flies with *E. faecalis* and found that *CrebA* RNAi flies were remarkably more susceptible to infection when compared to control flies ($p<0.0001$) (Fig 6B). In addition, *CrebA* RNAi flies died at a significantly faster rate than control flies when inoculated with *P. sneebia* ($p<0.0001$) (Fig 6C). Finally, infection with *Ecc15*, *S. marcescens* Type, and *E. coli* also killed more flies with *CrebA* expression blocked in the fat body than controls ($p=0.0013$ for *Ecc15*, $p=0.0004$ for *S. marcescens* Type, and $p=0.0028$ for *E. coli*) (Fig 6D-F). None of these latter three infections were lethal to wildtype control flies, but approximately 30% of *CrebA*-deficient flies succumbed to infection. Collectively, our results demonstrate that *CrebA* is generally required to survive bacterial infection.

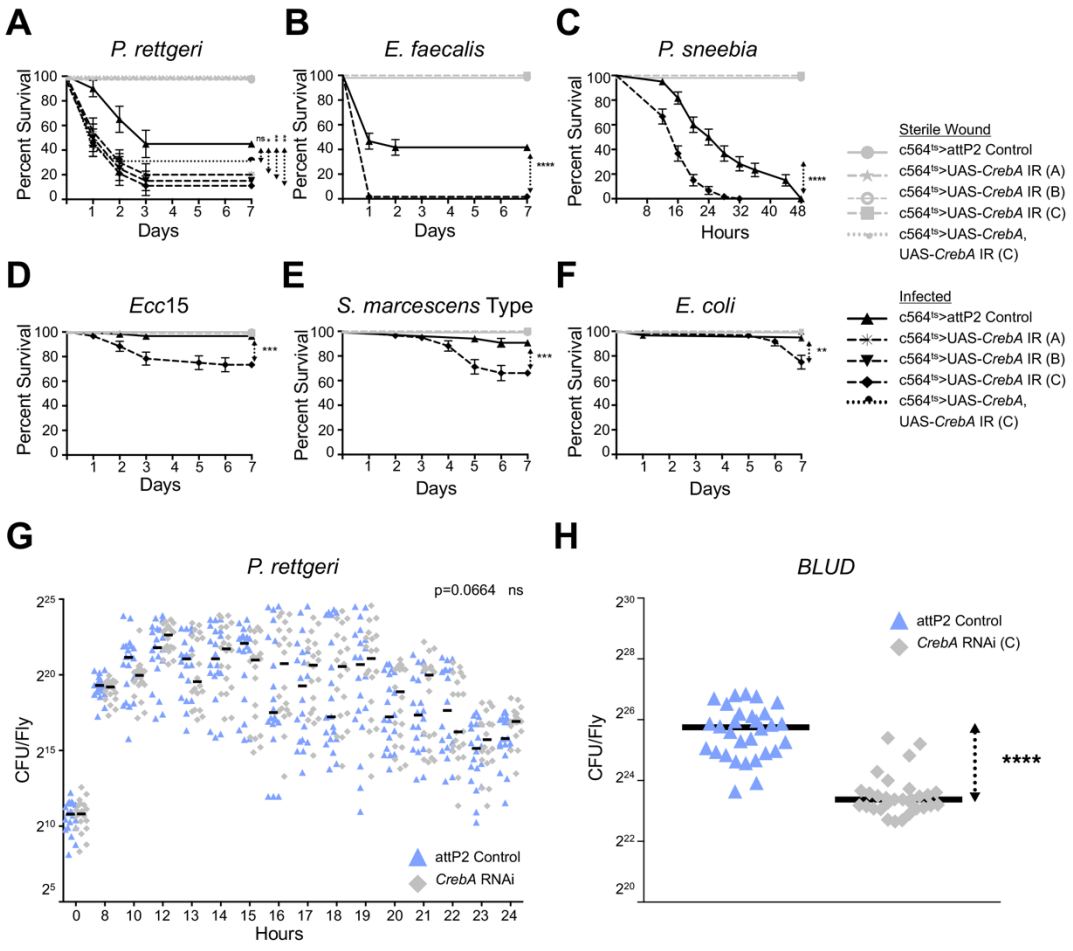

Figure III.6. *CrebA* promotes infection tolerance
Survival curves over 7 days (or 48 h in the case of *P. sneebia*) following infection of flies whose expression of *CrebA* is blocked with RNAi. *UAS-CrebA IR* (A), (B), and (C) indicate three distinct RNAi constructs that target *CrebA* transcripts. *UAS-CrebA*, *UAS-CrebA* IR refers to flies simultaneously co-expressing a *CrebA* RNAi and a *CrebA* overexpression construct. *attP2* is the background genotype control, in which *CrebA* is fully expressed. Knockdowns were driven in the fat body and hemocytes using a conditional c564 temperature sensitive driver. The curves represent the average percent survival ±SE of three biological replicates. *p<0.05 **p<0.01 ***p<0.001 ****p<0.0001 in a Log-rank test. Infections were performed with (A) *P. rettgeri*. (B) *E. faecalis*. (C) *P. sneebia*. (D) *Ecc15*. (E) *S. marcescens* Type. (F) *E. coli*. (G) Bacterial load time course of control flies and flies expressing *CrebA* RNAi in the fat body following infection with *P. rettgeri*. (H) *P. rettgeri* bacterial load upon death (*BLUD*) of wildtype controls and flies with *CrebA* expression knocked down by RNAi in the fat body. Three repeats are graphed together, with each symbol representing an individual fly's number of colony forming units (CFU). Horizontal lines represent median values for each condition. ****p<0.0001 in a Student's t-test.

To test whether the *CrebA* survival phenotype is due to a failure to control bacterial proliferation (a resistance defect) or a decrease in the ability to withstand infection (a tolerance defect), we monitored bacterial load in individual *CrebA* RNAi and control flies following *P. rettgeri* infection [37]. We focused our sampling on 1-2 h intervals over the first 24 h of infection, as this is the time when most of the *CrebA*-deficient flies succumbed. We did not find a significant difference in bacterial load between wildtype and *CrebA* knockdown flies at any measured time point (p=0.0664), indicating that *CrebA* RNAi flies are able to control bacterial load similarly to control flies (Fig 6G). To corroborate these results, we quantified bacterial load following infection with *P. rettgeri* in flies where *CrebA* was knocked down by a different RNAi construct and in flies co-expressing a *CrebA* RNAi construct and a *CrebA* overexpression construct (*Gal80^{ts}; c564-Gal4 > UAS-CrebA*, *UAS-CrebA-IR*). Again, we did not observe any significant difference in bacterial load between wildtype and *CrebA* knockdown flies (p=0.3208) or between wildtype and *CrebA* rescue flies (p=0.3030) (Fig S8C). To evaluate whether *CrebA* knockdown flies are less resistant to other pathogens, we measured bacterial load in individual flies following *E. faecalis* or *Ecc15* infection. In agreement with the results of our *P. rettgeri* experiments, we did not find a significant

difference between wildtype and *CrebA*-deficient flies at the time points sampled (p=0.4204 for *E. faecalis* and p=0.7253 for *Ecc15*) (Fig S8D-E), suggesting that *CrebA* knockdown flies do not have a defect in resistance to infection.

We previously demonstrated that flies die at a stereotypical and narrowly distributed bacterial load, the bacterial load upon death (*BLUD*), which represents the maximum quantity of bacteria that a fly can sustain while alive [38]. We therefore sought to determine whether *CrebA* RNAi flies have a lower *BLUD*, which would indicate a reduced tolerance of infection. We quantified the bacterial load of individual flies within 15 minutes of their death and found that *CrebA* RNAi flies died carrying a significantly lower bacterial load than control flies ($p<0.0001$) (Fig 6H). These data demonstrate that while *CrebA*-deficient flies control bacterial growth normally, they are more likely to die from infection, and they die at a lower bacterial load than wildtype flies. Therefore, the transcription factor *CrebA* acts to promote tolerance of infection.

Loss of *CrebA* alters the expression of secretory genes during infection

In order to identify the complete set of genes directly and indirectly regulated by *CrebA* upon infection, we performed RNA-seq on the fat bodies of wildtype flies and flies in which we knocked down *CrebA* in the fat body. We collected samples from both genotypes in unchallenged conditions and 12 h after infection with *P. rettgeri*. In total, we found that only 104 genes were downregulated in *CrebA* knockdown fat bodies compared to wildtype fat bodies following infection (S5 Table). These genes were associated with GO categories such as protein targeting to the ER, signal peptide processing, protein localization to the ER, and antibacterial humoral responses. Antimicrobial peptide genes of the *Cecropin* gene family (*CecA1*, *Cec*A2, *CecB*, and *Cec*C) showed partially reduced induction when *CrebA* expression was disrupted. Nevertheless,

they were still induced to extremely high levels (>200-fold) in *CrebA* knockdown fat bodies (Fig 7). Other antimicrobial peptide genes, such as *Dpt*, *Drs*, *Def*, and *AttC*, were expressed at similar levels in *CrebA* knockdown fat bodies compared to wildtype fat bodies, results corroborated by RT-qPCR analysis (Fig S9A-D). In contrast, a number of genes including sugar transporters and multiple lipases were upregulated upon infection in fat bodies deficient for *CrebA* but not in wildtype fat bodies. These data suggest that *CrebA* regulates immune, metabolic, and cellular functions during infection.

Gene Name	Function	*P. rettgeri* / UC: WT	*P. rettgeri* / UC: *CrebA* RNAi
SECRETORY PATHWAY			
ArfGAP1	Secretion	1.8	1.2
bai	Secretion	1.9	1.3
CG32276★	Secretion	3.0	2.0
CG5885★	Secretion	3.1	1.6
CG8860	Secretion	2.2	1.1
CrebA★	Secretion	7.3	4.1
ergic53★	Secretion	2.4	1.8
Grasp65★	Secretion	2.6	1.4
Gtp-bp	Secretion	2.3	1.2
loj	Secretion	2.5	2.1
Sec31	Secretion	1.5	1.3
Sec61beta★	Secretion	2.6	1.8
Sec63	Secretion	2.0	1.2
Spase12	Secretion	2.3	1.5
Spase25★	Secretion	2.6	1.5
Spp	Secretion	2.9	1.4
Srp19	Secretion	1.5	1.1
Srp72	Secretion	1.5	0.8
SrpRbeta	Secretion	1.7	1.1
Tapdelta	Secretion	2.4	1.7
TRAM★	Secretion	4.6	1.7
twr	Secretion	3.3	1.7
UNKNOWN			
CG30026★	Unknown	6.0	5.4
CG5791★	Unknown	1.3	1.0

Gene Name	Function	*P. rettgeri* / UC: WT	*P. rettgeri* / UC: *CrebA* RNAi
IMMUNITY			
CecA1★	Antimicrobial peptide	183.5	87.8
CecA2★	Antimicrobial peptide	422.5	352.0
CecB★	Antimicrobial peptide	1285.0	281.6
CecC★	Antimicrobial peptide	402.4	127.4
CG11313★	Coagulation	3.3	0.6
CG43114	Defense Response	0.7	0.4
Drs★	Antimicrobial peptide	77.5	50.7
GNBP-like3★	Antimicrobial response	3.3	2.8
IM14★	Antimicrobial response	2.2	1.7
METABOLISM			
SLC22A	Sugar transporter-like	3.9	6.2
CG32054	Sugar transporter-like	2.4	23.2
CG42825	Sugar transporter-like	0.7	3.9
Gld	Glucose dehydrogenase	0.7	2.9
CG17097	Lipase	0.9	9.1
CG18258	Lipase	1.0	6.3
CG18284	Lipase	1.1	11.3
CG31872	Lipid metabolic process	0.9	8.9
Uba5★	Mo-molybdopterin cofactor biosynthetic process	2.4	1.3
PROTEOLYSIS			
CG30091★	Serine-type endopeptidase activity	3.3	Not expressed
METAL ION HOMEOSTASIS			
ZnT86D★	Zinc ion transmembrane transporter activity	2.7	1.7
REPRODUCTION			
CG17271★	Multicellular organism reproduction	1.9	1.2

Color Legend ≥1.5 ≥2 ≥3 ≥5 ≥10 ≥100

★ Core gene

Figure III.7. *CrebA* regulates the expression of secretory pathway genes upon infection
Select list of 45 genes whose expression significantly changes in infected *CrebA* RNAi fat body samples compared to infected control samples. Gene symbols, functions, and fold enrichment of expression with infection (*P. rettgeri*/unchallenged) are indicated. Core genes are highlighted with a ★ symbol.

Previously, Fox and colleagues demonstrated that *CrebA* acts in the *Drosophila* embryo as

a direct regulator of secretory capacity and is both necessary and sufficient to activate the expression of many secretory pathway component genes [32]. We therefore asked whether *CrebA* controls secretion-related genes upon infection in the adult fat body. We found that the expression level of 32 secretion-related genes significantly increased upon infection with *P. rettgeri* in wildtype samples. However, the induction of these secretion-related genes was significantly lower ($p<0.05$) in *CrebA* RNAi fat body samples compared to wildtype fat body controls, a result that agrees with the findings of Fox et al. (Fig 7 and S5 Table). These 32 secretion-related genes we identified included core response genes that are central components of the cell's secretory machinery, including *TRAM*, *ergic53*, *Sec61β*, and *Spase25* (Fig 7). Using a separate set of samples from those of the RNA-seq, we further confirmed these findings by measuring *TRAM*, *ergic53*, *Sec61β*, and *Spase25* transcript levels by RT-qPCR in the fat bodies of flies infected with *P. rettgeri* at 12 h post-infection (Fig S9E-H). These four genes were significantly upregulated following infection with *P. rettgeri* in wildtype samples. However, we were not able to detect a significant increase in the levels of *TRAM*, *ergic53*, and *Sec61β* in *CrebA* RNAi fat bodies upon infection. The expression level of *Spase25* was significantly induced by infection with *P. rettgeri* even when *CrebA* expression was inhibited by RNAi in the fat body ($p<0.05$), but the induction was significantly lower ($p<0.001$) than the expression level observed in infected wildtype samples (Fig S9H). In sum, our data suggest that *CrebA* could act to regulate an increase in secretory capacity upon infection.

CrebA deficiency leads to ER stress upon bacterial challenge

Since our data suggested that *CrebA* may promote an increase in secretory capacity in the fat body upon infection, we hypothesized that loss of *CrebA* expression could lead to altered protein

secretion or defects in protein transport to the membrane. Accumulation of unfolded proteins or a decrease in protein secretion triggers endoplasmic reticulum (ER) stress, which in turn induces stereotypical pathways to limit the stress imposed on the cell. These pathways include IRE1α/XBP1-, PERK/ATF4-, and ATF6-mediated responses termed the unfolded protein response (UPR) [39,40]. Upon sensing of ER stress, *Xbp1* mRNA undergoes alternative splicing via IRE1α; *Xbp1* splicing is thus considered to be a marker of ER stress and of the activation of UPR [41,42]. To investigate whether loss of *CrebA* could trigger ER stress in fat body cells upon infection, we quantified the expression levels of both *Xbp1t* (total) and *Xbp1s* (spliced) in abdomens of wildtype and *CrebA*-knockdown flies under both unchallenged and infected conditions (Fig 8A-B). *Xbp1s* levels did not change upon infection in wildtype samples or differ between wildtype and *CrebA* RNAi samples in the absence of infection. However, *Xbp1s* levels spiked dramatically in *CrebA* RNAi fat body samples ($p=0.0289$) (Fig 8B) after infection, indicating that loss of *CrebA* upon bacterial challenge triggers ER stress in the fat body. Our data also revealed that *Xbp1t* expression was significantly higher in *CrebA* knockdown samples compared to wildtype samples following infection ($p=0.0144$) (Fig 8A). This result is in agreement with a previous study that suggested *Xbp1s* regulates *Xbp1* transcription [43]. To determine whether ER stress is induced in fat body cells directly, we labelled fat body cells *in vivo* by expressing a *dsRed* reporter under the control of the *Xbp1* regulatory sequence [44]. In agreement with our RT-qPCR experiments, we found that bacterial challenge did not induce *dsRed* expression in wildtype samples. However, infected *CrebA* RNAi fat body cells consistently expressed higher levels of *dsRed* compared to all other controls (Fig 8C). These results demonstrate that *CrebA* expression prevents the occurrence of ER stress in the fat body upon infection.

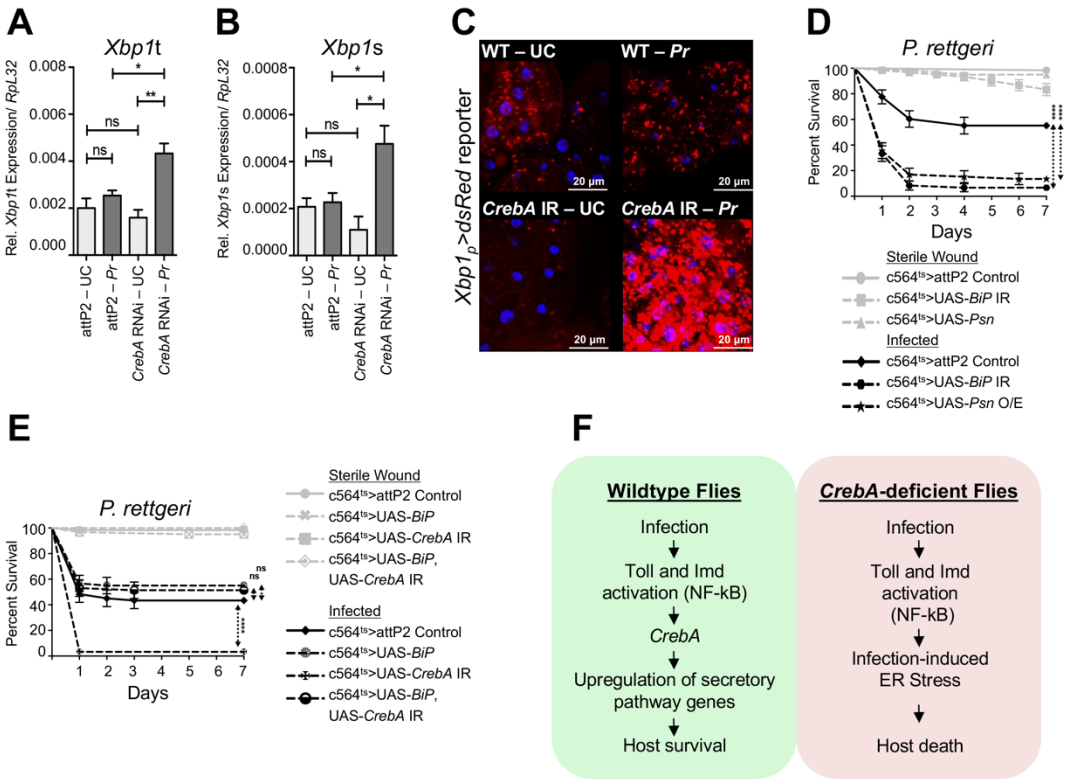

Figure III.8. Loss of *CrebA* triggers ER stress during infection
RT-qPCR of *Xbp1*t (unspliced, inactive) (A) and *Xbp1*s (spliced, active) (B) levels in the fat bodies of *CrebA* RNAi and wildtype flies in unchallenged and infected (*P. rettgeri*) conditions. An increase in the spliced form of *Xbp1* (*Xbp1*s) is a sign of ER stress. Mean values of three repeats are represented ±SE. *p<0.05 **p<0.01 in a Student's t-test. (C) Fat bodies from the $Xbp1_p$>*dsRed* reporter crossed to *CrebA* RNAi or wildtype flies in unchallenged (UC) and infected conditions (*Pr*). (D) Survival curves of flies with genetically-induced ER stress (*Psn* overexpression or *BiP* RNAi) in the fat body in unchallenged and infected conditions. (E) Survival curves over 7 days of flies co-expressing both the *CrebA* RNAi and *BiP* overexpression constructs in their fat bodies following infection with *P. rettgeri*. The curves represent the average percent survival ±SE of three biological replicates. ****p<0.0001 in a Log-rank test. (F) Upon infection, activation of the Toll and Imd pathways in the fat body transcriptionally upregulates the expression of the transcription factor *CrebA*. In turn, *CrebA* upregulates the expression of secretory pathway genes. In absence of *CrebA*, a failure to upregulate secretion machinery genes leads to infection-induced ER stress, followed by host death.

We next asked whether the failure of *CrebA*-deficient flies to prevent ER stress following infection could explain their increased susceptibility to bacterial challenge. To test this, we genetically induced ER stress in *Drosophila* fat bodies either by overexpression of *Psn* (*Gal80^{ts};*

c564-Gal4 > UAS-Psn), which disrupts calcium homeostasis, or by knockdown of *BiP* (*Gal80^{ts}; c564-Gal4 > UAS-BiP-IR*), a regulatory protein of the unfolded protein response [45,46]. Inducing ER stress in the fat body during infection made the flies more susceptible to *P. rettgeri* infection, phenocopying the result observed with *CrebA* knockdown flies ($p<0.0001$ for both constructs) (Fig 8D). Since the increased susceptibility of *CrebA* RNAi flies to infection stemmed from a tolerance defect (Fig 6G-H and Fig S8C-E), we sought to determine whether the increase in mortality observed in *BiP* RNAi and *Psn* overexpression flies following infection is also due to a tolerance deficiency. We monitored bacterial load in individual *BiP* RNAi and *Psn* overexpression flies following challenge with *P. rettgeri*. We did not observe a significant difference in bacterial load between wildtype and *BiP*-knockdown flies ($p=0.0624$) or between wildtype and *Psn* overexpression flies ($p=0.6462$) (Fig S10A). Quantification of bacterial load upon death (*BLUD*) following *P. rettgeri* infection in *BiP* RNAi flies showed that *BiP*-deficient flies perish carrying a significantly lower bacterial load than wildtype flies ($p<0.0001$) (Fig S10B). Altogether, our data indicate that induction of fat body ER stress during infection decreases fly survival by lowering host tolerance of infection.

Having demonstrated that *CrebA*-deficient flies experience fat body ER stress upon bacterial challenge and that flies with genetically induced fat body ER stress display increased mortality without a concomitant change in bacterial load following infection, thus phenocopying *CrebA*-deficient flies, we subsequently asked whether alleviating ER stress in *CrebA*-deficient flies could rescue the *CrebA* survival phenotype. To test this, we overexpressed *BiP* in fat body cells in which *CrebA* was knocked down by RNAi (*Gal80^{ts}; c564-Gal4 > UAS-CrebA-IR, UAS-BiP*). Previous work has shown that overexpression of *BiP* can ameliorate ER stress [47]. While overexpression of *BiP* alone did not alter host survival during infection, expression of *BiP* in *CrebA*

RNAi flies rescued fly survival upon challenge with *P. rettgeri* (Fig 8E). We observed no significant difference between the survival of infected control flies and that of infected flies co-expressing both the *CrebA* RNAi and *BiP* overexpression constructs (p=0.2786). These data indicate that reducing ER stress is sufficient to rescue the survival phenotype of *CrebA*-deficient flies during bacterial challenge. Excessive and prolonged ER stress can lead to apoptosis [48]. Therefore, we investigated whether *CrebA* RNAi flies are more susceptible to infection due to an increase in fat body cell apoptosis. We blocked apoptosis by overexpressing the apoptosis inhibitor P35 in the fat body of *CrebA*-knockdown flies (*Gal80^{ts}; c564-Gal4 > UAS-CrebA-IR, UAS-P35*) [49]. Expression of P35 in *CrebA* RNAi flies did not rescue the *CrebA* survival phenotype upon infection (Fig S10C), indicating that an increase in apoptosis is unlikely to explain the *CrebA* susceptibility defect. Collectively, our results show that *CrebA* is required in the fat body to prevent excessive and deleterious levels of ER stress upon infection.

Discussion

Bacteria trigger diverse and unique host responses

In this study, we have characterized the transcriptomic response of *Drosophila* to a wide range of bacterial infections. We found that the response to infection can involve up to 2,423 genes, or 13.7% of the genome. This is a considerably greater number of genes than what has been previously reported in similar transcriptomic studies [6,8]. As the response to infection was highly specific to each bacterium, the larger number of genes we identified is likely a consequence of having included more bacterial species in our experiment than previous studies. Likewise, we anticipate that future studies using different species of bacteria could further increase the number of genes found to be involved in the host response to infection. Our data clearly establish that while the core response to infection is narrow and conserved, every bacterium additionally triggers a very specific transcriptional response that reflects its unique interaction with host physiology.

At first, this high level of specificity may seem contrary to the traditional vision of the innate immune response. Early studies defined the innate immune system as generic, and the specificity of the *Drosophila* immune response was considered as a dichotomous activation of the Toll pathway by Gram-positive bacteria (Lys-type peptidoglycan) or the Imd pathway by Gram-negative bacteria (DAP-type peptidoglycan) [5,25]. Our data show that the host response to infection goes beyond the activation of the Toll and Imd pathways, with each bacterium also modulating host cell biology, metabolism, and stress responses in a microbe-specific manner. Although we did find that the type of bacterial peptidoglycan is a key factor shaping the response, we also found that each bacterium activates both the Toll and Imd pathways to quantitatively different levels, consistent with previous reports suggesting a much more complex coordination of

the immune response [50-53]. Activation of the Toll and Imd pathways depends on recognition of microbe-associated molecular patterns (MAMPs) and detection of damage-associated molecular patterns (DAMPs), suggesting that virulent bacteria could activate the Toll and Imd pathways to a higher degree [13,14]. However, we did not find a clear correlation between the virulence level of the bacterium or bacterial load sustained and the degree to which the canonical immune response is activated. In sum, our results support the notion that the response to infection comprises more than simple activation of immune functions, but instead is a function of precise physiological interactions between host and microbe.

Identification of a core response to infection

Although the response to infection appears to be largely specific, we identified a core set of genes that are regulated by infection with most bacteria. Induced genes include the classical targets of the Toll and Imd pathways, such as antimicrobial peptides and immune effectors (TEPs and IMs). However, genes involved in cell and tissue biology (translation, secretion, cell division) were also upregulated by the majority of infection conditions, possibly indicating a response to the stress imposed by infection. On the other hand, genes involved in metabolism (protease activity, oxidation-reduction, glucose metabolism, respiration), as well as digestive enzymes (e.g. the maltase cluster), were downregulated, suggesting a complete reshaping of host metabolism during infection [6]. It is tempting to speculate that the majority of core genes that do not fall under the immunity category could be part of a tolerance core response. Although the subject of tolerance mechanisms has attracted a lot of interest in recent years, identifying the genes and processes that define tolerance has remained somewhat elusive [54,55]. Further characterization of the core genes identified here may shed light on universal tolerance mechanisms.

The idea of a core response to infection has also been explored in other organisms. In *Caenorhabditis elegans*, for example, a study using four different pathogens to assay the transcriptional response to infection found that the core of the response included genes involved in proteolysis, cell death, and stress responses [56]. Comparative transcriptomics work in the honey bee, *Apis mellifera*, also revealed a core set of genes utilized in response to distinct pathogens, including genes involved in immunity, stress responses, and tissue repair [57]. In *Danio rerio*, immunity, metabolism, and cell killing have been implicated in host defense [58]. Collectively, these results and ours indicate that there is considerable overlap in the core response to infection across species, and that this consistency extends beyond classical immune sensing and signaling. Having a well-defined core response to infection in *Drosophila* will allow future studies to quantitatively assess differences in how distinct pathogens induce the core, as well as test the relative importance of various elements of the core in promoting resistance to and tolerance of infection.

A surprisingly high proportion (~40%) of the core response to infection was induced only by live microbes, but was not stimulated by challenge with heat-killed bacteria. One possibility is that MAMPs, such as peptidoglycan, are partially, if not fully, degraded at the sampled time points, obscuring our ability to appreciate the full extent of the response to MAMPs. An alternative explanation is that almost half of the core response to infection is a reaction to microbial activity, rather than just to the presence of MAMPs. This latter model involves the detection of the host's own DAMPs upon infection [12]. For example, bacterial growth and secretion of toxins can inflict damage to host tissues, leading to the generation of DAMPs, such as actin, proteases, and elastases [13,14,59]. In turn, DAMPs can activate the Toll, Imd, and JAK-STAT pathways, which may trigger higher levels of signaling in these pathways beyond that which is induced by the detection

of MAMPs [13,14,16,59]. Higher degrees of activation in these pathways could then translate into the induction of a larger set of target genes, which could partially account for the ~40% of core genes that are uniquely induced by live infections.

Bacterial infection triggers long term changes in host transcription

Interestingly, our study found that gene expression levels do not always reflect the changes in bacterial load during the course of infection. In chronically infected flies, we found that most genes downregulated at 12 h post-infection had returned to baseline expression levels by 132 h after infection. Likewise, many of the induced genes also decreased in expression or returned to basal levels even while flies still harbored bacteria. It is possible that the injury inflicted to systemically infected flies generates a complex early response, which is resolved at later time points. However, we note that injury alone did not generally trigger the downregulation of genes observed in live infections. An alternative explanation is that the bacteria have entered into a less aggressive state in the late stages of infection, persisting but with a reduced impact on the physiology of their host. Yet another hypothesis is that the host's initial response to infection is broad-spectrum and disproportionately strong, with the proactive goal of suppressing all bacteria before they can establish a highly detrimental infection. In this scenario, a subdued infection can be controlled with more nuance at later stages [22]. Finally, it is also possible that the percentage of recovered genes following infection with moderately virulent bacteria is overestimated because the RNA-seq is performed on pools of flies that may have distinct individual fates upon infection, and therefore distinct transcriptional kinetics. We have previously shown that flies infected with these same bacteria either die with a high bacterial load or survive with a low-level, persistent infection [38]. The individual flies at the 12 h RNA-seq data point comprise flies destined for both outcomes,

but only persistently infected flies are sampled at the 132 h time point after mortality has occurred. If flies fated to die induce genes that are not triggered in flies destined to survive, those genes may appear to be upregulated in the pooled 12 h RNA sample that contains a mix of flies destined for both outcomes. Likewise, those same genes will appear to have returned to baseline levels at the 132 h time point when just chronically infected flies are sampled, creating the false impression that they have recovered. Future work is required to evaluate these hypotheses and to provide insight into how the complex dynamics of gene expression relate to changes in pathogen burden [60].

We also observed seemingly long-term alterations to the transcription of some core response genes, even in the case of infections with bacteria, such as *M. luteus* and *Ecc15*, that are reduced to undetectable levels or cleared by the host. For example, the expression of several antimicrobial peptide genes (*Drs*, *Dro*, and *AttB*) as well as other effector molecules (*IM4* and *IM3*) never returned to basal levels, even multiple days after elimination of the infection. Such sustained reactions could provide long-lasting benefits in an environment with high risk of infection. Moreover, it should perhaps be considered that the baseline expression levels of these genes in laboratory-reared *Drosophila* are artificially low because of aseptic maintenance conditions as compared to those in natural environments.

The transcription factor *CrebA* prevents infection-induced ER stress

Among our core response genes, we identified *CrebA* as a key transcription factor that promotes host tolerance to infection. CrebA is the single *Drosophila* member of the Creb3-like family of transcription factors, which includes five different proteins in mammals: Creb3/Luman,

Creb3L1/Oasis, Creb3L2/BBF2H7, Creb3L3/CrebH, and Creb3L4/Creb4 [31]. A recent study demonstrated that *CrebA* is a master regulator of secretory capacity, capable of regulating the expression of the general machinery required in all cells for secretion [32]. *Drosophila CrebA* appears to have the same functional role as its mammalian counterparts. Exogenous expression of mammalian liver-specific *CrebH* caused upregulation of genes involved in secretory capacity and increased secretion of specific cargos [31]. Moreover, each of the five human CREB3 factors is capable of activating secretory pathway genes in *Drosophila*, dependent upon their shared ATB (Adjacent To bZip) domain [31]. In agreement with the function of CrebA and CREB3 proteins described in the literature, our study finds that *CrebA* regulates a rapid, infection-induced increase in the expression of secretory pathway genes in the fat body, an organ analogous to the liver and adipose tissues of mammals. Finally, it has been shown that proinflammatory cytokines act to increase the transcription of *CrebH*, and that CrebH becomes activated in response to ER stress [61]. Our data demonstrate that the two principal immune pathways in *Drosophila*, the Toll and Imd pathways, upregulate the expression of *CrebA* in response to bacterial challenge and that loss of *CrebA* in the fat body triggers ER stress upon infection. Collectively, the functions of mammalian *CrebH* as a regulator of secretory homeostasis under stress bear a striking resemblance to the role that we have attributed to *Drosophila CrebA* after bacterial challenge, suggesting that *CrebH* could have a similar role in mammals during infection.

CREB proteins are activated by phosphorylation from diverse kinases, including PKA and Ca2+/calmodulin-dependent protein kinases on the Serine 133 residue [62]. CrebA does not contain a PKA consensus phosphorylation site, and its transcriptional activity is only slightly enhanced by cAMP [36]. Rather, we found that the Toll and Imd pathways are both necessary and sufficient to regulate *CrebA* expression in the fat body. Loss of *CrebA* leads to ER stress, further

aggravating the physiological strains of infection. However, a lack of *CrebA* in unchallenged conditions does not lead to the induction of ER stress. We therefore propose a model in which the Toll and Imd pathways act early to upregulate *CrebA* in order to adapt the fat body cells for infection, thus preventing ER stress that would otherwise be triggered by the response to infection [63] (Fig 8F). This interpretation would suggest that immune activation generates a massive and rapid increase in translation [64] and secretion in response to infection, and thus triggers cellular stress in the fat body. In that context, the Toll and Imd pathways would proactively induce expression of *CrebA* to prevent some of the stress that comes from their own activation.

Lastly, *CrebA* knockdown flies are more likely to die from infection yet they show no increase in pathogen burden. This demonstrates that *CrebA* is required for tolerance of infection [65,66]. Considering that ER stress is induced upon infection in the absence of *CrebA*, our data suggest that *CrebA* is a tolerance gene that helps mitigate the stress imposed by the host response to infection. Fast induction of *CrebA* by the immune system upon infection can therefore be interpreted as an active tolerance mechanism that is generally required to survive bacterial infection.

Materials and Methods

Whole fly RNA-seq infections

Whole fly RNA-seq experiments were performed using wildtype strain *Canton S* flies. Flies were raised on standard yeast-cornmeal-sucrose medium (50 g baker's yeast, 60 g cornmeal, 40 g sucrose, 7 g agar, 26.5 mL Moldex (10%), and 12 mL Acid Mix solution (4.2% phosphoric acid, 41.8% propionic acid) per 1L of deionized H_2O) at 24°C and maintained at that temperature for the duration of the experiment. Individual males were infected with one of the ten experimental bacteria 5 to 8 days after eclosion from the pupal case. Control flies that were sterilely wounded or inoculated with heat-killed bacteria were handled equivalently. Flies were pin-pricked to generate septic injury. We standardized the initial inoculation dose across all bacteria to deliver ~3,000 colony-forming units (CFU) per fly. The following bacteria (from overnight cultures) were used: *Micrococcus luteus* (A_{600} = 100), *Escherichia coli* (A_{600} = 100), *Serratia marcescens* Type (A_{600} = 1), *Ecc15* (A_{600} = 1), *Providencia rettgeri* (A_{600} = 1), *Enterococcus faecalis* (A_{600} = 1), *Staphylococcus aureus* (A_{600} = 1), *Providencia sneebia* (A_{600} = 1), *Serratia marcescens* Db11 (A_{600} = 1), and *Pseudomonas entomophila* (A_{600} = 1). Three sets of controls were included in the experiment: unchallenged and uninjured flies, sterilely wounded flies, and challenge with either heat-killed *P. rettgeri* or heat-killed *E. faecalis*. For every control and bacterial infection, with the exception of the 4 highly virulent infections, 20 flies were collected at 12 h, 36 h, and 132 h post-infection. For the 4 highly virulent bacteria, only the 12 h sample was collected because the majority of the flies had died before the later time points. Additionally, 20 unchallenged, uninjured flies were also collected at time 0 h as an extra control. Each sample of 20 flies was homogenized, and total RNA was isolated using a modified TRizol extraction protocol (Life Technologies). All experiments were done in triplicate. The same methodology was employed for the RNA-seq

experiment focused specifically on the fat body.

3'-end RNA-seq library construction and sequencing

Following RNA extraction, the 3'end RNA-seq libraries were prepared using QuantSeq 3' mRNA-Seq Library Prep kit (Lexogen). The sample quality was evaluated before and after the library preparation using Fragment Analyzer (Advanced Analytical). Libraries were sequenced on two lanes of the Illumina Nextseq 500 platform using standard protocols for 75bp single-end read sequencing at the Cornell Life Sciences Sequencing Core.

Read processing, alignment, counts estimation, and PCA

On average, 6 million reads per sample were sequenced at their 3' termini. This is roughly equivalent in sensitivity to 20x coverage depth under a conventional random-priming RNA-seq method. Raw reads were first evaluated by fastqc for quality control (http://www.bioinformatics.bbsrc.ac.uk/projects/fastqc, version 0.11.3) and were then trimmed using Trimmomatic version 0.32 [67]. Trimmed reads were mapped to the *D. melanogaster* reference transcriptome, which was constructed with the *D. melanogaster* reference genome (version 6.80) using STAR RNA-seq aligner version 2.4.1a [68]. Read depth at each transcript was then calculated using htseq (version 0.6.1) [69]. Principal Component Analysis and extraction of the PC1/PC2 genes were performed by custom R scripts (available upon request).

Differential expression, functional category and pathway, and transcription factor enrichment

The software edgeR version 3.10.5 was used to call the genes that are differentially expressed among treatments [70]. Nine samples of unchallenged flies matching the 3 different time points post-infection (12 h, 36 h, and 132 h) were collapsed into a single control once it was determined that their transcriptomic profiles were very similar. Library sizes were normalized using a trimmed mean of M-values (TMM) approach implemented in edgeR. Genes with low counts (count-per-million < 1.2) were filtered out prior to differential expression analysis. Genes were considered statistically differentially expressed if they were differentially expressed between unchallenged condition and an infection condition of choice at the 5% false discovery rate (FDR). A fold-change cutoff was not applied to the data. Each gene was also evaluated for the number of infection conditions in which it was differentially regulated, where an "infection condition" refers to the transcriptomic profile in response to any of the live infections or controls at any point post-infection. Heatmaps were generated and clustering was performed using custom R scripts. Gene Ontology and KEGG pathway enrichment analysis was performed using the DAVID bioinformatics resource [71] and PANTHER [72]. The p-values from these analyses were corrected using the Benjamini and Hochberg procedure [73] with the FDR threshold set to 0.05. The search for putative transcription factor binding sites was performed using i-cisTarget under the default parameter values [26,27].

Defining the kinetics of the transcriptional response to infection

For each gene under each infection condition, an expression path was assigned based on the series of inferred induction or repression of infection relative to unchallenged controls at each successive time point. Genes that were significantly induced or repressed at 12 or 36 h but then returned to basal expression levels were deemed to have "recovered". To quantify the degree of recovery for

each gene, the level of fold change at 132 h after infection was compared to the fold change in expression at either 12 h or 36 h using custom R scripts (available upon request). The genes that were significantly induced (or repressed) at 12 h and then significantly repressed (or induced) at 36 h relative to the unchallenged conditions (1% of the genes) were excluded, as were genes that never changed expression in any of the time points.

Fly strains and crosses for *CrebA* experiments

Subsequent to the initial RNA-seq experiment, genetic manipulations of *CrebA* expression were performed. Flies for all of these experiments were reared at 18°C or 24°C. The Rel^{E20} and spz^{rm7} stocks have been previously described [74,75]. For manipulation of *CrebA* expression level, we used the *UAS/Gal4* gene expression system in combination with $Gal80^{ts}$ to restrict the expression of the constructs specifically to the adult stage. Male flies were collected 5 to 8 days after eclosion from the pupal case and then shifted to 29°C for an additional 8 days prior to any experiments. We used the following genotypes: 1. *c564-Gal4*; *tub-*$Gal80^{ts}$, *UAS-GFP* 2. *Lpp-Gal4*; *tub-*$Gal80^{ts}$, *UAS-GFP* 3. *c564-Gal4*; *tub-*$Gal80^{ts}$, *UAS-CrebA-IR* 4. *UAS-imd* 5. *UAS-spz** 6. *UAS-P35* 7. *UAS-Psn* (Bloomington 8305) 8. *UAS-BiP-IR* (Bloomington 32402) 9. *UAS-BiP* (Bloomington 5843) 10. TRiP control line *attP2* (Bloomington 36303) 11. TRiP control line *attP40* (Bloomington 36304) 12. $Xbp1_p$*>dsRed* 13-15. *UAS-CrebA-IR* (Bloomington 42562 (A), 31900 (B) and 27648 (C)).

Survival Experiments

Infection was done via septic pinprick to the thorax. After inoculation, death was recorded daily, and flies were transferred to fresh vials every 3 days. All experiments were performed at least 3

times. Statistical significance was determined using a Log-rank (Mantel-Cox) test.

Quantification of bacterial CFUs

At specified time points following infection, flies were individually homogenized by bead beating in 500 µl of sterile PBS using a tissue homogenizer (OPS Diagnostics). Dilutions of the homogenate were plated onto LB agar using a WASP II autoplate spiral plater (Microbiology International), incubated overnight at 29°C, and the CFUs were counted. All experiments were performed at least 3 times. Results were analyzed using a two-way (genotype and time) ANOVA in Prism (GraphPad Prism V7.0a, GraphPad Software, La Jolla, CA, USA).

RT-qPCR

For all experiments utilizing RT-qPCR, total RNA was extracted from pools of 20 flies using a standard TRIzol (Invitrogen) extraction. RNA samples were treated with DNase (Promega), and cDNA was generated using murine leukemia virus reverse transcriptase (MLV-RT) (Promega). qPCR was performed using the SSO Advanced SYBR green kit (Bio-Rad) in a Bio-Rad CFX-Connect instrument. Data represent the relative ratio between the Ct value of the target gene and that of the reference gene *RpL32* (also known as *Rp49*). Mean values of at least three biological replicates are represented ±SE. Data were normalized and then analyzed using an unpaired t-test in Prism (GraphPad Prism V7.0a; GraphPad Software, La Jolla, CA, USA). The primer sequences used in this study are available in Supplementary Table 6.

Fat body imaging

In some experiments, fat bodies were visualized microscopically. For these experiments,

Drosophila abdomens were dissected and fixed in a 4% paraformaldehyde in 1X PBS solution for 45 minutes and washed 3 times with 0.1% Triton-X in PBS. DNA was stained in 1:50,000 DAPI (Sigma-Aldrich) in PBS and 0.1% Triton-X for 45 minutes. Samples were then washed three times in PBS and mounted in antifadent medium (Citifluor AF1). Imaging was performed on a Zeiss LSM 700 fluorescent/confocal inverted microscope.

Acknowledgments

We thank all current and past members of the Buchon and Lazzaro labs for helpful discussions. We also thank the Andrew lab at Johns Hopkins University and the Ryoo lab at New York University for reagents and the Cornell Life Sciences Sequencing Core for assistance with sequencing.

REFERENCES

1. Kocks C, Cho JH, Nehme N, Ulvila J, Pearson AM, Meister M, et al. Eater, a transmembrane protein mediating phagocytosis of bacterial pathogens in Drosophila. Cell. 2005;123: 335–346. doi:10.1016/j.cell.2005.08.034

2. Guillou A, Troha K, Wang H, Franc NC, Buchon N. The Drosophila CD36 Homologue croquemort Is Required to Maintain Immune and Gut Homeostasis during Development and Aging. O'Riordan M, editor. PLoS Pathog. 2016;12: e1005961. doi:10.1371/journal.ppat.1005961

3. Boman HG, Nilsson I, Rasmuson B. Inducible antibacterial defence system in Drosophila. Nature. 1972;237: 232–235.

4. Tauszig S, Jouanguy E, Hoffmann JA, Imler JL. Toll-related receptors and the control of antimicrobial peptide expression in Drosophila. Proc Natl Acad Sci USA. 2000;97: 10520–10525. doi:10.1073/pnas.180130797

5. Buchon N, Silverman N, Cherry S. Immunity in Drosophila melanogaster--from microbial recognition to whole-organism physiology. Nat Rev Immunol. 2014;14: 796–810. doi:10.1038/nri3763

6. De Gregorio E, Spellman PT, Rubin GM, Lemaitre B. Genome-wide analysis of the Drosophila immune response by using oligonucleotide microarrays. Proc Natl Acad Sci USA. 2001;98: 12590–12595. doi:10.1073/pnas.221458698

7. De Gregorio E, Spellman PT, Tzou P, Rubin GM, Lemaitre B. The Toll and Imd pathways are the major regulators of the immune response in Drosophila. EMBO J. EMBO Press; 2002;21: 2568–2579. doi:10.1093/emboj/21.11.2568

8. Irving P, Troxler L, Heuer TS, Belvin M, Kopczynski C, Reichhart JM, et al. A genome-wide analysis of immune responses in Drosophila. Proc Natl Acad Sci USA. 2001;98: 15119–15124. doi:10.1073/pnas.261573998

9. Gobert V, Gottar M, Matskevich AA, Rutschmann S, Royet J, Belvin M, et al. Dual activation of the Drosophila toll pathway by two pattern recognition receptors. Science. 2003;302: 2126–2130. doi:10.1126/science.1085432

10. Leulier F, Parquet C, Pili-Floury S, Ryu J-H, Caroff M, Lee W-J, et al. The Drosophila immune system detects bacteria through specific peptidoglycan recognition. Nat Immunol. 2003;4: 478–484. doi:10.1038/ni922

11. Kaneko T, Yano T, Aggarwal K, Lim J-H, Ueda K, Oshima Y, et al. PGRP-LC and PGRP-LE have essential yet distinct functions in the drosophila immune response to monomeric DAP-type peptidoglycan. Nat Immunol. 2006;7: 715–723. doi:10.1038/ni1356

12. Matzinger P. Tolerance, Danger and the Extended Family. Annu Rev Immunol. Annual Reviews 4139 El Camino Way, P.O. Box 10139, Palo Alto, CA 94303-0139, USA;

1994;12: 991–1045. doi:10.1146/annurev.immunol.12.1.991

13. Gottar M, Gobert V, Matskevich AA, Reichhart J-M, Wang C, Butt TM, et al. Dual Detection of Fungal Infections in Drosophila via Recognition of Glucans and Sensing of Virulence Factors. Cell. 2006;127: 1425–1437. doi:10.1016/j.cell.2006.10.046

14. Schmidt RL, Trejo TR, Plummer TB, Platt JL, Tang AH. Infection-induced proteolysis of PGRP-LC controls the IMD activation and melanization cascades in Drosophila. FASEB J. Federation of American Societies for Experimental Biology; 2008;22: 918–929. doi:10.1096/fj.06-7907com

15. Chamy LE, Leclerc V, Caldelari I, Reichhart J-M. Sensing of 'danger signals' and pathogen-associated molecular patterns defines binary signaling pathways “upstream” of Toll. Nat Immunol. 2008;9: 1165–1170. doi:10.1038/ni.1643

16. Ming M, Obata F, Kuranaga E, Miura M. Persephone/Spätzle pathogen sensors mediate the activation of Toll receptor signaling in response to endogenous danger signals in apoptosis-deficient Drosophila. J Biol Chem. 2014;289: 7558–7568. doi:10.1074/jbc.M113.543884

17. Dionne MS, Pham LN, Shirasu-Hiza M, Schneider DS. Akt and foxo Dysregulation Contribute to Infection-Induced Wasting in Drosophila. Current Biology. 2006;16: 1977–1985. doi:10.1016/j.cub.2006.08.052

18. Buchon N, Broderick NA, Poidevin M, Pradervand S, Lemaitre B. Drosophila intestinal response to bacterial infection: activation of host defense and stem cell proliferation. Cell Host Microbe. Elsevier; 2009;5: 200–211. doi:10.1016/j.chom.2009.01.003

19. Buchon N, Broderick NA, Kuraishi T, Lemaitre B. Drosophila EGFR pathway coordinates stem cell proliferation and gut remodeling following infection. BMC Biol. BioMed Central; 2010;8: 152. doi:10.1186/1741-7007-8-152

20. Clark RI, Tan SWS, Péan CB, Roostalu U, Vivancos V, Bronda K, et al. MEF2 Is an In Vivo Immune-Metabolic Switch. Cell. The Authors; 2013;155: 435–447. doi:10.1016/j.cell.2013.09.007

21. Casadevall A, Pirofski LA. Host-pathogen interactions: redefining the basic concepts of virulence and pathogenicity. Infect Immun. American Society for Microbiology (ASM); 1999;67: 3703–3713.

22. Germain RN. The art of the probable: system control in the adaptive immune system. Science. American Association for the Advancement of Science; 2001;293: 240–245. doi:10.1126/science.1062946

23. Galac MR, Lazzaro BP. Comparative pathology of bacteria in the genus Providencia to a natural host, Drosophila melanogaster. Microbes and Infection. 2011;13: 673–683. doi:10.1016/j.micinf.2011.02.005

24. Johansson KC, Metzendorf C, Söderhäll K. Microarray analysis of immune challenged

Drosophila hemocytes. Exp Cell Res. 2005;305: 145–155. doi:10.1016/j.yexcr.2004.12.018

25. Lemaitre B, Hoffmann J. The host defense of Drosophila melanogaster. Annu Rev Immunol. Annual Reviews; 2007;25: 697–743. doi:10.1146/annurev.immunol.25.022106.141615

26. Herrmann C, Van de Sande B, Potier D, Aerts S. i-cisTarget: an integrative genomics method for the prediction of regulatory features and cis-regulatory modules. Nucleic Acids Res. 2012;40: e114–e114. doi:10.1093/nar/gks543

27. Imrichová H, Hulselmans G, Atak ZK, Potier D, Aerts S. i-cisTarget 2015 update: generalized cis-regulatory enrichment analysis in human, mouse and fly. Nucleic Acids Res. 2015;43: W57–64. doi:10.1093/nar/gkv395

28. Clark RI, Woodcock KJ, Geissmann F, Trouillet C, Dionne MS. Multiple TGF-β superfamily signals modulate the adult Drosophila immune response. Curr Biol. 2011;21: 1672–1677. doi:10.1016/j.cub.2011.08.048

29. Keestra-Gounder AM, Byndloss MX, Seyffert N, Young BM, Chávez-Arroyo A, Tsai AY, et al. NOD1 and NOD2 signalling links ER stress with inflammation. Nature. 2016;532: 394–397. doi:10.1038/nature17631

30. Meng X, Khanuja BS, Ip YT. Toll receptor-mediated Drosophila immune response requires Dif, an NF-kappaB factor. Genes Dev. Cold Spring Harbor Laboratory Press; 1999;13: 792–797.

31. Barbosa S, Fasanella G, Carreira S, Llarena M, Fox R, Barreca C, et al. An Orchestrated Program Regulating Secretory Pathway Genes and Cargos by the Transmembrane Transcription Factor CREB-H. Traffic. 2013;14: 382–398. doi:10.1111/tra.12038

32. Fox RM, Hanlon CD, Andrew DJ. The CrebA/Creb3-like transcription factors are major and direct regulators of secretory capacity. J Cell Biol. 2010;191: 479–492. doi:10.1083/jcb.201004062

33. Cartharius K, Frech K, Grote K, Klocke B, Haltmeier M, Klingenhoff A, et al. MatInspector and beyond: promoter analysis based on transcription factor binding sites. Bioinformatics. 2005;21: 2933–2942. doi:10.1093/bioinformatics/bti473

34. Georgel P, Naitza S, Kappler C, Ferrandon D, Zachary D, Swimmer C, et al. Drosophila immune deficiency (IMD) is a death domain protein that activates antibacterial defense and can promote apoptosis. Dev Cell. 2001;1: 503–514.

35. Pili-Floury S, Leulier F, Takahashi K, Saigo K, Samain E, Ueda R, et al. In vivo RNA interference analysis reveals an unexpected role for GNBP1 in the defense against Gram-positive bacterial infection in Drosophila adults. J Biol Chem. 2004;279: 12848–12853. doi:10.1074/jbc.M313324200

36. Rose RE, Gallaher NM, Andrew DJ, Goodman RH, Smolik SM. The CRE-binding protein

dCREB-A is required for Drosophila embryonic development. Genetics. Genetics Society of America; 1997;146: 595–606.

37. Ayres JS, Schneider DS. Tolerance of infections. Annu Rev Immunol. Annual Reviews; 2012;30: 271–294. doi:10.1146/annurev-immunol-020711-075030

38. Duneau D, Ferdy J-B, Revah J, Kondolf H, Ortiz GA, Lazzaro BP, et al. Stochastic variation in the initial phase of bacterial infection predicts the probability of survival in D. melanogaster. Elife. eLife Sciences Publications Limited; 2017;6: 245. doi:10.7554/eLife.28298

39. Moore KA, Hollien J. The unfolded protein response in secretory cell function. Annu Rev Genet. Annual Reviews; 2012;46: 165–183. doi:10.1146/annurev-genet-110711-155644

40. Ryoo HD. Drosophila as a model for unfolded protein response research. BMB Reports. 2015;48: 445–453. doi:10.5483/BMBRep.2015.48.8.099

41. Yoshida H, Matsui T, Yamamoto A, Okada T, Mori K. XBP1 mRNA is induced by ATF6 and spliced by IRE1 in response to ER stress to produce a highly active transcription factor. Cell. 2001;107: 881–891.

42. van Schadewijk A, van't Wout EFA, Stolk J, Hiemstra PS. A quantitative method for detection of spliced X-box binding protein-1 (XBP1) mRNA as a measure of endoplasmic reticulum (ER) stress. Cell Stress Chaperones. Springer Netherlands; 2012;17: 275–279. doi:10.1007/s12192-011-0306-2

43. Yoshida H, Matsui T, Hosokawa N, Kaufman RJ, Nagata K, Mori K. A time-dependent phase shift in the mammalian unfolded protein response. Dev Cell. 2003;4: 265–271.

44. Ryoo HD, Li J, Kang M-J. Drosophila XBP1 expression reporter marks cells under endoplasmic reticulum stress and with high protein secretory load. PLoS ONE. 2013;8: e75774–6. doi:10.1371/journal.pone.0075774

45. Demay Y, Perochon J, Szuplewski S, Mignotte B, Gaumer S. The PERK pathway independently triggers apoptosis and a Rac1/Slpr/JNK/Dilp8 signaling favoring tissue homeostasis in a chronic ER stress Drosophila model. Cell Death Dis. Nature Publishing Group; 2014;5: e1452. doi:10.1038/cddis.2014.403

46. Chow CY, Avila FW, Clark AG, Wolfner MF. Induction of excessive endoplasmic reticulum stress in the Drosophila male accessory gland results in infertility. Mollereau B, editor. PLoS ONE. Public Library of Science; 2015;10: e0119386. doi:10.1371/journal.pone.0119386

47. Xu H, Xu W, Xi H, Ma W, He Z, Ma M. The ER luminal binding protein (BiP) alleviates Cd2+-induced programmed cell death through endoplasmic reticulum stress–cell death signaling pathway in tobacco cells. Journal of Plant Physiology. 2013;170: 1434–1441. doi:10.1016/j.jplph.2013.05.017

48. Szegezdi E, Logue SE, Gorman AM, Samali A. Mediators of endoplasmic reticulum stress-induced apoptosis. EMBO Rep. EMBO Press; 2006;7: 880–885. doi:10.1038/sj.embor.7400779

49. Hay BA, Wolff T, Rubin GM. Expression of baculovirus P35 prevents cell death in Drosophila. Development. 1994;120: 2121–2129.

50. Lemaitre B, Reichhart JM, Hoffmann JA. Drosophila host defense: differential induction of antimicrobial peptide genes after infection by various classes of microorganisms. Proc Natl Acad Sci USA. National Academy of Sciences; 1997;94: 14614–14619.

51. Engström Y. Induction and regulation of antimicrobial peptides in Drosophila. Dev Comp Immunol. 1999;23: 345–358.

52. Hedengren-Olcott M, Olcott MC, Mooney DT, Ekengren S, Geller BL, Taylor BJ. Differential activation of the NF-kappaB-like factors Relish and Dif in Drosophila melanogaster by fungi and Gram-positive bacteria. J Biol Chem. 2004;279: 21121–21127. doi:10.1074/jbc.M313856200

53. Stenbak CR, Ryu J-H, Leulier F, Pili-Floury S, Parquet C, Hervé M, et al. Peptidoglycan molecular requirements allowing detection by the Drosophila immune deficiency pathway. J Immunol. 2004;173: 7339–7348.

54. Howick VM, Lazzaro BP. Genotype and diet shape resistance and tolerance across distinct phases of bacterial infection. BMC Evol Biol. BioMed Central; 2014;14: 56. doi:10.1186/1471-2148-14-56

55. Lefèvre T, Williams AJ, de Roode JC. Genetic variation in resistance, but not tolerance, to a protozoan parasite in the monarch butterfly. Proc Biol Sci. 2011;278: 751–759. doi:10.1098/rspb.2010.1479

56. Wong D, Bazopoulou D, Pujol N, Tavernarakis N, Ewbank JJ. Genome-wide investigation reveals pathogen-specific and shared signatures in the response of Caenorhabditis elegans to infection. Genome Biology. BioMed Central; 2007;8: R194. doi:10.1186/gb-2007-8-9-r194

57. Doublet V, Poeschl Y, Gogol-Döring A, Alaux C, Annoscia D, Aurori C, et al. Unity in defence: honeybee workers exhibit conserved molecular responses to diverse pathogens. BMC Genomics. BioMed Central; 2017;18: 207. doi:10.1186/s12864-017-3597-6

58. Stockhammer OW, Zakrzewska A, Hegedûs Z, Spaink HP, Meijer AH. Transcriptome profiling and functional analyses of the zebrafish embryonic innate immune response to Salmonella infection. J Immunol. American Association of Immunologists; 2009;182: 5641–5653. doi:10.4049/jimmunol.0900082

59. Srinivasan N, Gordon O, Ahrens S, Franz A, Deddouche S, Chakravarty P, et al. Actin is an evolutionarily-conserved damage-associated molecular pattern that signals tissue injury in Drosophila melanogaster. Elife. eLife Sciences Publications Limited; 2016;5: 72.

doi:10.7554/eLife.19662

60. Tate AT, Graham AL. Dissecting the contributions of time and microbe density to variation in immune gene expression. Proc Biol Sci. 2017;284: 20170727. doi:10.1098/rspb.2017.0727

61. Zhang K, Shen X, Wu J, Sakaki K, Saunders T, Rutkowski DT, et al. Endoplasmic Reticulum Stress Activates Cleavage of CREBH to Induce a Systemic Inflammatory Response. Cell. 2006;124: 587–599. doi:10.1016/j.cell.2005.11.040

62. Shaywitz AJ, Greenberg ME. CREB: a stimulus-induced transcription factor activated by a diverse array of extracellular signals. Annu Rev Biochem. 1999;68: 821–861. doi:10.1146/annurev.biochem.68.1.821

63. Richardson CE, Kooistra T, Kim DH. An essential role for XBP-1 in host protection against immune activation in C. elegans. Nature. Nature Publishing Group; 2010;463: 1092–1095. doi:10.1038/nature08762

64. Tirosh O, Cohen Y, Shitrit A, Shani O, Le-Trilling VTK, Trilling M, et al. The Transcription and Translation Landscapes during Human Cytomegalovirus Infection Reveal Novel Host-Pathogen Interactions. Dittmer DP, editor. PLoS Pathog. 2015;11: e1005288. doi:10.1371/journal.ppat.1005288

65. Råberg L. How to live with the enemy: understanding tolerance to parasites. PLoS Biol. 2014;12: e1001989. doi:10.1371/journal.pbio.1001989

66. Medzhitov R, Schneider DS, Soares MP. Disease tolerance as a defense strategy. Science. 2012;335: 936–941. doi:10.1126/science.1214935

67. Bolger AM, Lohse M, Usadel B. Trimmomatic: a flexible trimmer for Illumina sequence data. Bioinformatics. 2014;30: 2114–2120. doi:10.1093/bioinformatics/btu170

68. Dobin A, Davis CA, Schlesinger F, Drenkow J, Zaleski C, Jha S, et al. STAR: ultrafast universal RNA-seq aligner. Bioinformatics. 2013;29: 15–21. doi:10.1093/bioinformatics/bts635

69. Anders S, Pyl PT, Huber W. HTSeq--a Python framework to work with high-throughput sequencing data. Bioinformatics. 2015;31: 166–169. doi:10.1093/bioinformatics/btu638

70. Robinson MD, McCarthy DJ, Smyth GK. edgeR: a Bioconductor package for differential expression analysis of digital gene expression data. Bioinformatics. 2010;26: 139–140. doi:10.1093/bioinformatics/btp616

71. Huang DW, Sherman BT, Lempicki RA. Systematic and integrative analysis of large gene lists using DAVID bioinformatics resources. Nat Protoc. Nature Publishing Group; 2009;4: 44–57. doi:10.1038/nprot.2008.211

72. Mi H, Huang X, Muruganujan A, Tang H, Mills C, Kang D, et al. PANTHER version 11:

expanded annotation data from Gene Ontology and Reactome pathways, and data analysis tool enhancements. Nucleic Acids Res. 2017;45: D183–D189. doi:10.1093/nar/gkw1138

73. Benjamini Y, Hochberg Y. Controlling the False Discovery Rate: A Practical and Powerful Approach to Multiple Testing. Journal of the Royal Statistical Society. 2017;57: 1–13.

74. Hedengren M, Asling B, Dushay MS, Ando I, Ekengren S, Wihlborg M, et al. Relish, a central factor in the control of humoral but not cellular immunity in Drosophila. Mol Cell. 1999;4: 827–837.

75. Michel T, Reichhart JM, Hoffmann JA, Royet J. Drosophila Toll is activated by Gram-positive bacteria through a circulating peptidoglycan recognition protein. Nature. 2001;414: 756–759. doi:10.1038/414756a

CHAPTER IV

NEPHROCYTES MEDIATE IMMUNE TOLERANCE TO MICROBIOTA BY REMOVING PEPTIDOGLYCAN FROM SYSTEMIC CIRCULATION*

* Adapted from Katia Troha, Peter Nagy, Andrew Pivovar, Brian P. Lazzaro, Paul Hartley and Nicolas Buchon. Submitted to Immunity.

Abstract

Maintenance of immune tolerance to microbiota is essential to organismal homeostasis. Here, we report that the *Drosophila* nephrocyte, a cell type with molecular, anatomical, and functional similarity to the glomerular podocyte of the vertebrate kidney, promotes immune tolerance to Gram-positive microbiota. Flies deficient for *Klf15*, a transcription factor required for nephrocyte development and function, are viable but lack nephrocytes. *Klf15* mutants display constitutively elevated Toll pathway activity, and as a consequence, are both shorter-lived and more resistant to microbial infection. Our analysis revealed that nephrocytes uptake Lys-type peptidoglycan from systemic circulation and degrade it inside lysosomes. Without nephrocyte function, microbiota-derived peptidoglycan accumulates in circulation, triggering Toll pathway activation even in the absence of infection. These results unveil a role for hemolymph (insect blood) filtration in the maintenance of immune tolerance to microbiota and also identify a potential root cause for the chronic immune activation observed in animals suffering from impaired blood filtration.

Introduction

As the first line of defense against invading microorganisms, the innate immune system senses and responds to both MAMPs (microbe-associated molecular patterns) and DAMPs (damage-associated molecular patterns) (Kim Newton, 2012). Peptidoglycan, a major constituent of the microbial cell wall, is an immune-stimulatory MAMP found in all bacteria, pathogenic or not. Following infection, detection of MAMPs in systemic circulation triggers a cascade of immune reactions that can ultimately lead to sepsis (Cecconi et al., 2018). Even in the absence of infection, organisms do not live in a sterile environment. For instance, the animal gut harbors numerous microbial species, which constitute the microbiota. A consequence of the presence of microbiota is the translocation of microbiota-shed MAMPs from the gut lumen into systemic circulation. This is a phenomenon that has been documented in a variety of organisms, including *Drosophila* and mammals (Capo et al., 2017; Clarke et al., 2010; Corbitt et al., 2013; Gendrin et al., 2009; Zaidman-remy et al., 2006). Considering that MAMPs, such as peptidoglycan, are found in circulation, regulating their systemic concentration is critical to the maintenance of immune homeostasis. Despite recent advances, the mechanisms that allow the immune system to tolerate resident microbiota remain largely unknown. To date, no study has examined the contribution of renal filtration to the removal of translocated microbial products. The present work, therefore, seeks to understand the role of blood filtration in the maintenance of immune homeostasis.

Drosophila is a powerful system to study innate immune responses to both pathogens and gut microbes (Buchon et al., 2014; Liu et al., 2017). To resist infection, *Drosophila* relies on both cellular and humoral innate immune responses. The cellular response consists of encapsulation and phagocytosis, while the humoral response involves the melanization cascade and the synthesis

of antimicrobial peptides (AMPs) by the fat body (an organ analogous to the liver and adipose tissue of mammals). Production of AMPs is controlled by two principal signaling cascades, the Toll and Imd pathways. Both pathways are activated in response to peptidoglycan (PGN): Lys-type PGN from Gram-positive bacteria triggers the Toll pathway, while DAP-type PGN from Gram-negative bacteria induces the Imd pathway (Buchon et al., 2014). In the fly, peptidoglycan is detected by peptidoglycan recognition proteins (PGRPs). PGRP-LC and PGRP-LE sense DAP-type PGN, and PGRP-SA recognizes Lys-type PGN (Kaneko et al., 2006; Michel et al., 2001). The constant presence of gut microbes poses a challenge for an animal's immune system: it must tolerate the existing microbiota while simultaneously retaining the ability to detect and respond to pathogens. In *Drosophila*, multiple negative regulators of the Imd pathway prevent excessive activation of the immune system in response to microbiota. For instance, the transcription factor Caudal suppresses Imd-dependent expression of AMPs in the gut, thereby shaping microbiota composition (Ryu et al., 2008). Another regulator, PIMS, sequesters PGRP-LC to prevent its exposure to microbiota-derived PGN and subsequent activation of the Imd pathway (Lhocine et al., 2008). Finally, secreted PGRPs with amidase activity are able to degrade immunostimulatory DAP-type PGN (Paredes et al., 2011). A notable example of this is PGRP-LB, which is released into the hemolymph to degrade translocated, microbiota-derived PGN, thus preventing immune activation of the fat body (Zaidmanremy et al., 2006; Paredes et al., 2011). Remarkably, although the Toll pathway also responds to the presence of peptidoglycan, no immune tolerance mechanism to suppress Toll activation in response to microbiota has been described so far.

The excretory system of *Drosophila* is composed of nephrocytes, which regulate hemolymph (extracellular fluid analogous to blood) composition by filtration followed by filtrate

endocytosis, and Malpighian tubules, which modify and secrete urine (Denholm et al., 2009; Hartley et al., 2016). *Drosophila* nephrocytes can be divided into two distinct groups: the garland cells, which appear as a necklace-like structure surrounding the esophagus, and the pericardial cells that form two rows of cells flanking the heart (Aggarwal and King, 1967; Crossley, 1972; Na and Cagan, 2013). In the adult stage, pericardial nephrocytes serve as the primary filtration units (Zhang et al., 2013). Hemolymph filtration occurs in a stepwise manner. First, hemolymph is filtered across the nephrocytes' negatively charged basement membrane and a specialized filter known as the nephrocyte diaphragm. The filtrate then enters the lacunae, also known as the labyrinthine channels, which extend several microns into the nephrocyte's cortical region (Kosaka and Ikeda, 1983). It is in these chambers where the filtrate is finally endocytosed by nephrocytes (Denholm et al., 2009). Nephrocytes possess significant molecular, anatomical, and functional similarities to the glomerular podocyte, a cell type of the mammalian kidney important for the kidney's filtration function (Weavers et al., 2009; Zhuang et al., 2009). Both podocytes and nephrocytes possess a slit diaphragm and act as size- and charge-selective filters in the sequestration of materials from the blood and hemolymph (Reiser and Altintas, 2016; Weavers et al., 2009). The *Drosophila* ortholog of mammalian *Klf15*, a transcription factor required for podocyte differentiation (Mallipattu et al., 2012), is restricted to and essential for nephrocyte differentiation and function (Ivy et al., 2015). Flies mutant for *dKlf15* are viable but lack both garland and pericardial nephrocytes in the adult, making it an excellent tool to study the impact of hemolymph filtration on immune function (Ivy et al., 2015).

In the present work, we uncover a role for hemolymph filtration by the fly's podocytes in the maintenance of immune homeostasis. Through the use of both mutants and stage- and tissue-

specific RNAi, we show that flies devoid of nephrocytes, or with diminished nephrocyte function, are surprisingly more resistant to a variety of microbial infections. We demonstrate that both the improved survival against infection and shorter lifespan of *Klf15* mutants stem from abnormal Toll pathway activation. Our data reveal that aberrant Toll signaling in the mutant is exclusively dependent on the presence of Gram-positive microbiota. We further present evidence that nephrocytes uptake Lys-type peptidoglycan from systemic circulation via endocytosis and degraded it inside lysosomes. Without nephrocytes, microbiota-derived PGN accumulates in the hemolymph, triggering chronic stimulation of the Toll pathway. Our work describes the first immune tolerance mechanism for Toll-specific immunity, suggesting that both the Toll and Imd pathways are strongly constrained by microbiota-shed MAMPs. More importantly, we identify a potential role for renal filtration in the maintenance of immune tolerance to microbiota, a function likely conserved in mammals.

Results

Klf15 mutants are less susceptible to microbial infection

In order to evaluate the role of hemolymph (analogous to mammalian blood) filtration in immune function and homeostasis, we turned to flies mutant for the transcription factor *Klf15* (*Klf15*^{NN} null allele), which lack nephrocytes. First, we confirmed the previously published result that *Klf15* mutants fail to develop nephrocytes (Figure 1A) (Ivy et al., 2015). Our data also showed that *Klf15* mutants exhibited a significantly shorter basal lifespan compared to wildtype (WT) controls of the same genetic background (Figure 1B). Despite having a curtailed life expectancy, *Klf15* mutants survived sterile wounding comparably to WT animals (Figure 1C-1G). To determine whether immune competence was affected by the loss of hemolymph filtration, we conducted survival assays with *Klf15* mutants following systemic infection with the bacterial pathogens *Serratia marcescens* Type strain, *Salmonella typhimurium*, *Listeria innocua*, *Enterococcus faecalis*, *Staphylococcus aureus*, and *Providencia rettgeri*. Surprisingly, *Klf15* mutants displayed significantly increased survival against five of these infections (Figures 1C-1G). Although not to statistical significance, *Klf15* mutants also showed improved survival during challenge with two fungal agents, *Beauveria bassiana* and *Metarhizium anisopliae* (Figures S1A-S1B). The only exception was infection with *P. rettgeri*, to which the mutant proved more sensitive (Figure S1C). Overall, these results suggest that *Klf15* mutants are broadly protected against systemic infection by pathogens.

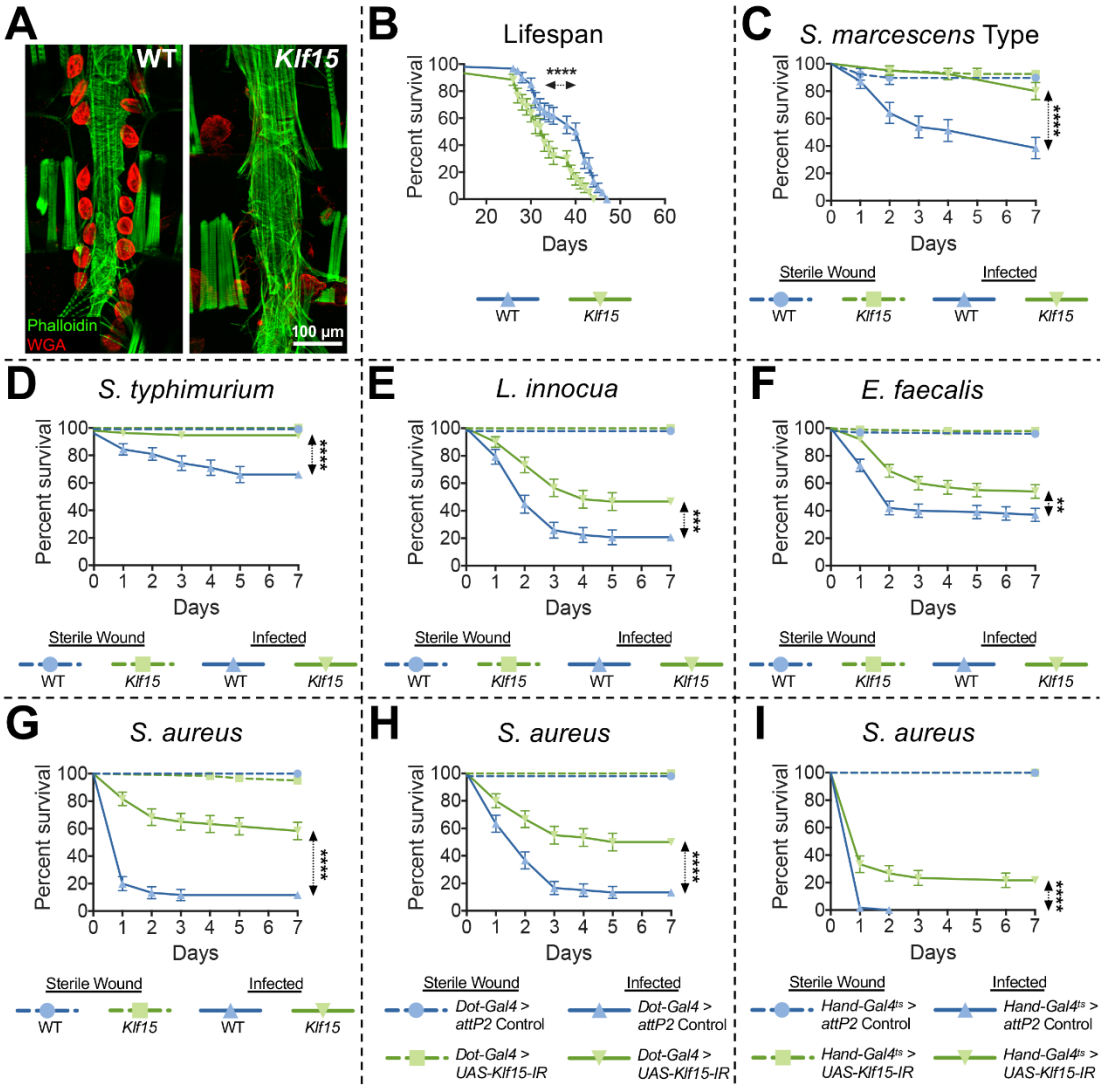

Figure IV.1. Loss of nephrocyte function increases survival against microbial challenge
(A) Adult pericardial nephrocytes stained with WGA Alexa Fluor 594 conjugate (red). Phalloidin-FITC (green) marks the heart tube. Staining is shown for both wildtype (WT) and *Klf15* mutants (*Klf15*^{NN} allele). (B) Lifespan curve comparing WT flies to *Klf15* mutants. (C-G) Survival curves over 7 days following infection of WT and *Klf15* mutant flies with the bacterial pathogens: *S. marcescens* Type strain (C), *S. typhimurium* (D), *L. innocua* (E), *E. faecalis* (F), and *S. aureus* (G). (H-I) Survival of flies expressing nephrocyte-specific RNAi against *Klf15* throughout development (*Dot-Gal4 > UAS-Klf15-IR*) (H) or only during the adult stage (*Hand-Gal4*^{ts} *> UAS-Klf15-IR)* (I) after infection with *S. aureus*. The curves represent the average percent survival ±SE of three or more biological replicates. **p<0.01 ***p<0.001 ****p<0.0001 in a Log-rank test.

To verify that the enhanced survival observed in the *Klf15* mutant was a direct consequence of the loss of nephrocytes, we generated nephrocyte-deficient flies through complementary means.

Using the nephrocyte-specific driver *Dot-Gal4*, we knocked down *Klf15* expression throughout development (*Dot-Gal4 > UAS-Klf15-IR*), which results in adult flies lacking nephrocytes (Ivy et al., 2015). Upon infection with *S. aureus* and *E. faecalis*, these flies also displayed increased survival relative to the WT controls, confirming our earlier findings (Figure 1H and Figure S1D). Next, we set out to determine whether the survival phenotype of *Klf15* mutants resulted from loss of hemolymph filtration in the mutant or from a developmental defect associated with the loss of nephrocytes. To distinguish between the two possibilities, we took advantage of the fact that adult-specific loss of *Klf15* halts the endocytic function of mature nephrocytes (Ivy et al., 2015). We knocked down *Klf15* specifically during the adult stage using the conditional, nephrocyte- and heart-specific driver *Hand-Gal4^{ts}* (*Hand-Gal4^{ts} > UAS-Klf15-IR*) and infected these flies separately with *S. aureus* and *E. faecalis*. Diminishing the endocytic competence of adult nephrocytes by *Klf15* knockdown was sufficient to increase survival to infection with both bacteria (Figure 1I and Figure S1E). Altogether, our results support the conclusion that loss of nephrocyte function generally increases survival against microbial infection.

Klf15 mutants are more resistant to infection, independent of phagocytosis and melanization

Multicellular organisms employ two complementary strategies to combat infection: resistance, to eliminate microbes, and resilience (also known as disease tolerance), to allow them to withstand the infection and/or its deleterious consequences (Ayres and Schneider, 2011; Ferrandon, 2013). To determine whether the increased survival of *Klf15* mutants was due to an increase in resilience, we compared the *BLUD* of WT and *Klf15* mutants following infection with *S. aureus* and *E. faecalis*. *BLUD*, which stands for bacterial load upon death, represents the maximal quantity of

bacteria that an infected fly can sustain (Duneau et al., 2017). We found that control flies and *Klf15* mutants die carrying similar numbers of each bacterium tested (Figure S2A), indicating that flies lacking nephrocytes are not more resilient to infection by these bacteria. Next, we tested whether the survival advantage of the mutant stemmed from improved resistance to infection. We monitored bacterial load during the course of *S. aureus*, *E. faecalis*, and *S. marcescens* infections (Figure 2A-2B and Figure S2B). *Klf15* mutants carried significantly lower bacterial burdens than wildtype flies as soon as 3 h post-infection with *S. aureus*, 4.5 h after challenge with *E. faecalis*, and 6 h post-inoculation with *S. marcescens*, demonstrating that flies without nephrocytes are more resistant to pathogens in the early stages of infection.

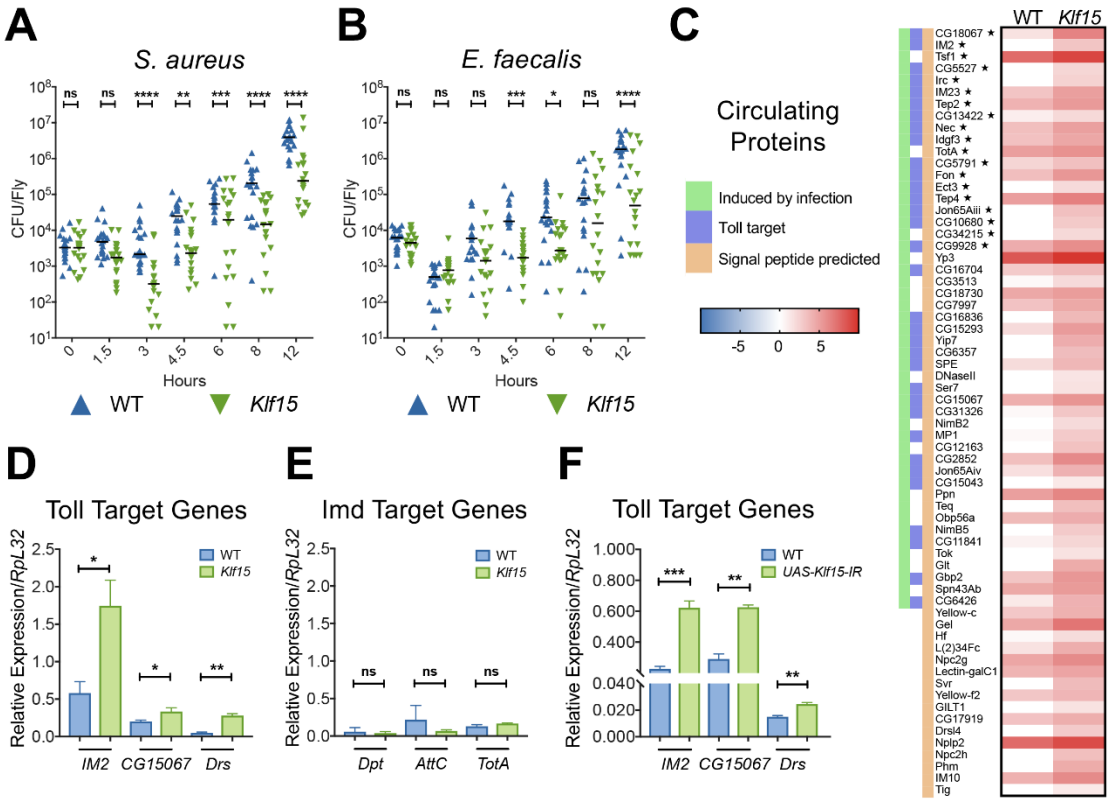

Figure IV.2. The Toll pathway is activated in *Klf15* mutant flies
(A-B) Bacterial load time course of control and *Klf15* flies following infection with *S. aureus* (A) and *E. faecalis* (B). Three repeats are graphed together, with each symbol representing an individual fly's number of colony forming units (CFU). Horizontal lines represent median values for each time point. Results were analyzed using a two-way ANOVA followed with Sidak's post-test for specific comparisons (*p<0.05 **p<0.01 ***p<0.001 ****p<0.0001). (C) Heat map showing a list of circulating proteins enriched (≥ 1.5-fold) in the hemolymph (insect blood) of *Klf15* mutants over WT or only present in *Klf15* flies but not WT. A color scale on the left side of the heat map denotes whether the gene that encodes each protein is transcriptionally induced by infection (green), a target of the Toll pathway (blue), or predicted to possess a signal peptide (orange). Core genes are highlighted with a ★ symbol [11]. (D-E) Whole fly RT-qPCR of Toll target genes *IM2*, *CG15067*, and *Drs* (D) and Imd target genes *Dpt*, *AttC*, and *TotA* (E) using unchallenged wildtype and *Klf15* samples. (F) Quantification of Toll target genes *IM2*, *CG15067*, and *Drs* via RT-qPCR in flies expressing RNAi against *Klf15* during the adult stage (Hand-Gal4ts > UAS-*Klf15*-IR). Mean values of three or more repeats are represented ±SE. *p<0.05 **p<0.01 ***p<0.001 in a Student's t-test.

Drosophila relies primarily on three effector mechanisms to control bacterial growth: phagocytosis, melanization, and the production of AMPs. First, we evaluated a role for phagocytosis in the resistance phenotype of the *Klf15* mutant. We injected nephrocyte-deficient

and WT flies with pH-sensitive pHrodo bacteria, which become fluorescent only after being engulfed into a fully mature, acidified phagosome (Guillou et al., 2016). After quantification, we observed close to 50% less fluorescence in *Klf15* mutant flies relative to controls (Figure S2C). Moreover, injection of flies with latex beads prior to systemic infection with both *S. aureus* and *E. faecalis*, a treatment that blocks phagocytosis (Elrod-Erickson et al., 2000), did not alter the survival phenotype of *Klf15* mutants (Figure S2D-S2E). These results demonstrate that phagocytic activity does not contribute meaningfully to the increased resistance of *Klf15* mutant flies. Assessment of phenoloxidase (PO) activity, the terminal enzymatic step driving melanization, revealed that while *Klf15* mutants had significantly higher levels of PO activity in basal conditions, they also displayed significantly lower levels of PO activity relative to controls 3 h post-infection with *S. aureus* and *E. faecalis* (Figure S2F). To clarify whether melanization played any role in the survival phenotype of *Klf15* mutants, we generated a mutant deficient for both *Klf15* and key genes required for the melanization response ($PPO1^{\Delta}$, 2^{Δ},3^{i}) (Binggeli et al., 2014; Dudzic et al., 2015). Upon infection with *S. aureus*, the quadruple mutant (*Klf15* ; $PPO1^{\Delta}$, 2^{Δ},3^{i}) exhibited improved survival relative to the triple mutant ($PPO1^{\Delta}$, 2^{Δ},3^{i}) (Figure S2G), suggesting that melanization is not required for the protection observed in nephrocyte-deficient flies. In sum, our data indicate that loss of nephrocytes confers increased resistance to hosts independent of phagocytosis and melanization.

The Toll pathway is constitutively active in *Klf15* mutants

Nephrocytes are major regulators of hemolymph (insect blood) content via filtration followed by filtrate endocytosis (Hartley et al., 2016; Soukup et al., 2009). Therefore, we considered whether changes in circulating proteins in the mutant could account for the increased resistance observed

in *Klf15* mutant flies. Previously, we performed a proteomic analysis of hemolymph composition in both WT and *Klf15* unchallenged flies (Hartley et al., 2016). An in-depth analysis of this dataset revealed that amongst 130 proteins enriched (≥ 1.5-fold) or detected only in the hemolymph of nephrocyte-deficient mutants, 65 proteins were annotated as having an immune-related function (Figure 2C). All 65 proteins were predicted to have a signal sequence (SignalP 4.1), which is expected for secreted hemolymph proteins. Of these 65 proteins, we found that 19 are encoded by core genes of the *Drosophila* immune response (i.e., genes upregulated in response to most bacterial infections, see (Troha et al., 2018)), 30 are the products of genes that are induced only by a subset of microbial infections, and 16 are coded by genes that, while not regulated in response to infection themselves, have been ascribed an immune function. Interestingly, we also noted that a majority (33 of 65) of these proteins are known targets of the Toll pathway (e.g., the antimicrobial peptide genes *IM2*, *IM23*, and *CG15067*). Our data therefore established that the hemolymph of *Klf15* mutants is enriched in proteins of immune function primarily encoded by target genes of the Toll pathway, and suggested that changes in Toll pathway activity could explain the increase in resistance to pathogens observed in *Klf15* mutant flies.

We developed two competing hypotheses to explain the accumulation of Toll pathway targets in the hemolymph of *Klf15* mutants. The first hypothesis posited that because nephrocytes are critical regulators of protein turnover in the hemolymph, the rise in immune effectors could be the result of a decrease in protein turnover in these flies. Alternatively, the accumulation of immune gene products could be due to aberrant activation of the Toll and/or Imd pathways in nephrocyte-deficient flies. In agreement with the latter hypothesis, our proteomic analysis also identified proteins that were depleted (≥ 1.5-fold) in the hemolymph of *Klf15* mutants relative to

controls (Figure S2H). Six of these proteins are encoded by genes that are typically downregulated in response to bacterial infection in a Toll-dependent manner (e.g., *Lsp1β* and *CG2233*) (Troha et al., 2018), arguing that changes in hemolymph protein content are due to Toll pathway activation rather than protein turnover. To test this idea directly, we surveyed the activation of the Toll and Imd pathways by measuring the expression level of 5 Toll target genes and 4 Imd target genes in WT and *Klf15* mutant flies under basal conditions. RT-qPCR data from whole fly showed that all 5 Toll target genes—*IM2*, *CG15067*, *Drs*, *CG18067*, and *CG15293*—were significantly upregulated in *Klf15* mutants compared to controls (Figure 2D and Figure S2I). In contrast, we did not find any appreciable differences in gene expression between WT and *Klf15* mutants for the Imd target genes *Dpt*, *AttC*, and *TotA*; the exception was *AttD*, for which the mutant had significantly lower levels of expression relative to WT (Figure 2E and Figure S2I). These data indicate that the Toll pathway, but not the Imd pathway, is constitutively activated in *Klf15* mutants in unchallenged conditions. In agreement with these data, we also detected abnormal Toll activation in flies in which *Klf15* was knocked-down by RNAi specifically during the adult stage (*Hand-Gal4^{ts} > UAS-Klf15-IR*), demonstrating that the loss of nephrocyte scavenging function is solely responsible for Toll activation in these flies (Figure 2F). In contrast to our results in unchallenged conditions, infection of *Klf15* mutants with either *S. aureus* or *E. faecalis* revealed no significant differences between WT and mutant in terms of Toll or Imd target gene expression at any of the time points surveyed (3, 8, and 12 h post-challenge) (Figure S2J-S2K). In conclusion, our data establish that *Klf15* mutants present elevated basal levels of Toll target gene induction in conjunction with increased immune resistance to pathogens.

Increased pathogen resistance in *Klf15* mutants is contingent on higher baseline levels

of Toll activity

Next, we asked whether Toll pathway activity could be responsible for the increased resistance observed in *Klf15* mutant flies. We began by verifying that the increase in baseline Toll target gene expression was dependent on the Toll pathway itself (an abbreviated schematic of the Toll pathway is provided as part of Supplementary Figure 3). RT-qPCR of the Toll target genes *IM2* (Figure 3A), *CG15067*, and *Drs* (Figure S3A-S3B) showed that a null mutation in the gene coding for the Toll cytokine Spz completely abolished the increase in Toll target gene expression found in *Klf15* mutants (*Klf15* ;; spz^{rm7} double mutants). This was also true for a null mutation in the gene coding for SPE (*Klf15* ;; SPE^{SK6}), a key enzyme involved in the maturation of Spz and subsequent activation of the Toll pathway (Figure S3C-S3E), demonstrating that the increase in Toll target gene expression in *Klf15* hosts is due to elevated Toll pathway activity. Notably, suppression of the Toll pathway by either spz^{rm7} or SPE^{SK6} completely abrogated the survival advantage of *Klf15* mutants against pathogenic infection (Figure 3B-3C and Figure S3F-S3G). These results indicate that a surge in Toll pathway signaling is directly accountable for the augmented resistance of *Klf15* flies to infection.

The Toll pathway can be induced by endogenous DAMPs, which trigger the maturation of the circulating serine protease Persephone (Psh), or by the recognition of MAMPs, leading to the activation of the serine protease ModSP (Buchon et al., 2009; Gottar et al., 2006; Ming et al., 2014). Consequently, we set out to investigate whether aberrant Toll signaling in *Klf15* mutants was dependent on the detection of DAMPs or MAMPs by the host. While a null allele of *psh* was unable to rescue the elevated basal expression of the Toll target genes *IM2* (Figure 3D), *CG15067*, and *Drs* (Figure S3H-S3I) in *Klf15* mutants (*Klf15* , psh^{1}), a null mutation in *modSP* fully reverted

this increase (*Klf15* ;; *modSP*^{1}) (Figure 3G and Figure S3J- S3K). Accordingly, while the improved survival phenotype of the *Klf15* mutant was still present in *Klf15*, *psh*^{1} flies (Figure 3E-3F), *Klf15* ;; *modSP*^{1} flies no longer exhibited it (Figure 3H-3I). Thus, our data support the conclusion that elevated Toll signaling in response to MAMPs is responsible for the *Klf15* phenotype.

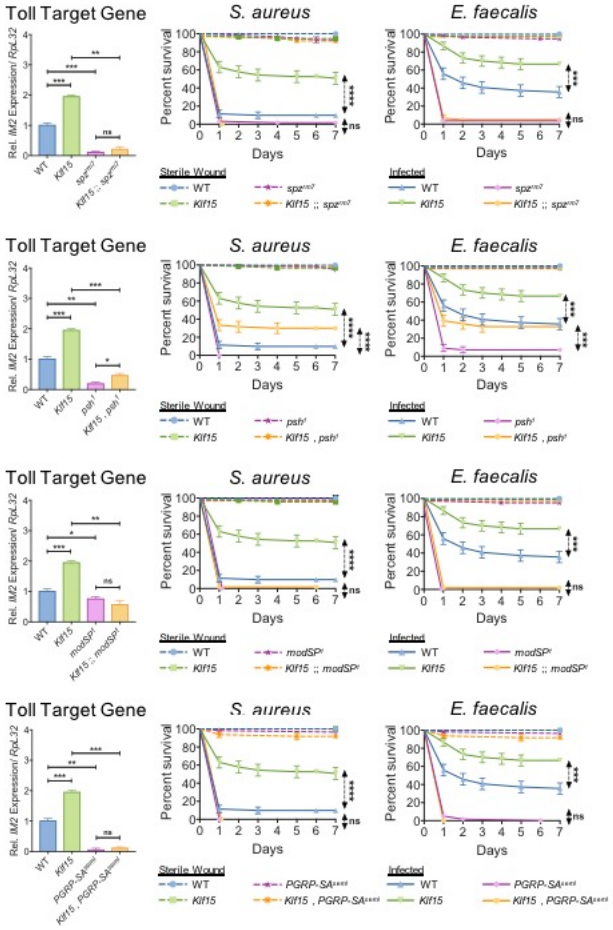

Figure IV.3. Increased resistance to infection in Klf15 mutants is PGRP-SA-dependent (A-C) Comparison of Klf15 ;; spzrm7 double mutants to WT, Klf15, and spzrm7 single mutants in experiments measuring IM2 (Toll target) gene expression via RT-qPCR (A), survival against S. aureus (B), and survival against E. faecalis (C). (D-F) Comparison of Klf15 ;; psh1 double mutants to WT, Klf15, and psh1 single mutants in experiments measuring IM2 gene expression via RT-qPCR (D), survival against S. aureus (E), and survival against E. faecalis (F). (G-I) Comparison of Klf15 ;; modSP1 double mutants to WT, Klf15, and modSP1 single mutants in experiments measuring IM2 gene expression via RT-qPCR (G), survival against S. aureus (H), and survival

against E. faecalis (I). (J-L) Comparison of Klf15 ;; PGRP-SAseml double mutants to WT, Klf15, and PGRP-SAseml single mutants in experiments measuring IM2 gene expression via RT-qPCR (J), survival against S. aureus (K), and survival against E. faecalis (L). For RT-qPCR experiments, mean values of three or more repeats are presented ±SE (*p<0.05 **p<0.01 ***p<0.001 in a Student's t-test). Survival curves show the average percent survival ±SE of three biological replicates (***p<0.001 ****p<0.0001 in a Log-rank test).

ModSP activity, and therefore Toll pathway signaling, can be induced by the binding of pattern recognition receptors (PRRs) to two types of MAMPs: β-(1,3)-glucan derived from the fungal cell wall is recognized by GNBP3 (Gottar et al., 2006), while bacterial peptidoglycan (PGN) is detected by PGRP-SA (Michel et al., 2001). Thus, we moved to resolve whether the increase in Toll pathway activity observed in *Klf15* mutants was due to sensing of PGN by PGRP-SA or β-(1,3)-glucan by GNBP3. RT-qPCR of the Toll target genes *IM2*, *CG15067*, and *Drs* demonstrated that the increase in basal Toll pathway signaling present in *Klf15* flies was downstream of PGRP-SA (*Klf15*, *PGRP-SA*^{seml}) (Figure 3J and Figure S3L-S3M) but not GNBP3 (*Klf15* ;; *GNBP3*^{Hades}) (Figure S3N-S3P). The enhanced survival phenotype of *Klf15* mutants was also lost in the double mutant *Klf15*, *PGRP-SA*^{seml} (Figure 3K-3L), but not in the double mutant *Klf15* ;; *GNBP3*^{Hades} (Figure S3Q-S3R), indicating that the surge in Toll signaling observed in nephrocyte-deficient flies is likely downstream of peptidoglycan recognition.

Microbiota-derived MAMPs trigger abnormal Toll pathway activation in *Klf15* mutants

Gut microbes are a source of MAMPs, such as peptidoglycan, and therefore can act as elicitors of the immune system (Kaneko et al., 2004; Clarke et al., 2010). In *Drosophila*, multiple immune tolerance mechanisms are in place to prevent errant activation of the Imd pathway in response to microbiota. These include the expression of a plethora of negative regulators (i.e., Caudal and

PIMS) and enzymes that degrade DAP-type PGN (i.e., PGRP-LB and PGRP-SC). However, no similar immune tolerance mechanism has been described for the Toll pathway despite the fact that it also senses PGN (Lys-type) (Wang et al., 2006; Bischoff et al., 2004; Park et al., 2007). Because the increase in Toll pathway activity in *Klf15* flies occurs downstream of PGRP-SA, we hypothesized that it could stem from a loss of immune tolerance to the gut microbiota (i.e. an aberrant increase in immune activation in response to innocuous microbes). To test this idea, we used RT-qPCR to measure the level of expression of the Toll target genes *IM2*, *CG15067* (Figure 4A), and *Drs* (Figure S4A) in wildtype and *Klf15* mutants reared in both conventionally reared (CR) and germ-free (GF) conditions. We found that the increase in Toll signaling in *Klf15* mutants was fully dependent on the presence of microbiota, as GF wildtype and GF *Klf15* flies displayed similar levels of expression for all measured Toll target genes. Since *Klf15* mutants did not have a higher microbiota load or show any alteration in gut barrier integrity—as determined by the SMURF assay and measurements of both circulating bacteria in the hemolymph and whole fly microbiota (Figure S4B-S4D)—our results indicate that *Klf15* mutants have lower immune tolerance to microbiota.

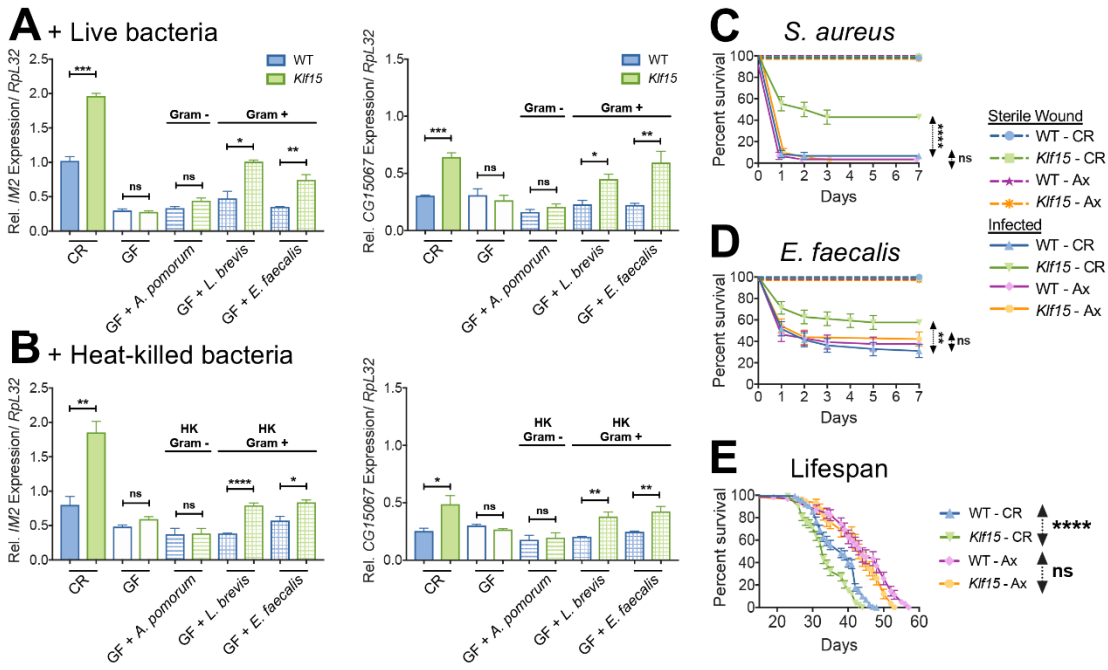

Figure IV.4. Nephrocytes mediate immune tolerance to Gram-positive microbiota (A) Assessment of gene expression levels in conventional (CR), germ-free (GF), and germ-free flies recolonized with either live A. pomorum (Gram-negative), live L. brevis (Gram-positive), or live E. faecalis (Gram-positive). RT-qPCR measurements of Toll target genes IM2 and CG15067 are shown. (B) Comparison of gene expression levels in conventional (CR), germ-free (GF), and germ-free flies fed either heat-killed A. pomorum (Gram-negative), heat-killed L. brevis (Gram-positive), or heat-killed E. faecalis (Gram-positive). RT-qPCR measurements of Toll target genes IM2 and CG15067 are presented. For RT-qPCR experiments, mean values of three or more repeats are presented ±SE. *p<0.05 **p<0.01 ***p<0.001 ****p<0.0001 in a Student's t-test. (C-D) Survival curve over 7 days after infection of WT and Klf15 mutant flies in both conventional (CR) and germ-free (GF) conditions with S. aureus (C) and E. faecalis (D). (E) Lifespan curve comparing WT flies to Klf15NN mutants in both conventional (CR) and germ-free (GF) conditions. Curves represent the average percent survival ±SE of three biological replicates (**p<0.01 ****p<0.0001 in a Log-rank test).

Because the increase in Toll pathway activity found in nephrocyte-deficient flies is both downstream of PGRP-SA and microbiota-dependent, we postulated that this phenotype could arise from a decrease in immune tolerance to microbiota-derived MAMPs. In agreement with this hypothesis, mono-colonization of GF *Klf15* flies with the Gram-positive, Lys-type PGN-carrying microbes *E. faecalis* and *Lactobacillus brevis* triggered aberrant Toll pathway activity, while recolonization with the Gram-negative, DAP-type PGN-containing *Acetobacter pomorum* did not

(Figure 4A-S4A). Of note, *E. faecalis*, *A. pomorum*, and *L. brevis* are normal constituents of the *Drosophila* gut microbiota (Broderick et al., 2014). This result suggested that the microbiota could act to elevate Toll pathway signaling in nephrocyte-deficient flies by providing a source of Lys-type PGN, thus stimulating PGRP-SA in the absence of infection. Additional experiments confirmed that gut microbiota-derived MAMPs were sufficient to trigger the Toll pathway in GF *Klf15* mutants. Feeding GF *Klf15* hosts with heat-killed *L. brevis* or *E. faecalis*, but not *A. pomorum*, was enough to elicit abnormal Toll pathway activity as measured by *IM2*, *CG15067*, and *Drs* expression (Figure 4B and Figure S4E). Altogether, these results established that in *Klf15* mutants, gut microbiota-derived Lys-type PGN induces an errant, Toll pathway-mediated immune response.

Next, we explored whether this rupture of tolerance to the microbiota could be responsible for the increase in resistance to infection observed in *Klf15* mutants. Unlike flies raised in CR conditions, GF *Klf15* flies infected with the bacterial pathogens *S. aureus* and *E. faecalis* did not exhibit increased survival to infection relative to GF wildtype controls (Figures 4C-4D). These results suggest that microbiota-derived Lys-type PGN primes the Toll pathway in *Klf15* mutants, leading to enhanced resistance. Chronic immune activation is costly and harmful to hosts (Charroux et al., 2018; Guo et al., 2014; Paredes et al., 2011). As we noted that flies devoid of nephrocytes had a shorter lifespan (Figure 1B), we asked whether this could also be due to a breach in immune tolerance to the microbiota. *Klf15* mutant flies reared in GF conditions significantly outlived their CR counterparts, and no difference in lifespan was found between *Klf15* and WT flies raised in GF conditions (Figure 4E). Thus, our results demonstrate that nephrocytes are part of an immune tolerance program that controls microbiota-dependent Toll pathway activation.

Nephrocytes endocytose peptidoglycan from the hemolymph to promote immune tolerance to the microbiota

We find that the Toll pathway is abnormally activated in response to microbiota-derived MAMPs in the absence of nephrocytes. This could be the result of either the presence of elevated amounts of microbiota-shed PGN in the hemolymph (as microbiota-shed MAMPs are commonly translocated from the gut lumen into systemic circulation) or the hyper-reactivity of these flies to MAMPs. SPE, a signaling component of the Toll pathway, accumulates in the hemolymph of *Klf15* mutants (Figure 2C) despite not being transcriptionally upregulated (Figure S4I). Overexpression of SPE is also sufficient to trigger Toll pathway activation (Jang et al., 2006). Consequently, we hypothesized that accretion of SPE could result in an aberrant response to the microbiota in *Klf15* mutant flies. While overexpression of SPE alone resulted in the upregulation of three target genes of the Toll pathway, *IM2*, *CG15067*, and *Drs* (Figure S4F-S4H), the level of induction was identical between CR and GF conditions, suggesting that this effect was not dependent on the presence of microbiota. It is therefore unlikely that the microbiota-dependent induction of Toll in *Klf15* flies is due to SPE accumulation. In light of this result, we moved on to the next hypothesis. As nephrocytes regulate hemolymph composition by filtration followed by filtrate endocytosis, we reasoned that in the absence of nephrocytes, microbiota-derived Lys-type PGN could accumulate in the hemolymph. We therefore measured the amount of PGN circulating in the hemolymph of WT and *Klf15* mutants in both CR and GF conditions. Using a colorimetric assay (SLP), we detected three times more circulating PGN in *Klf15* mutants than in WT controls under CR conditions, with no difference found between the two genotypes under GF conditions (Figure 5A). These data establish that nephrocytes participate in the removal of microbiota-shed PGN from

systemic circulation.

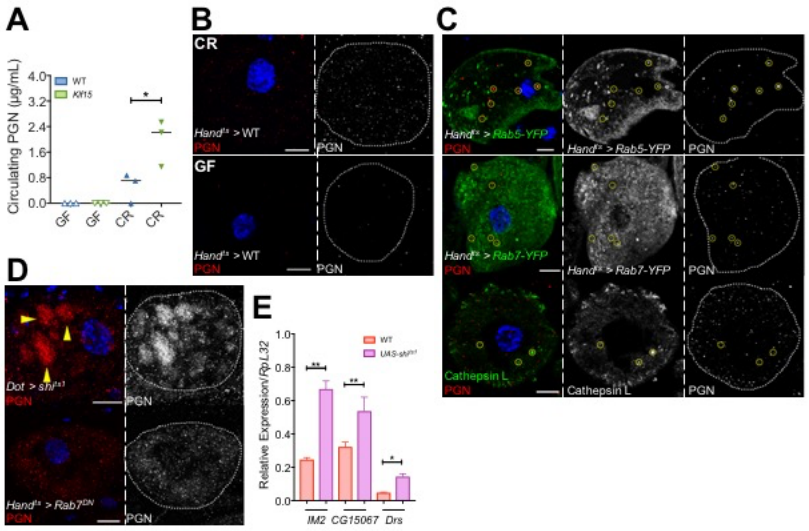

Figure IV.5. Nephrocytes endocytose peptidoglycan from systemic circulation
(A) Quantification of peptidoglycan levels in the hemolymph (insect blood) of WT and Klf15NN flies in germ-free (GF) and conventional (CR) conditions. *p<0.05 in a Student's t-test (B) Immunostaining of nephrocytes of CR and GF flies demonstrates that nephrocytes internalize microbiota-derived PGN. (C) Immunostaining against PGN reveals colocalization (yellow circles) with the early endosome marker Rab5 (Hand-Gal4ts > UAS- Rab5-YFP), the late endosome marker Rab7 (Hand-Gal4ts > UAS- Rab7-YFP), and the lysosomal compartment marker Cathepsin L. (D) Nephrocyte-specific expression of Shibirets (Dot-Gal4 > UAS-shits1) or Rab7DN (Hand-Gal4ts > UAS-Rab7DN) led to accumulation of PGN in nephrocytes when compared to control (B). (E) Whole fly RT-qPCR of Toll target genes IM2, CG15067, and Drs in unchallenged conditions. Gene expression was measured in flies expressing shibirets1 in a nephrocyte-specific manner (Dot-Gal4 > UAS-shits1). *p<0.05 **p<0.01 ***p<0.001 in a Student's t-test.

Subsequently, we focused on determining what mechanisms underlie nephrocyte-mediated PGN removal from the hemolymph. Nephrocytes are filtration devices. Their surface is covered by extensive membrane invaginations, which are sealed at the top by slit diaphragms. These chambers, known as lacunae or labyrinthine channels, are where most of their endocytic activity takes place. Once endocytosed, internalized cargo is either trafficked to lysosomes for degradation,

metabolized and released back into circulation, or stored in vacuoles for the lifespan of the fly (Denholm et al., 2009; Psathaki et al., 2018). To assess whether nephrocytes internalize circulating PGN, we immunostained nephrocytes with an anti-PGN antibody (raised against PGN from a Gram-positive Streptococcus sp.). Confocal sectioning of nephrocytes revealed a strong punctate signal pattern, indicating that nephrocytes do indeed internalize PGN (Figure 5B). PGN staining disappeared in flies reared in GF conditions, suggesting that nephrocytes take up microbiota-derived PGN in order to remove it from the hemolymph (Figure 5B). Immunostaining against PGN in nephrocytes expressing either a reporter for the early endosomal marker Rab5 (*Hand-Gal4^{ts} > UAS-Rab5-YFP*) or a reporter for the late endosomal marker Rab7 (*Hand-Gal4^{ts} > UAS-Rab7-YFP*) showed co-localization of PGN with both markers (Figure 5C). We also detected co-localization of PGN with the lysosomal marker cathepsin L (Figure 5C), implying that PGN is internalized by endocytosis and routed to the lysosomal compartment. We then moved to evaluate the role of endocytosis in the uptake of PGN by nephrocytes. The dynamin Shibire is involved in the early steps of endocytosis. Blocking Shibire triggers elongation of the lacunae/labyrinthine channels within the nephrocytes (Kosaka and Ikeda, 1983). Because the filtration and endocytic functions of nephrocytes are separate, blocking endocytosis but not filtration via expression of the thermosensitive *shibire^{ts1}* allele results in the accumulation of filtrate in the lacunae, a phenomenon previously observed with the circulating serpin Necrotic (Soukup et al., 2009). When we blocked the endocytic pathway using this same allele (*Hand-Gal4^{ts} > UAS-shi^{ts1}*), we observed massive accumulation of PGN in nephrocytes (Figure 5D), signifying that nephrocytes endocytose PGN by a Shibire-dependent mechanism. In addition, nephrocyte-specific expression of a dominant negative form of Rab7 (*Hand-Gal4^{ts} > UAS-Rab7^{DN}*)—which reroutes all traffic to clear vacuoles, thereby blocking access to the lysosome (Fu et al., 2017)—led to cytoplasmic accumulation of

endocytosed PGN relative to controls (Figure 5D). Taken together, these results demonstrate that PGN is endocytosed and degraded by nephrocytes in a Shibire- and Rab7-dependent manner.

Finally, we examined the consequences of arresting the endocytic function of nephrocytes on Toll pathway activity. Blocking endocytosis in nephrocytes via expression of the same *shibire*^{ts1} allele was sufficient to induce abnormally high transcription of Toll target genes (Figure 5E). These results are in agreement with the increase in Toll pathway signaling we detected in flies in which *Klf15* was knocked down in adult nephrocytes (Figure 2F), a condition known to block their endocytic capability (Ivy et al., 2015). Altogether, our results establish that nephrocytes remove microbiota-derived PGN from systemic circulation, thus preventing deviant immune activation in response to gut microbes.

Discussion

Regulation of circulating, microbiota-derived MAMPs is critical for maintenance of immune homeostasis. Toll and Imd, the two primary immune pathways in the fly, recognize the presence of invading bacteria through sensing of specific forms of PGN (peptidoglycan): Lys-type PGN from Gram-positive bacteria is recognized by the Toll pathway, while DAP-type PGN from Gram-negative bacteria is detected by the Imd pathway (Lemaitre and Hoffmann, 2007). Because the gut is constantly exposed to microbes and their MAMPs, it relies on specialized tolerance mechanisms to prevent local immune activation against the microbiota. Given that microbiota-shed PGN is translocated from the gut lumen into general circulation (Capo et al., 2017; Clarke et al., 2010; Gendrin et al., 2009), additional immune tolerance mechanisms are required to prevent systemic immune activation in response to the microbiota. Without such processes, chronic immune induction can lead to abnormal development (Bischoff et al., 2006) and/or a shortened lifespan, indicating that uncontrolled immune activity can be costly to the host's health (Charroux et al., 2018; Guillou et al., 2016; Paredes et al., 2011). Systemic immune tolerance mechanisms involve the secretion of amidase PGRPs into the hemolymph, where they act to degrade DAP-type PGN and prevent overactivation of the Imd pathway (Bischoff et al., 2006; Charroux et al., 2018; Guo et al., 2014; Paredes et al., 2011; Zaidmanremy et al., 2006). To date, no similar mechanism has been identified for the Toll pathway, although it seems like such mechanism should be necessary. Here, we propose that filtration of hemolymph by nephrocytes takes charge of this Toll-specific, immune homeostatic function. We find that nephrocytes endocytose Lys-type PGN from systemic circulation and route it to lysosomes for degradation, thus maintaining immune tolerance to Gram-positive microbiota.

Why distinct mechanisms to deal with the elimination of different types of PGN have evolved is an open question. One possibility is that efficient degradation of Lys-type PGN requires specialized enzymes, such as lysozymes, that work best in the acidified environment of a mature lysosome than in circulation. Optimal pH for lysozyme activity is ~6.6, with a rapid decrease in activity at pH values below 6.2 or above 7.0 (Smolelis and Hartsell, 1952). By contrast, hemolymph pH is considerably higher, with pH levels ranging from 7.3 to 7.4 (Ghosh and O'Connor, 2014). As nephrocytes are professional endocytic cells, they would be well suited to rapidly and proficiently uptake Lys-type PGN from the hemolymph and route it for degradation to lysosomes. In support of this idea, it is worth noting that nephrocytes express at least 7 lysozyme-like genes (Chintapalli et al., 2007). Interestingly, our data also established that the Imd pathway is not activated in the absence of nephrocytes. This could be a result of the efficient degradation of DAP-type PGN by amidase PGRPs, leaving no intact PGN of this class to be endocytosed. Alternatively, the intrinsic negative charge of the nephrocyte basement membrane, which is known to act as a charge-selective filter (Denholm et al., 2009), could act to exclude passage of DAP-type but not Lys-type PGN.

Recently, a study showed that nephrocytes uptake Nec, a secreted serpin and negative regulator of the Toll pathway, and target it for lysosomal degradation (Soukup et al., 2009). Our work not only confirmed this finding, as levels of Nec were higher in the hemolymph of *Klf15* mutants compared to wildtype, but also found that other key signaling components of the Toll pathway, such as SPE, accumulate in the hemolymph of *Klf15* mutants despite not being transcriptionally upregulated themselves. These results suggest that hemolymph filtration by nephrocytes may serve to regulate Toll pathway homeostasis on multiple levels: regulating both

Lys-type PGN hemolymph concentration and the amount of circulating Toll pathway components available in the hemolymph. Our results did not allow us to determine whether the accumulation of signaling components of the Toll pathway was also important for the loss of immune tolerance in flies lacking nephrocytes. However, the fact that GF *Klf15* mutants do not show an increase in Toll activity suggests that PGN filtration, rather than protein accumulation, is the critical immune tolerance mechanism. In addition, we note that the phenotype associated with a lack of nephrocytes is not easily predicted. At first glance, accumulation of Nec in flies devoid of nephrocytes would suggest a possible decrease in immune reactivity. However, our results proved the opposite, demonstrating that the loss of PGN filtration primes the immune system and increases resistance to infection.

Chronic kidney disease (CKD), characterized by a gradual loss of glomerular filtration rate, leads to alterations in plasma protein content similar to those observed in *Klf15* mutants. Specifically, Glorieux and colleagues found by proteomic analysis that patients with CKD progressively accumulate in their plasma high levels of 24 proteins involved in the complement system, with a large number of these proteins belonging to the alternative complement pathway (Glorieux et al., 2015). Further activation of the innate immune system was also evident in CKD patients, as their plasma was enriched for 62 proteins associated with the acute phase response (Glorieux et al., 2015). Given the remarkable functional, structural, and molecular similarities between nephrocytes and the glomerular podocytes of the mammalian kidney, we propose that renal filtration by the kidneys could also act to regulate the levels of microbiota-derived MAMPs, such as PGN, in the blood, thus maintaining immune homeostasis. In support of this idea, we highlight that the alternative complement pathway, several components of which were enriched in

the plasma of CKD patients, is known to be activated by peptidoglycan, including Lys-type peptidoglycan (Kawasaki et al., 1987). In both *Klf15* mutants and CKD patients, proteomic studies also showed accumulation of lysozymes in circulation, with lysozyme C increasing in the plasma and CG6426 rising in the hemolymph. It is possible that lysozyme accumulation could result, in both cases, from induction of the immune system in response to PGN, especially as CG6426 is a target of the Toll pathway (de Gregorio et al., 2001; Troha et al., 2018). Of note, it has also been proposed that nephrocytes are functionally analogous to endocytic scavenger cells of the mammalian reticuloendothelial system (Sørensen et al., 2012; Wigglesworth, 1970). Therefore, it is possible that additional cells with scavenging function, such as hepatocytes, could also be involved in the regulation of microbiota-shed MAMPs.

Altogether, our results reveal an unexpected role for podocyte filtration in the maintenance of insect immune homeostasis. They suggest that renal clearance could be a major and conserved mechanism to remove PGN from circulation, thus preventing aberrant immune activation in response to the gut microbiota. Because of the parallels between the filtration systems of flies and mammals, as well as the similar consequences of altering renal function in both species, we propose that at least part of the immune activation observed in patients suffering from glomerular diseases stems from the accumulation of PGN in plasma.

Materials and Methods

Rearing of Drosophila melanogaster

Flies were maintained on standard sucrose-cornmeal-yeast medium: 50 g baker's yeast, 60 g cornmeal, 40 g sucrose, 7 g agar, 26.5 mL Moldex (10%), and 12 mL Acid Mix solution (4.2% phosphoric acid, 41.8% propionic acid) per 1L of deionized H_2O. Wildtype and mutant flies were raised at 24 °C. Flies originating from crosses that employ the UAS-Gal4-Gal80^{ts} gene expression system were raised at 18 °C (Gal80^{ts} On, Gal4 Off) and transferred to 29 °C (Gal80^{ts} Off, Gal4 On) 5 days after eclosion. Males were used for all experiments, with the exception of immunostaining (larger female size is preferred for dissection and visualization of cells). For experiments with *UAS* transgenes, 10- to 14-day-old flies were used (to allow for the expression of the pertinent construct).

Drosophila melanogaster strains

Klf15^{NN}, *spz*^{rm7}, *SPE*^{SK6}, *psh*^{1}, *modSP*^{1}, *GNBP3*^{Hades}, *PGRP-SA*^{seml}, and *PPO1*$^{\Delta}$, *2*$^{\Delta}$*,3*^{1} mutants have been previously described (Buchon et al., 2009; Dudzic et al., 2015; Gobert et al., 2003; Gottar et al., 2006; Ivy et al., 2015; Jang et al., 2006; Michel et al., 2001; Ming et al., 2014). The nephrocyte-specific drivers, *Dot-Gal4* and *Hand-Gal4*^{ks}, are detailed in (Ivy et al., 2015). The following lines were purchased from the Bloomington *Drosophila* Stock Center: *UAS-shi*^{ts1} (44222), *UAS-Rab7*^{DN} (9778), *UAS-Rab5-YFP* (24616), *UAS-Rab7-YFP* (23270).

Culturing of microbes

The following bacteria were cultured overnight in LB broth and adjusted to the specified density: *Serratia marcescens* Type (OD_{600} =1), *Salmonella typhimurium* (OD_{600} =1), *Listeria innocua* (OD_{600}

=1), *Enterococcus faecalis* (OD_{600} =1), *Staphylococcus aureus* (OD_{600}=1), and *Providencia rettgeri* (OD_{600} =1). *S. typhimurium* and *L. innocua* were grown at 37 °C. All other bacteria were grown at 29 °C. The fungi *Beauveria bassiana* and *Metarhizium anisopliae* were grown at 29 °C on YPG-agar plates.

Infections, survival experiments, and recording of lifespan

Flies were systemically infected with bacteria via septic pinprick to the thorax. For natural infections with fungi, CO_2-anaestethized flies were placed directly on the sporulating lawn of a fungal culture plate and the plate was shaken for ~15 seconds to coat the flies in spores. Flies were then transferred to a new, clean food vial to recover. All flies, regardless of infection method, were maintained at 29 °C for the duration of the experiments. For survival experiments, death was recorded daily following inoculation, with flies transferred to fresh vials every 2 to 3 days. For lifespan measurements, adults were transferred to 29 °C 5 days post-eclosion and remained at that temperature for the duration of the experiment. All experiments were performed at least 3 times.

Quantification of bacterial CFUs

At specified time points following inoculation, flies were individually homogenized by bead beating in 500 µl of sterile PBS using a tissue homogenizer (OPS Diagnostics). Dilutions of the homogenate were plated onto LB agar plates using a WASP II autoplate spiral plater (Microbiology International), incubated overnight at 29 °C, and CFUs were counted. All experiments were performed at least 3 times.

RT-qPCR

For all experiments involving RT-qPCR, total RNA was extracted from pools of 20 flies using the standard TRIzol (Invitrogen) extraction. RNA samples were treated with DNase (Promega), and cDNA was generated using murine leukemia virus reverse transcriptase (MLV-RT-Promega). qPCR was performed using the SSO Advanced SYBR green kit (Bio-Rad) in a Bio-Rad CFX-Connect instrument. Data represent the relative ratio of the target gene and that of the reference gene *RpL32*. Mean values of at least three biological replicates are represented ±SE. The primer sequences used can be found in Table 1.

Phagocytosis assays

To assay phagocytosis, flies were injected in the thorax with 69 nl of pHrodo Red Bioparticles™ (Invitrogen) using a Nanoject (Drummond Scientific). The fluorescence within the abdomen of the flies was then imaged at 3 h post-injection with a Leica MZFLIII fluorescent microscope and quantified using ImageJ (NIH) as previously described (Guillou et al., 2016). To block phagocytosis, adult flies were pre-injected with a solution containing latex beads as previously described in (Elrod-Erickson et al., 2000). Twenty-four hours post injection, the flies were subjected to systemic infection as described above.

Hemolymph extraction

Hemolymph was collected using a centrifugation or capillary method. In the first method, ~100 anesthetized flies are loaded into a modified spin column (Qiagen), in which the filter was removed and thoroughly washed with water before use, and 2 metal beads are placed on top of the flies. Flies are then centrifuged twice at 5,000 g for 5 minutes at 4 °C. For the capillary method, a pulled glass needle is used to prick flies in the thorax. Hemolymph is extracted into the needle by capillary

action.

DOPA assay

Extracted hemolymph was immediately diluted in a 1:10 ratio using a protease inhibitor cocktail (Sigma: 11697498001) and kept on ice. Briefly, 50 µL of diluted hemolymph was combined with 150 μl of a 5 mM $CaCl_2$ solution and 800 µL of L-DOPA (Sigma: D9628) reagent. Following thorough mixing, 200 μl of sample/well was loaded into a 96-well plate. Using a spectrophotometer set to 29 °C, a kinetic assay was performed at OD_{492}.

Generation of germ-free and mono-colonized flies

Collected eggs were surface sterilized by immersion in 70% ethanol for 2 min. Eggs were then dechorionated via treatment with a 10% bleach solution for 10 min. This was followed by rinsing the eggs in sterile water 3 times to remove any leftover bleach. The eggs were then transferred to pre-autoclaved media vials, where they were allowed to develop. The entire procedure was performed using sterile technique in a laminar flow hood. For mono-colonized flies, pre-autoclaved media vials were seeded with 200 µL of the desired individual bacterial culture (OD_{600} =200). After the bacterial solution was absorbed into the media, adult germ-free flies were flipped into the mono-colonized media vial. Experiments with mono-colonized flies were carried out 5 days after the flies were first exposed to the bacteria.

PGN detection by Silkworm Larvae Plasma (SLP) assay

After diluting extracted hemolymph (1:10 ratio), 50 µL of hemolymph sample/condition was used for the SLP assay (Fujifilm Wako Pure Chemical Corporation: 297-51501) following the

manufacturer's instructions.

Gut barrier integrity (Smurf) assay

Adult flies were fed standard medium supplemented with Blue Dye No. 1 (2.5%). A fly was counted as a Smurf when the blue dye could be observed outside of the digestive tract.

UAS/GAL4/GAL80^{ts} gene expression system

For RNAi and overexpression experiments, we used the UAS/GAL4 gene expression system in combination with GAL80ts to restrict the expression of the constructs specifically to the adult stage. Flies were collected 5 to 8 days after eclosion from the pupal case and shifted to 29 °C for an additional 8 days prior to any experiments. See our *Rearing of Drosophila melanogaster* section for additional details.

Immunohistochemistry and fluorescence imaging

Dissected nephrocytes were fixed in a 4% paraformaldehyde solution in PBST (PBS with 0.5% Triton X-100) for 1 h. After repeated washes in PBST, samples were blocked in 3% BSA PBST for 3 h and incubated overnight with primary antibodies in 1% BSA PBST at 4 °C. Samples were labeled with secondary antibodies in 1% BSA PBST for 2 h. Samples were washed after each antibody labeling step with PBST containing 4% NaCl to reduce non-specific background labeling. The primary antibodies used in this study were: mouse anti-peptidoglycan (GeneTex: GTX39437) diluted 1:200, chicken anti-GFP (Invitrogen: A10262) diluted 1:1500, and rabbit anti-Cathepsin L (Abcam: ab58991) diluted 1:1000. The secondary antibodies were: Alexa Fluor 488 anti-chicken (A11039), Alexa Fluor 488 anti-rabbit (A21206), and Alexa Fluor 555 anti-mouse (A31570), all

diluted 1:1500 and from Invitrogen. Imaging was performed on a Zeiss LSM 700 confocal inverted microscope.

Statistical Analysis

Aside from one exception, all analyses were performed in Prism (GraphPad Prism V7.0a, GraphPad Software, La Jolla, CA, USA). For survival assays, the curves represent the average percent survival ±SE of three or more biological replicates (n=20 flies for each biological replicate). A Log-rank test was used to determine significance (*p<0.05 **p<0.01 ***p<0.001 ****p<0.0001). In bacterial load quantification assays, the horizontal lines represent median values for each time point. Three biological replicates were included. Following normalization, results were analyzed using a two-way ANOVA followed by Sidak's post-test for specific comparisons (*p<0.05 **p<0.01 ***p<0.001 ****p<0.0001). For all other experiments, mean values of three or more biological repeats are presented ±SE. Significance was calculated by a Student's t-test following normalization (*p<0.05 **p<0.01 ***p<0.001 ****p<0.0001). Whenever survival curves crossed, a Cox's proportional-hazards model was used instead of a Log-rank test to assay significance. In this case, SPSS (IBM Corp. Released 2017. IBM SPSS Statistics for Mac OS X, Armonk, NY: IBM Corp.) was used for the analysis.

Acknowledgements

We thank J. Rossi for assistance with manuscript editing. We also thank all members of the Buchon lab for helpful comments on the manuscript.

REFERENCES

Aggarwal, S.K., King, R.C., 1967. The ultrastructure of the wreath cells of Drosophila melanogaster larvae. Protoplasma 63, 343–352.

Ayres, J.S., Schneider, D.S., 2011. Tolerance of Infections. Annu Rev Immunol. doi:10.1146/annurev-immunol-020711-075030

Binggeli, O., Neyen, C., Poidevin, M., Lemaitre, B., 2014. Prophenoloxidase Activation Is Required for Survival to Microbial Infections in Drosophila. PLoS Pathog 10, e1004067. doi:10.1371/journal.ppat.1004067

Bischoff, V., Vignal, C., Duvic, B., Boneca, I.G., Hoffmann, J.A., Royet, J., 2006. Downregulation of the Drosophila immune response by peptidoglycan-recognition proteins SC1 and SC2. PLoS Pathog 2, e14. doi:10.1371/journal.ppat.0020014

Broderick, N.A., Buchon, N., Lemaitre, B., 2014. Microbiota-induced changes in drosophila melanogaster host gene expression and gut morphology. MBio 5, e01117–14. doi:10.1128/mBio.01117-14

Buchon, N., Poidevin, M., Kwon, H.-M., Guillou, A., Sottas, V., Lee, B.L., Lemaitre, B., 2009. A single modular serine protease integrates signals from pattern-recognition receptors upstream of the Drosophila Toll pathway. Proceedings of the National Academy of Sciences 106, 12442–12447. doi:10.1073/pnas.0901924106

Buchon, N., Silverman, N., Cherry, S., 2014. Immunity in Drosophila melanogaster - from microbial recognition to whole-organism physiology. Nat Rev Immunol 14, 796–810. doi:10.1038/nri3763

Capo, F., Chaduli, D., Viallat-Lieutaud, A., Charroux, B., Royet, J., 2017. Oligopeptide Transporters of the SLC15 Family Are Dispensable for Peptidoglycan Sensing and Transport in Drosophila. J Innate Immun 9, 483–492. doi:10.1159/000475771

Cecconi, M., Evans, L., Levy, M., Rhodes, A., 2018. Sepsis and septic shock. The Lancet 392, 75–87. doi:10.1016/S0140-6736(18)30696-2

Charroux, B., Capo, F., Kurz, C.L., Peslier, S., Chaduli, D., Viallat-Lieutaud, A., Royet, J., 2018. Cytosolic and Secreted Peptidoglycan-Degrading Enzymes in Drosophila Respectively Control Local and Systemic Immune Responses to Microbiota. Cell Host Microbe 23, 215–228.e4. doi:10.1016/j.chom.2017.12.007

Chintapalli, V.R., Wang, J., Dow, J.A.T., 2007. Using FlyAtlas to identify better Drosophila melanogaster models of human disease. Nat Genet 39, 715–720. doi:10.1038/ng2049

Clarke, T.B., Davis, K.M., Lysenko, E.S., Zhou, A.Y., Yu, Y., Weiser, J.N., 2010. Recognition of peptidoglycan from the microbiota by Nod1 enhances systemic innate immunity. Nat. Med. 16, 228–231. doi:10.1038/nm.2087

Corbitt, N., Kimura, S., Isse, K., Specht, S., Chedwick, L., Rosborough, B.R., Lunz, J.G., Murase, N., Yokota, S., Demetris, A.J., 2013. Gut Bacteria Drive Kupffer Cell Expansion via MAMP-Mediated ICAM-1 Induction on Sinusoidal Endothelium and Influence Preservation-Reperfusion Injury after Orthotopic Liver Transplantation. Am J Pathol 182, 180–191. doi:10.1016/j.ajpath.2012.09.010

Crossley, A.C., 1972. The ultrastructure and function of pericardial cells and other nephrocytes in an insect: Calliphora erythrocephala. Tissue Cell 4, 529–560.

de Gregorio, E., Spellman, P.T., Rubin, G.M., Lemaitre, B., 2001. Genome-wide analysis of the Drosophila immune response by using oligonucleotide microarrays. Proceedings of the National Academy of Sciences 98, 12590–12595. doi:10.1073/pnas.221458698

Denholm, B., development, H.S.C.O.I.G., 2009, 2009. Bringing together components of the fly renal system. Elsevier
. doi:10.1016/j.gde.2009.08.006
Dudzic, J.P., Kondo, S., Ueda, R., Bergman, C.M., Lemaitre, B., 2015. Drosophila innate immunity: regional and functional specialization of prophenoloxidases. BMC Biol 13, 81. doi:10.1186/s12915-015-0193-6
Duneau, D., Ferdy, J.-B., Revah, J., Kondolf, H., Ortiz, G.A., Lazzaro, B.P., Buchon, N., 2017. Stochastic variation in the initial phase of bacterial infection predicts the probability of survival in D. melanogaster. elife 6, e28298. doi:10.7554/eLife.28298
Elrod-Erickson, M., Mishra, S., Schneider, D.S., 2000. Interactions between the cellular and humoral immune responses in Drosophila 10, 781–784. doi:10.1016/S0960-9822(00)00569-8
Ferrandon, D., 2013. The complementary facets of epithelial host defenses in the genetic model organism Drosophila melanogaster: from resistance to resilience. Current Opinion in Immunology 25, 59–70. doi:10.1016/j.coi.2012.11.008
Fu, Y., Zhu, J.-Y., Zhang, F., Richman, A., Zhao, Z., Han, Z., 2017. Comprehensive functional analysis of Rab GTPases in Drosophila nephrocytes. Cell Tissue Res 368, 615–627.
Gendrin, M., Welchman, D.P., Poidevin, M., Hervé, M., Lemaitre, B., 2009. Long-range activation of systemic immunity through peptidoglycan diffusion in Drosophila. PLoS Pathog 5, e1000694. doi:10.1371/journal.ppat.1000694
Ghosh, A.C., O'Connor, M.B., 2014. Systemic Activin signaling independently regulates sugar homeostasis, cellular metabolism, and pH balance in Drosophila melanogaster. Proceedings of the National Academy of Sciences 111, 5729–5734. doi:10.1073/pnas.1319116111
Glorieux, G., Mullen, W., Duranton, F., Filip, S., Gayrard, N., Husi, H., Schepers, E., Neirynck, N., Schanstra, J.P., Jankowski, J., Mischak, H., Argilés, À., Vanholder, R., Vlahou, A., Klein, J., 2015. New insights in molecular mechanisms involved in chronic kidney disease using high-resolution plasma proteome analysis. Nephrol Dial Transplant 30, 1842–1852. doi:10.1093/ndt/gfv254
Gobert, V., Gottar, M., Matskevich, A.A., Rutschmann, S., Royet, J., Belvin, M., Hoffmann, J.A., Ferrandon, D., 2003. Dual activation of the Drosophila toll pathway by two pattern recognition receptors. Science 302, 2126–2130. doi:10.1126/science.1085432
Gottar, M., Gobert, V., Matskevich, A.A., Reichhart, J.M., Wang, C., Butt, T.M., Belvin, M., Hoffmann, J.A., Ferrandon, D., 2006. Dual detection of fungal infections in Drosophila via recognition of glucans and sensing of virulence factors. Cell 127, 1425–1437. doi:10.1016/j.cell.2006.10.046
Guillou, A., Troha, K., Wang, H., Franc, N.C., Buchon, N., 2016. The Drosophila CD36 Homologue croquemort Is Required to Maintain Immune and Gut Homeostasis during Development and Aging. - PubMed - NCBI. PLoS Pathog 12, e1005961. doi:10.1371/journal.ppat.1005961
Guo, L., Karpac, J., Tran, S.L., Jasper, H., 2014. PGRP-SC2 Promotes Gut Immune Homeostasis to Limit Commensal Dysbiosis and Extend Lifespan. Cell 156, 109–122. doi:10.1016/j.cell.2013.12.018
Hartley, P.S., Motamedchaboki, K., Bodmer, R., Ocorr, K., 2016. SPARC-Dependent Cardiomyopathy in Drosophila. Circ Cardiovasc Genet 9, 119–129. doi:10.1161/CIRCGENETICS.115.001254
Ivy, J.R., Drechsler, M., Catterson, J.H., Bodmer, R., Ocorr, K., Paululat, A., Hartley, P.S., 2015. Klf15 Is Critical for the Development and Differentiation of Drosophila Nephrocytes. PLoS

ONE 10, e0134620. doi:10.1371/journal.pone.0134620
Jang, I.-H., Chosa, N., Kim, S.-H., Nam, H.-J., Lemaitre, B., Ochiai, M., Kambris, Z., Brun, S., Hashimoto, C., Ashida, M., Brey, P.T., Lee, W.-J., 2006. A Spätzle-processing enzyme required for toll signaling activation in Drosophila innate immunity. Dev Cell 10, 45–55. doi:10.1016/j.devcel.2005.11.013
Kaneko, T., Goldman, W.E., Mellroth, P., Steiner, H., Fukase, K., Kusumoto, S., Harley, W., Fox, A., Golenbock, D., Silverman, N., 2004. Monomeric and polymeric gram-negative peptidoglycan but not purified LPS stimulate the Drosophila IMD pathway. Immunity 20, 637–649.
Kaneko, T., Yano, T., Aggarwal, K., Lim, J.-H., Ueda, K., Oshima, Y., Peach, C., Erturk-Hasdemir, D., Goldman, W.E., Oh, B.-H., Kurata, S., Silverman, N., 2006. PGRP-LC and PGRP-LE have essential yet distinct functions in the drosophila immune response to monomeric DAP-type peptidoglycan. Nat Immunol 7, 715–723. doi:10.1038/ni1356
Kawasaki, A., Takada, H., Kotani, S., Inai, S., Nagaki, K., Matsumoto, M., Yokogawa, K., Kawata, S., Kusumoto, S., Shiba, T., 1987. Activation of the Human Complement Cascade by Bacterial Cell Walls, Peptidoglycans, Water-Soluble Peptidoglycan Components, and Synthetic Muramylpeptides—Studies on Active Components and Structural Requirements. Microbiology and Immunology 31, 551–569. doi:10.1111/j.1348-0421.1987.tb03117.x
Kim Newton, V.M.D., 2012. Signaling in Innate Immunity and Inflammation. Cold Spring Harb Perspect Biol 4, a006049–a006049. doi:10.1101/cshperspect.a006049
Kosaka, T., Ikeda, K., 1983. Reversible blockage of membrane retrieval and endocytosis in the garland cell of the temperature-sensitive mutant of Drosophila melanogaster, shibirets1. J Cell Biol 97, 499–507. doi:10.1083/jcb.97.2.499
Lemaitre, B., Hoffmann, J.A., 2007. The host defense of Drosophila melanogaster. Annu Rev Immunol 25, 697–743. doi:10.1146/annurev.immunol.25.022106.141615
Lhocine, N., Ribeiro, P.S., Buchon, N., Wepf, A., Wilson, R., Tenev, T., Lemaitre, B., Gstaiger, M., Meier, P., Leulier, F., 2008. PIMS modulates immune tolerance by negatively regulating Drosophila innate immune signaling. Cell Host Microbe 4, 147–158. doi:10.1016/j.chom.2008.07.004
Liu, X., Hodgson, J.J., Buchon, N., 2017. Drosophila as a model for homeostatic, antibacterial, and antiviral mechanisms in the gut. PLoS Pathog 13, e1006277. doi:10.1371/journal.ppat.1006277
Mallipattu, S.K., Liu, R., Zheng, F., Narla, G., Ma'ayan, A., Dikman, S., Jain, M.K., Saleem, M., D'Agati, V., Klotman, P., Chuang, P.Y., He, J.C., 2012. Kruppel-like factor 15 (KLF15) is a key regulator of podocyte differentiation. Journal of Biological Chemistry 287, 19122–19135. doi:10.1074/jbc.M112.345983
Michel, T., Reichhart, J.M., Hoffmann, J.A., Royet, J., 2001. Drosophila Toll is activated by Gram-positive bacteria through a circulating peptidoglycan recognition protein. Nature 414, 756–759. doi:10.1038/414756a
Ming, M., Obata, F., Kuranaga, E., Miura, M., 2014. Persephone/Spätzle pathogen sensors mediate the activation of Toll receptor signaling in response to endogenous danger signals in apoptosis-deficient Drosophila. Journal of Biological Chemistry 289, 7558–7568. doi:10.1074/jbc.M113.543884
Na, J., Cagan, R.L., 2013. The Drosophila nephrocyte: back on stage. J. Am. Soc. Nephrol. 24, 161–163. doi:10.1681/ASN.2012121227
Paredes, J.C., Welchman, D.P., Poidevin, M., Lemaitre, B., 2011. Negative Regulation by

Amidase PGRPs Shapes the Drosophila Antibacterial Response and Protects the Fly from Innocuous Infection. Immunity 35, 770–779. doi:10.1016/j.immuni.2011.09.018

Psathaki, O.-E., Dehnen, L., Hartley, P.S., Paululat, A., 2018. Drosophila pericardial nephrocyte ultrastructure changes during ageing. Mech. Ageing Dev. 173, 9–20. doi:10.1016/j.mad.2018.04.006

Reiser, J., Altintas, M.M., 2016. Podocytes. F1000Res 5. doi:10.12688/f1000research.7255.1

Ryu, J.-H., Kim, S.-H., Lee, H.-Y., Bai, J.Y., Nam, Y.-D., Bae, J.-W., Lee, D.G., Shin, S.C., Ha, E.-M., Lee, W.-J., 2008. Innate immune homeostasis by the homeobox gene caudal and commensal-gut mutualism in Drosophila. Science 319, 777–782. doi:10.1126/science.1149357

Smolelis, A.N., Hartsell, S.E., 1952. Factors affecting the lytic activity of lysozyme. Journal of Bacteriology 63, 665–674.

Soukup, S.F., Culi, J., Gubb, D., 2009. Uptake of the Necrotic Serpin in Drosophila melanogaster via the Lipophorin Receptor-1. PLoS Genet 5, e1000532. doi:10.1371/journal.pgen.1000532

Sørensen, K.K., McCourt, P., Berg, T., Crossley, C., Le Couteur, D., Wake, K., Smedsrød, B., 2012. The scavenger endothelial cell: a new player in homeostasis and immunity. Am. J. Physiol. Regul. Integr. Comp. Physiol. 303, R1217–30. doi:10.1152/ajpregu.00686.2011

Troha, K., Im, J.H., Revah, J., Lazzaro, B.P., Buchon, N., 2018. Comparative transcriptomics reveals CrebA as a novel regulator of infection tolerance in D. melanogaster. PLoS Pathog 14, e1006847. doi:10.1371/journal.ppat.1006847

Wang, L., Weber, A.N.R., Atilano, M.L., Filipe, S.R., Gay, N.J., Ligoxygakis, P., 2006. Sensing of Gram-positive bacteria in Drosophila: GNBP1 is needed to process and present peptidoglycan to PGRP-SA. EMBO J 25, 5005–5014. doi:10.1038/sj.emboj.7601363

Weavers, H., Prieto-Sánchez, S., Grawe, F., Garcia-López, A., Artero, R., Wilsch-Bräuninger, M., Ruiz-Gómez, M., Skaer, H., Denholm, B., 2009. The insect nephrocyte is a podocyte-like cell with a filtration slit diaphragm. Nature 457, 322–326. doi:10.1038/nature07526

Wigglesworth, V.B., 1970. The pericardial cells of insects: analogue of the reticuloendothelial system. J Reticuloendothel Soc 7, 208–216.

Zaidmanremy, A., Hervé, M., Poidevin, M., Pili-Floury, S., Kim, M.-S., Blanot, D., Oh, B.-H., Ueda, R., Mengin-Lecreulx, D., Lemaitre, B., 2006. The Drosophila amidase PGRP-LB modulates the immune response to bacterial infection. Immunity 24, 463–473. doi:10.1016/j.immuni.2006.02.012

Zhang, F., Zhao, Y., Han, Z., 2013. An in vivo functional analysis system for renal gene discovery in Drosophila pericardial nephrocytes. J. Am. Soc. Nephrol. 24, 191–197. doi:10.1681/ASN.2012080769

Zhuang, S., Shao, H., Guo, F., Trimble, R., Pearce, E., Abmayr, S.M., 2009. Sns and Kirre, the Drosophila orthologs of Nephrin and Neph1, direct adhesion, fusion and formation of a slit diaphragm-like structure in insect nephrocytes. Development 136, 2335–2344. doi:10.1242/dev.031609

CHAPTER V

DISCUSSION

1. Summary of findings

In Chapter II, a thorough collection of current protocols and methodology to assess the host response to infection in *Drosophila* is presented. This review covers techniques for measuring the reaction to microbial infection both qualitatively and quantitatively. Specifically, we describe survival, bacterial load, *BLUD* (a measure of disease tolerance), phagocytosis, melanization, clotting, and ROS production assays, as well as efficient protocols to collect hemolymph and measure immune gene expression. We additionally offer an updated catalog of online resources and a collection of popular reporter lines and mutants to facilitate research efforts. Finally, this Chapter also includes a discussion of known environmental and genetics factors that affect the host response to infection.

In Chapter III, we sought to identify a comprehensive list of genes regulated by pathogenic and avirulent infections, and to determine what responses are general or specific to each infection. To do this, we used RNA-seq to profile the *D. melanogaster* transcriptomic response to systemic infection with 10 different species of bacteria that vary in their ability to grow within and kill the host. We found that each bacterium elicits a unique host transcriptional response. However, we also identified a small set of core genes that were differentially regulated in response to infection with the majority of bacteria. These genes are involved in a variety of immune and physiological functions, and a portion of them remained highly expressed even after bacteria were cleared from the host. Among the core genes was *CrebA*, a transcription factor. We found that *CrebA* expression is upregulated through both Toll and Imd signaling in the fat body following infection. Knockdown of *CrebA* significantly increased mortality from microbial challenge but did not alter bacterial load, suggesting that *CrebA* contributes to disease tolerance. *CrebA* regulates multiple genes involved in the secretory pathway, and the loss of *CrebA* triggered endoplasmic reticulum (ER) stress upon

infection. Our findings suggest that *CrebA* promotes disease tolerance through protection from cellular stress in the fat body during the rapid and dramatic response to infection. Altogether, this work reveals essential features of the response to bacterial infection and elucidates the function of a novel regulator of disease tolerance [1].

In Chapter IV, we evaluated the role of hemolymph (analogous to mammalian blood) filtration in immune function and homeostasis. We found that the *Drosophila* nephrocyte, a cell type that regulates hemolymph composition by filtration, promotes immune tolerance specifically to Gram-positive microbiota. We showed that flies without nephrocytes, or with diminished nephrocyte function, are more resistant to a variety of microbial infections. We demonstrated that both the improved survival against infection and shorter lifespan of nephrocyte-deficient flies stem from aberrant Toll pathway activation. Our data revealed that errant Toll signaling in these flies is exclusively dependent on the presence of Gram-positive microbiota. We further presented evidence that nephrocytes uptake Lys-type peptidoglycan from systemic circulation via endocytosis and degraded it inside lysosomes. Without nephrocytes, microbiota-derived peptidoglycan accumulated in the hemolymph, triggering chronic stimulation of the Toll pathway. This work describes the first immune tolerance mechanism for Toll-specific immunity, suggesting that both the Toll and Imd pathways are strongly constrained by microbiota-shed MAMPs. More importantly, we have identified a potential role for renal filtration in the maintenance of immune tolerance to microbiota, a function likely conserved in mammals.

2. The physiological response to infection in *Drosophila*

In Chapter III, we identified a list of biological processes differentially regulated in

response to infection that are not classically thought of as being part of the immune system—e.g., neuron-related, secretion, oxidation-reduction, metabolism, tissue repair, response to pheromone/olfactory behavior, etc. Although many of these processes had been found to be regulated by infection in previous studies [2] [3] [4] [5] [6], our study was the first to report (to our knowledge) a list of host processes that are regulated in response to a majority of bacterial infections, making these physiological responses part of a core response to bacterial infection. Interestingly, most of these core physiological responses appear to be essential for host survival to infection. A survival screen where core upregulated genes that are not part of the classical immune response (antimicrobial peptides and other genes involved in known immune processes were excluded) were knocked down via RNAi prior to infection with two separate pathogens (*P. rettgeri* and *E. faecalis*) showed that knockdown of a majority of these genes (~80%) severely reduced infection survival rates or resulted in the death of all infected subjects (unpublished data). This suggests that several of these genes/processes may be as important as the activation of the immune system to guarantee host survival. What the function of all these core physiological responses are during infection and how they might interact with the immune system remains an open question. Potential roles include countering the deleterious effects of activating the immune system (e.g. the role of *CrebA* during infection), activating general stress responses to prevent or limit damage caused by pathogens, and promoting nutritional immunity (a process by which a host organism sequesters essential trace minerals in an effort to resist the pathogen [7]). Future studies are required to elucidate the functions of these important core physiological responses.

Interestingly, in this Chapter (III) we also found that many non-immune genes remain differentially regulated (compared to unchallenged samples) several days after the infection is cleared by the host (*M. luteus* infection is an example). These genes are involved in processes such

as metabolism and antioxidant function. Although it is possible that these genes eventually return to basal, pre-infection levels of expression (perhaps after our last sampling time point—5.5 days post-challenge), it is also plausible that some aspects of fly physiology remain permanently altered following a single infection that has been cleared by the host. If so, the consequences of these changes in terms of their effect on reproduction and lifespan might prove an interesting point for future study.

3. *CrebA* and disease tolerance as a survival strategy

In the past few years, the subject of disease tolerance has attracted substantial attention [8] [9]. The interest in disease tolerance is partly based on the proposition that, unlike resistance mechanisms, disease tolerance mechanisms do not have a direct negative effect on pathogen burden. Thus, microbes are not predicted to evolve strategies to subvert disease tolerance mechanisms [10]. Despite the recent focus, identifying the genes and processes that define disease tolerance has remained somewhat elusive [11] [12]. In Chapter III, we identified one of the first known mechanisms of disease tolerance by a host—the activation and function of *CrebA* during infection [1].

Having identified a novel mechanism of disease tolerance, one of the first questions we had was: can the *CrebA* mechanism be exploited to further increase host survival during infection? During our work characterizing the function of *CrebA*, we overexpressed *CrebA* specifically in the fat body prior to infection with *P. rettgeri* and measured survival after infection. We did not detect any significant changes in fly survival following this treatment (unpublished data). However, it is important to note that infection with *P. rettgeri* does not trigger endoplasmic reticulum (ER) stress in a healthy, wildtype fly [1]. If the function of *CrebA* is to prevent ER stress during infection,

increasing expression of *CrebA* in the context of an infection that does not trigger ER stress would not necessarily improve fly survival. Nevertheless, it is possible that overexpression of *CrebA* could result in increased survival in the context of an infection that triggers ER stress in a wildtype fly. Ragheb and colleagues recently published work showing that overexpression of *CrebA* increases survival in the context of *P. entomophila* systemic infection [13]. While their study did not demonstrate that *P. entomophila* infection triggers ER stress in the fly, this hypothesis could offer an explanation as to why overexpression of *CrebA* results in increased survival in this context. Another context in which overexpression of *CrebA* could promote increased host survival to infection would involve infection of flies suffering from pre-existing ER stress. Indeed, ER stress is known to contribute to the pathogenesis of many diseases [14]. Our work in Chapter III provides evidence to support this idea. We genetically induced ER stress via expression of *BiP* (a regulatory protein of the unfolded protein response) RNAi in the fat body of flies and infected these flies with *P. rettgeri*. *BiP* RNAi-expressing flies proved to be more susceptible to infection. However, we were able to rescue this increase in susceptibility by combining the *BiP* RNAi with a different construct overexpressing *CrebA* in the fat body of flies, demonstrating that overexpression of *CrebA* is indeed able to increase host survival in specific conditions [1]. Altogether, these two examples support the idea that overexpression of *CrebA* may be exploited to further increase host survival during infection.

4. Loss of immune tolerance to microbiota as a survival strategy

Previous work has shown that loss of immune tolerance to microbiota is accompanied by a decrease in longevity [15] [16], indicating that there is a large cost associated with an overactive immune system. In Chapter IV, our work showing that nephrocytes are key mediators of immune

tolerance to Gram-positive microbiota confirmed this finding, as we observed that flies lacking nephrocytes exhibit shorter lifespans compared to wildtype flies. Given this large negative effect on lifespan, it is tempting to suggest that there is no advantage to a strategy that lowers immune tolerance to microbiota to increase survival to infection. However, this is not necessarily the case. In Chapter IV, infection of flies with impaired nephrocyte function using pathogens that typically kill ~100% of infected wildtype flies, such as *S. aureus*, resulted in ~60% of infected flies surviving infection. This is a sizeable improvement in survival. Thus, in the context of a lethal infection, lowering immune tolerance could provide some advantages in spite of the long term negative consequences that are associated with it, especially if lowering immune tolerance can be done in an controlled, inducible manner that can be reversed. The concept and usefulness of "unleashing the immune system" (in this case, as a result of lowering immune tolerance) to fight disease is not novel [17].Therefore, in the case of a lethal infection, perhaps one for which antibiotics are no longer available, there is merit to the idea of temporarily lowering immune tolerance to resident bacteria in an effort to better resist the infection.

5. Future directions

Future work on the major projects of this dissertation could focus on the following angles: In Chapter III, we identified a comprehensive list of genes and biological processes regulated in response to infection that are not classically thought of as being part of the immune system—e.g., neuron-related, secretion, oxidation-reduction, response to pheromone/olfactory behavior, etc. Followup work on this project will entail characterizing the function of these genes/biological processes during infection, especially those that are part of the core response to infection (i.e., genes regulated in response to the majority of infections tested). Regarding the *CrebA* component

of this project, future aims should focus on determining the mechanism through which ER stress is killing *CrebA*-deficient flies upon infection. Excessive and prolonged ER stress can lead to tissue apoptosis or a block in translation [18]. Our data suggested that fat body apoptosis was not responsible for the increased death observed in *CrebA*-deficient flies following infection [1]. However, a role for translational blockage was not tested, and it remains possible that an entirely different process triggered by ER stress is killing off *CrebA* RNAi flies. Finally, for the nephrocyte project of Chapter IV, future directions will concentrate on determining whether nephrocytes play a role in infection resolution. In Chapter IV, we showed that nephrocytes remove peptidoglycan from Gram-positive microbiota from systemic circulation and degrade it inside lysosomes. However, we never tested whether nephrocytes also function to eliminate peptidoglycan that is shed by Gram-positive bacterial pathogens during systemic infection. Because peptidoglycan is a major activator of the immune system in the fly [19] [20], an inability to remove peptidoglycan from circulation even after pathogen clearance could result is sustained immune activation. Hence, this is a significant point that needs to be addressed by future work.

REFERENCES

1. Troha K, Im JH, Revah J, Lazzaro BP, Buchon N. Comparative transcriptomics reveals CrebA as a novel regulator of infection tolerance in D. melanogaster. Schneider DS, editor. PLoS Pathog. 2018;14: e1006847. doi:10.1371/journal.ppat.1006847

2. Chambers MC, Song KH, Schneider DS. Listeria monocytogenes Infection Causes Metabolic Shifts in Drosophila melanogaster. Freitag NE, editor. PLoS ONE. Public Library of Science; 2012;7: e50679. doi:10.1371/journal.pone.0050679

3. De Gregorio E, Spellman PT, Rubin GM, Lemaitre B. Genome-wide analysis of the Drosophila immune response by using oligonucleotide microarrays. Proc Natl Acad Sci USA. 2001;98: 12590–12595. doi:10.1073/pnas.221458698

4. De Gregorio E, Spellman PT, Tzou P, Rubin GM, Lemaitre B. The Toll and Imd pathways are the major regulators of the immune response in Drosophila. EMBO J. EMBO Press; 2002;21: 2568–2579. doi:10.1093/emboj/21.11.2568

5. Dionne MS, Pham LN, Shirasu-Hiza M, Schneider DS. Akt and FOXO dysregulation contribute to infection-induced wasting in Drosophila. Curr Biol. 2006;16: 1977–1985. doi:10.1016/j.cub.2006.08.052

6. Buchon N, Broderick NA, Poidevin M, Pradervand S, Lemaitre B. Drosophila intestinal response to bacterial infection: activation of host defense and stem cell proliferation. Cell Host Microbe. Elsevier; 2009;5: 200–211. doi:10.1016/j.chom.2009.01.003

7. Núñez G, Sakamoto K, Soares MP. Innate Nutritional Immunity. J Immunol. 2018;201: 11–18. doi:10.4049/jimmunol.1800325

8. Medzhitov R, Schneider DS, Soares MP. Disease tolerance as a defense strategy. Science. 2012;335: 936–941. doi:10.1126/science.1214935

9. Ayres JS, Schneider DS. Tolerance of infections. Annu Rev Immunol. Annual Reviews; 2012;30: 271–294. doi:10.1146/annurev-immunol-020711-075030

10. Schneider DS, Ayres JS. Two ways to survive infection: what resistance and tolerance can teach us about treating infectious diseases. Nat Rev Immunol. 2008;8: 889–895. doi:10.1038/nri2432

11. Lefèvre T, Williams AJ, de Roode JC. Genetic variation in resistance, but not tolerance, to a protozoan parasite in the monarch butterfly. Proc Biol Sci. 2011;278: 751–759. doi:10.1098/rspb.2010.1479

12. Howick VM, Lazzaro BP. Genotype and diet shape resistance and tolerance across distinct phases of bacterial infection. BMC Evol Biol. BioMed Central; 2014;14: 56. doi:10.1186/1471-2148-14-56

13. Ragheb R, Chuyen A, Torres M, Defaye A, Seyres D, Kremmer L, et al. Interplay between

trauma and Pseudomonas entomophila infection in flies: a central role of the JNK pathway and of CrebA. Sci Rep. 2017;7: 16222. doi:10.1038/s41598-017-14969-7

14. Ozcan L, Tabas I. Role of Endoplasmic Reticulum Stress in Metabolic Disease and Other Disorders. Annual Review of Medicine. 2012;63: 317–328. doi:10.1146/annurev-med-043010-144749

15. Paredes JC, Welchman DP, Poidevin M, Lemaitre B. Negative regulation by amidase PGRPs shapes the Drosophila antibacterial response and protects the fly from innocuous infection. Immunity. 2011;35: 770–779. doi:10.1016/j.immuni.2011.09.018

16. Zaidman-Rémy A, Hervé M, Poidevin M, Pili-Floury S, Kim M-S, Blanot D, et al. The Drosophila amidase PGRP-LB modulates the immune response to bacterial infection. Immunity. 2006;24: 463–473. doi:10.1016/j.immuni.2006.02.012

17. Pardoll DM. The blockade of immune checkpoints in cancer immunotherapy. Nat Rev Cancer. Nature Publishing Group; 2012;12: 252–264. doi:10.1038/nrc3239

18. Oakes SA, Papa FR. The role of endoplasmic reticulum stress in human pathology. Annu Rev Pathol. 2015;10: 173–194. doi:10.1146/annurev-pathol-012513-104649

19. Lemaitre B, Hoffmann J. The host defense of Drosophila melanogaster. Annu Rev Immunol. Annual Reviews; 2007;25: 697–743. doi:10.1146/annurev.immunol.25.022106.141615

20. Buchon N, Silverman N, Cherry S. Immunity in Drosophila melanogaster--from microbial recognition to whole-organism physiology. Nat Rev Immunol. 2014;14: 796–810. doi:10.1038/nri3763

SUPPLEMENTARY DOCUMENTS FOR CHAPTER III

COMPARATIVE TRANSCRIPTOMICS REVEALS *CREBA* AS A NOVEL REGULATOR OF INFECTION TOLERANCE IN *D. MELANOGASTER**

* Adapted from Katia Troha, Joo Hyun Im, Jonathan Revah, Brian P. Lazzaro and Nicolas Buchon. Copyright 2018. PLOS Pathogens.

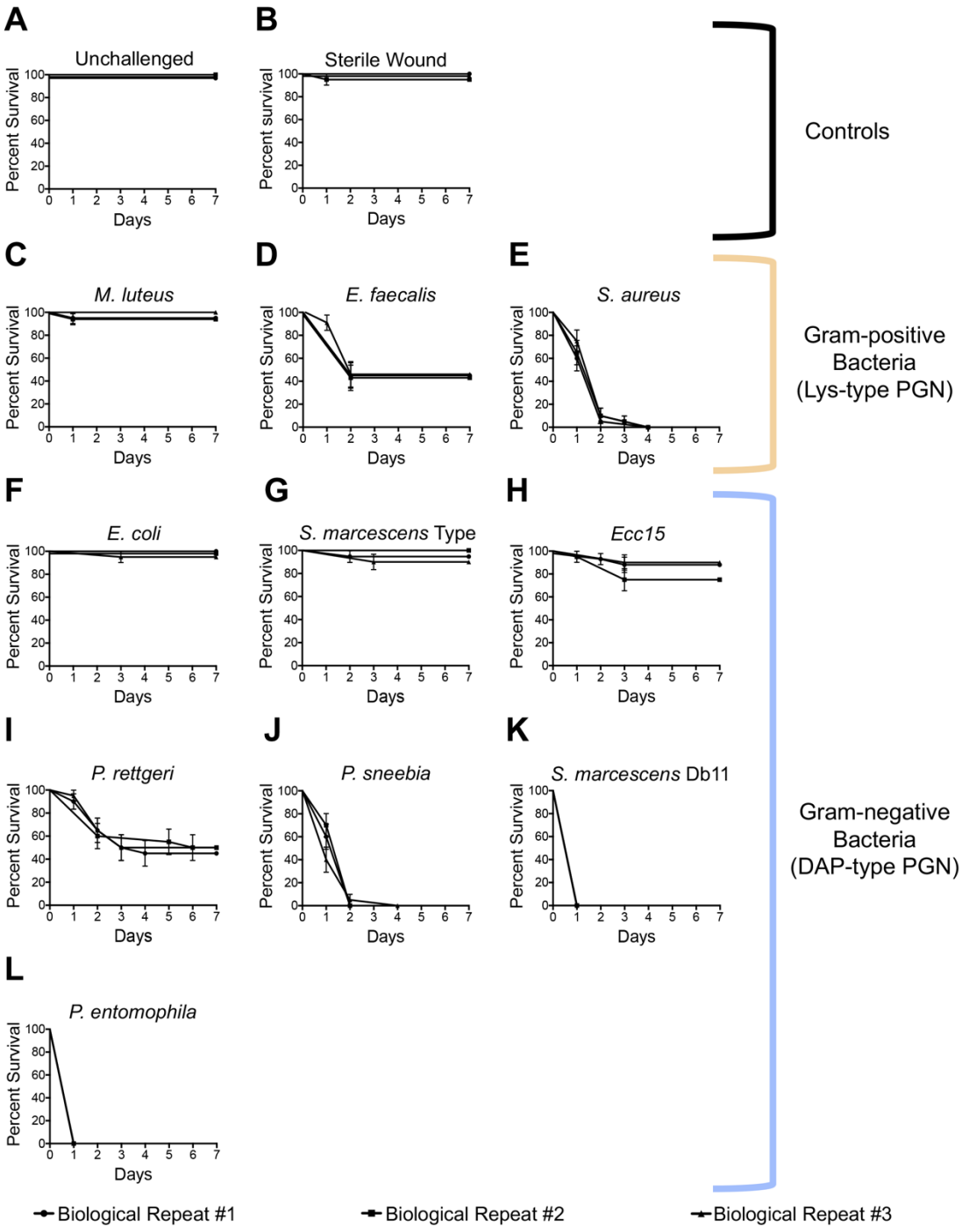

Supplementary Figure III.1. 10 bacteria cause different mortalities in *Drosophila*
Survival curves (in %) over time of control and infected *Canton S* flies. Three biological replicates are graphed independently for each condition. Treatments are as follows: (A) Unchallenged. (B) Sterile wound. (C) *Micrococcus luteus*. (D) *Enterococcus faecalis*. (E) *Staphylococcus aureus*. (F) *Escherichia coli*. (G) *Serratia marcescens* Type strain. (H) *Pectinobacterium* (formerly *Erwinia*) *carotovora Ecc15*. (I) *Providencia rettgeri*. (J) *Providencia sneebia*. (K) *Serratia marcescens* strain Db11. (L) *Pseudomonas entomophila*.

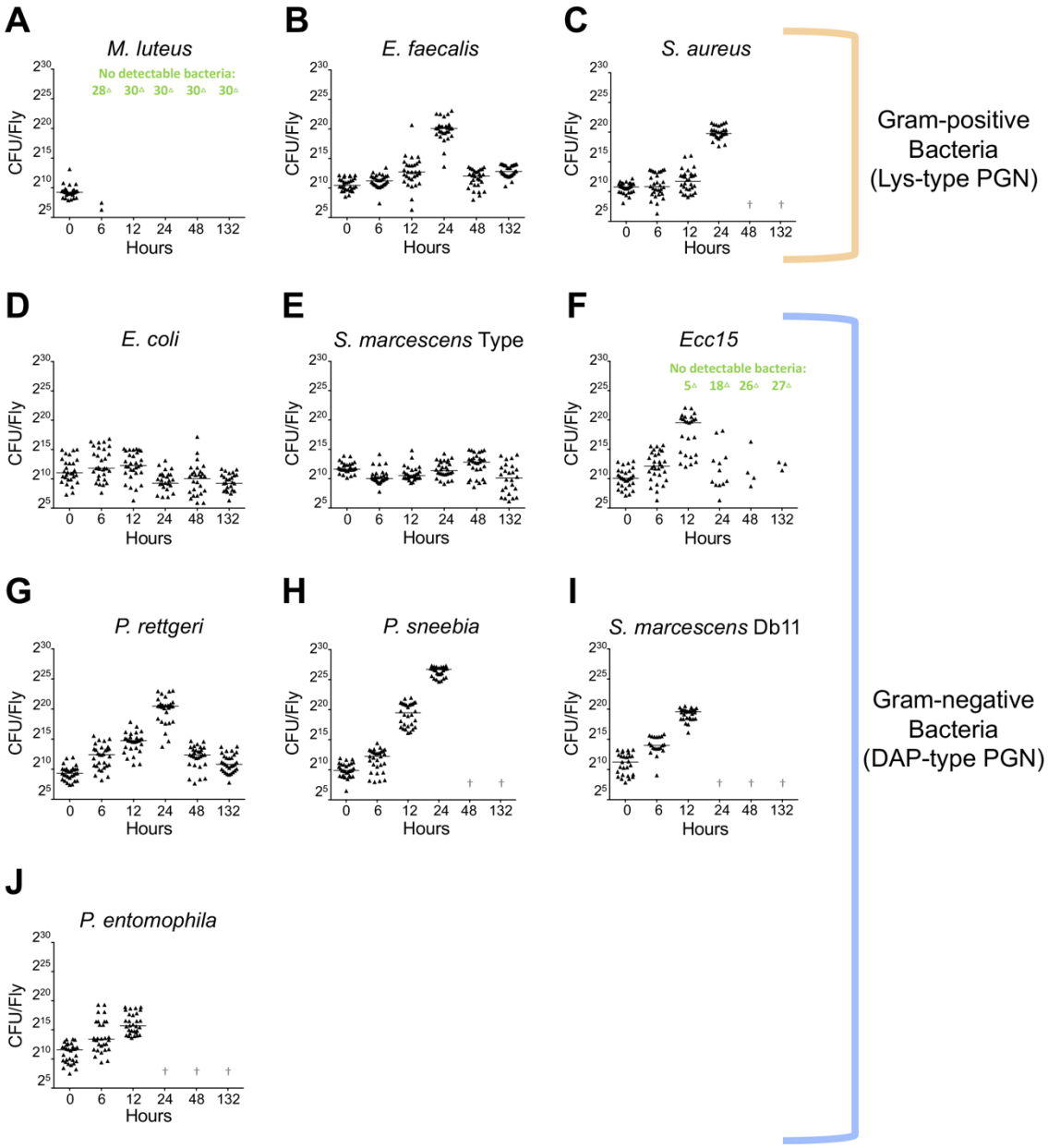

Supplementary Figure III.2. 10 bacteria differ in their rate of growth in the fly
Bacterial load time courses of infected *Canton S* flies over 132 h following infection. Three biological repeats are graphed together, with each triangle representing the bacterial burden in an individually sampled fly. (A) *M. luteus*. (B) *E. faecalis*. (C) *S. aureus*. (D) *E. coli*. (E) *S. marcescens* Type. (F) *Ecc15*. (G) *P. rettgeri*. (H) *P. sneebia*. (I) *S. marcescens* Db11. (J) *P. entomophila*. The symbol † denotes no flies were sampled because most, if not all, flies had succumbed by that time point. A number followed by the symbol Δ indicates the number of flies found to have no bacteria (flies that carry undetectable levels of bacteria or that have cleared the infection) at the specified time point.

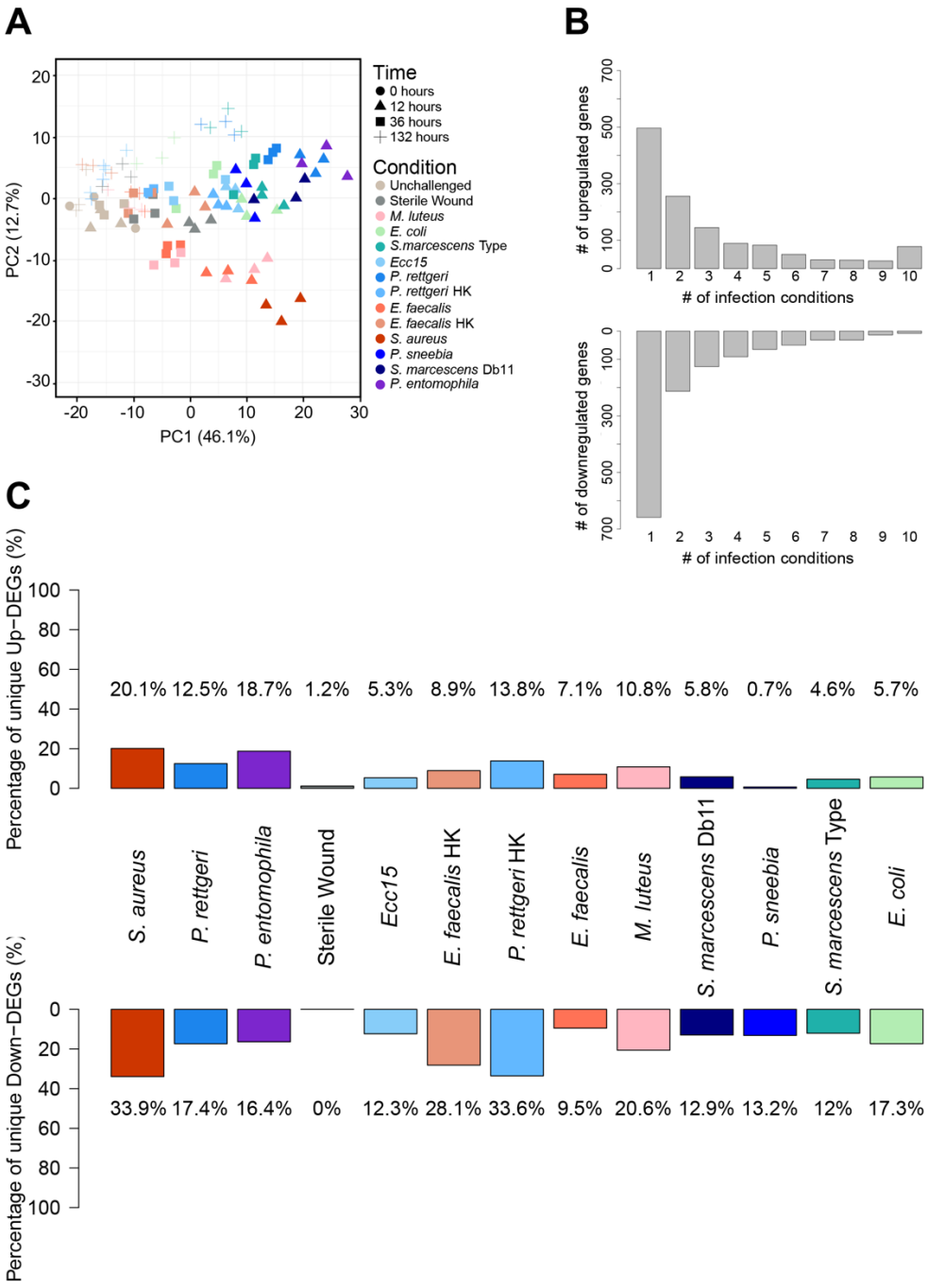

Supplementary Figure III.3. Each bacterial infection induces a unique host response
(A) PCA plot showing the first two principal components of the entire dataset. Pink, orange, and red (warm) colors show infections with Gram-positive (Lys-type PGN) bacteria, while green, blue, and purple (cool) colors denote infections with Gram-negative (DAP-type PGN) bacteria. HK indicates stimulation with heat-killed bacteria. (B) Histogram of differentially upregulated (top) or downregulated (bottom) genes by the number of infection conditions in which a given gene was differentially expressed. (C) Percentage of genes that are uniquely upregulated (top) or downregulated (bottom) by each infection.

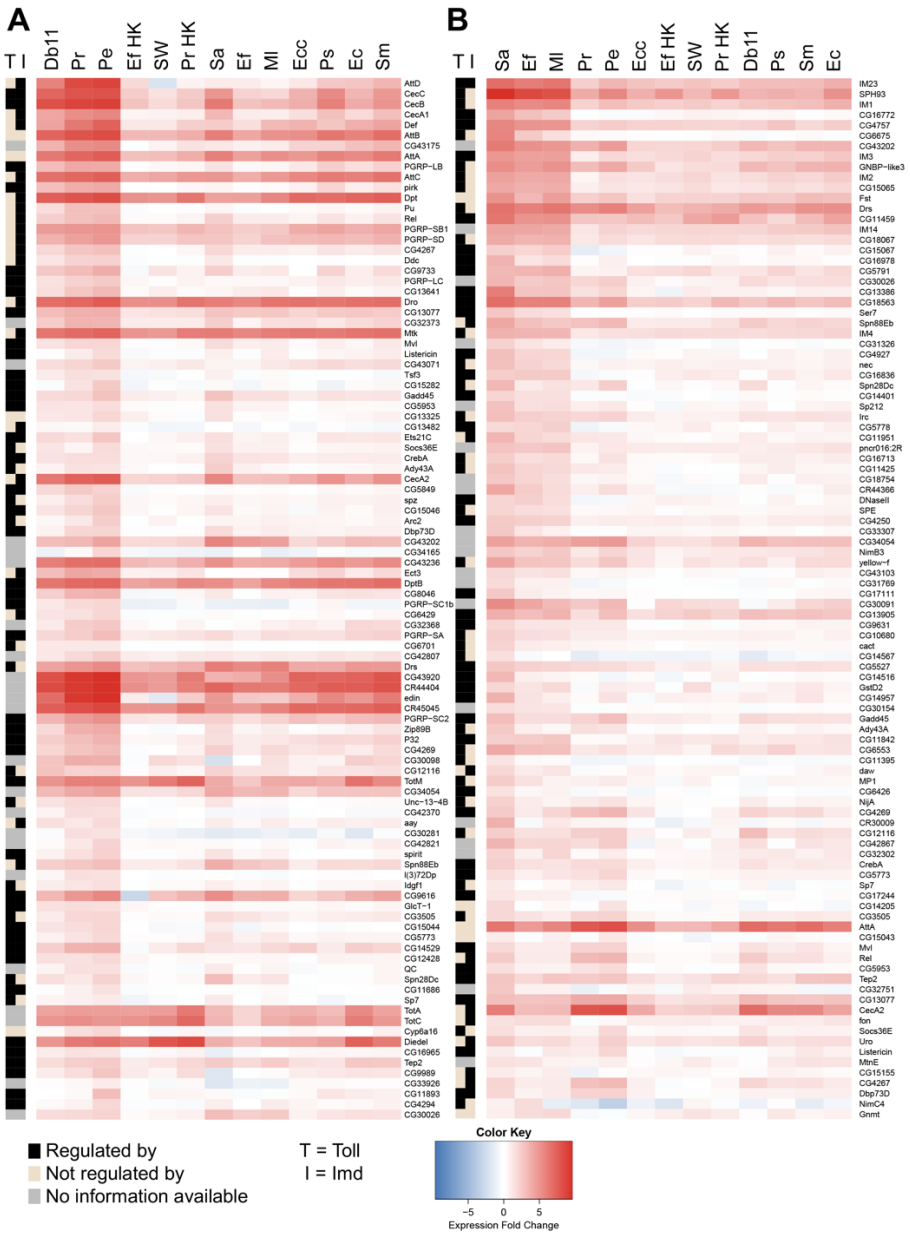

Supplementary Figure III.4. Individual infections differ in their ability to induce the Toll and Imd pathways and reshape host metabolism.

Heatmap (log_2 fold change) of top 100 genes that contribute the most to PC1 (A) and of top 100 genes that most contribute to PC2 (B). A gene was deemed to be regulated by the Toll or Imd pathways if the absence of the key genes in each pathway (*spz* for Toll and *Rel* for Imd) changed the expression level of said gene by 20% or more compared to the expression level of the gene in wildtype, as previously reported [7]. A color scale on the left side of each heatmap indicates whether each gene is regulated by Toll (T) or Imd (I). In the first column (T), genes regulated by the Toll pathway are marked in black, while genes not regulated by Toll are marked in beige. Similarly, in the second column (I), genes regulated by Imd are marked in black, while genes not regulated by Imd are marked in beige. Genes were marked in gray when no information was available about their regulation by Toll or Imd.

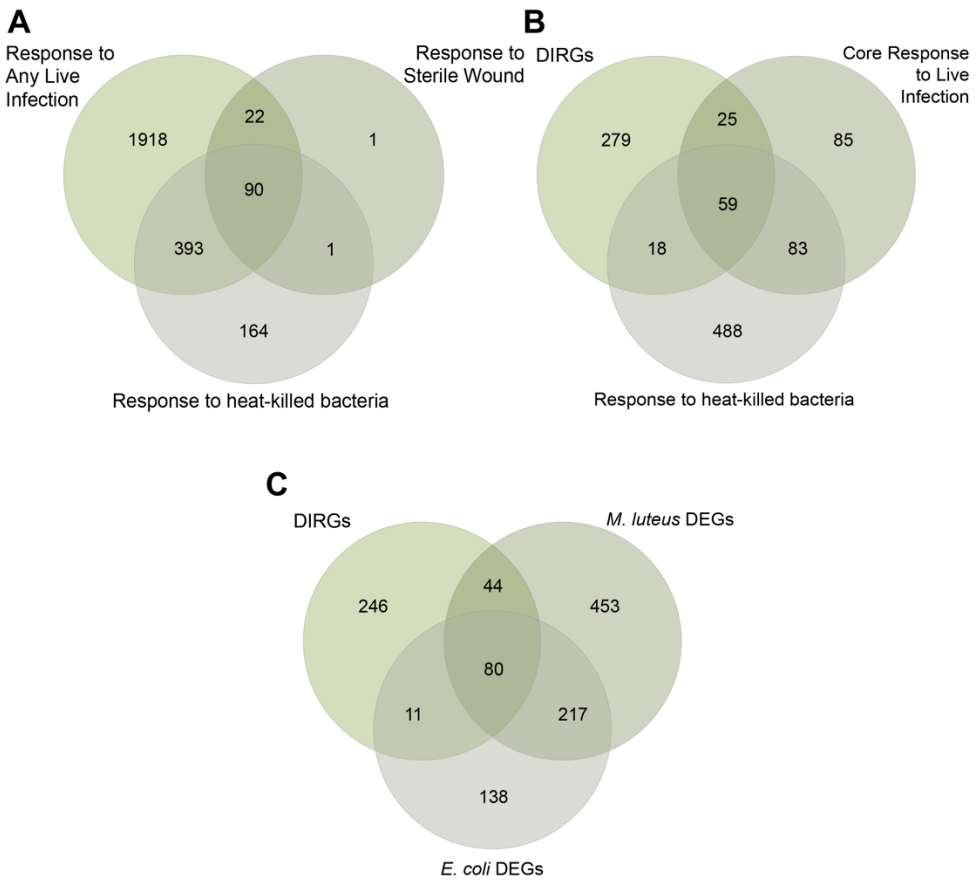

Supplementary Figure III.5. Overlap between genes responding to live infection, sterile wound, heat-killed bacteria, and the DIRGs

(A) Venn diagram showing the intersection between genes that are differentially regulated in response to at least one live infection, sterile wound, and challenge with heat-killed bacteria. (B) Venn diagram depicting the overlap between the previously described *Drosophila* Immune-Regulated Genes (DIRGs) [6], core genes differentially regulated in response to live infection, and genes differentially expressed in response to heat-killed bacteria. (C) Venn diagram illustrating the overlay between genes differentially regulated in response to *M. luteus* infection and, separately, *E. coli* infection in the present study and the DIRGs, which were previously identified from infection with a mixed cocktail of *E. coli* and *M. luteus* [6].

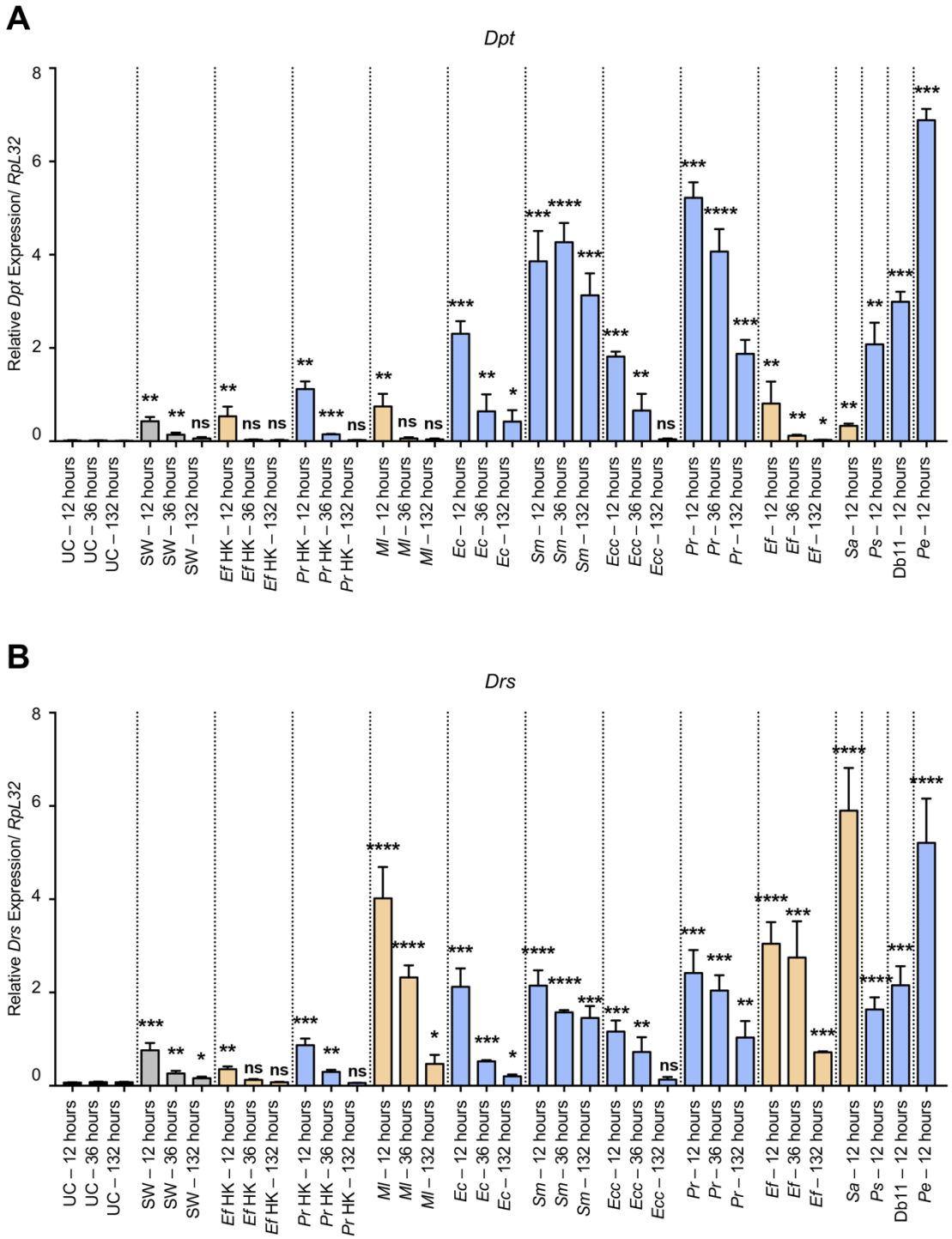

Supplementary Figure III.6. 10 bacteria induce different expression levels of antimicrobial peptide genes

RT-qPCR measuring (A) *Diptericin* and (B) *Drosomycin* expression levels in control and infected *Canton S* flies at 12, 36, and 132 h post-infection. These samples are separate biological replicates, distinct from those used in the RNA-seq experiment. Mean values of three biological repeats are represented ±SE. *p<0.05 **p<0.01 ***p<0.001 ****p<0.0001 in a Student's t-test.

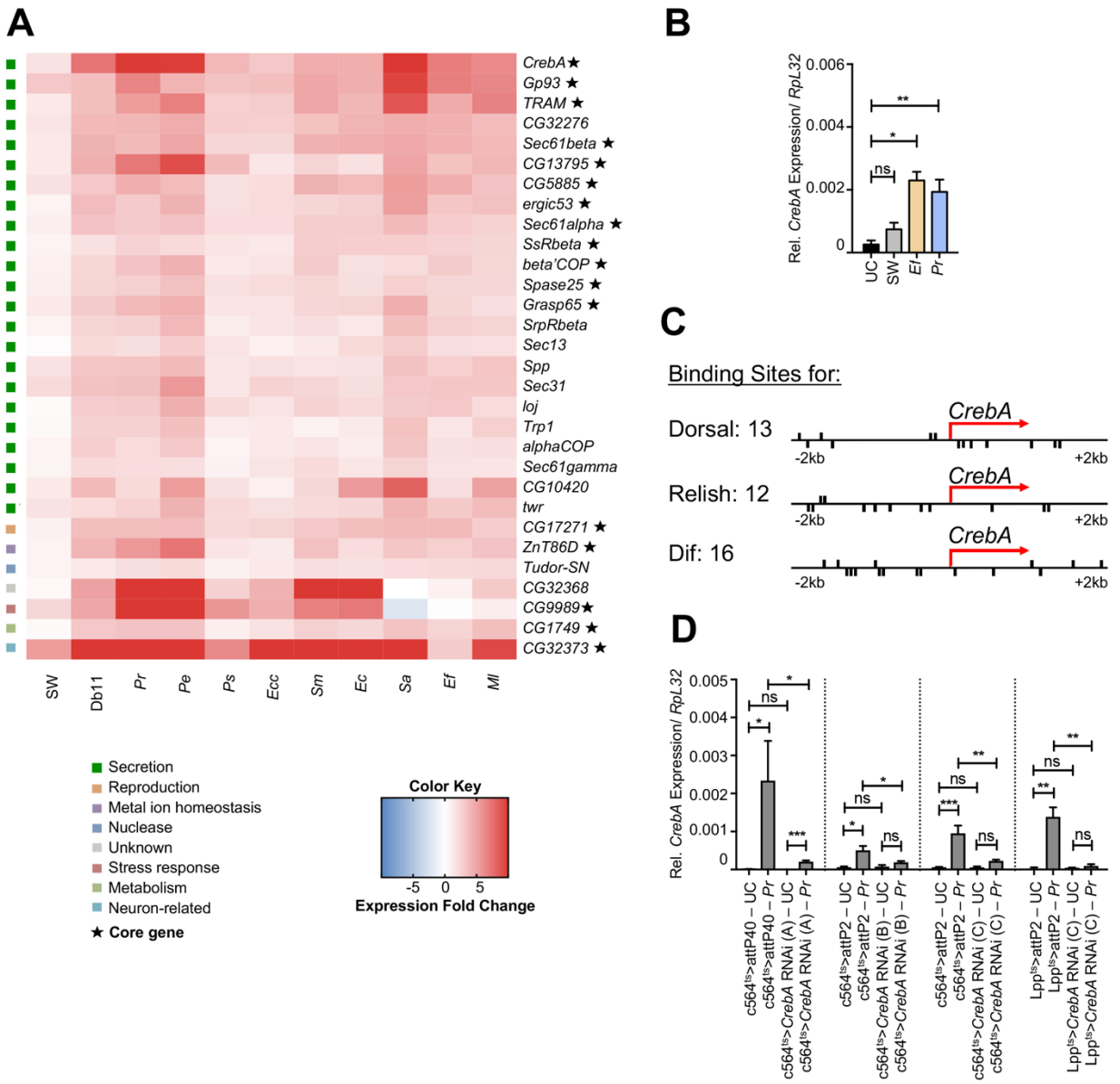

Supplementary Figure III.7. *CrebA* is a target of Toll and Imd and a putative regulator of core genes in the fat body

(A) Heatmap showing the expression levels ($\log_2$ fold change) of a select group of putative *CrebA* target genes found to be significantly upregulated by infection. Core genes (marked by a ★) and their functions are highlighted. (B) RT-qPCR validation of *CrebA* induction levels 12 h after infection with *P. rettgeri* (*Pr*) and *E. faecalis* (*Ef*) using samples distinct from those used in the RNA-seq. (C) Schematic of predicted Dif, Dorsal, and Relish binding sites on the *CrebA* promoter region (+/-2kb from the start site). (D) Whole fly RT-qPCR of flies with *CrebA* knockdown in the fat body following infection with *P. rettgeri*. *CrebA* RNAi (A), (B), and (C) denote three distinct RNAi constructs used to target *CrebA* mRNA. Mean values of three or more repeats are represented ±SE. *p<0.05 **p<0.01 ***p<0.001 in a Student's t-test.

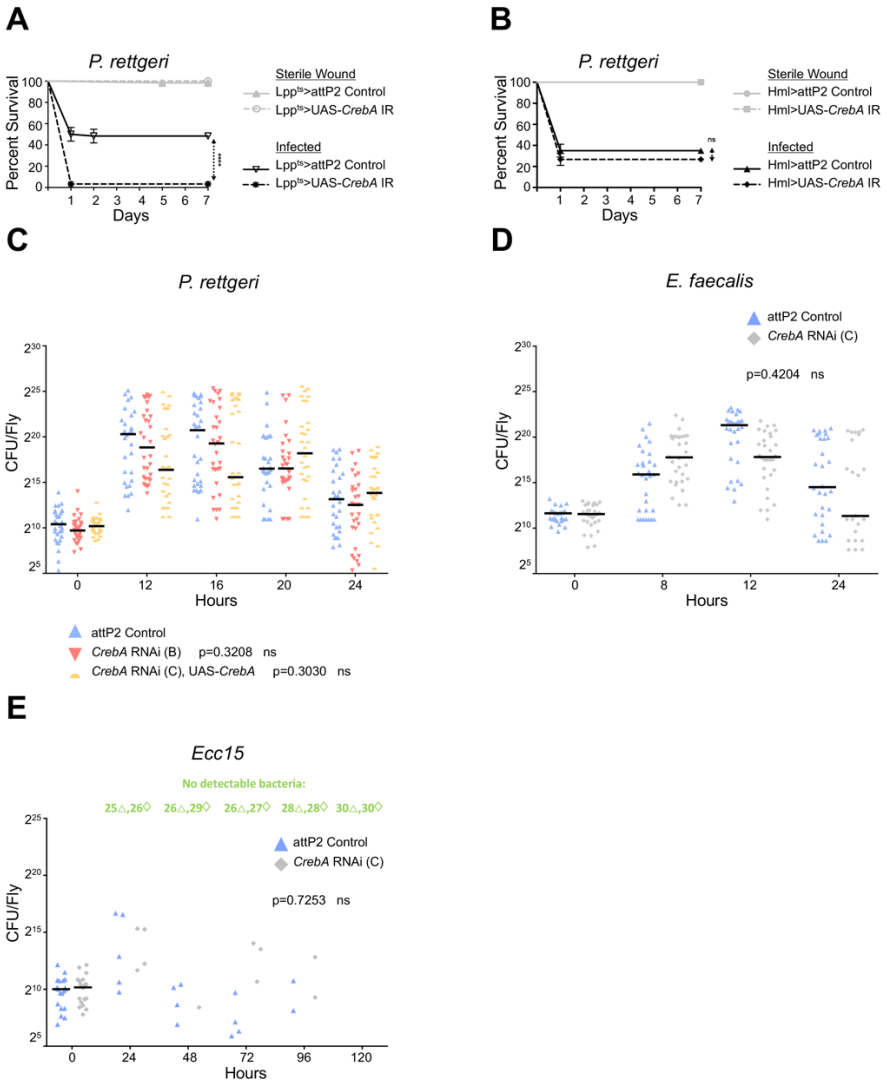

Supplementary Figure III.8. *CrebA* RNAi flies do not carry a larger bacterial burden than wildtype flies upon infection

(A) Survival curves over 7 days following *P. rettgeri* infection of flies whose expression of *CrebA* is blocked with RNAi specifically in the fat body with a second driver, *Lpp-Gal4* (*Gal80^{ts}; Lpp-Gal4 > UAS-CrebA-IR*). *attP2* is the background genotype control, in which *CrebA* is fully expressed. (B) Survival of unchallenged and infected (*P. rettgeri*) control flies and flies expressing *CrebA* RNAi in hemocytes only (*Hml-Gal4* driver). The curves represent the average percent survival ±SE of three biological replicates. ****p<0.0001 in a Log-rank test. (C) Bacterial load time course of control flies, flies expressing a separate *CrebA* RNAi construct (construct B), and flies simultaneously co-expressing a *CrebA* RNAi and a *CrebA* overexpression construct in the fat body following infection with *P. rettgeri*. Bacterial load time course of *CrebA* knockdown and control flies after infection with (D) *E. faecalis* and (E) *Ecc15*. Three repeats are graphed together, with each symbol representing an individual fly's number of colony forming units (CFU). Horizontal lines represent median values for each condition. A number followed by the symbol Δ (*attP2* control flies) or the symbol ◊ (*CrebA* RNAi flies) indicates the number of flies found to have no bacteria (flies that carry undetectable levels of bacteria or that have cleared the infection) at the specified time point.

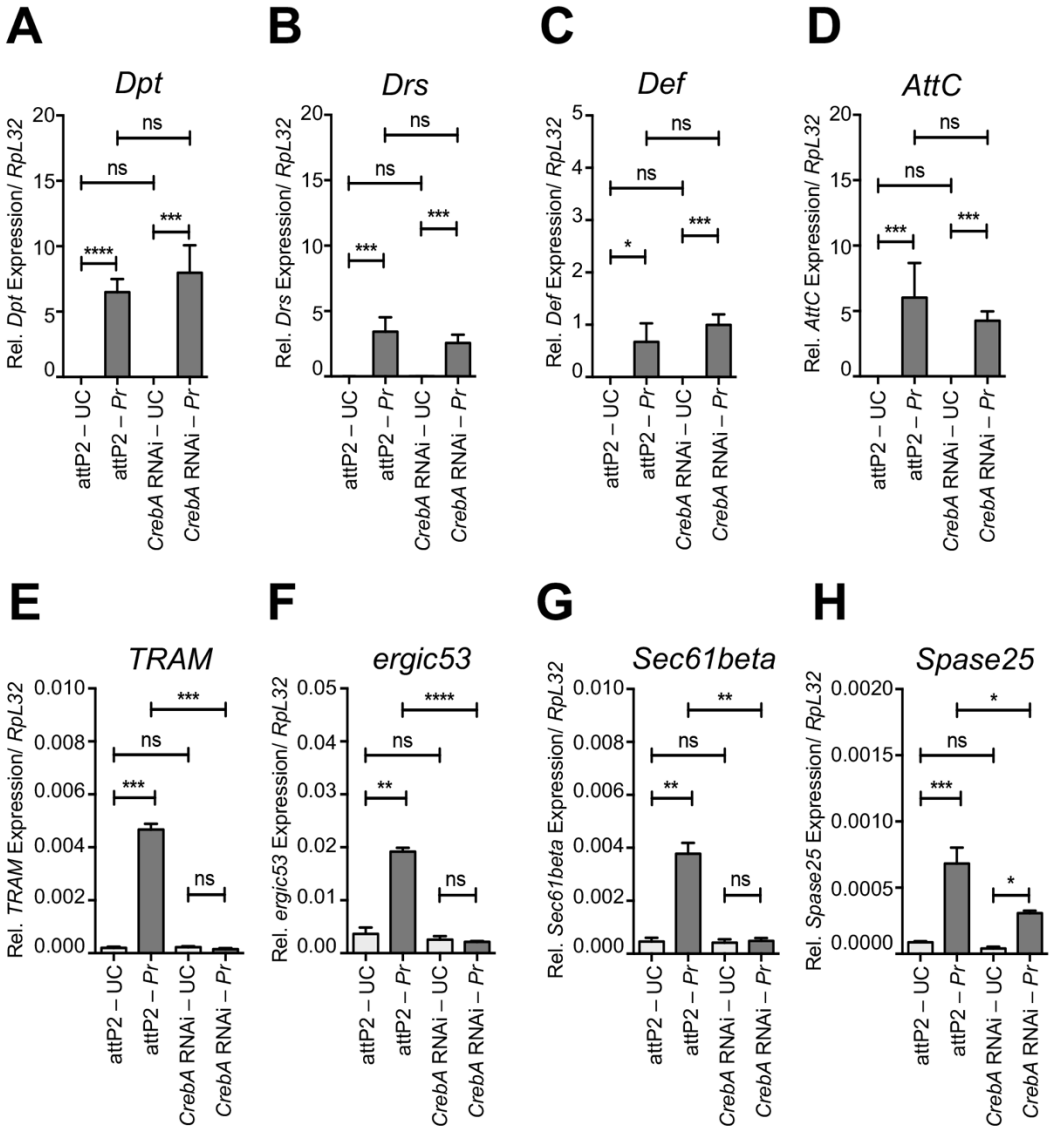

Supplementary Figure III.9. *CrebA* regulates secretory capacity during infection
Expression level of predicted *CrebA* target genes in unchallenged (UC) or infected (*Pr*) conditions in control (*attP2*) and *CrebA* RNAi fat body samples. Assayed genes encoding antimicrobial peptides are (A) *Diptericin*, (B) *Drosomycin*, (C) *Defensin*, and (D) *Attacin C*. Surveyed genes encoding secretory factors are (E) *TRAM*, (F) *ergic53*, (G) *Sec61beta*, and (H) *Spase25*. Mean values of three biological replicates are represented ±SE. *p<0.05 **p<0.01 ***p<0.001 ****p<0.0001 in a Student's t-test.

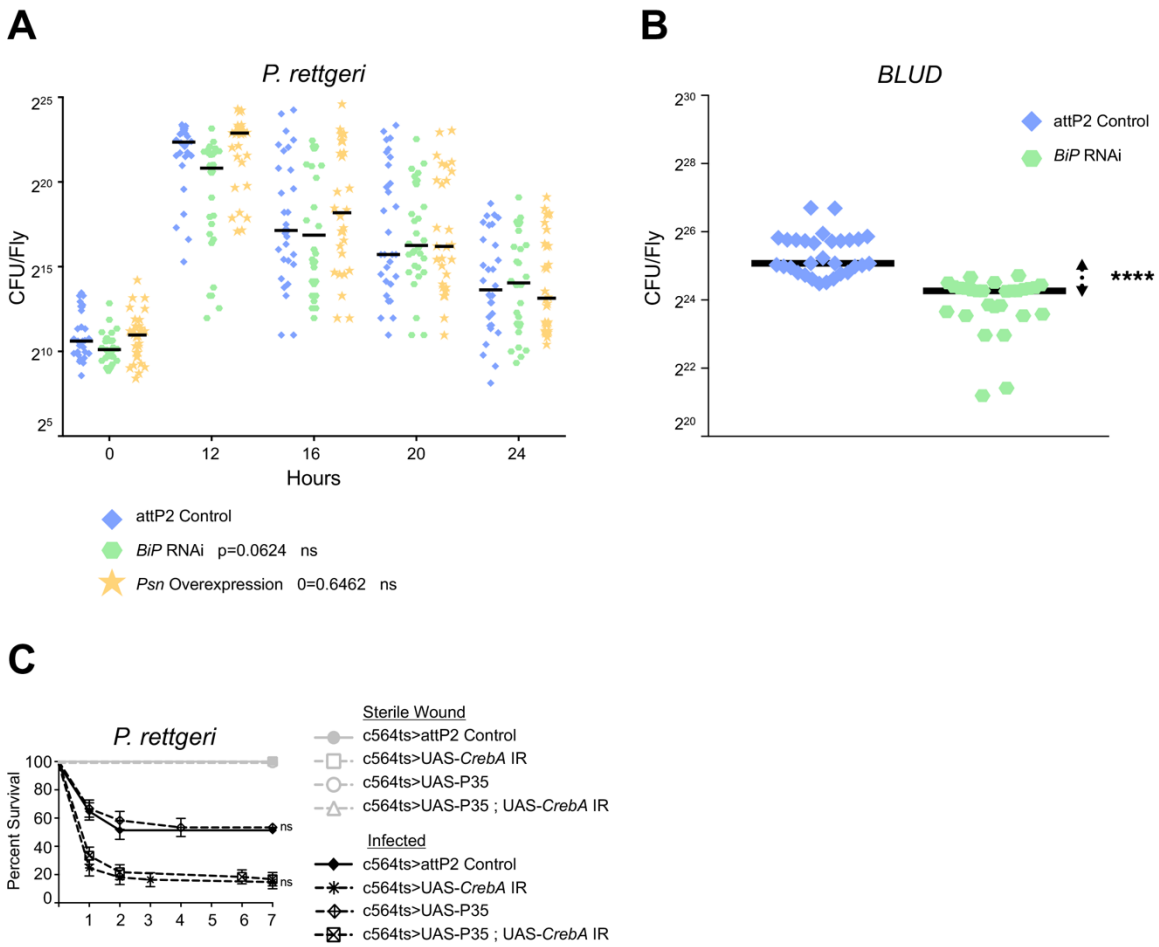

Supplementary Figure III.10. *CrebA* expression prevents ER stress upon infection
(A) Bacterial load time course of control flies and flies expressing *BiP* RNAi or *Psn* overexpression in the fat body following infection with *P. rettgeri*. (B) Bacterial load upon death (*BLUD*) following *P. rettgeri* infection of wildtype controls and flies with *BiP* expression knocked down by RNAi in the fat body. Three repeats are graphed together, with each symbol representing an individual fly's number of colony forming units (CFU). Horizontal lines represent median values for each condition. ****p<0.0001 in a Student's t-test. (C) Survival curves of flies co-expressing *CrebA* RNAi and the apoptosis inhibitor P35 in fat body cells. The curves represent the average percent survival ±SE of three biological replicates.

SUPPLEMENTARY DOCUMENTS FOR CHAPTER IV

NEPHROCYTES MEDIATE IMMUNE TOLERANCE TO MICROBIOTA BY REMOVING PEPTIDOGLYCAN FROM SYSTEMIC CIRCULATION*

* Adapted from Katia Troha, Peter Nagy, Andrew Pivovar, Brian P. Lazzaro, Paul Hartley and Nicolas Buchon. Submitted to Immunity.

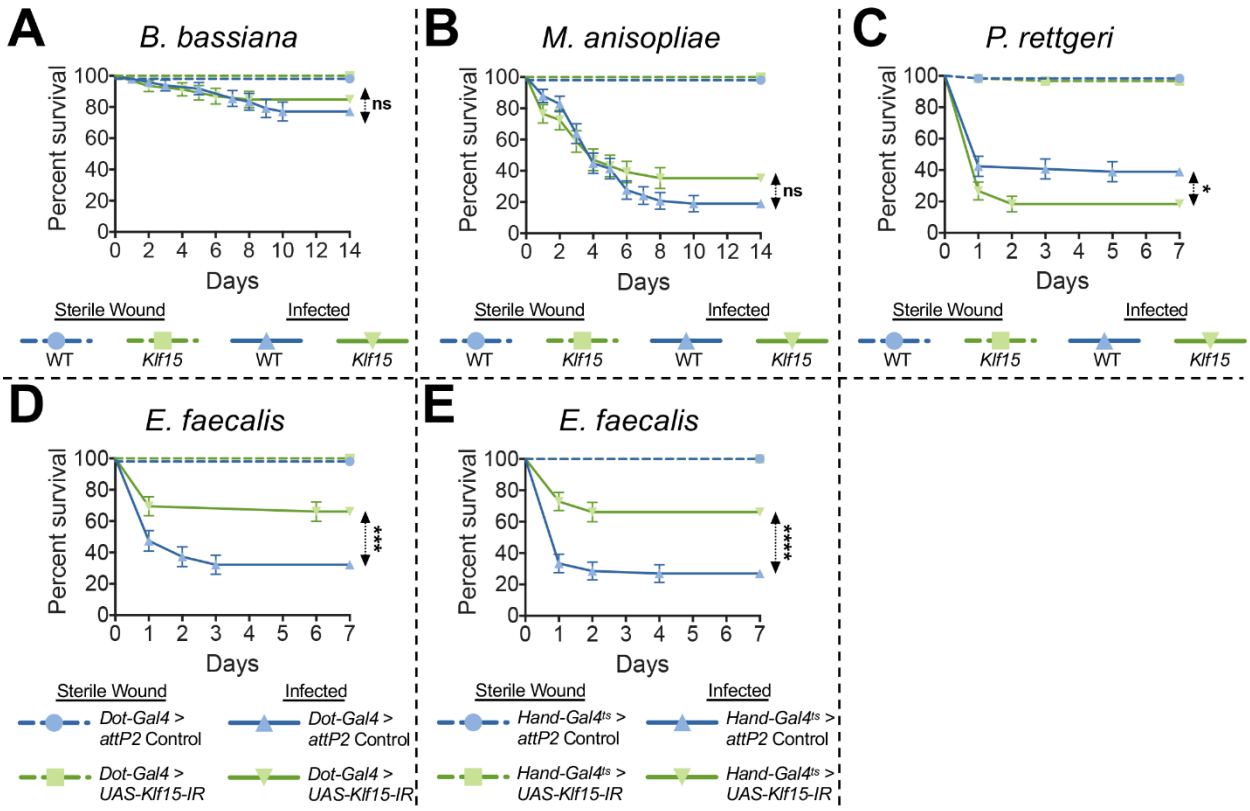

Supplementary Figure IV.1. *Klf15* flies are less susceptible to a variety of microbial infections (A-B) Survival curves over 14 days following natural infection of WT and *Klf15*^{NN} flies with the fungal pathogens *B. bassiana* (A) and *M. anisopliae* (B). (C) Survival curve of *Klf15* and WT flies infected with P. *rettgeri*. *p<0.05 in a Log-rank test. (D-E) Survival of flies expressing nephrocyte-specific RNAi against *Klf15* throughout development (*Dot-Gal4 > UAS-Klf15-IR*) (D) or only during the adult stage (*Hand-Gal4*^{ts} *> UAS-Klf15-IR*) (E) after infection with *E. faecalis*. The curves represent the average percent survival ±SE of three biological replicates. ***p<0.001 ****p<0.0001 in a Log-rank test.

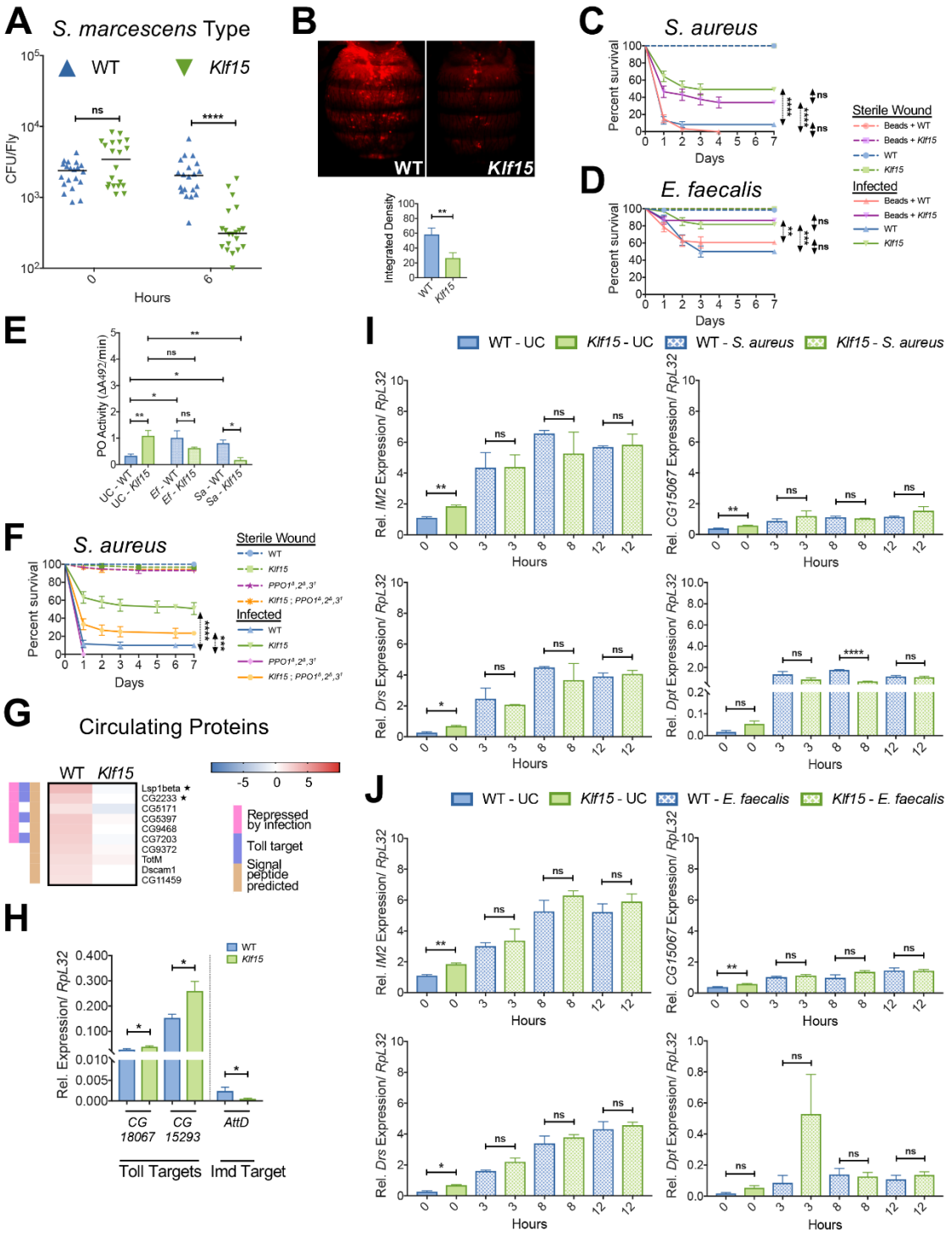

Supplementary Figure IV.2. Toll pathway activation makes *Klf15* mutants more resistant to infection

(A) Bacterial load time course of control and *Klf15*^{NN} flies following infection with *S. marcescens* Type strain. Three repeats are graphed together, with each symbol representing an individual fly's number of colony forming units (CFU). Horizontal lines represent median values for each time point. Results were analyzed using a two-way ANOVA followed with Sidak's post-tests for specific comparisons (****p<0.0001).

(B) Representative fluorescence images of the abdomen of control and *Klf15* mutants 3 h post-injection with pHrodo bacteria. Fluorescence was quantified and the average plotted. **p<0.01 in a Student's t-test. (C-D) Survival curves over 7 days following infection of WT and *Klf15* mutant flies that were pre-injected with latex beads 24 h prior to infection with the pathogens *E. faecalis* (C) and *S. aureus* (D). **p<0.01 ***p<0.001 ****p<0.0001 in a Log-rank test. (E) Phenoloxidase activity was measured via the L-DOPA assay. WT and *Klf15* samples were measured in unchallenged conditions as well as following infection with *E. faecalis* and *S. aureus*. *p<0.05 **p<0.01 in a Student's t-test. (F) Comparison of *Klf15* ;; $PPO1^{\Delta}, 2^{\Delta},3^{1}$ quadruple mutants to WT, *Klf15*, and $PPO1^{\Delta}, 2^{\Delta},3^{1}$ mutants in experiments measuring survival against *S. aureus*. ***p<0.001 ****p<0.0001 in a Log-rank test.(G) Heat map showing a list of circulating proteins depleted (≥ 1.5-fold) in the hemolymph (insect blood) of *Klf15* mutants over WT. A color scale on the left side of the heat map denotes whether the gene that encodes each protein is transcriptionally downregulated by infection (green), a target of the Toll pathway (blue), or predicted to possess a signal peptide (orange). Core genes are highlighted with a ★ symbol (Troha et al., 2018). (H) Whole fly RT-qPCR of Toll target genes *CG18067* and *CG15293* and Imd target gene *AttD* using unchallenged wildtype and $Klf15^{NN}$ samples. *p<0.05 in a Student's t-test.
(I-J) Whole fly RT-qPCR of Toll target genes *IM2*, *CG15067*, and *Drs* and Imd target gene *Dpt* following infection with *S. aureus* (I) and *E. faecalis* (J). *p<0.05 **p<0.01 in a Student's t-test.

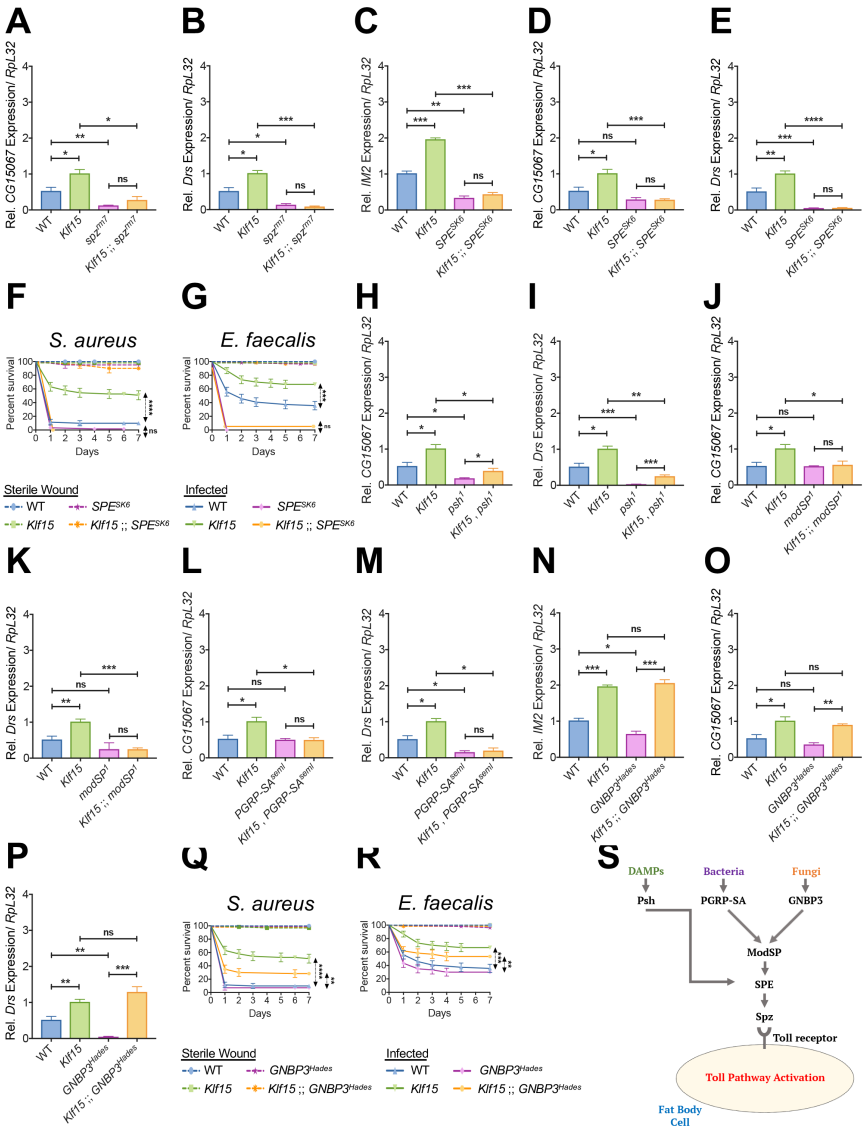

Supplementary Figure IV.3. Increased resistance to infection in *Klf15* flies is Toll-dependent
(A-B) Comparison of *Klf15* ;; *spz*^{rm7} double mutants to WT, *Klf15*, and *spz*^{rm7} single mutants in experiments measuring expression levels of Toll target genes *CG15067* (A) and *Drs* (B) via RT-qPCR. (C-G) Comparison of *Klf15* ;; *SPE*^{SK6} double mutants to WT, *Klf15*, and *SPE*^{SK6} single mutants in experiments measuring expression levels of Toll target genes *IM2* (C), *CG15067* (D), and *Drs* (E) via RT-qPCR as well as survival against *S. aureus* (F) and *E. faecalis* (G). (H-I) Comparison of *Klf15* ;; *psh*^{1} double mutants to WT, *Klf15*, and *psh*^{1} single mutants in experiments measuring expression levels of Toll target genes *CG15067* (H) and *Drs* (I) via RT-qPCR. (J-K) Comparison of *Klf15* ;; *modSP*^{1} double mutants to WT, *Klf15*, and *modSP*^{1} single mutants in experiments measuring expression levels of Toll target genes *CG15067* (J) and *Drs* (K) via RT-qPCR. (L-M) Comparison of *Klf15* ;; *PGRP-SA*^{seml} double mutants to WT, *Klf15*, and *PGRP-SA*^{seml} single mutants in experiments measuring expression levels of Toll target genes *CG15067* (L) and *Drs* (M) via RT-qPCR. (N-R) Comparison of *Klf15* ;; *GNBP3*^{Hades} double mutants to WT, *Klf15*, and *GNBP3*^{Hades} single mutants in experiments measuring expression levels of Toll target genes *IM2* (N), *CG15067* (O), and *Drs* (P) via RT-qPCR as well as survival against *S. aureus* (Q) and *E. faecalis* (R). (S) Abbreviated schematic of the Toll pathway.

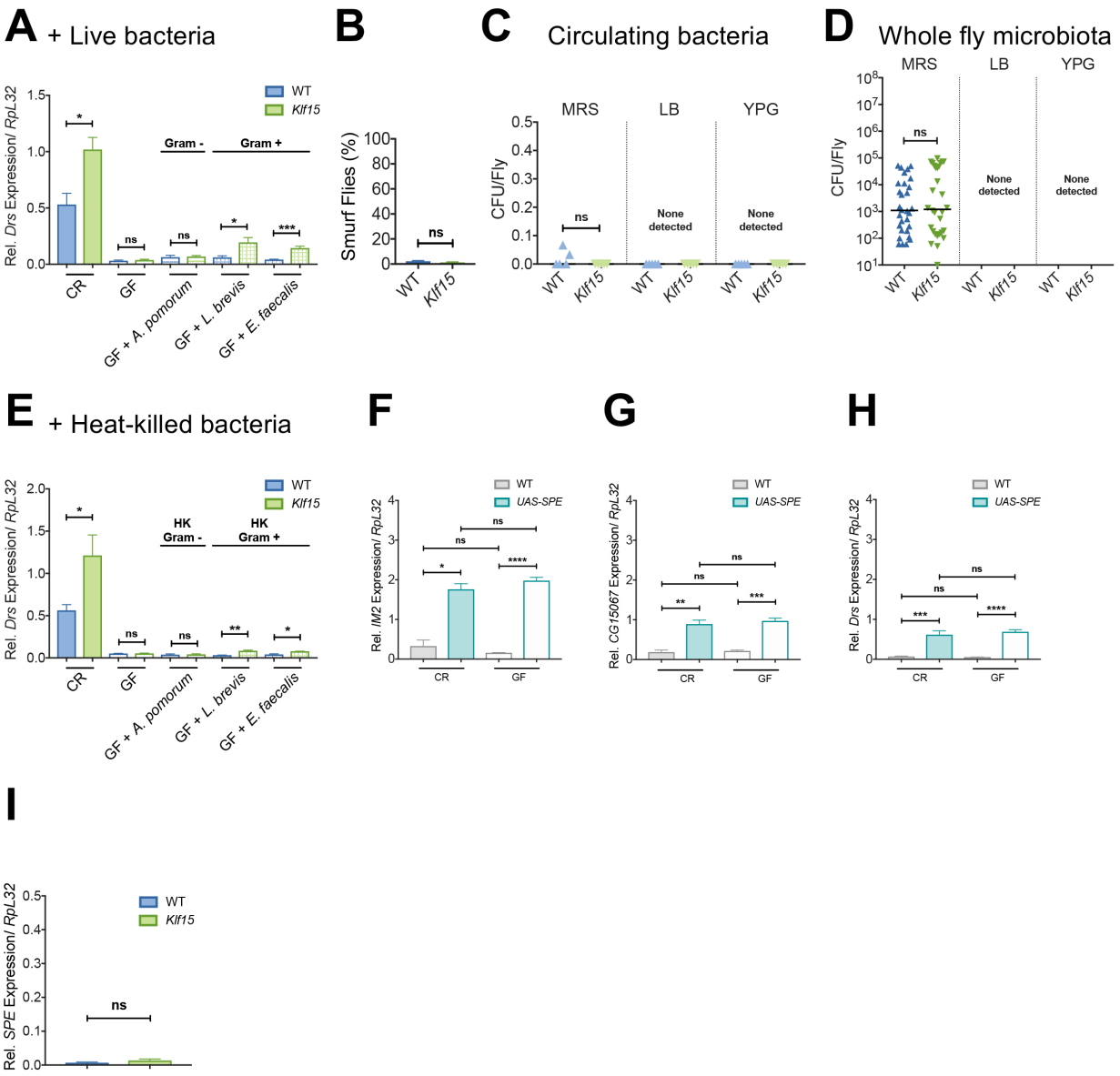

Supplementary Figure IV.4. Nephrocytes mediate immune tolerance to gut microbes
(A) Assessment of gene expression levels in conventional (CR), germ-free (GF), and germ-free flies recolonized with either live *A. pomorum* (Dap-type PGN), live *L. brevis* (Lys-type PGN), or live *E. faecalis* (Lys-type PGN). RT-qPCR measurements of Toll target gene *Drs* is shown.
(B) Percent SMURF flies found after feeding a diet containing 2.5% Blue 1 Dye for both WT and *Klf15*^{NN} flies. (C) Comparison of circulating (hemolymph) bacteria between *Klf15* and control flies. Samples were plated on three separate media: De Man, Rogosa and Sharpe (MRS), Luria-Bertani (LB), and yeast-peptone-glucose (YPG) agar. (D) Comparison of whole fly microbiota between *Klf15* and control flies. Samples were plated on three separate media: De Man, Rogosa and Sharpe (MRS), Luria-Bertani (LB), and yeast-peptone-glucose (YPG) agar. (E) Comparison of gene expression levels in conventional (CR), germ-free (GF), and germ-free flies fed either heat-killed *A. pomorum* (Dap-type PGN), heat-killed L. brevis (Lys-type PGN), or heat-killed *E. faecalis* (Lys-type PGN). RT-qPCR measurements of Toll target gene *Drs* is presented. For RT-qPCR experiments, mean values of three or more repeats are presented ±SE. *p<0.05 **p<0.01

***p<0.001 ****p<0.0001 in a Student's t-test. (F-H) Assessment of gene expression levels in flies overexpressing SPE (*c564-Gal4^{ts} > UAS-SPE*) in both conventional (CR) and germ-free (GF) conditions. RT-qPCR measurements of Toll target gene *IM2* (F), *CG15067* (G), and *Drs* (H) is shown. (I) Whole fly RT-qPCR of SPE using unchallenged wildtype and Klf15 samples.